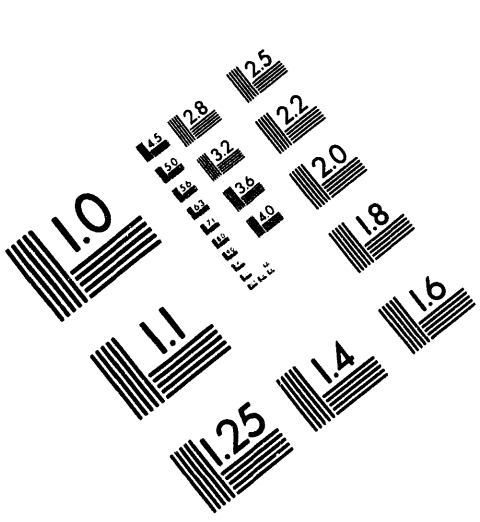

AIIM

Association for Information and Image Management
1100 Wayne Avenue, Suite 1100
Silver Spring, Maryland 20910
301/587-8202

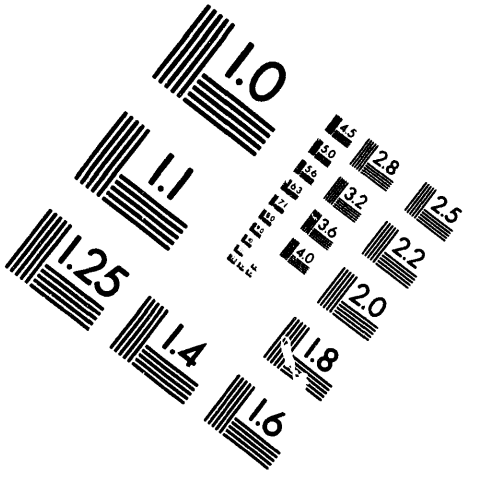

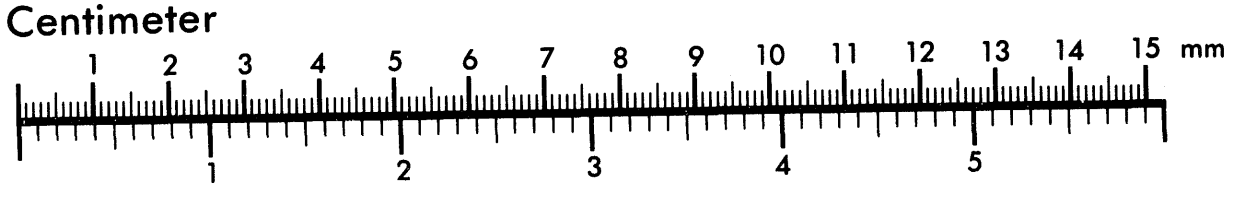

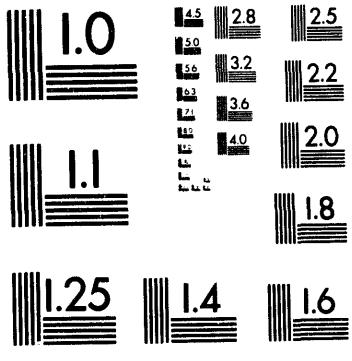

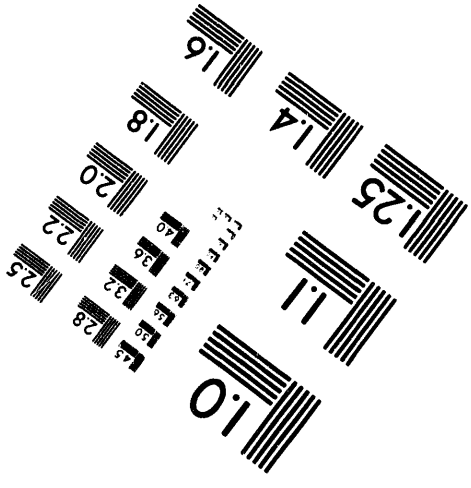

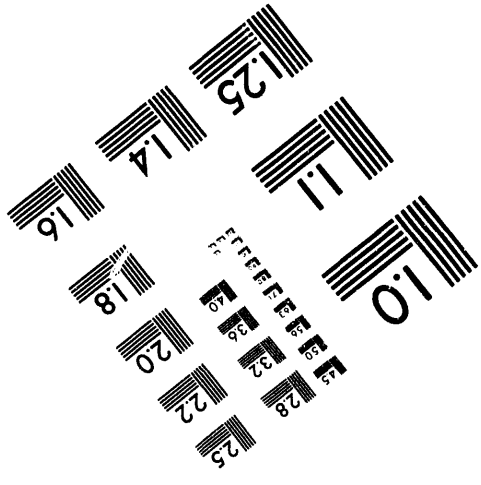

MANUFACTURED TO AIIM STANDARDS
BY APPLIED IMAGE, INC.

1 of 3

NUREG/CR-6193
NEA/CSNI/R(94)2
ORNL/TM-12681

Primary System Fission Product Release and Transport

A State-of-the-Art Report to the Committee on the Safety of Nuclear Installations

Manuscript Completed: April 1994
Date Published: June 1994

Prepared by
A. L. Wright

Oak Ridge National Laboratory
Managed by Martin Marietta Energy Systems, Inc.

Oak Ridge National Laboratory
Oak Ridge, TN 37831-6050

Prepared for
Division of Systems Research
Office of Nuclear Regulatory Research
U.S. Nuclear Regulatory Commission
Washington, DC 20555-0001
NRC FIN L2250
Under DOE Contract No. DE-AC05-84OR21400

Abstract

This report presents a summary of the status of research activities associated with fission product behavior (release and transport) under severe accident conditions within the primary systems of water-moderated and water-cooled nuclear reactors. For each of the areas of fission product release and fission product transport, the report summarizes relevant information on important phenomena, major experiments performed, relevant computer models and codes, comparisons of computer code calculations with experimental results, and general conclusions on the overall state of the art. Finally, the report provides an assessment of the overall importance and knowledge of primary system release and transport phenomena and presents major conclusions on the state of the art.

Contents

List of Figures

List of Tables

Executive Summary

ES.1 Overview

The objective of this report is to present the status of research activities associated with fission product behavior (release and transport) within the primary systems of water-moderated and water-cooled reactors. This category of reactors includes pressurized-water reactors (PWRs), boiling-water reactors (BWRs), and Canadian Deuterium-Uranium (CANDU) reactors. The report has been prepared at the request of the Nuclear Energy Agency (NEA) of the Organization for Economic Cooperation and Development (OECD) Committee on the Safety of Nuclear Installations (CSNI), and the U.S. Nuclear Regulatory Commission (NRC). It summarizes relevant information on important phenomena, computer models and codes, experiments, and comparisons of calculations with experiments. Implications of the information assessed in the report are discussed, and suggestions are made for future work by the PWG-2 task group.

Developing an improved understanding of primary system fission product release and transport is important to permit realistic estimates of reactor accident source terms to be made. Fission product release and transport in the primary system play three important roles in terms of reactor accident source terms:

1. release from fuel defines a significant component of the potential containment source term,
2. the primary system can act as a "reaction chamber" that can chemically and physically condition and modify the timing of vapor and aerosol release to containment, and
3. there can be significant fission product vapor/aerosol retention in the primary system.

This report provides a complete overview of fission product release and transport in the primary system. The report considers in-vessel release and transport up to the reactor coolant system (RCS) pressure boundary and so excludes molten-core-concrete interactions, containment fission product behavior, and pool scrubbing phenomena. It discusses areas where substantial progress has been made in understanding fission product release and transport phenomena. It also identifies areas where additional information is needed. The report covers material that has been documented up to January 1993. References are provided at the end of each report section so that readers can readily obtain more information on selected topics.

Chapter 1 of the report presents background information on major international studies that have been performed related to in-vessel fission product release and transport. Chapter 2 presents a discussion of overall accident sequence phenomena and system boundary conditions that are expected to have a major influence on primary system fission product and core material release and transport. Chapter 3 discusses the major phenomena, experiments, computer codes/models, and code-to-data comparisons performed in the area of in-vessel fission product and core material release. Chapter 4 presents a similar discussion for the area of primary system fission product transport. Finally, Chap. 5 summarizes the main conclusions from the studies documented in Chaps. 3 and 4 and lists recommendations for future work in this area.

This executive summary presents a detailed overview of the information given in the body of this report. It also presents the specific conclusions and recommendations given at the end of Chaps. 3 and 4 and the broad conclusions and recommendations from Chap. 5.

ES.2 Chapter 2 Summary: Accident Sequence Phenomena and Boundary Conditions

The objective of Chap. 2 is to define representative severe accident sequences, and the associated core and RCS boundary conditions, affecting the release and transport of fission products and core materials in Western type water reactors.

The plants considered in Chap. 2 are those with reactors that are UO_2-fueled and light water moderated and cooled. This includes light water reactors (LWRs), that is, PWRs and BWRs of U.S. and European origin for which information is readily available. The primary rationale for this choice is that it includes plants designed, built, and operated by OECD member countries. Furthermore, over the next 10 to 20 years, most of the new plants that are constructed are likely to be LWRs. Advanced design plants are not explicitly discussed in this report, although advanced light water reactors (ALWRs), including passive plants, would be expected to have RCS accident boundary conditions similar to low-pressure sequences for existing LWRs. (While fission product release and transport for CANDU reactors are considered in Chaps. 3 and 4, the Chap. 2 discussion of accident sequences is limited to LWRs.)

The information for the boundary conditions comes mainly from two sources: work done in support of the NRC-sponsored risk analysis of five U.S. plants and the Phebus-FP Phase A studies and related analysis performed within the Commission of the European Communities (CEC) programs on nuclear safety. The German

Risikostudie, Phase B was also used. While a number of analyses of this type have been and are being produced, the ones referenced are considered to be representative and sufficient for the objective of this study.

Because the scope of this state-of-the-art assessment is confined to the RCS, only accident sequence conditions up to the RCS boundary are considered. Thus, ex-vessel debris coolability, core-concrete interaction, and containment thermal-hydraulic conditions are not addressed. Similarly, fission product transport is not considered in systems beyond the RCS [e.g., secondary side of steam generators in steam generator tube rupture (SGTR) accidents and systems interfacing with the RCS in interfacing loss-of-coolant accidents].

In addition to providing information on calculated boundary conditions for severe accident sequences, Chap. 2 also provides a discussion on chemical and physical phenomena that influence RCS release and transport and implications of core-damage progression phenomena on RCS release and transport.

ES.3 Chapter 3 Summary: In-Vessel Release from Core Materials

The study of fission product release to model the various phenomena in accident conditions has generated a large body of data and many different approaches. This chapter gives an overview of the phenomena of fission product and core material release, a summary of the experimental programs that have been conducted to investigate release phenomena, an overview of the models and computer codes that have been developed to describe release behavior, and finally a comparison between code calculations and experimental data. Conclusions are presented at the end of the chapter.

The in-vessel release phenomena discussed in Chap. 3 include the following:

- concentration and chemical forms of fission products;
- distribution and mobility of fission products;
- transport in the fuel-cladding gap;
- effects of UO_2 oxidation, UO_2-Zircaloy chemical interactions, microcracking, and quenching/reflood;
- release from debris beds and molten pools;
- release from molten fuel-coolant interactions; and
- non-fission product material releases (Ag-In-Cd, Sn, boric acid, and other structural materials).

Section 3.2 presents information on the major in-reactor and out-of-pile experiments that have been performed related to fission product and structural material release phenomena. Tables of information related to the major experiments are also presented in this section.

Computer codes for modeling in-vessel fission product (FP) release may be divided into two categories: (1) **systems codes**, that cover all aspects of severe accident phenomena and that usually treat FP release using models from (2) **special FP release codes** that are stand-alone code for calculating FP release. The special FP release codes can be split into two additional categories: (1) **empirical** models, based on an Arrhenius-type of correlation for the release rate with the constants and exponents found by fitting experimental data, and (2) **mechanistic** models, which define serially connected steps to calculate FP release.

The FP release code review presented in Chap. 3 covers eight system codes: ATHLET/CD, KESS, ICARE-2 (and ESCADRE), ESTER, RELAP5/SCDAP, MELCOR, MAAP and THALES; seven FP release codes: CORSOR (and CORSOR-M), CORSOR-Booth, GRASS (FASTGRASS, PARAGRASS), VICTORIA, FREEDOM, MITRA and FIPREM (including FPRATE); and two stand-alone FP release models: the NUREG-0772 and the Kelly models.

The information presented in the code/experiment section of Chap. 3 is taken from published reports of the comparisons of calculated and measured fission product releases from fuel. The section is organized by comparisons of experimental data with specific code calculations and is concluded by a discussion of the insights provided by the detailed comparisons. Code comparisons with data produced in the Severe Fuel Damage (SFD) tests, the OECD Loss of Fluid Test (LOFT) LP-FP, the HI-series, the VI-series, the ACRR ST-series, and the HEVA tests are presented and the results of the comparisons are discussed.

ES.3.1 Chapter 3 Conclusions (from Sect. 3.5)

The current state-of-the-art understanding of in-vessel fission product/core-material release is well developed for most aspects of release behavior, particularly for the noble gases and volatile fission products (I and Cs). The dominant phenomena have been recognized and are understood to the level that has permitted development of both empirical and some fundamental/mechanistic models for predicting the rates of fission product release. The existing experimental data are mostly adequate for continued development and improvement of the empirical

models. On the other hand, continued development and validation of the mechanistic models require data from further well-characterized separate-effect and integral experiments.

Several weaknesses have been identified in the current understanding of fission product release. These weaknesses have variable impact on fission product releases from the fuel. The two most important weaknesses identified with respect to potential source terms were (1) long-term releases of low-volatility fission products from molten fuel and (2) releases at high temperature in air/high oxygen potential conditions (i.e., postvessel failure scenario). Other potentially important weaknesses include the effects of quenching/reflood, releases from debris beds, and the effects of UO_2 liquefaction.

A general overview follows, based on the subsections of Chap. 3. Specific weaknesses in the current state of the art are identified, and recommendations are provided for future undertakings.

ES.3.1.1 In-Vessel Release Phenomena

A physically based description of fission product release behavior requires a knowledge of the concentration, chemical form, spatial distribution and mobility of fission products within the fuel. A detailed model of the fuel morphology and its evolution is also required.

The concentration of fission products in the fuel is considered to be well established. Concentrations can be calculated to the required level of accuracy using time-dependent irradiation data in a nuclear production/capture/decay code.

The chemical form of fission products can be predicted as a function of burnup, temperature, and oxygen potential, based on thermodynamic data, although uncertainties exist for some of the data. The chemical form is important for the determination of volatility and, hence, release rates for some fission products (e.g., Mo, Cs), which can form a variety of different compounds in the fuel. Also, once released from the fuel, the chemical form of the gaseous species will determine their subsequent transport and deposition. The spatial distribution of fission products within the fuel (i.e., intragranular bubbles, grain boundaries, gap, etc.) has also been studied, but limited quantitative data have been produced (except for gap inventories) because of the difficulty in performing such measurements.

The individual processes that contribute to fission product release from the UO_2 matrix have been identified. The main processes include atomic diffusion, intragranular bubble migration, grain-boundary sweeping, intergranular bubble coalescence, microcracking, liquefaction, and matrix volatilization. Physically based descriptions have been developed for all of these processes; however, there is still considerable uncertainty regarding the dominant processes controlling release behavior during the various stages of transient heating and core-damage progression.

Fission product transport in the fuel-rod gap is also understood qualitatively, and models exist for describing behavior of defective fuel in intact geometries.

The individual phenomena controlling the release rates of most non-fission product materials are generally well understood. Ag-In-Cd control rod material releases depend on the timing of the failure of the stainless steel cladding, which varies between high- and low-pressure accident scenarios. Releases of tin from Zircaloy are known to be influenced by cladding oxidation, which raises the tin activity leading to a higher vapor pressure and more rapid releases. Boric acid aerosols can be formed by flashing of borated reactor coolant. Uranium-bearing aerosols may be produced by volatilization of exposed UO_2 at high oxygen potentials via formation of gaseous UO_3 or other volatile uranium species.

ES.3.1.2 Experimental Programs on In-Vessel Release Phenomena

An extensive experimental data base of integral and kinetic release measurements is available to support both phenomenological understanding and the development of models or codes for describing release behavior. The data base includes information derived from small-scale single-effect out-of-reactor tests, large-scale multiple-effect in-reactor tests, and the Three Mile Island Unit 2 (TMI-2) accident. Experiments have been conducted under a variety of conditions representative of those expected to arise in reactor accidents. The data base, however, is not sufficiently complete that it can be used to formulate empirical release correlations that could be used confidently for the range of accidents of interest. Furthermore, the data base is most focused on cesium. More scattered data are available for noble gases or iodine. Release data are scarce for tellurium and the lower-volatility radionuclides.

In general, the experimental data base indicates that cesium, iodine, and the noble gases show the highest release rates for most conditions and that the rates are similar for these species. Oxidizing conditions can produce significant releases of ruthenium and molybdenum. Reducing conditions cause increased europium and barium releases. Tellurium and antimony releases are shown to increase when the cladding is oxidized.

Some weaknesses have been identified in the existing experimental data base. The release rates from molten fuel, particularly for the less-volatile fission products, are not available. Only limited release data are currently available for postvessel failure conditions involving air/oxygen-rich conditions at high temperatures. The FP source term from the fuel/debris under these conditions would be significantly different from steam/H_2 mixtures because of the high oxygen potential and increased volatility of many fission products, actinides, and other core materials. Data on releases from debris beds are lacking, and the effect on releases of UO_2 dissolution by Zircaloy have not been quantified. Irradiated fuel behavior in hydrogen-rich conditions at high temperatures is not well understood with respect to UO_2 "foaming" and its potential effect on fission product release. Data on fission product release under quenching/reflood conditions are inadequate for model development. Finally, the existing data base is not adequate for the wide range of burnup, including both low- and high-burnup fuels. By addressing these weaknesses, a more complete basis for quantifying releases from intact or degraded geometries would be available.

The data base for non-fission product material releases has some uncertainties, but is generally adequate.

ES.3.1.3 Release Modeling and Codes

Two types of models have been developed for calculating the release rates of fission products or core materials during severe accident conditions: empirical models and mechanistic models. The empirical models are based on correlations between experimental conditions and release rates and have achieved widespread use because of their simplicity and functional reliability. This simplicity, however, tends to produce inaccurate results for calculations done under boundary conditions that differ from those on which the correlations are based.

Mechanistic models, on the other hand, are based on fundamental principles and in most cases include microstructural information in the calculations. These models embody the understanding of individual release phenomena and, when implemented correctly, are regarded as powerful tools with general applicability. For certain cases, it can be shown that the mechanistic calculations give better agreement with data than do empirical calculations. However, the mechanistic models require a significant computational effort and demand boundary conditions and constitutive laws to be defined at a microstructural level. The mechanistic models must be linked to system codes in order to have adequately defined fuel morphology and cladding conditions, without which the user is faced with complex input requirements.

Many of the mechanistic codes are still under development. In some cases, the existing mechanistic models appear to be leading the experimental data base. The most obvious area in which the mechanistic codes require data is in the spatial distribution of fission products within the fuel (e.g., the grain boundary inventory of fission products, which is calculated by all of the mechanistic codes). Other needs include data for the development of mechanistic fission product release models under quenching/reflood conditions. On the other hand, empirical models seem to be lagging the experimental data base. They should be extended to include data on the effect of burnup, fuel oxidation, and perhaps other phenomena such as liquefaction, quenching/reflood, and fuel morphology considerations.

Code validation is currently an area requiring some attention. This applies primarily to both verification of model implementations within codes and validation by comparison to experimental data. There is a lack of clearly identified versions of mechanistic codes with documented validation.

ES.3.1.4 Comparisons between Experimental Results and Code Calculations

Measured data from both in-reactor and out-of-reactor fission product release experiments have been compared with computer code calculations using both mechanistic and empirical models. The number of documented comparisons is considerable, but none of the calculations have been blind; thus no conclusions can be drawn about the validity or robustness of the various models over a wide range of conditions. Very few comparisons are available for fission products other than the noble gases or iodine and cesium.

In general, the simple empirical models tended to overpredict the measured volatile fission product release data; however, this is not surprising, given that the majority of comparisons were based on experiments with trace-irradiated or low-burnup fuel. The releases of barium and strontium tended to be overpredicted. The releases of control rod materials were overpredicted by models that did not take into account relocation of melts to cooler regions lower in the core.

The mechanistic models were able to match some measured integral release data fairly well for open calculations that permitted tuning of model parameters. Release rates were more difficult to reproduce. It should be noted, however, that the mechanistic codes require detailed fuel conditions to achieve useful results.

ES.3.1.5 Recommendations

The existing experimental data, combined with planned experiments in the near future, generally appear to be adequate for the needs of understanding most aspects of release phenomena and model development. However, specific studies involving a mixture of single-effect and integral experiments should be conducted to address the need for data in the following areas: high-temperature releases of low-volatile fission products from molten fuel, high-temperature air/high oxygen potential conditions, quenching/reflood, release from debris beds, and release during liquefaction of UO_2. The mechanistic models should also be further developed to include more fundamental descriptions of these processes.

Model development and validation efforts should be continued for both empirical and mechanistic codes. The empirical models should be updated to include recent data and extended to include some simple additional features such as burnup, fuel oxidation, and perhaps other phenomena such as liquefaction, quenching/reflood, and fuel morphology considerations.

International Standard Problems (ISPs), preferably blind or semiblind single-effect and integral tests, should be encouraged as a forum for code validation. However, well-defined thermal-hydraulic boundary conditions are necessary in the experiments to enable blind predictions to be judged and interpreted. As such, these exercises would be valuable for assessing the true capabilities of existing codes and to highlight areas for improvement. In addition, ISPs encourage a wider exchange between modelers and experimentalists; this in turn should promote a more objective assessment of analytical tools and improve the validation efforts.

ES.4 Chapter 4 Summary: Primary System Fission Product Transport

Following release from the fuel, fission products could be transported through some portion of the RCS before being emitted to the containment (or environment in the event of containment failure or an accident sequence that bypasses the containment building). Processes within the RCS will determine the magnitude, nature, and timing of this radioactive emission.

The RCS can attenuate the extent of the release by removing a significant fraction of fission products through a variety of aerosol and vapor removal mechanisms. Extensive experimental and code development studies undertaken over the last 10 years have demonstrated that significant attenuation can occur within the primary system and that analyses conducted before this time (which consciously assumed no retention) were oversimplified.

More recently there has been a growing appreciation of the role that the primary circuit can play as a reaction chamber in defining the timing and physical and chemical forms of the radioactive emission. The role of the primary circuit as a reaction chamber has also been emphasized by recent plant analyses that indicate the potential importance of revaporization (whereby fission products initially deposited in the circuit are released due to decay heating of the surfaces at a time when the containment may no longer be intact).

The discussion in Chap. 4 considers the main physical and chemical phenomena that occur within the primary circuit during a severe accident. These phenomena follow an approximately chronological order (i.e., from release from fuel to transport to the containment):

- Vapor-phase phenomena
  - — Thermodynamics and speciation
  - — Vapor condensation
  - — Vapor/surface and vapor/aerosol reactions
- Aerosol nucleation and characterization
  - — Nucleation
  - — Growth (final particle size distribution)
- Aerosol transport and relocation
  - — Transport and deposition
  - — Resuspension
  - — Revaporization

Section 4.2 provides a detailed analysis of the phenomena just identified. The basic principles of each topic are initially reviewed, followed by a detailed description of the status of experimental and modeling work in the area; each subsection concludes with a discussion of the main uncertainties associated with the individual phenomenon.

All the major experimental programs examining RCS fission product transport phenomena are considered in Sect. 4.3, both in terms of basic input to models (small-scale, separate-effects studies) and examination of the coupling between models and validity of the source term codes (large-scale, integral studies). Emphasis is placed on those experiments that have been compared with code predictions.

Substantial efforts have been made to model the transport phenomena based either on application of empirical models or a more mechanistic approach. Modeling within

both system codes and codes dedicated to fission product transport issues is reviewed in Sect. 4.4. The fission product transport codes reviewed include: (1) detailed transport codes, including VICTORIA, TRAP-MELT2.2 and TRAP-MELT3, RAFT Version 1.0, SOPHIE Version 2.1, AEROSOLS B2, MACRES, HORN, and ECART; and (2) systems codes, including SCDAP/RELAP Mod3, MELCOR Version 1.8.2, MAAP Version 3.0B, ICARE2 (and ESCADRE), ATHLET-CD, and ESTER.

In Sect. 4.5 fission product code/experiment comparisons are presented. These include comparisons with results from the Marviken tests, LWR Aerosol Containment Experiment (LACE) tests, Aerosol Transport Tests (ATTs) and Aerosol Resuspension Tests (ARTs) performed at ORNL, Falcon experiments, the French TUBA, TRANSAT, and DEVAP tests, and PBF tests, and also include pretest calculations for the Phebus-FP tests.

ES.4.1 Chapter 4 Conclusions (from Sect. 4.6)

ES.4.1.1 Thermodynamics and Speciation

The chemical form of the fission products will influence their transport within the RCS both as vapors and aerosols. Thermodynamic data are required to predict the main species stabilized and their likely properties. There has been good progress in recent years in the understanding of the vapor and condensed phase chemistry that can occur within the reactor coolant circuit during a severe accident. A substantial data base of thermodynamic properties has been assembled of species likely to be present in the RCS. Efforts are under way to ensure that the data base is self-consistent and broadly accepted.

However, there are fewer data on species such as hydroxides and hydrides that may become more important at high pressures of steam and hydrogen. Furthermore, the effects of intense radiation fields on chemistry in the reactor coolant circuit have received little attention. The major uncertainty for code validation purposes is believed to be the lack of data on the chemical forms of the fission products stabilized within the RCS. The Phebus-FP program is expected to provide an indication on the fission product speciation from experiments using a realistic source.

ES.4.1.2 Vapor Interactions with Surfaces and Aerosols

Interactions of fission product vapors with primary circuit surfaces and aerosols can substantially modify the magnitude and nature of the source term to the containment. However, the relative importance of the processes is uncertain: while the extensive surface area of the aerosol surfaces indicates that vapor-aerosol interactions should predominate, heat and mass transfer limitations can considerably affect the balance.

A number of deposition kinetics studies have been conducted using the following vapor species: CsOH, I_2, HI, Te, SnTe and CsI. Other vapors could well play important roles, and the data base needs to be extended to include them. It should also be noted that, in reality, surfaces could be oxidized and coated with aerosols, and work is required on such representative surfaces. The effect of carrier gas oxidation potential is also an important consideration.

Some data are available on vapor interactions with deposited aerosols, but few studies have addressed vapor interactions with suspended aerosols. Consideration of time scales indicates that the latter process will be governed by diffusion limitations rather than chemical kinetics. Lack of data on the diffusion of fission product vapors through reactor gases prevents accurate prediction of condensation phenomena.

Representative data are required (e.g., from Phebus-FP) to indicate the nature of the surface deposits and the competition between vapor-surface and vapor-aerosol reactions. Such data should guide the requirement for separate-effects studies and the development of more sophisticated models to treat these processes.

ES.4.1.3 Aerosol Nucleation and Growth

The behavior of fission product aerosols within the RCS will be determined predominately by the size and, to a lesser extent, the shape of the aerosol. The chemical form of the fission product vapors will determine the point at which condensation will occur to form aerosols, their size distribution, and morphology. Uncertainties in defining the chemical speciation of the fission product vapors represent an important uncertainty in determining the subsequent aerosol transport.

Experimental studies have shown that chemically distinct aerosols can be produced with different transport properties, although their significance with respect to transport in the RCS remains to be assessed. The role of pressure on aerosol nucleation is uncertain; however, scoping tests have indicated that the primary size of aerosol particles decreases with increasing system pressure.

The general requirement for a detailed treatment of aerosol nucleation has not been demonstrated (e.g., while a sophisticated model is used in RAFT, only a limited

approach is adopted within VICTORIA). The need for a detailed understanding of these phenomena should be assessed through sensitivity studies and additional scoping experiments, if appropriate.

ES.4.1.4 Aerosol Transport and Deposition

The basic processes governing aerosol transport are generally well understood, although the neglect of electrostatic forces within the codes remains a concern. Areas of weakness include:

1. deposition in bends,
2. application of the fundamental aerosol physics models to treatment of complex structures at a large scale (such as steam separators or steam dryers),
3. aerosol deposition arising from abrupt changes in the flow channel width, and
4. thermophoretic deposition from turbulent flows.

ES.4.1.5 Resuspension and Revaporization

Two processes may lead to a significant release of radioactivity at late stages of the accident:

1. physical resuspension (or re-entrainment) of aerosols (increased flow and shock and vibration in the substrate) and
2. revaporization of deposits (increased temperature or variation in gas composition).

Resuspension of aerosols has been demonstrated in a number of experiments; however, the importance of this phenomenon in determining the consequences of severe accidents is uncertain. All experimental studies conducted to date have relied on the use of simple aerosol stimulants, and more realistic experiments such as Phebus-FP are required to define the nature of the initial deposit more clearly. Uncertainties persist as to the size distribution of the resuspended material and the synergisms between the effects of gas flow and structural vibration on resuspension. However, the complexity of physical resuspension for realistic systems (involving multicomponent, multilayered deposits in a variety of thermal-hydraulic conditions) makes it unlikely that a fully mechanistic analysis will be possible.

Plant calculations and code analyses indicate the potential importance of revaporization to the consequences of severe reactor accidents. In the absence of interactions with surfaces and other materials, revaporization can be modeled simply on the basis of the temperature and partial vapor pressures of the system. However, reactions could modify any release significantly. The study of a number of key systems is recommended to acquire the relevant activity coefficients. More detailed modeling of the interactions of deposits with surfaces is also needed to interpret and apply these data.

ES.4.1.6 Codes and Benchmarks

A large number of alternative codes and different versions of transport codes are available. In many cases there is no documented evidence that some of the current versions of codes have ever been checked against experiments. The production of validation statements (as for VICTORIA and MAAP, for example) is recommended.

While assumptions and approximations are made, no code appears to be significantly better than the others in predicting deposition. In general, code comparison exercises show that the codes are capable of predicting which aerosol deposition mechanism will dominate, but they are less successful in determining the extent of deposition. Few integral experiments have been conducted to allow the vapor models to be tested.

There is a general consensus that sedimentation, thermophoresis, turbulent diffusion, and impaction are important aerosol phenomena in the RCS. However, significant variety in the treatment of the deposition processes within each code has been observed. Comparison of the models within the codes would clarify differences and inconsistencies. Such an exercise would assist in identifying the best models that warrant continued use and development.

Detailed code comparison exercises are needed both to validate individual models (separate-effects studies) and assess the coupling between models and the applicability of the source term programs (integral tests). Data from the Falcon ISP and Phebus-FP program should address some of these concerns.

Parametric assessments/sensitivity studies (e.g., variation of aerosol size, concentration, composition) are urgently needed to link the primary circuit calculations to eventual accident-specific source terms to the containment and environment. Such analyses should assist in defining the requirements for a detailed understanding of speciation calculations, the treatment of aerosol nucleation and resuspension, and the assessment of multicomponent aerosol behavior. The risk-dominant phenomena can be highlighted, allowing future work to concentrate on those phenomena contributing most to uncertainties in the consequences of the accident. Such calculations are planned as part of the CEC Reinforced Concerted Action on Source Term.

ES.4.1.7 Thermal-Hydraulics

There has been a significant change over the last 10 years in the understanding of flows in the RCS during core degradation, particularly for the accidents in which the circuit remains pressurized during core degradation. Complex natural circulation loops are predicted to develop that could markedly influence aerosol and vapor behavior. The uncertainties in the results of source term calculations stem as much from uncertainties in the thermal-hydraulic boundary conditions as from limitations in source term modeling. Examples of thermal-hydraulic uncertainties include the treatment of late-phase core behavior, the effect of the carrier gas on fission product speciation and transport, the one- or two-dimensional (1- or 2-D) approach adopted within the majority of severe accident thermal-hydraulic codes, decay heat effects, and the coupling of source term with thermal-hydraulic modeling. Decay heat is important in determining local surface temperatures and, hence, phenomena such as revaporization. The relocation of liquid and slurry deposits under hydrodynamic and gravity forces therefore merits attention.

ES.5 Chapter 5 Summary: Main Conclusions and Recommendations

Chapter 5 summarizes the main conclusions and recommendations that have been derived from the information presented in this report. It takes the specific conclusions and other information presented in Chaps. 2–4 and integrates and summarizes those issues that the writing group believes are the most important from the standpoint of source term analyses for severe accident conditions. Recommendations to the CSNI are also presented.

There has been a significant improvement in the understanding of fission product release and transport in the RCS since the TMI accident. The ability to predict behavior of radionuclides in the RCS under severe accident conditions has advanced greatly. These capabilities have demonstrated that radionuclide retention in the RCS can significantly attenuate and transform the potential release of radioactivity from a nuclear power plant during an accident. Careful modeling of these release and transport phenomena is an essential element of reactor accident analyses. For example, in accident scenarios involving containment bypass through lines connected to the RCS (V sequence) or late containment failure and revaporization of radionuclides, the in-vessel behavior of radionuclides would have a direct bearing on the consequences of the accident.

However, the phenomena associated with RCS release and transport are complex, and not all of the relevant source term issues have been resolved. The conclusions and recommendations presented in Chap. 5 concern the phenomena and issues that the writing group considered to have the greatest need for further understanding and potential impact on our ability to perform realistic source term analyses for severe accidents.

Both Chaps. 3 and 4 included discussions of the major phenomena that must be modeled to assess RCS fission product release and transport. The writing group qualitatively assessed the importance of each of these phenomena to the prediction of RCS release and transport and the need for additional experimental data to resolve uncertainties in the phenomena.

Tables ES.1 and ES.2 (also Tables 5.1 and 5.2 from Chap. 5) summarize the rankings that members of the writing group gave to each of the phenomena in terms of importance and the data needs. These rankings ["high, medium, low" (HML)] represent our best effort to prioritize the needs for further release and transport phenomena assessments in terms of importance to source term issues for severe accident analyses. A high ranking for a release phenomena means that the writing group believes that it has a strong influence on the release from the core. A high ranking for a transport phenomena means that the writing group believes that it has a strong influence on the source to the containment or, in the case of bypass sequences, to the auxiliary building. It should be noted that a range (such as L-M) was agreed to for phenomena where there was not a consensus on the HML rankings. The experimental needs identified when assigning knowledge rankings are in addition to and not alternative to existing programs such as Phebus-FP and Falcon and potential future programs such as STORM.

The writing group believes that an adequate data base exists for understanding and model development for many release and transport phenomena. A limited number of phenomena were ranked high in importance and were viewed by the writing group as needing additional experiments to permit the phenomena to be understood and included in RCS release and transport codes. The writing group recommends additional experiments (with supporting analysis and model development) concerning the following release and transport phenomena:

1. For fission product release, new experiments, or extension of planned experiments, are needed to characterize the fission product release from fuel under air or highly oxidizing conditions and low-volatile fission product release from molten pools in the reactor vessel. In our view, these release phenomena have the potential (depending on the plant design characteristics) for high impact on accident

Table ES.1 Phenomena summary table for RCS fission product release

Phenomena affecting FP release	Importance (High-Med-Low)[a]	Knowledge ranking (1–4)[b]	Comments
Chemistry of FPs in fuel	M-H	2	Thermodynamic data are mostly adequate for current needs, and modeling tools exist for equilibrium calculations.
FP mobility in fuel	H	2	Extensive data exist, but they need to be consolidated and reviewed. More data may be required on the effect of oxygen potential and burnup on diffusion rates.
Evolution of fuel microstructure	M	3	Important for early phase of release (e.g., venting of grain boundaries). Need data to support model calculations at different grain sizes, burnups, and power histories.
UO_2 liquefaction	M	3	Need separate-effect test data to support models.
UO_2 oxidation	H	3	Important for postvessel failure releases with air oxidation of exposed fuel. Data are required at high temperatures.
Quenching/reflood	M	3	Requires tests with high burnup fuel.
Debris bed formation/heatup	L-M	3	Requires integral test data. Need knowledge of local temperatures, fuel morphology, and carrier gas conditions.
Molten pool formation	H	3	Data required for low-volatile FPs after extended melt duration.
Molten fuel-coolant interaction	L	4	Not expected to contribute significantly to source term.
Non-FP material releases	H-L	2	Ag-In-Cd, boric acid, and Sn-Zr releases rated M/H; others as M/L. Data need to be reviewed/consolidated. Some integral test data, particularly at high pressures, may be required.

[a]Importance ranking (level of importance with respect to impact on FP source term from the core).
[b]Knowledge ranking (level of understanding for each phenomena):

1. Current understanding (data and modeling) is adequate.
2. Further modeling or review/consolidation of data is required. Existing data appear to be adequate.
3. Understanding is incomplete. New experimental data would provide adequate information to develop the necessary understanding, and this could be achieved in the near future.
4. Understanding is incomplete. New experimental data would be required to provide adequate information to develop the necessary understanding, but the data are not likely to be available in the near future.

Table ES.2 Phenomena summary table for RCS fission product transport

FP transport phenomena	Importance (High, Med., Low)[a]	Knowledge ranking (1–4)[b]	Comments
Thermodynamic data	H	1[c]	Generally well understood, but there is a need for high-pressure data and data for more complex compounds.
Vapor interactions with surfaces and aerosols	H	3	There is a clear need for vapor-aerosol interaction data. Vapor-surface interaction tests may need to be done with more complex FP species. Data on appropriate species will hopefully come from Phebus-FP tests.
Aerosol nucleation and growth	M	2	The need for detailed nucleation/growth modeling in the codes has not been clearly established.
Aerosol deposition and transport	H-M	1[c]	Generally well understood in terms of basic physics, though there is a need for improved understanding of deposition in bends and in complex geometries.
Aerosol resuspension	L-M	3	The need for detailed resuspension models in the codes has not been clearly established. Phebus-FP can help to define the aerosol species to be used in any tests.
Revaporization	H	3	There is a need for revaporization tests performed with appropriate FP chemical species. Again, Phebus-FP can help.

[a]Importance ranking (level of importance with respect to FP source term from the RCS).

[b]Knowledge ranking (level of understanding for each phenomena):

1. Current understanding (data and modeling) is adequate.
2. Further modeling or review/consolidation of data is required. Existing data appear to be adequate.
3. Understanding is incomplete. New experimental data would provide adequate information to develop the necessary understanding, and this could be achieved in the near future.
4. Understanding is incomplete. New experimental data would be required to provide adequate information to develop the necessary understanding, but the data are not likely to be available in the near future.

[c]As noted in the comments, the knowledge base for these phenomena is generally well understood. Although there were outstanding data needs, the writing group did not think that these needs warranted giving these phenomena a "2" or "3" knowledge ranking.

source term analyses, and adequate information is not available to model them in the release codes.

2. For fission product transport, additional experiments are needed to address vapor interactions with aerosols and surfaces and material revaporization phenomena. We assess these to be of high importance to RCS transport and source term analysis and believe that an adequate experimental data base is not available to permit appropriate code models to be developed.

Section 5.3 of Chap. 5 presents additional conclusions and recommendations from this state-of-the-art assessment; these were developed from the specific conclusions presented at the end of Chaps. 3 and 4.

1. Two types of FP release codes are presently in use—empirical and mechanistic codes. The empirical codes are based on correlations between experimental conditions and release rates and are widely used because of their simplicity. However, they are often used under conditions differing from those on which they are based.

   We recommend that the CSNI encourage efforts to extend the usefulness of the empirical codes by including recent experimental data on the effects of burnup, fuel oxidation, and perhaps other phenomena such as liquefaction, quenching, etc. This will make the empirical codes applicable to a wider range of accident conditions.

2. The release code-to-data comparisons presented in Chap. 3 illustrate that (1) empirical release codes tend to overpredict volatile FP release data and (2) mechanistic release codes are capable of producing better agreement with experiment but appear to require very careful application (detailed fuel conditions) to obtain good results. However, detailed assessments of FP release code–experiment comparisons have never been performed (and none of the comparisons have been blind), so it is difficult to assess the validity and robustness of the models.

   We recommend that coordinated efforts be made to assess the validity of the FP release models and codes (current and future versions), using both benchmarks and ISPs. Comparisons with both simplified and well-controlled separate-effects tests, as well as with more global tests—especially with Phebus-FP data—should guide the need for further model improvements and developments. The additional experiments recommended in Sect. 5.2, point 1 (FP release from fuel under air-oxidizing conditions and low-volatile FP release from molten pools in the reactor vessel) will also be necessary as a data base for future code development.

3. The FP transport code-comparison results presented in Chap. 4 indicate that the codes have not been sufficiently validated for reliable use in reactor source term analyses. From the standpoint of aerosol transport, the codes can correctly predict which deposition phenomena are most important in an experiment but are not capable of predicting the magnitude and distribution of the deposition when compared with experimental data. Few of the benchmark experiments discussed in Chap. 4 permit definitive validation of the vapor interaction models presently in the codes.

   We recommend the continued development and assessment of the FP transport codes. This should, at a minimum, include (a) improved transport code models based on the experimental needs highlighted in Sect. 5.2, (b) well-coordinated comparisons of code predictions to results from Falcon and Phebus-FP experiments (ISPs) and assessment of the FP transport codes based on these comparisons, and (c) additional code-comparison exercises to identify differences in code models used to analyze the same phenomena (e.g., bend deposition).

4. The importance of mechanistically modeling aerosol nucleation has not been assessed. At issue is whether *ad hoc* treatments of nucleation phenomena are adequate for the purposes of reactor safety analyses. In addition, the importance of mechanical resuspension of aerosols (and mechanistic modeling of this process) has not been clearly established. Consequently, while additional experiments would be useful to permit appropriate models for these phenomena to be developed, it is not possible to make a clear case for doing so.

   We recommend that coordinated efforts be initiated to determine the importance of aerosol nucleation and aerosol resuspension phenomena to RCS fission product transport analyses. These assessments would provide the basis for determining if experiments are needed in addition to those already performed or planned.

Other writing group comments include the following:

1. With regard to any future integral FP release and transport experiments, and particularly the Phebus-FP tests, the writing group recommends that attention be given to using the test data to guide future separate-effects tests. For example, appropriate analyses of deposition samples may indicate the fission product chemical species that should be included in future small-scale revaporization tests.

2. Although the writing group did not perform any detailed assessments of the impact of thermal-hydraulic and core-degradation uncertainties on FP release and

transport and the importance of scaling of experiments, we view these issues as sufficiently important that they should be considered with regard to release and transport analyses and experimental design. For example, the core degradation codes should provide sufficiently accurate information on fuel conditions to the mechanistic FP release codes for release calculations. The writing group encourages efforts to link existing mechanistic release models with existing mechanistic core degradation models.

Acknowledgments

Completion of this report was a major effort, and the authors are pleased to acknowledge the contributions of many people and organizations. We first wish to thank the OECD/NEA for their support of this effort, and in particular Heikki Holmström of the OECD/NEA, who coordinated all of the OECD efforts associated with preparation of this report. We thank the CSNI Principal Working Group 2 and the In-Vessel Degraded Core Behavior Task Group for their guidance of the report preparation efforts. We also wish to thank the NRC for sponsoring the efforts of the writing group chairman and for publishing the final version of the report. Specifically, we thank Farouk Eltawila, Richard Lee, and Alan Rubin of the NRC for their overall assistance.

The individual writing group section chairmen wish to acknowledge the contributions of the following people who assisted in preparing the individual report sections:

Section 1: T. S. Kress, ORNL/USA

Section 2: R. Hammersley for providing information from MAAP calculations, and the DOE Advanced Reactor Severe Accident Program for providing support for preparing this section.

Sections 3.1, 3.2: B. J. Lewis and S. R. Mulpuru from AECL/Canada, R. A. Lorenz and M. F. Osborne from the ORNL/USA, C. G. Benson and R. Williamson from the UKAEA, O. Gotzmann from Germany, F. Panisko from the PNL/USA, and D. J. Osetek from the USA.

Section 3.3: J. Starflinger from the University of Bochum in Germany, who assisted in much of the comparison and table preparation efforts, and Professor H. Unger of the University of Bochum, who provided financial and technical review assistance in preparation of this section. Also T. Heames and R. M. Summers from SNL/USA, M. Kajimoto from JAERI, J. Rest from the ANL/USA, L. N. Carlucci from the AECL Chalk River Laboratories, C. Ronchi from the Institut fur Transuranu/CEC, M. Plys from the Westinghouse Inc./USA, J. K. Hohorst from the INEL/USA, M. R. Gonzales from the IPSN, CEN/Cadarache, M. Z. Podowski from the Rensselaer Polytechnic Institute/USA, and M. R. Kuhlman from the BCL/USA.

Section 3.4: The NRC for providing financial assistance for preparing this report section. P. Chatelard from CEA/IPSN-Cadarache and J. P. Leveque from CEA/DRN-Grenoble, who provided assistance in preparing this section.

Sections 4.1, 4.3: A. L. Nichols from the UKAEA, who provided assistance in preparing these sections and in reviewing the report. T. J. Haste, S. R. Kinnersly, and D. A. Williams from the UKAEA, who provided report review assistance. Finally, the U.K. Health and Safety Executive for funding the AEA involvement in preparing this report.

Section 4.4: Y. Waaranpera from the ABB/Sweden, J. Sugimoto from JAERI, F. Parozzi from the ENEL/Italy, D. A. Williams from the UKAEA, L. Kmetyk from the SNL/USA, and E. Hontañon from the JRC in Ispra/Italy. J. L. Cheissoux and M. Granga from CEA/IPSN-Cadarache for assistance in preparing and reviewing this section.

Section 4.5: D A. Williams from the UKAEA, F. Parozzi from the ENEL/Italy, and L. Kmetyk from the SNL/USA for providing report copies and answering many questions. J. Jokiniemi from VTT Finland for providing report comments.

We would in addition like to acknowledge A. Mailliat, P. Dumaz, and V. Layly from the CEA/IPSN for their participation in the Cadarache writing group meeting, and J. C. Crestia from the CEA/IPSN for participation in the Bethesda writing group meeting. We would also like to acknowledge Carolyn Pollard, Judith Hickman, and Diana Love, who are secretaries in the ORNL Engineering Technology Division (ETD); they provided excellent support in preparing the draft versions and portions of the final version of this report. We thank members of the ETD Word Processing center for preparing the tables in the report. Finally, we sincerely appreciate the assistance provided by members of the ORNL Engineering Technology/Fusion Energy Division Publications Office; they did an exceptional job of preparing the final version of this report.

1 Introduction

1.1 Report Objectives and Scope

The objective of this report is to present the status of research activities associated with fission product behavior (release and transport) within the primary systems of water-moderated and water-cooled reactors. This category of reactors includes pressurized-water reactors (PWRs), boiling-water reactors (BWRs), and Canadian deuterium-uranium (CANDU) reactors. The report has been prepared at the request of the Nuclear Energy Agency (NEA) of the Organization for Economic Cooperation and Development (OECD) Committee on the Safety of Nuclear Installations (CSNI), and the U.S. Nuclear Regulatory Commission (U.S. NRC). It summarizes relevant information on important phenomena, computer models and codes, experiments, and comparisons of calculations with experiments. Implications of the information assessed in the report are discussed, and areas for future work by the Principal Working Group 2 (PWG-2) task group are suggested.

Developing an improved understanding of primary system fission product release and transport is important to permit realistic estimates of reactor accident source terms to be made. Fission product release and transport in the primary system play three major roles in the determination of reactor accident source terms:

1. release from fuel defines a significant component of the potential containment source term,

2. the primary system can act as a "reaction chamber" that can chemically and physically condition the vapors/aerosols released to containment, and

3. there can be significant fission product vapor/aerosol retention in the primary system.

This report provides a complete overview of fission product release and transport in the primary system. The report considers in-vessel release and transport up to the reactor coolant system (RCS) pressure boundary and so excludes molten-core-concrete interactions, containment fission product behavior, and pool scrubbing phenomena. It discusses areas where, in our opinion, substantial progress has been made in understanding fission product release and transport phenomena. It also identifies areas where additional information is needed. The report covers material that has been documented up to January 1993. At the end of each report section, references are provided so that readers can readily obtain more information on selected topics.

1.2 Background

Studies of primary system fission product release and transport in support of reactor accident source term analysis did not really play an important role until after the Three-Mile Island Unit-2 (TMI-2) accident in 1979. Before 1979, little account for the influence of primary system phenomena on source terms was assumed. In the United States, the document TID-14844 (Ref. 1) provided a set of assumptions for estimating consequences of maximum credible accident for reactor site suitability purposes. The assumed TID-14844 source term to containment was 100% of the core noble gases, 50% of the core halogens (iodine assumed to be predominantly be I_2), and 1% of the solid fission products. It was acknowledged in TID-14844 that this was an approximate and perhaps poor source term estimate but that the state of the art at that time did not support a better one.

The 1974 Reactor Safety Study (WASH-1400)[2] was the first systematic attempt to estimate source terms for nuclear accidents that might lead to core melt. However, again because of the state of the art at that time, the assumptions on primary system fission product release and transport used in WASH-1400 were not realistic; for example, no primary system radionuclide retention was assumed in most of the evaluated accident sequences. A few years after WASH-1400, the German Risk Study (Phase A) was completed.[3] This study was performed for a representative 1300-MW(e) German PWR and relied on many of the assumptions and methods used in WASH-1400. Despite differences in U.S. and German plants, many of the insights from the German study were in agreement with WASH-1400.

The extremely low radionuclide releases that occurred in the 1979 TMI-2 accident led to significant international efforts to reassess the technical bases for estimating reactor source terms from severe accidents. It became evident from these assessments that phenomena associated with primary system fission product release and transport—including fission product vapor/aerosol chemistry and vapor/aerosol retention—had been ignored in the past and that these phenomena played a major role in the realistic estimation of accident source terms. Major international activities related to source term reassessment subsequent to the TMI-2 accident have included the following:

- In 1980, the NRC reviewed the state of the art for estimating fission product behavior in severe reactor accidents. This was a response to questions on the

adequacy of the WASH-1400 study in light of results from the TMI-2 accident. This report, "Technical Bases for Estimating Fission Product Behavior During LWR Accidents,"[4] NUREG-0772, set the basis for future NRC work to develop capabilities to perform realistic source term assessments.

- United Kingdom activities on source term estimates performed in the early 1980s included the Sizewell-B source term study[5] and the Phase-1 and Phase-2 PWR Severe Accident Containment Studies.[6,7] "Primary System Material Transport and Deposition" were among the important phenomena evaluated in the Phase-1 and Phase-2 reports.

- The NRC funded a source term study at Battelle Columbus Laboratories that led to preparation in 1983 of the BMI-2104 series of reports.[8] This study involved development of the "Source Term Code Package" (STCP), which couples a number of severe accident codes to permit detailed calculations of source terms. The original version of the STCP uses the CORSOR model to calculate fission product release from fuel and the TRAP-MELT2 code to calculate primary system fission product transport.

- The U.S. Industry Degraded Core Rulemaking (IDCOR) Program* completed in 1984 a significant nuclear industry effort to perform source term calculations for severe accidents. As part of this program, the integrated Modular Accident Analysis Program (MAAP) computer code was developed.

- In 1986 the NRC reassessed of the technical basis for estimating U.S. LWR source terms; this resulted in preparation of the NUREG-0956, "Reassessment of the Technical Bases for Estimating Source Terms."[9] This reassessment involved reviewing experimental and analytical results—with a major emphasis on the STCP and the calculations performed in the BMI-2104 study—from the severe accident research programs that were emphasized after the TMI-2 accident.

- The results of the European shared cost action were published in 1988.† This study was devoted to reactor accident sequence calculations in support of the Phebus-FP project, with the objective of identifying the phenomena that dominate fission-product release, transport, and deposition mechanisms in given accident sequences.

- The German Risk Study, Phase B, published in 1989 (Ref. 10), focused on the assessment of systems, techniques, and plant technology aspects for a German Standard PWR. Selected accident sequences were analyzed using STCP codes such as MARCH3 and TRAP-MELT3.

- More recently there have been significant efforts to use improved understandings of severe accident behavior to update source term and risk assessments for reactor accidents. These efforts include the NUREG-1150 report,[11] which provides an updated risk assessment for five U.S. nuclear power plants; an effort by the NRC to define a revised accident source term (compared with that from TID-14844) for regulatory application for future LWRs;[12] and a U.S. industry effort to develop a "physically based source term" for use in advanced LWRs.[13] All of these efforts have benefitted from improved understanding of primary system behavior.

Improvements in understanding the behavior of fission product vapors and aerosols in the primary system have resulted from the following activities:

1. the performance of separate effects experiments to study relevant phenomena and to develop computer code models,

2. the continued development and evaluation of computer codes to predict primary system behavior, and

3. the performance of large-scale tests to investigate integrated phenomena and to evaluate computer code performance.

Some of these efforts are briefly summarized:

- Development of primary system release and transport computer codes in the United States, Europe, and Japan relies heavily on separate effects tests to define relevant phenomena and provide code model parameters. Separate effects studies on fission product release, fission product chemical behavior, and aerosol and vapor transport have been and are being performed throughout the world. These studies are discussed in Chaps. 3 and 4.

- Important large-scale primary system release and transport experiments include the Marviken Aerosol Transport Tests; the Light Water Reactor (LWR) Aerosol Containment Experiments (LACE); the OECD Loss of Fluid Test (LOFT) FP1 and FP2 tests; the NRC Severe Fuel Damage (SFD) tests; the NRC HI, VI, and ACRR-ST tests; and the forthcoming French Phebus-FP release and transport tests. These are also discussed in Chaps. 3 and 4.

*Technology for Energy Corporation, "IDCOR Technical Summary Report: Nuclear Power Plant Response to Severe Accidents," Atomic Industrial Forum, November 1984.

†A. Mailliat, "Comparison of Phase A Studies, Phebus-FP Shared Cost Action," IPSN/DRS/SEMAR (March 1988).

- In the area of primary system release and transport code development, there have been efforts to develop and/or improve code models, to identify code differences by performing code-to-code comparisons, and to compare code results with those produced in large-scale experiments. Numerous code comparison exercises have been performed (particularly on fission product transport behavior) and international groups of analysts have participated.

International collaboration on defining and developing research programs; defining conditions for important experiments; and exercising, comparing, and evaluating computer codes has played a major role in developing an improved understanding of fission product behavior in the primary system. International collaboration activities have been important because: (1) in many cases, experimental conditions have been determined based on the expert advice of the international participants; (2) for many of the large-scale tests, code-comparison activities led to significant improvements in the release and transport codes; and (3) support for the large-scale tests in many cases included performance of small-scale support tests that enhanced the knowledge base on release and transport phenomena.

Some of the more important ongoing collaboration efforts include the NRC Cooperative Severe Accident Research Program (CSARP), the ongoing European Reinforced Concerted Effort (RCA) on source terms (being performed to achieve consensus in Europe on key areas of agreement and uncertainty affecting the source term), the Commission of the European Communities (CEC)/French Commissariat à l' Energie Atomique (CEA) international collaboration effort on the Phebus-FP experiments,[14] and NEA/OECD/CSNI-sponsored efforts on fission product behavior and source terms.

The CSNI has been active for a number of years in evaluating source term technology development. In 1979, a group of experts prepared a state-of-the-art report on nuclear aerosols in reactor safety,* and in 1985 a supplemental report was prepared that discussed further relevant aerosol information.† In addition, a 1987 CSNI report on "Selected Source Term Topics" contained information on fission product release from fuel, fission product chemistry in the RCS, and aerosol resuspension phenomena.[15] The CSNI has also sponsored two specialist meetings, in 1980 in Gatlinburg, Tennessee,[16] and in 1984 in Karlsruhe, Federal Republic of Germany,[17] dedicated specifically to evaluating the role of aerosol behavior in nuclear reactor safety. The CSNI has also recently sponsored an International Standards Problem (ISP) (ISP-34) related to the U.K. Falcon test program; this ISP deals with fission product transport in the RCS under severe accident conditions.

Although the Chernobyl Unit-4 reactor accident in 1986 was certainly the most significant severe accident that has occurred to date, the source term from that accident has little relevance to LWR severe accident source terms. However, the accident did lead to some efforts by the technical community to evaluate the chemical and physical nature of the fission products released.

A number of major international meetings have included a significant emphasis on primary system fission product release and transport. Some of the most important of these meetings were the ANS Topical Meeting on Fission Product Behavior and Source Term Research[18] (1984), the IAEA Symposium on Source Term Evaluation for Accident Conditions[19] (1985), the Water-Cooled Reactor Aerosol Code Evaluation and Uncertainty Workshop[20] (1988), the Workshop on Chemical Processes and Products in Severe Nuclear Reactor Accidents[21] (1988), the IAEA Severe Accident Symposium[22] (1988), the International Seminar on Fission Product Transport Processes in Reactor Accidents[23] (1989), and the OECD/CSNI Containment Aerosol and Thermal Hydraulic Behavior meeting in Fontenay-aux-Roses (1990).‡

The net result of all of the activities just briefly discussed has been a significant effort to improve capabilities for assessing primary system fission product release and transport in severe reactor accidents. The remainder of this report presents in some detail a summary of the state of the art in this area. Chapter 2 presents a discussion of overall accident sequence phenomena and system boundary conditions that are expected to have a major influence on primary system fission product and core material release and transport. Chapter 3 presents a discussion of the major phenomena, experiments, computer codes/models, and code-to-data comparisons performed in the area of in-vessel fission product and core material release. Chapter 4 presents a similar discussion for the area of primary system fission product transport. Finally, Chap. 5 summarizes the main conclusions from the studies documented in Chaps. 3 and 4 and presents a list of recommendations for future work in this area.

*"Nuclear Aerosols in Reactor Safety, A State-of-the-Art Report by a Group of Experts of the CSNI," NEA, OECD (1979).

†"Nuclear Aerosols in Reactor Safety, Supplementary Report," NEA, OECD (1985).

‡OECD/CSNI, Workshop on Aerosol Behavior and Thermal Hydraulics in the Containment, Fontenay-aux-Roses, France, November 1990.

1.3 References

1. J. J. DiNunno et al., "Calculation of Distance Factors for Power and Test Reactor Sites," TID-14844, U.S. Atomic Energy Commission, March 1962.

2. U.S. Nuclear Regulatory Commission, "The Reactor Safety Study: An Assessment of Accident Risk in U.S. Commercial Nuclear Power Plants," USNRC Report NUREG 75/014 (WASH-1400), October 1975.*

3. The Federal Minister of Research and Technology, *The German Risk Study—Summary*, Gesellschaft für Reaktorsicherheit, Köln (August 15, 1979).

4. U.S. Nuclear Regulatory Commission, "Technical Bases for Estimating Fission Product Behavior During LWR Accidents," USNRC Report NUREG-0772, June 1981.*

5. M. R. Hayns et al., "The Technical Basis of 'Spectral Source Terms' for Assessing Uncertainties in Fission Product Release During Accidents in PWRs with Special Reference to Sizewell-B," Atomic Energy Authority, SRD-R-256, United Kingdom (November 1982).

6. A. T. D. Butland et al., "Report on Phase 1 of the PWR Severe Accident Containment Study," Atomic Energy Authority, AEEW-R 1842, United Kingdom (December 1984).

7. A. T. D. Butland et al., "Report on Phase 2 of the PWR Severe Accident Containment Study," Atomic Energy Authority, AEEW-R1964, United Kingdom (April 1986).

8. J. A. Gieseke et al., Battelle Memorial Laboratories, "Radionuclide Release Under Specific LWR Accident Conditions," BMI-2104, Vols. I–VII, 1983.*

9. M. Silberberg et al., "Reassessment of the Technical Bases for Estimating Source Terms," USNRC Report NUREG-0956, July 1986.*

10. "German Risk Study Nuclear Power Plants, Phase B, A Summary," Gesellschaft für Reaktorsicherheit mbH, GRS-74, Köln (June 1990).

11. U.S. Nuclear Regulatory Commission, "Severe Accident Risks: An Assessment for Five U.S. Nuclear Power Plants," USNRC Report NUREG-1150, December 1990.*

12. L. Soffer et al., *Accident Source Terms for Light-Water Nuclear Power Plants*, USNRC Draft Report NUREG-1465, June 1992.*

13. D. E. Leaver et al., "Passive ALWR Source Term," EG&G Idaho, DOE/ID-10321, February 1991.

14. W. Krischer and M. C. Rubinstein, Eds., *THE PHEBUS FISSION PRODUCT PROJECT: Presentation of the Experimental Programme and Test Facility* (Elsevier Applied Science, 1992).

15. P. N. Clough and F. Abbey, "Selected Source Term Topics, Report to the CSNI by an OECD/NEA Group of Experts," Committee on Safety of Nuclear Installations Report 136, France (April 1987).

16. T. S. Kress, Ed., *Proceedings of the CSNI Specialist's Meeting on Nuclear Aerosols in Reactor Safety, Gatlinburg, Tenn.*, USNRC Report ORNL/NUREG/TM-404 (CSNI-45), 1980.*

17. W. O. Schikarski and W. Schock, Eds., *Proceedings of the CSNI Specialists' Meeting on Nuclear Aerosols in Reactor Safety*, Kernforschungszentrum Karlsruhe, KfK-3800/CSNI-95, Germany (1985).

18. *Proceedings of the ANS Topical Meeting of Fission Product Behavior and Source Term Research, Snowbird, Utah, July 1984*, Electric Power Research Institute, NP-4113-SR, July 1985.†

19. *Proceedings of the Symposium on Source Term Evaluation for Accident Conditions, Columbus, Ohio, October 1985*, International Atomic Energy Agency, IAEA-SM-281, Austria (1986).†

20. E. della Loggia and J. Royen, Eds., *Proceedings of the Water-Cooled Reactor Aerosol Code Evaluation and Uncertainty Assessment Workshop*, CEC/OECD Nuclear Science and Technology, EUR 11351 EN (1988).

21. *Chemical Processes and Products in Severe Nuclear Reactor Accidents-Report of a Workshop* (National Academy Press, 1988).

22. *Proceedings of Symposium on Severe Accidents in Nuclear Power Plants, Sorrento, Italy,* International Atomic Energy Agency, IAEA-SM-296, Austria (March 1988).

23. J. T. Rogers, Ed., "Fission Product Transport Processes in Reactor Accidents," *Proceedings of ICHMT Seminar, Dubrovnik, Yugoslavia, May 1989* (Hemisphere Publishing Corporation, 1990).

---

*Available for purchase from the National Technical Information Service, Springfield, VA 22161.
†Available in public technical libraries.

2 Accident Sequence Phenomena and Boundary Conditions

2.1 Introduction

The objective of this chapter is to define representative severe accident sequences, and the associated core and reactor coolant system (RCS) boundary conditions, affecting the release and transport of fission products and core materials in Western type water reactors.

The accident sequence core and RCS boundary conditions and phenomena are major determinants of the ultimate fission product release and transport from the RCS to the containment. However, it is not the purpose of this report to assess the state of the art of degraded core behavior. Rather, this was accomplished in an earlier Nuclear Energy Agency (NEA)/Committee on the Safety of Nuclear Installations (CSNI) report.[1] Thus, this chapter provides the framework for subsequent chapters by giving realistic boundary conditions to be expected in severe accident sequences.

2.2 Plant Types and Initial Conditions

The plant types considered in this chapter are those with reactors that are uranium dioxide (UO_2) fueled, and light water moderated and cooled. This includes light water reactors (LWRs), that is, pressurized-water reactors (PWRs) and boiling-water reactors (BWRs) of U.S. and European origin for which information is readily available. The primary rationale for this choice is that it includes plants designed, built, and operated by Organization for Economic Cooperation and Development (OECD) member countries. Furthermore, over the next 10 to 20 years, most of the new plants are likely to be LWRs. Advanced design plants are not explicitly discussed in this report, although advanced light water reactors (ALWRs), including passive plants, would be expected to have RCS accident boundary conditions similar to low-pressure sequences for existing LWRs. While fission product release and transport for Canadian deuterium-uranium (CANDU) reactors are considered in Chaps. 3 and 4, the Chap. 2 discussion of accident sequences is limited to LWRs.

The information for the boundary conditions comes from several sources: work done in support of the U.S. Nuclear Regulatory Commission (NRC) sponsored risk analysis of five U.S. plants;[2] the Phebus-FP Phase A studies* and related analysis performed within the Commission of the European Communities (CEC) programs (i.e., the Shared Cost and the Reinforced Concerted Action) on nuclear safety; the German Risk Study, Phase B;[3] and recent analyses using the Modular Accident Analysis Program (MAAP) code, which is the accident analysis tool being used for individual plant examinations (IPEs) for operating plants in the United States. While several analyses of this type have been and are being produced, including a limited number of new analyses with the MELCOR code,[4] the ones noted are considered to be representative and sufficient for the objective of this study.

2.2.1 PWR Initial Conditions

Many families of PWRs exist even within the same supplier. Sizes range from the single loop 510-MW(t) Zorita plant in Spain to large four-loop 3570-MW(t) units, such as the Sequoyah plant in the United States. Despite such differences, which are mainly reflected in the fission product and core material inventories, there are not substantial differences in the basic nuclear and thermal-hydraulic parameters. Table 2.1, taken from various sources, reflects such differences for representative plants.

Table 2.2 gives the amounts and properties of the structural materials in a typical PWR core.[5] The initial fission product inventories for the end of an equilibrium cycle in a typical PWR [the 2441-MW(t) Surry plant] are given in Table 2.3. These inventories are based on the ORIGEN code and are reproduced from Ref. 6. The fission product inventories are generally in proportion to reactor thermal power, other conditions such as fuel burnup being equal. Table 2.3 also includes melting points, boiling points, and vapor pressures for the most important fission product forms expected in reactor accidents.

2.2.2 BWR Initial Conditions

There also exist many families of BWRs that range from the small 150-MW(t) Dodewaard plant in the Netherlands to the large 3833-MW(t) Grand Gulf station in the United States.

Table 2.4 gives the basic nuclear and thermal parameters, taken from different sources, for some prototypical BWRs. Table 2.3 gives the fuel fission product and actinide inventories for a 3293-MW(t) GE-BWR, at the end-of-cycle equilibrium core, calculated by ORIGEN.

*A. Mailliat, "Comparison of Phase A Studies Phebus-FP Shared Cost Action, Part A: Reactor Coolant System," ISPN/DRS/SEMAR (March 1988).

Accident

Table 2.1 Typical PWR core and RCS parameters

Reactor model	Thermal power [MW(t)]	Nominal pressure (MPa)	Inlet temperature (°C)	Outlet temperature (°C)	Power density (kW/L)
W-3LOOP	2696	15.5	291	326	101
W-4LOOP	3411	15.5	291	326	86
KWU-3LOOP	3010	15.5	293	326	93
KWU-4LOOP	3765	15.8	293	326	93
FRAMATOME-N325	3200	15.5	290	323	98
FRAMATOME-P4	3800	15.5	292	323	100
FRAMATOME-N4	4250	15.5	292	323	105

2.3 Degraded Core Accident Sequence Description

In NUREG-1150, severe accident sequences have been defined for internal initiators leading to core damage and fission product release and transport.[2] Although there are differences among the plants analyzed, the dominant sequences tend to be the same; differences appear mainly in their expected frequencies and uncertainties. In Table 2.5 the dominant accident groups, each one including similar sequences, are identified for PWRs and in Table 2.6 for BWRs. Sequence frequencies provide perspective for the reader on the relative likelihood of various sequence types and the fact that any core damage sequence is very unlikely.

Because the scope of this state-of-the-art assessment is confined to the RCS, only accident sequence conditions up to the RCS boundary are considered. Thus, ex-vessel debris coolability, core concrete interaction, and containment thermal-hydraulic conditions are not addressed. Similarly, fission product transport is not considered in systems beyond the RCS boundary [e.g., secondary side of steam generators in steam generator tube rupture (SGTR) and systems interfacing with the RCS in interfacing loss of coolant accidents (LOCAs)].

2.3.1 PWR Accident Sequences

Station blackout sequences are initiated by a loss of offsite power (LOSP). With safety systems functioning normally, the LOSP would result in reactor trip, emergency diesel actuation, and decay heat removal via the secondary side. However, in station blackout sequences, the emergency diesels fail, leading to a loss of the injection and cooling to the reactor coolant pumps seals, creating a small LOCA. Failure of the auxiliary feedwater causes a pressure increase with the opening of the relief valves, which may not close, also producing a LOCA. Because the safety injection systems are inoperable due to the lack of ac power, core damage will result.

Transient sequences can be initiated by a number of events that result in a reactor trip. Additional failures leading to loss of decay heat removal would be required to cause core damage. Transients tend to lead to similar RCS conditions (e.g., high pressure) as station blackouts.

Within the class of LOCAs in PWRs, various sequences are evaluated including large, intermediate, and small breaks with failure of the emergency core cooling systems (ECCSs). Only passive accumulators are assumed to be operational. These sequences lead to core degradation at different times, depending on the location and size of the break.

Small LOCAs are associated with RCS ruptures with blowdown rates equivalent to double-ended circumferential breaks in pipes <5 cm in diameter. The RCS pressure tends to remain high, and a reactor trip is assumed. As the break size is insufficient to provide core cooling, even with high-pressure injection, decay heat removal through the secondary side or through primary feed and bleed is necessary. Moreover, long-term cooling must be provided for. The failure to accomplish high-pressure injection or the decay heat removal function will produce core damage.

Intermediate LOCAs are associated with RCS ruptures and flow through open valves with blowdown rates equivalent to double-ended circumferential breaks between 5 and

Table 2.2 Amounts and properties of structural materials in a PWR core

Material	Components		Aerosol species			
	Element	Weight (kg)	Possible form	MP (°C)	BP (°C)	Vp at 2400°C (Pa)
Control rod	Ag	2.260	Ag	961	2210	2.5×10^5
	In	425	In	156	2080	4.5×10^5
			In_2O_3		850	
	Cd	142	Cd	321	765	$\sim 8.5 \times 10^7$
			$Cd(OH)_2$	d 300[a]		
			CdO	≥1500	d 1000	
Boric acid	B	120[b]	H_3BO_3	169→HBO_2		
			HBO_2	300→B_2O_3		
			B_2O_3	450	1860	9.0×10^5
Borosilicate glass	B	82				
	Si	64	SiO_2	1700	2230	8.0×10^4
Zircaloy-4	Zr	16.200	Zr	1852	4380	2
			ZrO_2	2700	~5000	
	Sn	240	Sn	232	2270	1.5×10^5
Stainless steel	Fe	1.360	Fe	1535	2750	2.0×10^4
			FeO	1370		
			Fe_2O_3	1565		
			Fe_3O_4	1595		
	Cr	380	Cr	1860	2670	6.0×10^4
			Cr_2O_3	2270	4000	
	Ni	200	Ni	1455	2730	1.0×10^4
			NiO	1984		
	Mn	40	Mn	1244	1962	4.1×10^5
			MnO			
			Mn_2O_3	~0.1080		
			Mn_3O_4	1564		
Urania fuel	U	10^3	UO_2	2880		2.0×10^2

[a] d = decomposes.
[b] Boric acid present in primary circuit cooling water only (in a severe accident a maximum of 39 tonnes of boric acid could be delivered to the core).
Source: Ref. 7.

Table 2.3 Amounts and properties of fuel and fission products in a core

Constituent	Amount[a] PWR (mol)	Amount[a] BWR (mol)	Mol fraction in phase[b]	Evaporating material Form	Melting point (°C)	Boiling point (°C)	Temperature = 2700 K (2427°C) Vapor pressure (bar)	Effective vapor pressure[c] (bar)	Maximum pressure[d] (bar) PWR	Maximum pressure[d] (bar) BWR
				Semivolatiles						
I, Br	146	308		I_2	114	183	High	[e]	0.059	0.12
Cs, Rb	1624	3222		Cs	29	700	High	[e]	0.65	1.4
Te	253	533		Te	450	998	High	[e]	0.10	0.21
				Oxide fuel matrix						
U	2.95×10^5	6.22×10^5	0.97	UO_2	2830		0.002	0.002	118.0	249.0
Ba, Sr	1279	2696	0.0042	BaO	1920	(2750)	3.2	0.014	0.51	1.08
Rare earths	4471	9421	0.015	La_2O_3	2320		0.06	1×10^{-3}	1.78	3.74
Zr, Nb	2402	5060	0.0089	ZrO_2	2720	(4300)	Low	Low	1.09	2.29
				Noble metal inclusions						
Mo	2179	4591	0.39	Metal	2610	5560	5.3×10^{-6}	2.1×10^{-6}	0.87	1.8
Ru	1527	3323	0.28	Metal	2500	4900	2.3×10^{-5}	6.4×10^{-6}	0.63	1.3
Pd	914	1927	0.16	Metal	1552	3980	0.076	0.012	0.37	0.77
Tc	518	1091	0.095	Metal	2200		1×10^{-4}	9.5×10^{-6}	0.21	0.44
Rh	296	624	0.053	Metal	1966	4500	5.3×10^{-4}	2.8×10^{-5}	0.12	0.25
Ag	58	122	0.010	Metal	961	2210	2.42	0.024	0.023	0.049

[a]Quantities of fission products are based on an ORIGEN calculation for the Browns Ferry BWR at essentially infinite time at initial unloading. The differences between a PWR and a BWR are simply the differences in core fuel mass.

[b]In assumed phases: phase 1 (UO_2-La_2O_3-BaO-ZrO_2); phase 2 (noble metals).

[c]Vapor pressure times mol fraction in phase.

[d]Pressure exerted if completely vaporized within confines of pressure vessel, all at 2700 K. A volume of 548 m^3 (BWR) was used for both PWR and BWR calculations even though the PWR will have a smaller volume.

[e]Completely vaporized.

Source: Ref. 6.

Table 2.4 Typical BWR core and RCS parameters

Reactor model	Thermal power [MW(t)]	Nominal pressure (MPa)	Inlet temperature (°C)	Outlet temperature (°C)	Specific power (W/gU)
GE-BWR 4	1381	7.1	183	287	40.6
GE-BWR 6	2894	7.3	214	288	52.4
KWU-BWR 69	1912	7.1	190	285	50.6
KWU-BWR 72	2575	7.1	215	286	51.1
ASEA-BWR	1700	7.0	180	286	22.9
ASEA-BWR 75	3000	7.0	215	286	24.6

Table 2.5 Expected frequency of PWR accident groups from internal events contributing to core damage, mean values in year^{-1}

Accident group	Surry	Sequoyah	Zion
Station blackout	2.7×10^{-5}	1.5×10^{-5}	6.3×10^{-6}
Transients	3.7×10^{-6}	4.4×10^{-6}	1.0×10^{-5}
LOCAs	6.0×10^{-6}	3.6×10^{-5}	3.0×10^{-4}
Interfacing LOCAs and SGTR	3.4×10^{-6}	2.3×10^{-6}	1.5×10^{-6}

Source: Ref. 2.

Table 2.6 Expected frequency of BWR accident groups from internal events contributing to core damage, mean values in year^{-1}

Accident group	Peach Bottom	Grand Gulf
Station blackout	2.2×10^{-6}	4.0×10^{-6}
ATWS	1.9×10^{-6}	1.1×10^{-7}
LOCAs	2.6×10^{-7}	
Transients	1.4×10^{-7}	

Source: Ref. 2.

15 cm in diameter; **large LOCAs** are beyond that size. In this presentation only large breaks are considered because the severe accident phenomenology is similar to that of intermediate breaks.

Large and intermediate breaks cause a rapid coolant blowdown, lasting seconds to minutes. The rapid depressurization causes the reactor shutdown, which is later maintained by injecting borated water. The decay heat removal function must be assured, which requires the correct actuation of the low-pressure systems and systems for the containment cooling function. If such safety functions are not accomplished, core damage will occur.

SGTR and interfacing LOCA sequences will generally have RCS conditions that are bounded by the sequences previously discussed and, as noted previously, are not within the scope of this report.

2.3.2 BWR Accident Sequences

A BWR **station blackout** begins with a turbine trip followed by the loss of all ac power. The reactor is shutdown, and it can be depressurized, but the removal of decay power can only be accomplished with passive systems, such as isolation condensers or high-pressure injection systems operating with turbine-driven pumps. Nevertheless, the former can only provide cooling if there is water in the secondary side, and the latter depends on station dc power. If such systems become depleted before ac power is restored, core damage occurs.

Transients, including anticipated transient without scram (ATWS), require the intervention of operators to depressurize the system, manually scram the reactor, or actuate the secondary shutdown system, that is, the standby liquid control system. Core damage occurs relatively rapidly, ~15 min, if the reactor cannot be made subcritical; otherwise the time to core melt will depend upon the success or failure of the decay heat removal systems.

Several BWR ATWS sequences could be considered, involving various combinations of failure to shut down the reactor through manual scram and the secondary shutdown system. If shutdown is achieved by the secondary shutdown system, but the vessel is not manually depressurized, then the high-pressure injection system may take decay heat out to the suppression pool, which is assumed not to be cooled. This produces failure of the high-pressure system, and core damage results.

If shutdown is not achieved and there is a stuck open relieve valve, then the outcome of the process will depend on the extent to which the core is cooled with the low-pressure injection and recirculation systems.

LOCAs tend to be lower frequency in BWRs due to the lower coolant pressure, the existence of jet pumps in some designs, and larger redundancies in the ECCSs, active and sometimes passive, plus the possibility of automatic or manual depressurization. The average time to core failure will be between 1 to 2 h.

2.3.3 Degraded Core Accident Progression Phenomena

Accidents that lead to core damage can result from a number of different types of event sequences as described earlier. However, all of these core damage accidents have certain common chemical and physical phenomena affecting fission product release and transport.

These chemical and physical phenomena are briefly described in their approximate order of occurrence in a degraded core accident. More detailed information on these phenomena can be found in Refs. 6–9.

After the core is uncovered, heat transfer from the fuel to the steam is low compared to decay heat, and the fuel temperature increases. This in turn leads to oxidation of the Zircaloy fuel cladding and hydrogen generation and can also lead to clad ballooning.

While the effect of clad ballooning and rupture on accident progression is uncertain in severe accident analysis, calculations indicate that ballooning may reduce natural circulation flows between the core and upper plenum, causing reduced heat transfer and therefore more rapid heatup of the core.[10]

Zircaloy cladding oxidation by steam causes acceleration of the core heatup rate and increases the melting temperature of the debris. Heatup rate due to decay heat alone is in the range of 0.4 to 1.0 K/s, depending on the location in the core and the particular accident sequence, and can increase to well above 1 K/s as the local temperature increases above ~1300 K due to rapid oxidation of Zircaloy and the strongly exothermic nature of the reaction. Oxidation of Zircaloy increases its melting temperature, and high oxygen content in molten Zircaloy limits UO_2 dissolution.[11]

The core melt and initial relocation portion of accident progression encompasses low-temperature materials interaction, metallic blockage, UO_2 liquefaction, and molten pool formation. Temperatures of various core damage phenomena are shown in Fig. 2.1 (Ref. 12).

Core melt progression is initiated as a result of eutectic reactions of core materials at temperatures well below the melting temperatures of the fuel and its cladding. These reactions involve control rods, burnable poison rods, clad, and structural materials forming relatively low temperature liquid phases.[1] PWR control rod material (Ag-In-Cd) is molten at ~1100 K (Ref. 13), and the molten Ag-In-Cd alloy will chemically dissolve Zircaloy. However, due to chemical compatibility of Ag-In-Cd with its stainless steel clad, control rod failure would not be expected to occur until about 1500 K for low-pressure sequences and 1700 K for high-pressure sequences.[14] In BWRs, the major low-temperature reaction is between the BWR control material, boron carbide (B_4C) and stainless steel, at about 1500 K (Ref. 1).

Metallic melts generated by these low-temperature interactions flow downward in the core until they reach cooler

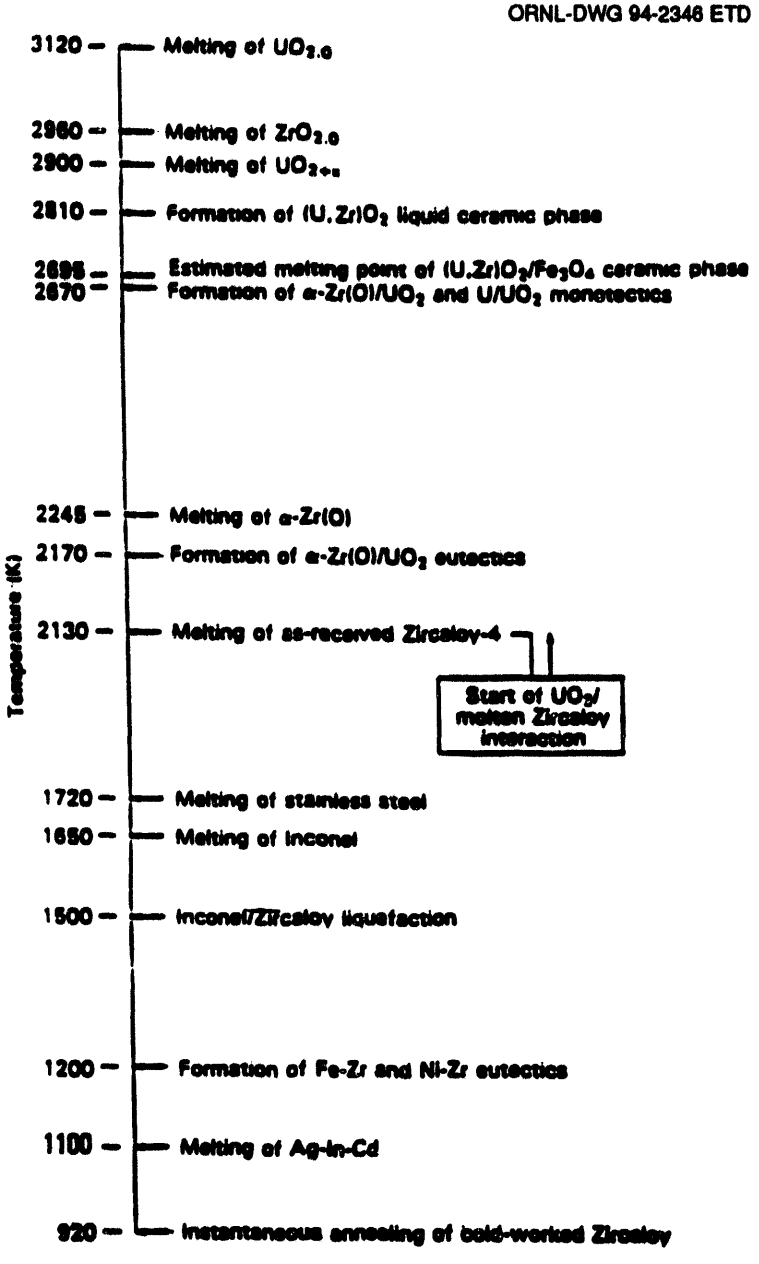

Figure 2.1 Temperature of core damage phenomena (based on Ref. 12)

locations where the melts tend to solidify, forming partial blockages in the flow channels between fuel rods, particularly in PWRs. (Due to lower steaming rates and potentially higher temperatures in the lower part of the core, metallic melt can drain out of the core in BWRs).[8] The metallic blockages can restrict flow and cause accelerated heatup of the core. UO_2 fuel can be liquefied at temperatures well below its melting point (3100 K) by dissolution in molten Zircaloy (melting point ~2200 K, depending upon oxygen content). This can lead to a primarily ceramic blockage at a higher elevation in the core than the metallic blockage due to the higher freezing temperature (up to ~2800 K) of the primarily ceramic $(U,Zr)O_2$ melt.[7]

As a result of diversion of steam around the blockage and the low thermal conductivity of the ceramic material, heat transfer from the ceramic blockage is slow, and a molten pool can form within a ceramic crust. This has been observed to some extent in integral experiments that were run to lesser damage levels and to a significant extent in the Three Mile Island Unit-2 (TMI-2) accident. Lower melting point structural and other materials resistant to oxidation (e.g., nickel and silver) have been observed in the $(U,Zr)O_2$ ceramic melt.

The oxidation potential within molten pools has been estimated from measurements of the chemical forms (metals compared to oxides) within the melt.[7] Examination of the TMI-2 debris and in-pile tests indicates the presence of oxides of iron and chromium, both metallic and oxidized forms of nickel and indium, and metallic antimony. Application of these observations to the Fig. 2.2 plot of the free energies of formation of core material oxides vs temperature indicates that the oxygen potential is fairly high,

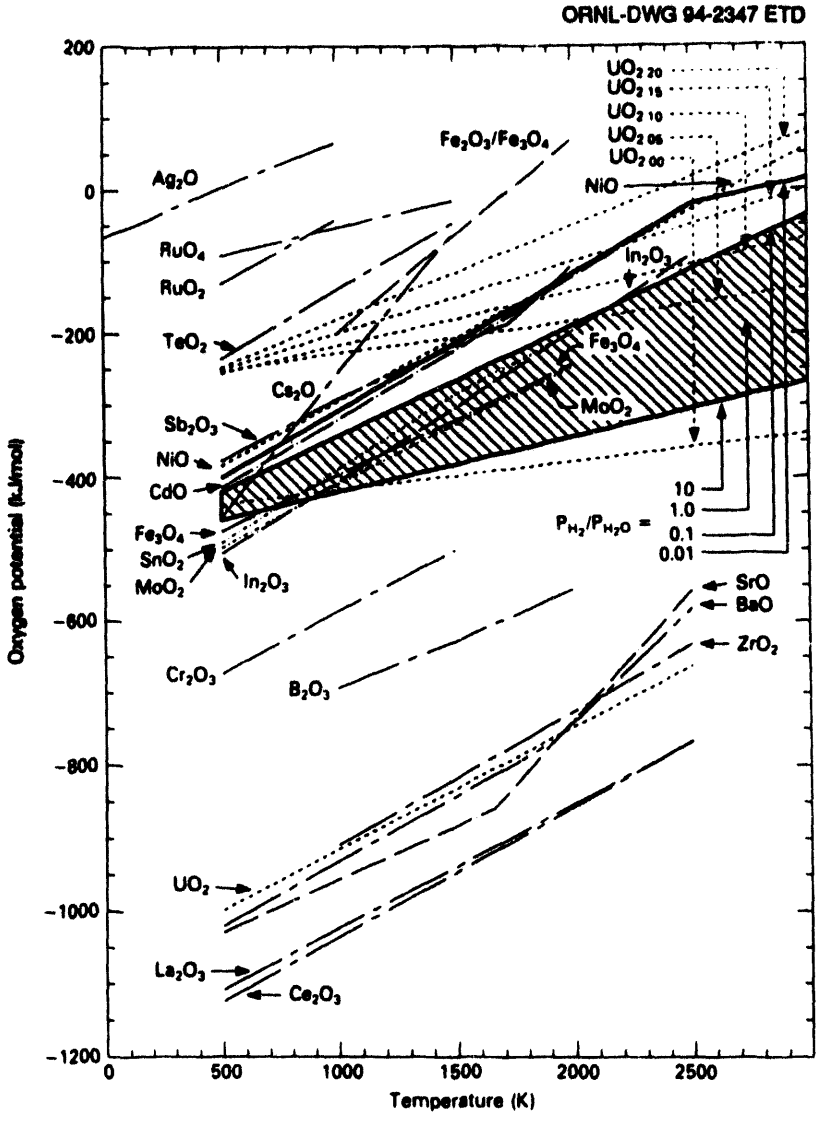

Figure 2.2 Free energies of formation in core material oxide

that is, in the range of –120 to +20 kJ/mol at 2800 K. As indicated in Fig. 2.2, this is the expected range of oxidation potential for hydrogen-to-steam partial pressure ratios of the order of 0.01 to 1 and is indicative of oxidizing conditions. This is the range predicted for bulk gas flows in LWR degraded core accidents.

A steam-starved environment can cause higher hydrogen-to-steam partial pressure ratios, which can result in reducing conditions. However, steam starvation over large volumes of the core is inconsistent with experience (i.e., the noncoherent nature of core melt progression and the large amounts of water that would still be present at this stage of the accident). Further, reducing conditions are not expected for extended periods of time because the duration of steam starvation is likely to be limited. Thus, such conditions should not have a major effect on fission product speciation.

Crust failure and melt relocation to the lower plenum are late-phase core damage progression phenomena for which the uncertainties are greater than for the early phase phenomena. The general understanding of the late-phase phenomena is based on examination of the damaged TMI-2 core, because large-scale experiments have not been run at high enough temperatures and for long enough time periods for the phenomena to occur fully. The TMI-2 accident progression suggests that, if unmitigated, the molten interior will relocate into the lower region of the reactor vessel, either as a result of crust failure or of pool overflow from over the top of the crust. Approximately 20 tons of ceramic melt relocated into the lower plenum in the TMI-2 accident. The relocation to the lower plenum is likely to be rate limited due to the localized nature of the breach in the ceramic crust and the presence of structures that intercept and redirect the melt streams. This rate-limited relocation is expected to increase the extent of oxidation as well as steam generation.[1]

Natural circulation has been identified as an important phenomenon in PWRs, particularly when the RCS pressure is high. Three potential natural circulation flow paths exist: in-vessel circulation; hot leg countercurrent flow, including flow into the steam generator tubes; and flow through the coolant loops.[1] The two main effects of natural circulation are enhancing heat transfer from the core region to other structures in the RCS and enhancing steam flow in the core, thus holding down core temperatures and delaying melt progression.

As noted, variations can exist within a sequence depending upon the status of plant systems and operator actions to manage the accident. The accident management strategy for a core damage accident while the core is still in the reactor vessel would consist of two main actions: (1) water makeup into the reactor vessel to reflood the partially damaged core and terminate the accident and (2) RCS depressurization to allow low-pressure makeup and to avoid high-pressure melt ejection should the core melt through the reactor vessel lower head.

Several of the integrated core damage progression tests have been reflooded, resulting in production of significant amounts of steam, with further oxidation and hydrogen production. Also, reflooding can produce a debris bed of fragmented fuel particles that lose their cladding restraint due to oxygen embrittlement. It is estimated that about one-third of the total hydrogen generated in the TMI-2 accident was produced during reflood from the B-loop transient.[15]

During the period of in-vessel melt progression before reactor vessel lower head penetration, a significant fraction of the fission products released from fuel will deposit on RCS surfaces either by aerosol or vapor deposition. Subsequent heating of these surfaces can lead to the revaporization of volatile fission products from surfaces, their redistribution to other surfaces further down the flow path, and, for some fraction of the originally deposited radionuclides, release to the containment atmosphere. The amount of the deposited fission products that will revaporize depends on the temperature of the surface and the volatility of the chemical species. The ambient atmosphere within the RCS can also affect fission product revaporization. In an accident that involves an open flow path (two holes in the system), air can be drawn through the vessel, potentially oxidizing the fission products if the temperature is sufficiently high and sweeping airborne vapors and aerosols into the containment. Design features of the plant, such as reactor cavity flooding, can reduce the extent of this effect.

Recently there has been significant interest and activity in the area of risk during shutdown conditions. This is due to several factors, including a number of refueling outage incidents that occurred at U.S. plants in the last several years: the Vogtle loss of ac power incident[16,17] in 1990; recent probabilistic risk assessment (PRA) work suggesting that shutdown conditions contribute significantly to the total risk of core damage;[17,*] and the fact that the characteristics of plant conditions during shutdown may be less

*S. Hirschberg et al., "Modeling of Accident Sequences During Shutdown and Low Power Conditions," IAEA Meeting Report, Vienna, Austria, November 1991.

forgiving than during power operation. This less forgiving nature is due to reduced technical specifications, higher dependence on operator action, and the potential for the RCS and containment to be open.

The boundary conditions for fission product release and transport in the RCS during shutdown conditions are different from the boundary conditions for accidents at power. First, decay heat levels are lower, leading to lower fuel heatup rates, on the order of 0.1 to 0.3 K/s. Rapid temperature escalation at 1500 K is less likely because the thick oxide layer formed on the clad outer surface tends to reduce the oxidation reaction rate. Second, the RCS is typically open to containment. In addition to resulting in low RCS pressure, this also means that the RCS is likely to be exposed to air, causing more oxidizing conditions compared to accidents at power. Third, radioactive decay has significantly reduced the fission product inventory in the core, particularly for volatiles, compared to immediately after shutdown.

2.3.4 Fission Product Release and Transport Implications

Details of fission product release and transport are found in Chaps. 3 and 4. This section provides a brief summary of the important implications of the previous core damage progression phenomena on fission product release and transport.

Fuel can be in a solid state in some regions of the core for the duration of the accident (e.g., peripheral locations, debris bed of fragmented fuel particles). In these regions volatile fission product release is limited by temperatures less than ~2200 K and by the fact that the fuel particles are at least several orders of magnitude larger than the fuel grain size (10 μm). Low volatile fission product release is even more limited. Transgranular and intergranular fuel cracking as a result of quenching during reflood can enhance volatile fission product release from fuel in the solid state. Measurements indicate that only about 20% of the iodine and cesium is retained in a fuel debris bed.[7] High burnup fuel (exceeding ~10 MWd/kgU) enhances volatile fission product release from fuel in a solid state during accidents by increasing grain boundary porosity.

Changing fuel to a liquid state enhances volatile fission product release because bubble migration in a liquid is more rapid than in a solid. Measurements indicate that only about 10% of the iodine and cesium are retained in liquefied fuel.[7] Low melting point structural materials (e.g., Ag-In-Cd, Fe, Zr, Ni) vaporize during core heatup and in the ceramic melt, and they can condense into aerosols resulting in aerosol release during the same period of time that fission products are being released. This can have a significant effect on fission product transport due to interactions of fission product vapor and aerosol with structural aerosol.[18] Recent experimental data suggest that the quantity of structural aerosol mass released is in the range of 1 to 3 times the fission product mass release.*

Oxidation potential is a primary determinant of the form, and therefore the magnitude, of the fission product release. From Fig. 2.2 and the fact that the oxidation potential of core material oxides ranges from –120 to +20 kJ/mol, it may be seen that fission product barium, strontium, cerium, and lanthanum are in oxide form. These oxide species have very low vapor pressure, thus tending to make the release magnitude small. Ruthenium would be in metallic form. Metallic ruthenium has low vapor pressure and tends to alloy itself with other metals, so its release magnitude would also tend to be small. Local variations of oxygen potential are possible and could result in increased rates of release of strontium, cerium, and other low volatiles. Such increases are, however, expected to be of short duration relative to the time of core damage progression and therefore to be of minor importance to total release magnitude.

Measurements indicate that tellurium tends to be sequestered in metallic Zircaloy cladding until oxidation becomes extensive. Oxidation greater than about 90% active clad will cause a significant increase in the tellurium release.[19] The transport behavior of tellurium is consistent with a telluride or tellurite form rather than elemental tellurium.

The transport of both cesium and iodine within the primary circuit is likely to be as aerosol. Cesium and iodine are expected to be stabilized in the reducing steam conditions of the primary circuit initially as cesium hydroxide and cesium iodide or other metallic iodides. However, depending upon the characteristics of the accident sequence, both materials can react with boric acid to generate low-volatility cesium borate and volatile hydrogen iodide (HI).[20] Low-pressure, rapid core damage sequences tend to minimize the boric acid reaction because much of the boric acid is expelled from the RCS during the blowdown. Furthermore, the boric oxide tends to be retained in the

*D. A. Petti et al., "The Composition of Aerosols Generated During a Severe Reactor Accident: Experimental Results from the Power Burst Facility Severe Damage Test," accepted for publication in *Nucl. Technol.*

fuel matrix during core melt. Thus, for example, as described in Refs. 21 and 22, only small amounts of HI are expected for the design basis source term in the U.S. ALWR where low-pressure core damage sequences are dominant, and rapid core damage is assumed. High-pressure, slow core melt sequences would tend to make the boric acid reaction more important, which would decrease the cesium hydroxide (CsOH) and cesium iodide (CsI) and increase the amount of cesium borate and HI. However, HI is a reactive, volatile gas and is predicted to react rapidly with metallic aerosols released from the control rods to form either cadmium or silver iodide (CdI_2 or AgI). Direct evidence for cesium borate and CdI formation is given from the Falcon experiments;[23] the existence of either CdI_2 or AgI has been inferred from analyses of the loss of fluid test (LOFT) FP-2 experiment.[18]

The enhanced heat transfer from the core to RCS structures resulting from natural circulation will increase structural temperatures and can reduce fission product retention in the RCS. The prolonged heatup at lower temperatures may result in more extensive clad oxidation.

2.4 Degraded Core Accident Sequence Boundary Conditions

From this discussion of degraded core accident progression phenomena, it is evident that the accident sequence boundary conditions that have the most significant effect on fission product release are core temperature (and time at temperature), fuel morphology (a function of burnup and grain boundary microcracking due to reflood), RCS pressure, clad oxidation, hydrogen-to-steam partial pressure ratio, and molar flow rates. Additional conditions affecting fission product transport are production of structural aerosols, gas temperatures, and RCS structure temperatures. Initial conditions and structural material quantities have been defined in Sect. 2.2. High (or at least equilibrium) burnup fuel is assumed. Remaining boundary conditions are estimated below for each of the sequence types defined in Sect. 2.3.

The boundary conditions are estimated as a function of time in the respective sequences. The times for which boundary conditions are provided correspond to five major events in the accident sequence: core uncovery, melt initiation, melt relocation, lower head dryout, and lower head failure. The boundary condition values must be considered as approximations due to the uncertainties in such calculations, the differences in results from different computer codes, variations in plant design and accident sequences, and the fact that the values at times other than those provided in the tables may be different.

For the PWR, LOCA and transient (station blackout) were selected for evaluation on the basis of Table 2.5 probability estimates. For the BWR, ATWS and station blackout were selected based on Table 2.6.

2.4.1 PWR Small LOCA

In the PWR small LOCA the accident event timing, RCS pressure, average core temperature, fraction core melted, and fraction clad reacted, given in Table 2.7, are rounded off values from Source Term Code Package (STCP) calculations for the Zion Plan[24] performed in support of NUREG-1150. For this and other sequences discussed later, a peak core temperature of 2550 K was assumed for melt initiation. This is based on several factors including the STCP value and the fact that a number of other codes predict this temperature.[25] Also, this temperature is not unreasonable based on the significant oxygen content in the clad that tends to limit UO_2 dissolution, which would otherwise occur at ~2200 K. A peak core temperature of 3000 K was assumed for melt relocation based upon TMI-2 data, which indicated temperatures in the upper central core region of 3000 to 3100 K (Ref. 26), and the fact that transition metal oxides present in the ceramic phase form eutectics with ZrO_2 to lower the liquidus temperature by about 100 K (Ref. 7). The Table 2.8 values for gas and structure temperatures, as well as the remaining Table 2.7 boundary conditions of hydrogen-to-steam partial pressure ratio and core exit gas flow, were taken from Ref. 27. Reference 27 developed a model for predicting RCS thermal-hydraulic conditions during degraded core accidents and used MARCH code results as source conditions.

Tables 2.7 and 2.8 values compare reasonably well with other published PWR small LOCA sequence boundary conditions, given the differences in plant designs and specifics of the sequence. Reference 10, which utilized the SCDAP/RELAP5 computer code, predicted core melt initiation ~30 min after core uncovery, a peak node core heatup rate of ~0.9 K/s over a peak core temperature range of 600 K to ~2500 K, a peak core temperature near 3000 K, and an RCS pressure of ~8 MPa at core uncovery and ~4 MPa at the beginning of core melt. The calculation in Ref. 10 was terminated at ~200 min with no lower head failure having occurred. Reference 10 predicted somewhat higher fraction clad reacted (80%) whereas the average of the NUREG-1150 expert elicitations for PWR in-vessel, ~7 to 10 MPa, was about 40% equivalent clad oxidation.[28] To provide additional perspective, Tables 2.9 and 2.10 summarize MAAP code results for a small LOCA.* MAAP is

*R. J. Hammersley, Fauske & Associates, Inc., Letter to D. E. Leaver, Polestar Applied Technology, Inc., December 4, 1992.

Table 2.7 Core response to PWR small LOCA (based on STCP)

Accident event	Time (min)	RCS pressure (MPa)	Average core temperature (K)	Peak core temperature (K)	Fraction clad reacted	Fraction core melted	P_{H_2}/P_{H_2O}	Core exit gas flow (moles/s)
Core uncovery	0	8.8	580	585	0	0	0	3400
Melt initiation	30	6.8	1300	2550	0.06	0.04	4	75
Melt relocation	45	4.8	2300	3000	0.43	0.69	0.8	600
Lower head dryout	60	8.5	2200	3000	0.47			
Lower head dryout	70	6.1	2350	3000	0.47			

Table 2.8 RCS gas and temperature response to PWR small LOCA

Accident event	Time (min)	Core exit gas (K)	Upper plenum gas (K)	Upper plenum structure (K)	Hot leg gas (K)
Core uncovery	0	575	575	575	575
Melt initiation	30	2100	1600	1050	1200
Melt relocation	45	1400	1500	1300	1200

Table 2.9 Core response to PWR small LOCA (based on MAAP)

Accident event	Time (min.)	Average core temperature (K)	Peak core temperature (K)	Fraction clad reacted	Fraction core melted	P_{H_2}/P_{H_2O}	Core exit gas flow (moles/s)
Core uncovery	0	550	566	0.0	0.0	0.0	630
Melt initiation	231	836	3000	0.033	0.01	0.04	260
Melt relocation	468	2290	3050	0.569	0.14	0.05	46
Lower head dryout	502	1630	2860	0.578	0.33	0.08	442
Lower head failure	586	1820	2610	0.578	0.66	0.05	0

Table 2.10 RCS gas and temperature response to PWR small LOCA (based on MAAP)

Accident event	Time (min)	Core exit gas (K)	Upper plenum gas (K)	Upper plenum structure (K)	Hot leg gas (K)
Core uncovery	0	531	532	543	544
Melt initiation	231	2980	1410	974	766
Melt relocation	468	2480	1570	1550	721

the U.S. industry-developed code that is being used by most U.S. utilities as part of the IPE PRA work. While MAAP predicted considerably longer times than STCP (probably due to differences in plant design and accident sequence input assumptions), the core temperatures, clad oxidation, gas flows, and gas and structure temperatures compare reasonably well. Mailliat's comparison* contains calculations performed as part of PHEBUS-FP Phase A studies by Germany, United Kingdom, France, and Italy, using national codes applied to their respective PWRs. Table 2.11 summarizes these results.

It can be concluded that for the PWR small LOCA pressure remains at intermediate levels (above about 4 MPa) during core degradation; average core temperature is about 2000 K with maximum value up to 3000 K. Clad oxidation is about 50%; the fraction of core melted is high, as would be the release of volatile fission products. Gas and structure temperatures are in the range of 1000 to 1500 K.

*A. Mailliat, "Comparison of Phase A Studies Phebus-FP Shared Cost Action, Part A: Reactor Coolant System," ISPN/DRS/SEMAR (March 1988).

2.4.2 PWR Station Blackout

The PWR station blackout accident event timing, RCS pressure, average core temperature, fraction core melted, and fraction clad reacted, given in Table 2.12, are rounded off STCP calculations for the Zion Plant[24] performed in support of NUREG-1150. Table 2.13 values for gas and structure temperatures, as well as the remaining Table 2.12 boundary conditions, hydrogen-to-steam partial pressure ratio and core exit gas flow, were taken from Ref. 29, which is an extension of the Ref. 27 work.

Tables 2.12 and 2.13 values compare favorably with other boundary conditions. Reference 6 reported timing, RCS pressure, fraction of core melted, and gas and structure temperature values for a PWR transient based on MARCH U. K., which compare reasonably well with the results from Tables 2.12 and 2.13. Reference 10, which utilized the SCDAP/RELAP5 computer code, predicted initiation of fuel cladding failure ~20 min after core uncovery, peak node core heatup rate of ~1 K/s over a peak core temperature range of 600 K to 1800 K before loop seal clearing,

Table 2.11 Small-break main parameters before core collapse

Accident sequences		Pressure range (MPa)	Core maximum average temperature or maximum temperature (K)	Temperature slope (K/s)	FP release duration 5–90% (s)	Flow rate range (kg/s)	FP fraction release before core collapse	Oxidation before core collapse (%)
S_2D	G	8.2–5.7	2000	1.4 0.6	1000	15 0.4	Cs : 36%[a]	23[b]
S_2D	GB	8.6–1.7	1300–2740	1.5 0.3	1560	<1 0.4–0.1	100%	54[b]
S_LD	I	7.9–1.9					>98%	59
S_LCD	F	NA	NA	NA	1800	NA	95%	67

[a]FP release not modeled during reaction.
[b]Accumulator not activated.
Source: Ref. 3.

Table 2.12 Core response to PWR station blackout (based on STCP)

Accident event	Time (min)	RCS pressure (MPa)	Average core temperature (K)	Peak core temperature (K)	Fraction clad reacted	Fraction core melted	P_{H_2}/P_{H_2O}	Core exit gas flow (moles/s)
Core uncovery	0	16.1	627	630	0	0	0	2450
Melt initiation	24	16.1	1337	2550	0.06	0.01	1.2	18
Melt relocation	54	16.1	2731	3000	0.33	0.57	5.3	17
Lower head failure	65	16.1	2507	3000	0.52	≥0.86		

Table 2.13 RCS gas and structure temperature response to PWR station blackout

Accident event	Time (min)	Core exit gas (K)	Upper plenum gas (K)	Upper plenum structure (K)	Hot leg gas (K)
Core uncovery	0	666	645	645	645
Melt initiation	24	2100	1000	750	715
Melt relocation	54	2465	1200	1025	795

peak core temperature near 2000 K before loop seal clearing, and RCS pressure of about 16 MPa at core uncovery. While the SCDAP/RELAP5 results are not directly comparable with the STCP results because the SCDAP/RELAP5 model accounted for loop seal clearing, data up to the time of loop seal clearing agree reasonably well with Tables 2.12 and 2.13. Tables 2.14 and 2.15 summarize MAAP code results for a station blackout.* Again, the MAAP code predicts considerably longer times than STCP, but the remaining parameter values compare reasonably well. A station blackout sequence has been analyzed as part of the PHEBUS-FP Phase A effort for different European PWRs, using national codes based mainly on STCP. The results obtained are summarized in Table 2.16.

It is evident from these results that the pressure stays high throughout the accident (close to operating pressure), average core temperature is somewhat higher than the small LOCA, and fraction core melted and, thus, fission product release are slightly higher.

*R. J. Hammersley, Fauske & Associates, Inc., Letter to D. E. Leaver, Polestar Applied Technology, Inc., December 4, 1992.

Table 2.14 Core response to PWR station blackout (based on MAAP)

Accident event	Time (min)	Average core temperature (K)	Peak core temperature (K)	Fraction clad reacted	Fraction core melted	P_{H_2}/P_{H_2O}	Core exit gas flow (moles/s)
Core uncovery	0	647	664	0.0	0.0	0.0	1436
Melt initiation	52	1300	2630	0.076	0.034	0.038	958
Melt relocation	173	2240	2990	0.404	0.118	0.529	100
Lower head dryout	220	1710	2700	0.511	0.359	0.092	206
Lower head failure	298	1980	2850	0.512	0.709	0.098	0.1

Table 2.15 RCS gas and temperature response to PWR station blackout (based on MAAP)

Accident event	Time (min)	Core exit gas (K)	Upper plenum gas (K)	Upper plenum structure (K)	Hot leg gas (K)
Core uncovery	0	627.8	628.8	625.3	629.1
Melt initiation	52	2165	1230	919.6	1132
Melt relocation	173	2088	994.6	780.2	875.7

Table 2.16 Transient main parameters before core collapse

Accident sequences		Pressure range (MPa)	Core maximum average temperature or maximum temperature (K)	Temperature slope (K/s)	FP release duration 5–90% (s)	Flow rate range (kg/s)	FP fraction release before core collapse (%)	Oxidation before core collapse (%)
TMLB'	G				NA			
TMLB'	GB	16.5	1600–2760		2000	1→0 0.2	95	67
TMLB'	I	17.45	1300–2400	0.25 0.1	2400	1→0 0.05	>90	26
TMLB'	SP	17.4	2200	–0.8	NA	15→0 0.12		22
TLCD	F	16.0	NA	NA	2400	NA	100	2 (?)
TMLB'β/δ	F	8.0–15.5	1400–2300	1.2 0.5	1300	14→0 0.3	77	45

Source: Ref. 3.

2.4.3 PWR Large LOCA

The PWR large LOCA accident event timing, RCS pressure, average core temperature, fraction core melted, and fraction clad reacted given in Table 2.17, are rounded off values from STCP calculations for the Surry Plant[30] performed in support of NUREG-1150. The large LOCA sequence modeled for Surry is a long-term sequence, consisting of failure of ECCS recirculation at about 50 h due to loss of containment heat removal. Table 2.18 values for gas and structure temperatures, as well as the remaining Table 2.17 boundary conditions, hydrogen-to-steam partial pressure ratio, and core exit gas flow, were taken from Ref. 29.

Some values in Tables 2.17 and 2.18 differ from other published data, due primarily to the fact that core uncovery does not begin until 50 h after shutdown when decay heat has decreased significantly. This resulted in extended accident times and lower core heatup rates (~0.3 K/s). PHEBUS-FP Phase A studies in Table 2.19 show significantly faster core heatup, as high as 2 K/s.

For the large LOCA, it is evident that the RCS pressure is rapidly reduced to low values. The initial RCS inventory will be discharged quickly, with accumulators providing inventory makeup for some period of time. Continued evaporation of this inventory will affect revolatilization of condensed vapors and deposited aerosols in RCS structures. High fractions of core melt and clad oxidation occur.

2.4.4 BWR Station Blackout

The BWR station blackout accident event timing, RCS pressure, average core temperature, fraction core melted, and fraction clad reacted, given in Table 2.20, are rounded-off values from STCP calculations for the Peach Bottom Plant[31] performed in support of NUREG-1150. Table 2.21 values for gas and structure temperatures, as well as the remaining Table 2.20 boundary conditions, hydrogen-to-steam partial pressure ratio, and core exit gas flow, were taken from Ref. 29.

The NUREG-1150 expert elicitation for BWR in-vessel, high RCS pressure conditions was about 25% equivalent clad oxidation,[28] which agrees very well with the previous results. Tables 2.22 and 2.23, taken from MAAP calculations,* agree quite well for core conditions, but differ significantly in gas and structure temperatures, probably due to differences in natural circulation modeling or sequence differences that affect natural circulation.

It is evident from these results that the RCS pressure remains high throughout the station blackout sequence with average core temperature somewhat lower than other sequences and relatively low clad oxidation.

2.4.5 BWR ATWS

The BWR ATWS accident event timing, RCS pressure, average core temperature, fraction core melted, and fraction clad reacted, given in Table 2.24, are rounded-off values from STCP calculations for the Peach Bottom Plant[31] performed in support of NUREG-1150.

Table 2.25 values for gas and structure temperatures, as well as the remaining Table 2.24 boundary conditions, hydrogen-to-steam partial pressure ratio, and core exit gas flow, were taken from Hammersley.*

The ATWS sequence results in low RCS pressures and is a somewhat shorter event with less core melt than the station blackout.

2.5 Conclusions

This chapter has defined representative severe accident sequences, and associated core and RCS boundary conditions, affecting the release and transport of fission products and core materials in Western type LWRs. The main conclusions from the chapter are as follows:

- While LWRs have been designed with engineered systems to prevent core damage and any accident sequence involving a degraded core is very unlikely, the international nuclear community has performed significant research work evaluating the effects of core damage sequences in order to better understand the risk implications and to improve upon containment design.

- While analytical and experimental work continues, a number of studies have been performed to predict degraded core accident progression and associated boundary conditions. The most widely used tools for integrated evaluation of degraded core accident conditions are STCP and MAAP. A limited number of evaluations using the MELCOR code have also recently become available.

*R. J. Hammersley, Fauske & Associates, Inc., Letter to D. E. Leaver, Polestar Applied Technology, Inc., December 4, 1992.

Table 2.17 RCS gas and structure temperature response to PWR large LOCA (based on STCP)

Accident event	Time (min)	RCS pressure (MPa)	Average core temperature (K)	Peak core temperature (K)	Fraction clad reacted	Fraction core melted	P_{H_2}/P_{H_2O}	Core exit gas flow (moles/s)
Core uncovery	0	0.126	383	383	0	0	0	2400
Melt initiation	75[a]	0.10	1336	2550	0.12	0.09	5.9	23
Melt relocation	128[a]	0.10	2550	3000	0.70	0.80	6.6	29
Lower head dryout	157[a]	0.10	1481	3000	0.71			
Lower head failure	291[a]	0.21	2227	3000	0.71			

[a]Core melt progression timing is extended because this is a long-term sequence consisting of ECCS recirculation failure at 50 h due to loss of containment heat removal.

Table 2.18 RCS gas and structure temperature response to PWR station large LOCA

Accident event	Time (min)	Core exit gas (K)	Upper plenum gas (K)	Upper plenum structure (K)	Hot leg gas (K)
Core uncovery	0	454	492	601	492
Melt initiation	75	2094	1225	660	1100
Melt relocation	128	2491	1537	780	1172

Table 2.19 Large-break main parameters before core collapse

Accident sequences	Pressure range (MPa)	Core maximum average temperature or maximum temperature (K)	Temperature slope (K/s)	FP release duration 5–90% (s)	Flow rate range (kg/s)	FP fraction release before core collapse (%)	Oxidation before core collapse (%)
AH G hot leg	0.14	2200		1200	75→0 NA	>90	60
AB GB hot leg	0.35/0.3	1600–2760	1.4 0.3	0.1320	5→0 0.3/0.1	100	46
AF F cold leg	0.36	1400–2000	0.6 0.05	7200	6→0 0.1	88	93
ALB F cold leg	0.2	1400–2300	1.1 0.2	1450	16.1→0 0.1	>80	35
AB F hot leg	Low pressure	NA	NA	1200	3→0 0.1	99	26

Source: Ref. 3.

Table 2.20 RCS gas and structure temperature response to BWR station blackout (based on STCP)

Accident event	Time (min)	RCS pressure (MPa)	Average core temperature (K)	Peak core temperature (K)	Fraction clad reacted	Fraction core melted	P_{H_2}/P_{H_2O}	Core exit gas flow (moles/s)
Core uncovery	0	7.2	565	568	0	0	0	407
Melt initiation	114	7.3	1795	2550	0.08	0.0	2.1	35
Melt relocation	167	7.8	2170	3000	0.22	0.61	9.0	70
Lower head dryout	177	7.7	1604	3000	0.25	0.65		
Lower head failure	205	7.4	1776	3000	0.25			

Table 2.21 RCS gas and structure temperature response to BWR station blackout

Accident event	Time (min)	Core exit gas (K)	Upper plenum gas (K)	Upper plenum structure (K)	Hot leg gas (K)
Core uncovery	0	469	469	1258	469
Melt initiation	114	1660	1600	750	600
Melt relocation	167	2320	2290	1258	756

Table 2.22 Core response to BWR station blackout (based on MAAP)

Accident event	Time (min)	RCS pressure (MPa)	Average core temperature (K)	Peak core temperature (K)	Fraction clad reacted	Fraction core melted	P_{H_2}/P_{H_2O}	Core exit gas flow (moles/s)
Core uncovery	0	7.4	574.6	583.6	0.0	0.0	0.0	800
Melt initiation	73	7.2	1361	2504	0.076	0.027	0.098	913
Melt relocation	136	7.2	2191	3042	0.309	0.27	0.238	0.0
Lower head dryout	158	7.3	1180	2130	0.383	0.63	2×10^{-4}	1337
Lower head failure	330	7.4	1399	1885	0.383	0.87	1×10^{-4}	0.0

Table 2.23 RCS gas and structure temperature response to BWR station blackout (based on MAAP)

Accident event	Time (min)	Core exit gas (K)	Upper plenum gas (K)	Upper plenum structure (K)
Core uncovery	0	564.4	563.2	545.3
Melt initiation	73	906	575.3	553.5
Melt relocation	136	915.6	630	593.8

Table 2.24 Core response to BWR ATWS (based on STCP)

Accident event	Time (min)	RCS pressure (MPa)	Average core temperature (K)	Peak core temperature (K)	Fraction clad reacted	Fraction core melted	P_{H_2}/P_{H_2O}	Core exit gas flow (moles/s)
Core uncovery	0	8.2	667	731	0	0	0	2885
Melt initiation	40.2	0.23	1475	2550	0.06	0.01	9.0	40
Melt relocation	72.2	0.14	2123	3000	0.18	0.30	9.6	39
Lower head dryout	108	0.75	1769	3000	0.26			
Lower head failure	137	0.11	2017	3000	0.26			

Table 2.25 RCS gas and structure temperature response to BWR ATWS

Accident event	Time (min)	Core exit gas (K)	Mixing plenum gas (K)	Stand pipe structure (K)	Steam line gas (K)
Core uncovery	0	1001	575	575	569
Melt initiation	24.5	2017	1950	725	575
Melt relocation	53	2200	2128	897	575

Accident

- Based upon PRA frequency estimates, LOCA and transient (station blackout) sequences were selected for reporting boundary conditions for the PWR, and ATWS and station blackout sequences for the BWR.

- Based upon the available studies of core and RCS response to degraded core conditions, the key boundary conditions that have a major effect on fission product release and transport are core temperature (including time at temperature), fuel morphology (a function of burnup and grain boundary microcracking due to reflood), RCS pressure, clad oxidation, hydrogen-to-steam partial pressure ratio, and molar flow rates. Additional conditions affecting fission product transport are production of structural aerosols, gas temperatures, and RCS structure temperatures.

2.6 References

1. S. R. Kinnerly et al., "In-Vessel Core Degradation in LWR Severe Accidents: A State-of-the-Art Report to CSNI," NEA/CSNI/R (91) 12, November 1991.

2. U.S. Nuclear Regulatory Commission, "Severe Accident Risks: An Assessment for Five U.S. Nuclear Power Plants," USNRC Report NUREG-1150, June 1989.*

3. "German Risk Study Nuclear Power Plants, Phase B," Gesellschaft für Reaktorsicherheit mbH, GRS-72, Köln (June 1989).

4. A. Alonzo et al., "Analysis of Three Severe Accident Sequences (AB, SGTR, and V) in a Three Loop W-PWR 900 MWe with the MELCOR Code," Catedra de Technologia Nuclear, CTN-35/93 (1992).

5. B. R. Bowsher, "Fission Product Chemistry and Aerosol Behavior in the Primary Circuit of a Pressurized Water Reactor Under Severe Accident Conditions," *Progr. Nucl. Energy*, 20 (3), 199 (1987).†

6. R. P. Wichner and R. D. Spence, "Quantity and Nature of LWR Aerosols Produced in the Pressure Vessel During Core Heatup Accidents—A Chemical Equilibrium Estimate," USNRC Report NUREG/CR-3181, March 1984.*

7. R. R. Hobbins et al., "Review of Experimental Results on Light Water Reactor Core Melt Progression," *Nucl. Technol.*, 95 (September 1991).†

8. R. W. Wright et al., *Core Degradation and Fission Product Release, The Phebus Fission Product Project* (Elsevier Science Publishers, Essex, England, 1992).

9. C. Allison et al., "Severe Core Damage and Associated Fission Product Release," *Prog. Nucl. Energy*, 20 (2), 1987.†

10. P. Bayless et al., *Feedwater Transient and Small Break Loss of Coolant Accident Analyses for the Bellafonte Nuclear Plant*, USNRC Report NUREG/CR-4741, March 1987.*

11. B. Adroguer et al., "Analysis of the Fuel Cladding Chemical Interaction in PHEBUS SFD Tests Using ICARE2 Code," p. 137 in *Proceedings of IAEA Meeting on Behavior of Core Materials and Fission Product Release in Accident Conditions in LWRs, Aix-en-Provence, France, March 1992*, International Atomic Energy Agency, IAEA-TEC DOC-706 (June 1993).

12. D. W. Akers et al., "Core Materials Inventory and Behavior," *Nucl. Technol.*, 87 (August 1989).†

13. B. R. Bowsher et al., "Silver-Indium-Cadmium Control Rod Behaviour During a Severe Reactor Accident," Atomic Energy Authority AEEW-R 1991, United Kingdom (1986).

14. D. A. Petti, "Silver-Indium-Cadmium Control Rod Behavior in Severe Reactor Accidents," *Nucl. Technol.*, 84, 128 (1989).†

15. P. Ruan et al., "Thermal Interactions During the Three Mile Island Unit 2 2-B Coolant Pump Transient," *Nucl. Technol.*, 87 (August 1989).†

16. U.S. Nuclear Regulatory Commission, "Loss of Vital AC Power and the Residual Heat Removal System During Mid-Loop Operations at Vogtle Unit 1 on March 20, 1990," USNRC Report NUREG-1410, June 1990.*

17. U.S. Nuclear Regulatory Commission, "Evaluation of Shutdown and Low Power Risks," SECY-91-283, September 9, 1991.*

18. C. G. Benson et al., p. 447 in *Proceedings of ICHMT Seminar on Fission Product Transport Processes in Reactor Accidents, 22–26, May 1989, Dubrovnik*, J. T. Rogers, Ed. (Hemisphere Publishing, 1990).

19. J. L. Collins et al., "Fission Product Tellurium Release Behavior Under Severe Light Water Reactor Accident Conditions," *Nucl. Technol.*, 77, 18 (1987).†

20. B. R. Bowsher et al., "The Interaction of Cesium Iodide with Boric Acid in the Temperature Range 100 to 1000°C," p. 253 in *Proceedings of CSNI Specialists' Workshop on Iodine Chemistry in Reactor Safety, AERE Harwell, September 1985*, Atomic Energy Authority, AERE-R 11974, United Kingdom (1986).

21. D. E. Leaver et al., "Passive ALWR Source Term," EG&G Idaho, DOE/ID-10321, February 1991.

22. E. C. Beahm et al., "Iodine Chemical Form in LWR Severe Accidents," USNRC Report NUREG/CR-5732, June 1991.*

23. A. M. Beard et al., The Falcon Programme: Characterization of Multicomponent Aerosols in Severe Nuclear Reactor Accidents," *J. Aerosol Sci.*, 23, S831 (1992).†

24. R. S. Denning et al., "Radionuclide Release Calculations for Selected Severe Accident Scenarios," Vol. 5 (Zion), USNRC Report NUREG/CR-4624, July 1986.*

25. D. W. Golden et al., "Summary of the Three Mile Island Unit 2 Analysis Exercise," *Nucl. Technol.*, 87 (August 1989).†

26. C. S. Olsen et al., "Materials Interactions and Temperature in the Three Mile Island Unit 2 Core," *Nucl. Technol.*, 87 (August 1989).†

27. A. T. Wassel et al., "Thermal-Hydraulic Modeling of the Primary Coolant System of Light Water Reactors During Severely Degraded Core Accidents," Electric Power Research Institute, EPRI NP-3563, July 1984.

28. Sandia National Laboratories, "Evaluation of Severe Accident Risks: Quantification of Major Input Parameters—In Vessel Issues," Vol. 2, USNRC Report NUREG/CR-4551, Rev. 1, Part 1, December 1990.*

29. A. T. Wassel et al., "Estimate of Primary System Temperatures in Severe Reactor Accidents," Electric Power Research Institute, EPRI NP-3120, May 1983.

30. R. S. Denning et al., "Radionuclide Release Calculations for Selected Severe Accident Scenarios," Vol. 3 (Surry), USNRC Report NUREG/CR-4624, May 1986.*

31. R. S. Denning et al., *Radionuclide Release Calculations for Selected Severe Accident Scenarios*, Vol. 1 (Peach Bottom), USNRC Report NUREG/CR-4624, May 1986.*

---

*Available for purchase from the National Technical Information Service, Springfield, VA 22161.
†Available in public technical libraries.

3 In-Vessel Release of Fission Products and Core Materials

The study of fission product release in accident conditions has generated a large body of data and many different attempts at modeling. This chapter gives an overview of the phenomena of fission product and core material release, a summary of the most important experimental programs that have been conducted to investigate release phenomena, an overview of the models and computer codes that have been developed to describe release behavior, and finally a comparison between code calculations and experimental data. The conclusions are presented at the end of the chapter.

3.1 Description of Release Phenomena

3.1.1 Fission Product Releases

A physically based description of fission product release from uranium dioxide (UO_2) fuel during accident conditions requires information about

- the concentration and chemical forms of the fission products within the fuel;
- the spatial distribution of the fission products within the fuel (i.e., solid solution within the UO_2 matrix, as bubbles, on grain boundaries or in the free volume of the fuel); and
- the effective mobility of the fission products at each site in the fuel.

All of these quantities are direct or indirect time-dependent functions of temperature, pressure, oxygen potential, and irradiation history (i.e., fission rate and burnup). In the following subsections, the factors that influence chemical form, distribution, and mobility of fission products are described.

3.1.1.1 Concentration and Chemical Forms of Fission Products

Fission of uranium and plutonium produces stable and radioactive fission products. More than 800 isotopes can be formed by the combination of fission and other nuclear reactions such as transmutation by neutron capture or various decay reactions. For UO_2 fuels, the most abundant fission product elements by mass are Xe, Mo, Nd, Ce, Cs, Zr, Ru, Ba, and La. The concentration and activity of these various isotopes can be calculated using time-dependent irradiation data in a nuclear production/capture/decay computer program such as the ORIGEN-2 code.[1] These calculations have been assessed by comparison with post-irradiation chemical analyses, and for the important fission products the uncertainty is not considered to be important with respect to reactor accident calculations.

The most abundant fission products and actinides constitute about 30 different chemical elements that can be classified into four groups: noble gases (Xe and Kr); volatile species (I, Cs, Br, Rb); semivolatile species (Te, Ru, Mo, Tc, Sb, Sn, Ag); and low-volatility species (Ba, Sr, Y, Zr, Nb, Rh, Pd, La, Ce, Pr, Nd, Pm, Sm, Eu, U, Np, Pu, Am). The distinction between the latter two classifications is not rigid, because some fission products may be classified as either low-volatile or semivolatile depending on the temperature and oxygen potential, as discussed later.

The fission products and actinides exist in various chemical forms. The noble gases do not form chemical compounds in the fuel and are therefore the simplest species to model.

The volatile classification of fission products (I, Cs, Br, Rb) is generally regarded as being released in a similar manner to the noble gases; however, it differs from the noble gases because these elements can form compounds that are volatile only at temperatures much above those of normal coolant operation (e.g., CsI, CsOH, CsBr, Cs uranates, molybdates etc.).

The semivolatile classification of fission products (Te, Ru, Mo, Tc, Sb, Sn, Ag) includes elements that are not significantly volatile at moderate temperatures in their elemental form but can become volatile at higher temperatures or as oxides or other compounds. For example, elemental ruthenium has a very high melting temperature and is not volatile, but if an oxidizing environment exists, then the ruthenium can be converted to an oxide of high volatility and releases would occur.

The low-volatility classification of fission products and actinides (Ba, Sr, Y, Zr, Nb, Rh, Pd, La, Ce, Pr, Nd, Pm, Sm, Eu, U, Np, Pu, Am) tend to either remain in solid solution in the UO_2 or form stable compounds of high melting temperature. These species are not normally released from the UO_2, except in extreme accident scenarios in which the fuel is vaporized.

The chemical forms of fission products within the UO_2 have been the subject of much work, based primarily on thermodynamic assessments[2–4] and electron probe microanalyses.[5–8] The possible chemical forms include elements, oxides, metallic alloys, oxide compounds (i.e., uranates, zirconates, or molybdates) and intermetallics. A single fission product element may exist in several different chemical states, depending on temperature, oxygen potential, pressure, and concentrations (a function of

burnup). The phase compositions in the fuel at equilibrium can be calculated, although uncertainty remains for some of the thermodynamic properties of the fission product compounds.

The chemical forms of the fission products are essential in calculating the release behavior, because they control the volatility of the fission products.[9] During the reactor accident conditions, the fuel temperatures escalate from normal operating conditions, and the oxygen potential within the fuel may either decrease due to Zircaloy-UO_2 interactions or increase due to oxidation by the external steam atmosphere. Thus, fuel damage progression phenomena contribute to changes in the volatility of the various fission products.

3.1.1.2 Distribution of Fission Products

Fission products are generated throughout the UO_2 matrix during irradiation. The distribution of fission products within the fuel is affected by the irradiation history and operating characteristics of the fuel. The power level and heat transfer characteristics to the coolant control the temperature distribution in the fuel and therefore control processes such as grain growth and densification. Partitioning of the various fission products between sinks, such as the UO_2 matrix, intragranular bubbles, the grain boundary, and fuel/sheath gap, can be calculated by fuel performance codes for normal operating conditions. Measurements of fission product concentrations within the different sinks, such as bubbles or grain boundaries,[10–15] are rare and have not been compared with calculations by fuel performance codes.

The noble gases have a low solubility in UO_2 and therefore tend to form bubbles within the ceramic matrix (intragranular) and on grain boundaries (intergranular) at elevated temperatures. During normal operation, irradiation-induced re-solution of the bubbles tends to limit the intragranular bubble populations. With increasing burnup the grain boundaries accumulate bubbles that grow, coalesce, and eventually interlink along grain edges to permit venting of the gas pressure to the internal volume of the fuel rod. The dynamics of intergranular and intragranular bubble evolution are strongly influenced by stress-state (local pressure). During normal operation of the fuel, the largest contribution to pressurization of the fuel rod is due to releases of noble gas fission products.

The volatile fission products also form bubbles similar to the noble gases. However, after release from the UO_2 these species condense on cooler free surfaces of the fuel rod; as a result, I, Cs, and Br do not contribute significantly to the internal pressure of a fuel rod under normal conditions. At elevated temperatures (>800°C) in an accident, I, Cs, and Br would be released, not only from the UO_2, but also due to vaporization of the previously released amounts on the free surfaces of the fuel.

The size of fission gas bubbles is governed by equilibrium between the local state of stress (i.e., total pressure in bubbles) and the surface tension of the UO_2. During accident conditions, the stresses in the UO_2 are affected by depressurization of the primary circuit and changing temperature distributions in the fuel and can lead to rapid growth of bubbles and release of fission products. Under decay power conditions re-solution is reduced, and more intragranular bubbles can form; these bubbles become less mobile as they grow. This process can act as a means of retaining fission gas within the ceramic in the absence of collection at grain boundaries as a result of grain boundary motion (termed grain boundary sweeping).

The solubility of the semivolatile and low-volatile fission products in UO_2 varies with temperature, pressure, and oxygen potential. Some of the insoluble species accumulate at grain boundaries or in intragranular bubbles where they precipitate to form metallic alloys (Mo, Ru, Rh, Tc, Pd) or other compounds, such as zirconates, molybdates or uranates. The stability and composition of these phases are functions of temperature, oxygen potential, pressure, and local fission product concentrations, as discussed in Sect. 3.1.1.1.

3.1.1.3 Mobility of Fission Products

In general, the processes by which fission products can be released from the UO_2 matrix include diffusion, knockout, and recoil.[16] The latter two processes make only a small contribution and would be negligible in accident conditions. The effective mobility of fission products within the fuel depends on many parameters, including the aforementioned chemical forms. The effective mobility is required for calculating the rates of fission product transport from the UO_2 matrix to the grain boundaries. The diffusion process may involve either atomic species, fission product/defect clusters, or bubbles. Migration on grain boundaries, in cracks and pellet interfaces, and in the fuel/sheath gap can also be described in terms of effective mobilities.

The release of short-lived fission gases from UO_2 during irradiation has been extensively studied in a number of experiments with single and polycrystalline fuel specimens,[17–20] and with swept assemblies in which the fuel-cladding gap of an intact operating fuel rod was continually purged.[21–24] These experiments generally demonstrate that diffusion of noble gas atoms and iodine in UO_2 is the rate-determining mechanism for release during

steady-state operation. At lower fuel temperatures (<1000°C), diffusion is independent of temperature but is enhanced as a result of the fission process;[19,25] however, for the shorter-lived isotopes, recoil effects also become important.[26,27] As shown in these various experiments, the diffusion coefficients of krypton, xenon, and iodine were found to be similar in magnitude and in their temperature-dependent behavior. Both thermally activated and athermal diffusion are implicated in the main release studies because the release-to-birth rate (R/B) ratio is observed to vary inversely as the square root of the isotopic decay constant λ. This type of behavior was predicted over 30 years ago by Booth, using diffusion theory.[28] A more general solution by Kidson,[29] which included transient conditions and precursor effects, was modified and used in the ANS 5.4 standard model.[30] However, any implementation requires assumptions about fission product concentrations on the grain boundary, because this is a boundary condition for the grain diffusion problem. The accepted approach for describing the required diffusion coefficients is to include both thermal and athermal components with a factor to include an increasing value with burnup.

A diffusional release of noble gas and volatile fission products (e.g., Xe, Kr, Cs, I) has been observed in a number of high-temperature, postirradiation annealing experiments with trace-irradiated polycrystalline UO_2 fuel samples[31] and high-burnup specimens taken from commercial spent fuel rods.[32–39] In particular, the idealized Booth model[28] has been used extensively to interpret the diffusive release of the more volatile fission products in these postirradiation annealing experiments. The equivalent-sphere model has also been generalized in that a nonuniform fission product concentration is assumed to exist in the grains during the irradiation period when the fuel temperatures are sufficiently high to allow diffusion to occur.[40] However, in many out-of-pile experiments in which polycrystalline UO_2 is annealed at high temperature, the release is found to be much more rapid than expected from ideal release kinetics based on diffusion theory. For example, an initial burst (due to a release from the grain boundary inventory) followed by a slower diffusional component, has been reported by Peehs et al., based on a number of Knudsen cell experiments with small UO_2 samples from spent light water reactor (LWR) fuel rods.[35–37] In experiments performed with bare fuel fragments from spent Canadian deuterium-uranium (CANDU) reactor rods, a slow diffusional release occurred, followed by a more rapid release (in accordance with first-order kinetics) when the fuel was oxidized in steam to small values of the stoichiometry deviation in the UO_{2+x} phase.[41] On the other hand, only a diffusional release of cesium was observed for spent fragments annealed in a reducing (hydrogen-rich) atmosphere.[41,42]

Aside from temperature, stoichiometry of the UO_2 is the most important parameter controlling fission product mobilities. The effects of UO_2 oxidation are discussed below in Sect. 3.1.1.5.

3.1.1.4 Transport in the Fuel-Cladding Gap

Historically, a number of steady-state models have been proposed to describe the transport behavior of volatile fission products in the fuel-cladding gap of defective fuel rods during normal reactor operation. The early work of Helstrom suggested that the rate-determining process for noble gas transport in the gap was atomic diffusion within a bulk steam environment.*,[43] The empirical model of Allison and Rae estimated the effect of the axial path length on the holdup of the radioactive noble gases.[44] In other treatments, in accordance with a first-order rate process, the coolant release was assumed to be proportional to the total inventory in the gap where the proportionality constant was defined as an "escape-rate" coefficient.[45–47] The chemical holdup of iodine, presumably on the internal sheath surface, was also modeled with an adsorption isotherm. This latter method has been used extensively in the analysis of the gap release of fission product iodine and noble gases in defective fuel rods in pressurized-water reactors (PWRs).[45–50] The treatment of Kalfsbeek also considered competing diffusive and bulk-convective transport processes in boiling-water reactor (BWR) fuel pins.[51] More recently, a kinetic model was used for estimating the effect of defect size on the release behavior of iodine and noble gases from defective fuel pins in LWRs and CANDU reactors.†,[52–55] A more general treatment has considered axial diffusion along the gap where release into the coolant is modeled as a surface-exchange process, thereby accounting for the effects of defect location and size.[56]

During a loss-of-coolant temperature transient, iodine and cesium transport from the fuel-to-sheath gap have been modeled empirically as a burst release that is carried out by the escaping plenum gas when the rod ruptures, followed by a diffusional-release component.[57]

3.1.1.5 Effects of UO_2 Oxidation

UO_2 fuel may become oxidized to varying degrees during normal irradiation, after failure of a fuel rod under normal operating conditions, or during severe accident conditions. The consequence of even small increases in the oxygen content (leading to formation of hyperstoichiometric

*C. Helstrom, "Emission Rate of Fission Products from a Hole in the Cladding of a Reactor Fuel Element," AECU 3220, July 1956.

†D. L. Burman, "Methods for Estimating Numbers of Failed Rods from Coolant Activity Analysis," presented at the EPRI Workshop on Fuel Integrity Monitoring by Coolant Activity Analysis, Charlotte, North Carolina, May 21, 1986.

UO_{2+x}) is a general increase in the release rates for many fission products. The phenomena associated with UO_2 oxidation and significance to fission product release are described in this subsection.

During irradiation, fission of uranium and plutonium causes the average oxygen/metal (O/M) ratio (stoichiometry) to increase with burnup due to the different oxidation states of the fission products and the fuel. The O/M ratio is predicted to vary across the UO_2 radius due to the radial temperature profile and corresponding variation in oxygen potential.[58] This deviation from stoichiometry can lead to increased fission product mobilities and is important for modeling the behavior of fuel at extended burnup, but it is of minor importance to severe accident conditions, aside from its effect on the chemical forms of fission products in the fuel before the accident sequence.

If the Zircaloy fuel cladding fails under normal operation or in accident conditions, the environment inside the fuel rod can become oxidizing with respect to the UO_2. The UO_2 can incorporate excess oxygen to form hyperstoichiometric UO_{2+x} or be converted to higher oxides such as U_4O_9, U_3O_7, or U_3O_8, depending on the temperature and oxygen potential.[59] In air at atmospheric pressure, the UO_2 can be oxidized to U_3O_8 at temperatures below about 1500°C; at higher temperatures UO_{2+x} is the highest oxide formed. The oxygen potential of steam is lower than air and varies with temperature and total pressure. In steam, UO_{2+x} is the oxidation limit above about 1050°C, and U_4O_9 is formed at lower temperatures. U_3O_8 is predicted to form below about 900°C in steam at atmospheric pressure. At higher steam pressures, the oxygen partial pressure increases, and U_3O_8 can be formed at higher temperatures.[60]

The consequences of U_3O_8 formation include enhanced fission product releases and degradation of the fuel. There is a volume expansion of about 32% upon oxidation to U_3O_8, and this results in fragmentation of the fuel matrix with production of a fine powder (2- to 10-μm particles) in the temperature range 400 to 700°C. At higher temperatures, the U_3O_8 is more plastic and does not form a fine powder. The releases of noble gases and volatile fission products due to U_3O_8 formation have been measured in experiments.[61–66] Up to 100% of the noble gases and large fractions of the inventory of iodine and cesium are rapidly released during air oxidation in the temperature range 400 to 1100°C. These releases were attributed to enhanced diffusion in U_3O_8, sweeping by the phase transformation from UO_2 to U_3O_8, and cracking of the matrix from the volumetric expansion. Below 400°C, the releases of noble gas were 5 to 8% of the inventory and were attributed to the phase transformation.[67]

The oxidation of UO_2 in steam has been studied by a number of investigators in experiments performed out-of-pile.[68–72] In the early work of Bittel et al.,[68] it was suggested that the oxidation process was controlled by oxygen diffusion through the fuel matrix. However, Carter and Lay[69] subsequently showed that the oxidation in mixtures of CO_2/CO was controlled by a reaction at the solid/gas interface, characterized by a surface-exchange coefficient. The surface exchange coefficient in steam was determined experimentally by Cox et al.,[72,73] in the temperature range 800 to 1600°C. In mixtures of steam and hydrogen, the equilibrium UO_2 stoichiometry decreases with increasing hydrogen content; however, even a few percent of steam in a hydrogen-rich gas can be oxidizing to stoichiometric UO_2 at high temperatures.

An increase in the UO_2 stoichiometry without transformation to a higher oxide (i.e., oxidation in steam/H_2 mixtures) results in the direct enhancement of the diffusional release of fission products from the fuel matrix.[73–77] Recent experimental work has indicated that xenon diffusion occurs as a neutral tri-vacancy in UO_2 (Ref. 76), in agreement with the theoretical calculations of Grimes and Catlow.[78] However, these calculations also indicate that in UO_{2+x} the most stable solution site is the uranium vacancy. This finding supports the model of Killeen and Turnbull[77] for the noble gas diffusion coefficient in UO_{2+x} (for x in the range of 0.005 to 0.1), where it has been assumed that the gas atom mobility is influenced by the presence of the uranium cation vacancies in which Frenkel and Schottky equilibria govern the isolated point defects. This model for the diffusion coefficient is in agreement with the experimental work of Lindner and Matzke.[73] It has been used to describe the in-pile steady-state release of fission gas from detective fuel rods[79] and the cesium release kinetics from bare and Zircaloy-clad fuel specimens taken from commercial spent fuel rods and annealed at high temperature in steam. In particular, it has been shown that hydrogen production from the Zircaloy-steam reaction can inhibit the oxidation of the UO_2 fuel that, in turn, can delay the release of cesium from the Zircaloy-clad fuel relative to the release from the bare UO_2.

Another phenomenon that contributes to fission product releases in oxidizing accident conditions is volatilization of the fuel. Volatilization of the UO_2 is a process by which the condensed phase is vaporized due to the formation of a volatile uranium-bearing species. In air, steam, or steam/H_2 mixtures, the process is incongruent vaporization with the formation of gaseous UO_3. Volatilization can be rapid at temperatures above 1500°C (Ref. 72). As the matrix is volatilized, the low-volatility fission products that were previously inside the fuel become concentrated at the surface, where they can accumulate or else be vaporized or

entrained in the flowing gases as particulates. This process has been described by Alexander[80–82] as "matrix stripping." Experiments with bare UO_2 in air at 1800 to 2100°C produced significant UO_2 volatilization and resulted in >50% release of the low-volatility Zr, La, Nb, and Ce fission products.[83] In steam, or in the presence of unoxidized Zircaloy, the volatilization rate and corresponding fission product release rates are expected to be lower.[84]

3.1.1.6 UO_2-Zircaloy Chemical Interactions

The chemical interactions between Zircaloy cladding and UO_2 have been extensively studied up to the melting point of Zircaloy-4 (Refs. 85 and 86) and at higher temperatures.[87,88] The UO_2 can be liquefied by dissolution with molten Zircaloy at temperatures as low as about 1900°C. During the interaction process, a uranium-rich molten metallic phase is produced on the UO_2 grain boundaries in response to oxygen removal by interaction with the Zircaloy. This metallic melt results in liquefaction of the grain boundaries and can act as a pathway for escape of fission products to the pellet surface by bubble migration.[89] Complete liquefaction of the UO_2 can also result from interaction with molten Zircaloy, and this may cause further fission product releases as the crystalline matrix is dissolved and gas bubbles migrate through the bulk melt phase. Because bubble migration in liquids is much faster than diffusion in solids, it is expected that dissolution of UO_2 should lead to enhanced fission product releases. However, it is possible that the liquid phase could act as a trap for large gas bubbles, producing a foamlike microstructure in which large gas bubble are stable. Such microstructures have been observed in the Annular Core Research Reactor (ACRR) ST-1 experiment,[90] the FLHT-4 and FLHT-5 tests (unpublished results), and the out-of-pile Oak Ridge National Laboratory (ORNL) VI-4 test (unpublished result). Enhanced releases during UO_2 dissolution have been confirmed with small pieces of fuel in out-of-pile tests,[91] but no definitive in-reactor data have been produced.

3.1.1.7 Microcracking and the Effect of Quenching/Reflood

Microcracking of the UO_2 ceramic in response to transient heating or rapid quenching has been proposed as a mechanism for releasing noble gases and volatile fission products. During rapid transient heating or cooling, steep temperature gradients exist in the UO_2, and the corresponding stresses are thought to be responsible for microcracking along grain boundaries (intergranular) or across the grains (intragranular). Out-of-pile tests in the Argonne Direct-Electric-Heating (DEH) program[92] indicated that the presence of gas bubbles on the grain boundaries enhanced microcracking and radial constraint of the fuel tended to inhibit microcracking.

Extensive cracking, both intergranular and transgranular, has been observed in fuel fragments in the upper debris beds in Three Mile Island Unit 2 (TMI-2)[93] and a severe fuel damage scoping test (SFD-ST).[94] The intersection of microcracks with porosity trapped at grain boundaries has been used to explain fission gas release upon cooling from high-temperature transients[95] and reflooding.[93,94] Most of the fission product release in Power Burst Facility (PBF) SFD-ST occurred after reflood was initiated.[94] It should also be noted that reflooding a hot core can cause a temperature excursion due to accelerated Zircaloy-water reaction that, in turn, can cause enhanced fission product release. The majority of fission product release in the loss-of-fluid test (LOFT) FP-2 test has been attributed to a temperature excursion upon reflood.[96]

It is expected that the enhancement upon reflood of the release of noble gases and volatile fission products should be strongest for trace-irradiated and low-burnup (<5-MWd/kg U) fuels. In the low-burnup fuels, volatile fission products would be transported to grain boundaries in the heatup transient and be available for release during reflood due to grain boundary cracking or the formation of microcracks that intersect grain boundaries. On the other hand, volatile fission products in high-burnup fuel would have collected at grain boundaries during normal operation and would have been released during the heatup, leading to relatively minor additional releases upon reflood.

3.1.1.8 Release from Debris Beds

Debris beds can be formed by fragmentation of fuel denuded of cladding and fuel rods having oxygen-embrittled cladding. Thermal shock following liquid coolant introduction into a hot core can fragment fuel in either of these conditions.[94,97,98] Additionally, cladding melting and runoff in regions of the core with a reducing atmosphere in a steam-starved transient can cause loss of cladding restraint and fuel disassembly.[99] In debris beds formed by any of these mechanisms, the mean particle size is about 1 mm and is related to the cracking pattern within the fuel developed before the accident by power changes associated with reactor startups and shutdowns.[100] This particle size is 2 orders of magnitude larger than fuel grain size. As a consequence, the release of noble gases and volatile fission products from debris beds should be little different from that in rod geometry where release is governed principally by migration to grain boundaries and subsequent release through interconnected tunnels.

3.1.1.9 Release from Molten Pools

Molten pools of primarily $(U,Zr)O_2$ ceramic formed in the TMI-2 accident[98] and in SFD tests.[94,97,101–104] Analysis of fission product release from the molten ceramic pool in the TMI-2 accident indicates that the

fission product chemical form and concentration dominated the release of medium- and low-volatile fission products and that bubble dynamics dominated the release of fission gases and volatile fission products.[93]

Fission product chemical forms are influenced by the oxygen potential of the molten pool. Fission products such as lanthanum, cerium, and strontium would exist as oxides (La_2O_3, Ce_2O_3 or CeO_2, and SrO) in most accidents in all but the most reducing conditions (H_2/H_2O ratio >100). La_2O_3 and Ce_2O_3 are soluble in $(U,Zr)O_2$, which reduces their already low volatilities. Ruthenium and antimony would be present as metals immiscible in the ceramic melt but soluble in other metallic melts such as nickel, which reduces their volatility. Low releases are calculated for these materials primarily because of the low concentration and low volatility (including the decrease in chemical activity due to solubility) of these species in the melt and the low surface-to-volume ratio of the molten region.[93] Virtually all of the fission gases and volatile fission products should be released from the melt due to bubble coalescence and buoyancy.[93] However, cesium has been found in the molten debris transported to the lower plenum of the TMI-2 reactor vessel.[105,106] The retention of cesium in a previously molten ceramic was unexpected and suggests that some cesium may have been present in a chemical form stable at very high temperatures.

In addition to the unfavorable surface-to-volume ratio, molten ceramic pools are surrounded by oxidic crusts. These crusts tend to be self-healing so that fission products released from the melt must diffuse through the crust to escape. There may be a strong temperature gradient through the crust, from the temperature of the $(U,Zr)O_2$ melt on the inside surface to much lower temperatures on the outside. The rate-limiting process for fission product release from such a geometry may be diffusion through the crust or vaporization from the surface of the crust.

The long-term (10- to 20-h) release of fission products, primarily the lower volatility species such as Ba, Sr, and La, from molten pools that may be contained in the lower head of a reactor vessel following core melting and relocation is uncertain and of significance for accident management strategies.

3.1.1.10 Release from Molten Fuel-Coolant Interaction

Molten fuel-coolant interactions (MFCIs) may occur during the relocation of fuel-bearing melt into a pool of liquid coolant. This phenomenon took place in the TMI-2 accident during the relocation of ceramic fuel-bearing melt from the core to the lower plenum. A transitional geometry that is between the starting molten ceramic pool geometry and the final solid debris geometry is produced. Release during an MFCI is probably a function of the melt surface area produced by the MFCI and the time duration of the interaction. The gravity drain of melt into a reactor lower plenum is a fairly rapid process as evidenced by the 1- to 2-min duration of the melt relocation event in the TMI-2 accident.[98] If the molten fuel pour breaks up into fragments as fine as the smallest of the resulting debris (≈1 mm in the case of TMI-2), a large surface area could be produced. However, little remains of the noble gases and volatile fission products to be released at this stage of a severe accident, and the short time duration of the MFCI strongly limits the release of less volatile fission products. Although there have been no direct measurements of fission product release during a MFCI, all indications from the analyses of the TMI-2 accident are that the releases must be small relative to releases due to other phenomena already treated.[93,100]

3.1.2 Nonfission Product Material Releases

3.1.2.1 Ag-In-Cd Release

PWRs utilize stainless steel clad Ag-In-Cd control rods (80% Ag, 15% In, and 5% Cd) that are housed in Zircaloy guide tubes. The control alloy is molten at temperatures above 1100 K but is contained within the stainless steel cladding. Pressures exerted by the cadmium vapor and fill gas are sufficient to cause the stainless steel cladding to balloon out and contact the Zircaloy guide tube in accidents with low system pressure (<1 MPa). It has been observed in out-of-pile low-pressure tests that, at points of contact, chemical interaction between the stainless steel and Zircaloy causes control rod failure due to liquid formation at about 1500 K.[107,108] In high-pressure accident scenarios, control rod failure does not occur until stainless steel melting at about 1700 K.[109]

The molten Ag-In-Cd alloy is incompatible with Zircaloy, dissolving it very rapidly at temperatures in the neighborhood of 1500 K (Refs. 108 and 110) There is a tendency at low system pressure for the molten Ag-In-Cd alloy to be widely dispersed throughout the core, driven by overpressure within the control rod at the time of failure.[109] In high-pressure sequences, the alloy is released less energetically and is more likely to flow down the inside and outside of the guide tubes.

Some of the molten Ag-In-Cd alloy vaporizes in the core and condenses into aerosols as it enters cooler regions above the core. The releases of Ag, In, and Cd from the core are fairly modest in high-pressure accident scenarios, as is demonstrated by results from the PBF SFD 1-4 test[100] (6.95 MPa) in which the measured release fractions were

2.7×10^{-4} (Ag), 8.8×10^{-4} (In), and 6.2×10^{-2} (Cd). Nonetheless, these releases accounted for 3% (Ag), 2% (In), and 40% (Cd) of the nonfission product release from this core-melt experiment. In the low-pressure LOFT LP-FP-2 experiment[111] (1.1 MPa), the fractional release of silver was much greater (1.7×10^{-3}) and accounted for 86% of the aerosol released from the core.

3.1.2.2 Tin Releases

Zircaloy-4 is the principal material used in a PWR for the fuel cladding and guide tubes. It comprises 98.5% zirconium and 1.5% tin, together with minor alloying elements, and melts at ~2075 K. The vapor pressure of tin is much higher than for zirconium, and it is therefore possible that tin could be a significant source of aerosols in a severe accident. However, the situation is complicated by a number of factors associated with zirconium oxidation[112] and the reduced activity of tin in zirconium.[112, 113]

A few studies have examined the release of tin from Zircaloy at high temperatures. Mulpuru[114] has reported release rates for tin and other constituents of Zircaloy-4 at 2273 to 2473 K. Bowsher has conducted mass spectrometric studies that characterize the release of tin from unoxidized and oxidized Zircaloy samples.[115] No release of tin was observed from unoxidized Zircaloy up to ~2120 K, implying a reduction in activity by a factor of at least 10^3. A simple Raoult's law analysis predicted reduction in activity by a factor of 0.015. At ~1820 K no release was detected from the pre-oxidized sample, but on raising the temperature to 2020 K a weak signal was observed, indicating a tin activity of 2×10^{-4}. A similar study by Alexander and Ogden measured the thermodynamic activities of tin in Zircaloy by using Knudsen cell mass spectrometry over a wide temperature range.[113] An expression for the activity coefficient of tin in Zircaloy-4 (γ) was derived:

$$\ln \gamma = \frac{(2700 \pm 670)}{T} - (5.57 \pm 0.41) ,$$

where T is the absolute temperature in degrees kelvin. It was also concluded that, even though Zircaloy oxidizes under the steam conditions of an accident, the conditions will be sufficiently reducing to leave tin in its elemental form. Alexander and Ogden[113] concluded that SnTe would become the predominant vapor-phase species at tin activities of 0.1 or higher.

3.1.2.3 Boric Acid

The behavior of boric acid in a severe accident represents a significant uncertainty in defining the source term. The principal source of boric acid in most PWRs is in the primary circuit coolant where it is used as a soluble moderator. The concentration is varied during the fuel cycle so that it is at a maximum of ~1200 ppm (boron) with fresh fuel and is systematically reduced to 50 ppm (boron).[115,116] Typically, 700 kg boric acid is present in the primary circuit, with an additional 40,000 kg present in the emergency core cooling system (ECCS) and other sources such as accumulators.[117] The role of boric acid will be very much sequence dependent. In a low-pressure sequence, such as an AB hot-leg break, much of the primary circuit coolant will be ejected from the primary circuit; in a containment bypass sequence such as a V sequence, 95% of the coolant is predicted to be lost before fission product release. However, in a TMLB high-pressure sequence, the loss of coolant will be relatively slow and will result in significant concentrations of boric acid present at the time of fission product release. Boric acid is not used in the primary coolant system of a BWR, although it has been postulated that the boron carbide control fins could react with steam in an accident to form an oxidized boron species.[118] Release of boric acid from the core of an LWR would be expected to occur via a number of mechanisms:

1. flashing and violent boiling of the reactor coolant early in the accident sequence, resulting in the formation of boric acid aerosols;
2. overheating of the core resulting in some vaporization of boric acid and crystallization of boric oxide;
3. injection of the borated ECCS, resulting in flash boiling and formation of boric acid aerosols; and
4. vaporization of boric oxide deposits on the fuel and reactor circuit surfaces by flashing of water when the core slumps into water in the lower plenum.

It has been proposed that boric acid can modify the transport and deposition of fission products in two main ways:

1. Chemical reactions in which the speciation (and therefore physical properties) of the released fission products is changed. The most important examples of this are CsOH and CsI, which react with boric acid to form $CsBO_2$ and HI. $CsBO_2$ is less reactive and volatile than either CsOH or CsI; HI is considerably more reactive and volatile than CsI.
2. Aerosol particles formed by condensation of vapor-phase boron species can act as centers for condensation of fission products. Studies conducted at Winfrith Technology Centre[119] have demonstrated that two types of particle are formed when boric acid solution comes into contact with a hot surface (i.e., a situation representative of flash boiling in an accident): (1) large (≈20-μm volume equivalent diameter) deposits with complex crystalline features and (2) small (0.1-μm volume equivalent diameter) spherical particles that

agglomerated to form deposits of 1.0-μm volume equivalent diameter.

The larger particles were formed by flashing of the aqueous solution in contact with the hot steel surface and the smaller ones by vaporization and subsequent condensation of boric acid. The size distribution and density of the boric acid aerosol will significantly affect the subsequent transport and deposition of fission products in the primary circuit and containment. Because of the hygroscopic nature of CsOH, CsOH aerosol particles transported to the containment would tend to absorb water, even at low relative humidities. This will lead to an enhanced deposition rate. However, the $CsBO_2$ aerosol formed in the presence of boric acid would not absorb water so rapidly (or at all) and would therefore remain suspended for a greater time. This could have the effect of increasing the potential source term to the environment.

3.1.2.3 Other Structural Materials

Other structural materials that might contribute to the non-fission product material releases under severe accident conditions include the constituents of Inconel and stainless steels (primarily Fe, Ni, Cr); BWR control blade materials (stainless steel with boron carbide); and a variety of burnable poison materials such as alumina with boron carbide, dysprosia, and gadolinia. UO_2 is excluded from consideration here because uranium-bearing releases were described in Sect. 3.1.1.5 as part of UO_2 oxidation discussions. Compared with the Ag, In, Cd, Sn and boric acid, all of these other materials are expected to make small contributions to the total material releases.

3.1.3 References

1. A. G. Croff, Union Carbide Corp. Nucl. Div., Oak Ridge National Laboratory, "ORIGEN-2: A Revised and Updated Version of the Oak Ridge Isotope Generation and Depletion Code," ORNL-5621, 1980.*

2. E. H. P. Cordfunke and R. J. M. Konings, Eds., *Thermodynamic Data for Reactor Materials and Fission Products* (North Holland, Amsterdam, 1990).

3. E. H. P. Cordfunke and R. J. M. Konings, "Chemical Interactions in Water-Cooled Nuclear Fuel: A Thermochemical Approach," *J. Nucl. Mater.* 152, 301 (1988).†

4. S. Imoto, "Chemical State of Fission Products in Irradiated UO_2," *J. Nucl. Mater.* 140, 19 (1986).†

5. H. Kleykamp, "The Chemical State of the Fission Products in Oxide Fuels," *J. Nucl. Mater.* 131, 221 (1985).†

6. K. Naito, T. Tsuji, T. Matsui, and A. Date, "Chemical State, Phases and Vapor Pressures of Fission-Produced Noble Metals in Oxide Fuel," *J. Nucl. Mater.* 154, 3 (1988).†

7. C. Ronchi and C. T. Walker, "Determinations of Xenon Concentrations in Nuclear Fuels by Electron Microprobe Analysis," *J. Phys. D.: Appl. Phys.* 13, 2175 (1980).†

8. M. Mogensen, J. Als-Nielsen, and N. H. Andersen, "Determination of Fission Products in Irradiated Fuel by X-Ray Fluorescence," Riso National Laboratory, RISO-M-2599, Denmark (1986).

9. D. Cubicciotti and B. R. Sehgal, "Vapor Transport of Fission Products in Postulated Severe Light Water Reactor Accidents," *Nucl. Technol.* 65, 266 (1984).†

10. L. H. Johnson and H. H. Joling, "Fission Product Leaching Form Used CANDU Fuel: An Estimate of Fuel-Sheath Gap and Grain Boundary Inventories and Probable Release After Disposal," Atomic Energy of Canada Limited Technical Record, TR-280, Canada (1984).

11. C. T. Walker and K. Lassmann, "Fission Gas and Cs Gradients in Single Grains of Transient Tested UO_2 Fuel: Results of an EPMA Investigation," *J. Nucl. Mater.* 138, 155 (1986).†

12. S. Ukai, T. Hosokawa, I. Shibahara, and Y. Enokido, "Evaluation of the Fission Gas Release Behavior From Fast Reactor Mixed Oxide Fuel Based on Local Concentration Measurement of Retained Xenon," *J. Nucl. Mater.* 151, 209 (1988).†

13. C. E. L. Hunt et al., "Fission Product Grain Boundary Inventory," *Proceedings of CNS 10th Annual Conference, Ottawa, June 7–10, 1989*, Atomic Energy of Canada Limited, Report AECL-10036, Canada (1989).

14. H. Kleykamp, Post-Irradiation Examinations and Composition of the Residues from Nitric Acid

Dissolution Experiments of High-Burnup LWR Fuel, *J. Nucl. Mater.* 171, 181 (1990).†

15. M. Mogensen, C. Bagger, and C. T. Walker, "An Experimental Study of the Distribution of Retained Xenon in Transient-Tested UO_2 Fuel," *J. Nucl. Mater.* 199, 85 (1993).†

16. I. J. Hastings, C. E. L. Hunt, J. J. Lipsett, and R. D. MacDonald, "Test to Determine the Release of Short-Lived Fission Products from UO_2 Fuel Operating at Linear powers of 45 and 60 kW/m: Method and Results," Atomic Energy of Canada Limited Report AECL-7920, Canada (September 1985)

17. C. A. Friskney and M. V. Speight, "A Calculation on the In-Pile Diffusional Release of Fission Products Forming a General Decay Chain," *J. Nucl. Mater.* 62, 89 (1976).†

18. Friskney, C. A. and J. A. Turnbull, "The Characteristics of Fission Gas Release from Uranium Dioxide during Irradiation," *J. Nucl. Mater.* 79, 184 (1979).†

19. J. A. Turnbull et al., "The Diffusion Coefficients of Gaseous and Volatile Species during the Irradiation of Uranium Dioxide," *J. Nucl. Mater.* 107, 168 (1982).†

20. J. A. Turnbull, R. J. White, and C. Wise, "The Diffusion Coefficient for Fission Gas Atoms in Uranium Dioxide," *Proceedings of the IAEA Technical Committee Meeting on Water Reactor Fuel Element Computer Modelling in Steady State, Transient and Accident Conditions, Preston, United Kingdom, September 18–22, 1988*, International Atomic Energy Agency, IAEA-IWGFPT-32, Austria (1988).

21. I. J. Hastings, C. E. L. Hunt, and J. J. Lipsett, "Release of Short-Lived Fission Products from UO_2 Fuel: Effects of Operating Conditions," *J. Nucl. Mater.* 130, 407 (1985).†

22. B. J. Lewis, C. E. L. Hunt, and F. C. Iglesias, "Source Term of Iodine and Noble Gas Fission Products in the Fuel-to-Sheath Gap of Intact Operating Nuclear Fuel Elements," *J. Nucl. Mater.* 172, 197 (1990).†

23. A. D. Appelhans and J. A. Turnbull, "Measured Release of Radioactive Xenon, Krypton, and Iodine from UO_2 at Typical Light Water Reactor Conditions, and a Comparison with Release Models," USNRC Report NUREG/CR-2298, 1981.*

24. I. Ursu, C. Gheorghiu, C. Soare, and E. Gheorghiu, "Behavior of Short-Lived Fission Products in UO_2 Fuel Elements during Steady Power Operation," *Rev. Roum. Phys., Tome* 32 (9) 951–960 (1987).

25. Hj. Matzke, "Diffusion in Ceramic Oxide Systems," *Adv. Ceramics* 17, 1 (1986).†

26. C. Wise, "Recoil Release of Fission Products from Nuclear Fuel," *J. Nucl. Mater.* 136, 30 (1985).†

27. B. J. Lewis, "Fission Product Release from Nuclear Fuel by Recoil and Knockout," *J. Nucl. Mater.* 148, 28 (1987).†

28. A. H. Booth, "A Method for Calculating Fission Gas Diffusion from UO_2 Fuel and Its Application to the X-2-f Loop Test," Atomic Energy of Canada Limited Report, AECL-496, Canada (1957).

29. G. V. Kidson, "A Generalized Analysis of the Cumulative Diffusional Release of Fission Product Gases from an Equivalent Sphere of UO_2," *J. Nucl. Mater.* 88, 299 (1980).†

30. S. E. Turner et al., "*Background and Derivation of the ANS 5.4 Standard Fission Product Release Model*," USNRC Report NUREG/CR-2507, 1982.*

31. S. G. Prussin, D. R. Olander, W. K. Lau, and L. Hansson, "Release of Fission Products (Xe, I, Te, Mo and Tc) from Polycrystalline UO_2," *J. Nucl. Mater.* 154, 25 (1988).†

32. M. F. Osborne, J. L. Collins, and R. A. Lorenz, "Experimental Studies of Fission Product Release from Commercial Light Water Reactor Fuel Under Accident Conditions," *Nucl. Technol.* 78, 157 (1987).†

33. M. F. Osborne, R. A. Lorenz, J. L. Collins, and T. Nakamura, "Time-Dependent Release of Fission Products from LWR Fuel Under Severe Accident Conditions," p. 1293 in *Proceedings of the International Conference on Thermal Reactor Safety, Avignon, France, October 2–7, 1988*, Societé Francaise d' Energie Nucleaire, Paris, France (1988).

In-Vessel

34. T. S. Kress, R. A. Lorenz, T. Nakamura, and M. F. Osborne, "Correlation of Recent Fission Product Release Data," ICHMT Seminar on Fission Product Transport Processes in Reactor Accidents, Dubrovnik, Yugoslavia, May 22–26, 1989, in *Fission Product Transport Processes in Reactor Accidents*, J. T. Rogers, Ed. (Hemisphere Publishing, 1990).

35. M. Peehs, G. Kaspar, and K. H. Neeb, "Cs and I Source Terms of Irradiated UO_2," *Proceedings of Topical Meeting on Fission Product Behavior and Source Term Research, Snowbird, Utah, July 15–19, 1984*, Electric Power Research Institute, 1985.

36. M. Peehs, G. Kaspar, and F. Sontheimer, *Cs and I Source Terms of Irradiated UO_2*, IAEA Technical Committee on Fuel Rod Internal Chemistry and Fission Product Behavior, Karlsruhe, FRG, November 11–15, 1985, International Atomic Energy Agency, IWGFPT/25, Austria (October 1986).

37. G. Kaspar and M. Peehs, 'Transient Release of Iodine and Cesium from Irradiated UO_2 in Presence of Zircaloy and Oxygen," p. 444 in *Proceedings of the Workshop on Chemical Reactivity of Oxide Fuel and Fission Product Release, Gloucestershire, United Kingdom, April 7–9, 1987*, Central Electricity Generating Board (1987).

38. D. S. Cox et al., "Fission-Product Release Kinetics from CANDU and LWR Fuel During High-Temperature Steam Oxidation Experiments," *Proceedings of IAEA Technical Committee Meeting on Fission Gas Release and Fuel Rod Chemistry Released to Extended Burnup, Pembroke, Ontario, Canada, April 28–May 1, 1992*, International Atomic Energy Agency, IAEA-TEC-DOC-697, Austria (April 1993).

39. D. S. Cox, Z. Liu, R. S. Dickson, and P. H. Elder, "Fission-Product Release During Post-Test Annealing of High-Burnup CANDU Fuel," Third International Conference on CANDU Fuel, Pembroke, Ontario, Canada, October 4–8, 1992, Canadian Nuclear Society (1992).

40. B. J. Lewis and F. C. Iglesias, "A Model for Calculating Fission Gas Diffusion in Annealing Experiments," *J. Nucl. Mater.* 154, 228 (1988).†

41. B. J. Lewis, F. C. Iglesias, C. E. L. Hunt, and D. S. Cox, "Release Kinetics of Volatile Fission Products Under Severe Accident Conditions," *Nucl. Technol.* 99, 330 (1992).†

42. J. M. Dumas, G. Lhiaubet, G. Lemarois, and G. Ducros, "Fuel Behavior and Fission Product Release Under Realistic Hydrogen Conditions: Comparison Between HEVA 06 Test Results and VULCAIN Computations," ICHMT Seminar on Fission Product Transport Processes in Reactor Accidents, Dubrovnik, Yugoslavia, May 22–26, 1989, in *Fission Product Transport Processes in Reactor Accidents*, J. T. Rogers, Ed. (Hemisphere Publishing, 1990).

43. B. Lustman, "Irradiation Effects in Uranium Dioxide," in J. Belle, *Uranium Dioxide: Properties and Nuclear Applications* (U.S. Government Printing Office, Washington, D.C., 1961), Chap. 9, pp. 431–666.

44. G. M. Allison and H. K. Rae, "The Release of Fission Gases and Iodine from Defected UO_2 Fuel Elements of Different Lengths," Atomic Energy of Canada Limited Report AECL-2206, Canada, June 1965.

45. P. Bourgeois and J. P. Stora, "Behavior of Fission Products in PWR Primary Circuits and Defected Fuel Rod Evaluation," p. C1/1 (1–8) in *Proceedings of the 5th International Conference on Structural Mechanics in Reactor Technology, Berlin, Federal Republic of Germany, March 20, 1979*, North Holland, Amsterdam (1979).

46. P. Beslu, C. Leuthrot, and G. Frejaville, "PROFIP Code: A Model to Evaluate the Release of Fission Products from Defected Fuel in PWRs," *Proceedings of the Specialists' Meeting on Defected Zirconium Alloy Clad Ceramic Fuel in Water Cooled Reactors, Chalk River, Canada, September 1979*, International Atomic Energy Agency, IWGFPT/6, Austria (1980).

47. R. Beraha, G. Beuken, G. Frejaville, C. Leuthrot, and Y. Musante, "Fuel Survey in the Light Water Reactors Based on the Activity of the Fission Products," *Nucl. Technol.* 49, 426 (1980).†

48. C. Leuthrot, A. Brissaud, and J. P. Missud, "Relationships Between the Characteristics of Cladding Defects and the Activity of the Primary Coolant Circuit and Aid for the Management of Leaking Fuel Assemblies in PWR," pp. 324 in *Proceedings of the International Topical Meeting on LWR Fuel Perfor-*

mance, Avignon, France, April 21–24, 1991, Societé Francaise d' Energie Nucleaire, Paris, France (1991).

49. J. T. Mayer, E. T. Chulick, and V. Subrahmanyam, *B&W Radiochemical Analyses for Defective Fuel*, pp. 221 in *Proceedings of the Specialists' Meeting on Defected Zirconium Alloy Clad Ceramic Fuel in Water Cooled Reactors, Chalk River, Canada, September 17–21, 1979*, International Atomic Energy Agency, IWGFPT/6, Austria (1980).

50. H. Zanker, "Defective Fuel Rod Detection in Operating Pressurized Water Reactors During Periods of Continuously Decreasing Fuel Rod Integrity Levels," *Nucl. Technol.* 86, 239 (1989).†

51. H. W. Kalfsbeek, "The Abundance of Fission Gases in the Off Gas of a Boiling Water Reactor," *Nucl. Technol.* 61, 7 (1983).†

52. D. L. Burman et al., *Development of a Coolant Activity Evaluation Model and Related Application Experience*, pp. 363 in *Proceedings of the International Topical Meeting on LWR Fuel Performance, Avignon, France, April 21–24, 1991*, Societé Francaise d' Energie Nucleaire, Paris, France (1991).

53. C. E. Beyer, "Methodology Estimating Number of Failed Fuel Rods and Defect Size," Electric Power Research Institute, EPRI NP-6554, September 1989.

54. C. E. Beyer, "An Analytical Model for Estimating the Number and Size of Defected Fuel Rods in an Operating Reactor," pp. 437 in *Proceedings of the International Topical Meeting on LWR Fuel Performance, Avignon, France, April 21–24, 1991*, Societe Francaise d' Energie Nucleaire, Paris, France (1991).

55. B. J. Lewis, R. J. Green, and C. W. T. Che, "A Prototype Expert System for the Monitoring of Defected Nuclear Fuel Elements in CANDU Reactors," *Nucl. Technol.* 98, 307 (1992).†

56. B. J. Lewis, "A Generalized Model for Fission-Product Transport in the Fuel-to-Sheath Gap of Defective Fuel Elements," *J. Nucl. Mater.* 175, 218 (1990).†

57. R. A. Lorenz, J. L. Collins, and A. P. Malinauskas, "Fission Product Source Terms for the Light Water Reactor Loss-of-Coolant Accident,' *Nucl. Technol.* 46, 404 (1979).†

58. I. Johnson, C. E. Johnson, C. E. Crouthamel, and C. A. Seils, "Oxygen Potential of Irradiated Urania-Plutonia Fuel Pins," *J. Nucl. Mater.* 48, 21 (1973).†

59. K. Naito and N. Kamegashira, "High Temperature Chemistry of Ceramic Nuclear Fuels with Emphasis on Nonstoichiometry," in *Advances in Nuclear Science and Technology*, E. J. Henley and J. Lewins, Eds. (Academic Press, 1976), Vol. 9, 99–180.

60. D. R. Olander, "Oxidation of UO_2 by High Pressure Steam," *Nucl. Technol.* 74, 215 (1986).†

61. H. C. Stoner, J. R. Matthews, and M. H. Wood, "Possible Effects of Oxidation on Transient Release of Fission Gas from UO_2," Report AERE-M.3152, United Kingdom (January 1981).

62. P. Wood and G. H. Bannister, "Release of Fission Products During and After Oxidation of Trace-Irradiated Uranium Dioxide at 300–900°C," *Proceedings of IAEA Specialists' Meeting on Fission Product Release and Transport in Gas Cooled Reactors, Berkeley, United Kingdom, October 22–25, 1985*, International Atomic Energy Agency, IWGGCR/13, Austria, 1986.

63. C. E. L. Hunt et al., "Fission Product Release During UO_2 Oxidation," p. 508 in *Proceedings of the International Conference on CANDU Fuel, Chalk River Nuclear Laboratories, Chalk River, Ontario, Canada, October 6–8, 1986*, Canadian Nuclear Society (1987).

64. F. C. Iglesias et al., "UO_2 Oxidation and Fission Product Release," *Proceedings of the Workshop on Chemical Reactivity of Oxide Fuel and Fission Product Release, Gloucestershire, United Kingdom, April 7–9, 1987*, Central Electricity Generating Board (1987).

65. D. S. Cox et al., "Fission Product Release from UO_2 in Air During Temperature Ramps," *Proceedings of the Canadian Nuclear Society 8th Annual Conference, Saint John, New Brunswick, 1987 June 14–17*, Canadian Nuclear Society (1987).

66. C. E. L. Hunt, F. C. Iglesias, and D. S. Cox, "Measured Release Kinetics of Iodine and Cesium

from UO_2 at High Temperatures under Reactor Accident Conditions," ICHMT Seminar on Fission Product Transport Processes in Reactor Accidents, Dubrovnik, Yugoslavia, May 22–26, 1989, p. 163 in *Fission Product Transport Processes in Reactor Accidents*, J. T. Rogers, Ed. (Hemisphere Publishing, 1990).

67. R. Williamson and S. A. Beetham, "Fission Product and U_3O_8 Particulate Emission Arising from the Oxidation of Irradiated Uranium Dioxide: Preliminary Studies," ICHMT Seminar on Fission Product Transport Processes in Reactor Accidents, Dubrovnik, Yugoslavia, May 22–26, 1989, in *Fission Product Transport Processes in Reactor Accidents*, J. T. Rogers, Ed. (Hemisphere Publishing, 1990).

68. J. T. Bittel, L. H. Sjohdal, and J. F. White, "Steam Oxidation Kinetics and Oxygen Diffusion in UO_2 at High Temperatures," *J. Amer. Ceram. Soc.* 52 (8), 446 (1968).†

69. R. E. Carter and K. W. Lay, "Surface-Controlled Oxidation-Reduction of UO_2," *J. Nucl. Mater.* 36, 77 (1970).†

70. J. A. Meachen, "Oxygen Diffusion in Uranium Dioxide: A Review," *Nucl. Energy* 28, 221 (1989).†

71. D. S. Cox et al., "Oxidation of UO_2 in Air and Steam with Relevance to Fission Product Releases," pp. 2–35 in *Proceedings of the Symposium on Chemical Phenomenon Associated with Radioactivity During Severe Nuclear Plant Accidents, Anaheim, California*, USNRC Conference Proceeding NUREG/CP-0078, September 1986.*

72. D. S. Cox et al., "High-Temperature Oxidation Behavior of UO_2 in Air and Steam," *Proceedings of the International Symposium on High-Temperature Oxidation and Sulphidation Processes, Hamilton, Ontario, Canada, August 26–30, 1990* (Pergamon Press, 1990).

73. R. Lindner and H. Matzke, *Z. Naturforschg.* 14a, 582 (1959).

74. W. Miekeley and F. Felix, *J. Nucl. Mater.* 42, 297 (1972).†

75. G. T. Lawrence, "A Review of the Diffusion Coefficient of Fission-Product Rare Gases in Uranium Dioxide," *J. Nucl. Mater.* 71, 195 (1978).†

76. H. Matzke, "Gas Release Mechanisms in UO_2—a Critical Review," *Radiation Effects* 53, 219 (1980).†

77. J. C. Killeen and J. A. Turnbull, "An Experimental and Theoretical Treatment of the Release of ^{85}Kr from Hyperstoichiometric Uranium Dioxide," p. 387 in *Proceedings of the Workshop on Chemical Reactivity of Oxide Fuel and Fission Product Release, Gloucestershire, United Kingdom, April 7–9, 1987*, Central Electricity Generating Board, 1987.

78. R. W. Grimes and C. R. Catlow, "The Stability of Fission Products in Uranium Dioxide," *Phil. Trans. R. Soc. London A*, 335, 609 (1991).

79. B. J. Lewis, F. C. Iglesias, D. S. Cox, and E. Gheorghiu, "A Model for Fission Gas Release and Fuel Oxidation Behavior for Defected UO_2 Fuel Elements," *Nucl. Technol.* 92, 353 (1990).†

80. C. A. Alexander, J. S. Ogden, and L. Chan, "Actinide Release from Irradiated Fuel at High Temperatures," p. 77 in *Source Term Evaluation for Accident Conditions*, International Atomic Energy Agency, IAEA-SM-281/10, Vienna (1986).

81. C. A. Alexander, J. S. Ogden, L. Chan, and R. W. Wright, "Matrix Stripping and Fission Product Release at High Temperatures," *Proceedings of an IAEA/OECD International Symposium on Severe Accidents in Nuclear Power Plants, Sorrento, Italy*, International Atomic Energy Agency, IAEA-SM-296/99, Austria (March 1988).

82. C. A. Alexander and J. S. Ogden, "Vaporization of UO_2 at High Temperatures and High Pressures. A generic relation for volatilization," *High Temp.-High Pres.*, 21 149 (1990).†

83. D. S. Cox et al., "Fission-Product Releases from UO_2 in Air and Inert Conditions at 1700-2350 K: Analysis of the MCE-1 Experiment," *Proceedings of the American Nuclear Society International Topical Meeting on Safety of Thermal Reactors, Portland, Oregon, U.S.A., July 21–25, 1991*, also AECL-10438, Atomic Energy of Canada Limited (1991).

84. D. S. Cox et al., "A Model for the Release of Low-Volatility Fission Products in Oxidizing Conditions," *Proceedings of the 12th Annual Conference of the Canadian Nuclear Society, Saskatoon, June 9–12, 1991*, also AECL-10440, Atomic Energy of Canada Limited (1991).

85. P. Hofmann and D. W. Kerwin-Peck, "UO_2/Zircaloy-4 Chemical Interactions and Reaction Kinetics from 1000 to 1700°C under Isothermal and Transient Conditions," *J. Nucl. Mater.* 124, 80–105 (1984).†

86. P. Hofmann et al., "Reactor Core Materials Interactions at Very High Temperatures," *Nucl. Technol.* 87, 146–186 (1990).†

87. K. T. Kim and D. R. Olander, "Dissolution of Uranium Dioxide by Molten Zircaloy," *J. Nucl. Mater.* 154, 85 (1988).†

88. P. Hofmann et al., "Dissolution of Solid UO_2 by Molten Zircaloy and its Modelling," *International Symposium on Severe Accidents in Nuclear Power Plants, Sorrento, Italy, March 21–25, 1988*, International Atomic Energy Agency, IAEA-SM-2986/1, Austria (March 1988).

89. J. Rest and A. W. Cronenberg, "Modelling the Behavior of Xe, I, Cs, Te, Ba and Sr in Solid and Liquefied Fuel during Severe Accidents," *J. Nucl. Mater.* 150, 203 (1987).†

90. M. D. Allen, H. D. Stockman, K. O. Reil, and J. W. Fisk, "Fission Product Release and Fuel Behavior of Irradiated Light Water Reactor Fuel under Severe Accident Conditions: The ACRR ST-1 Experiment," USNRC Report NUREG/CR-5345, September 1991.*

91. G. Kaspar, W. Haas, and A. Bleier, "Unterschung der Spaltproduktexhalation aus abgebranntem Brennstoff unter Anwesenheit von Zircaloy und Sauerstoff," *Proceedings of the Symposium on Source Term Evaluation for Accident Conditions, Columbus, Ohio, September 28–October 1, 1985*, International Atomic Energy Agency, IAEA-SM-281, Austria (1986).

92. S. M. Gehl, "The Release of Fission Gas During Transient Heating of LWR Fuel," USNRC Report NUREG/CR-2777 (ANL-80-108), May 1982.*

93. D. A. Petti, J. P. Adams, J. L. Anderson, and R. R. Hobbins, "Analysis of Fission Product Release Behavior from the Three Mile Island Unit 2 Core," *Nucl. Technol.* 87, 243 (1989).†

94. A. D. Knipe, S. A. Ploger, and D. J. Osetek, "PBF Severe Fuel Damage Scoping Test-Test Results Report," USNRC Report NUREG/CR-4683, March 1986.*

95. P. J. Fehrenbach et al., "High Temperature Transient Fission Product Release from UO_2 Fuel: Microstructural Observations," *Proceedings of the International Topical Meeting Thermal Reactor Safety, San Diego, February 2–6, 1986*, Vol. 5, American Nuclear Society, 1986.

96. S. M. Modro and M. L. Carboneau, "The LP-FP-2 Severe Fuel Damage Scenario and Discussion of the Relative Influence of the Transient and Reflood Phase in Affecting the Final Condition of the Bundle," *Proceedings of the Open Forum on the OECD/LOFT Project, Achievements and Significant Results, Madrid, Spain, May 9–11, 1990*, Organization for Economic Cooperation and Development, Paris, France (1991).

97. S. M. Jensen, D. W. Akers, and B. A. Pregger, "Postirradiation Examination Data and Analyses for OECD LOFT Fission Product Experiment LP-FP-2," Organization for Economic Cooperation and Development, OECD LOFT-T-3810, Vol. 1, Paris, France (December 1989).

98. J. M. Broughton, P. Kuan, D. A. Petti, and E. L. Tolman, "A Scenario of the Three Mile Island Unit 2 Accident," *Nucl. Technol.* 87, 34 (1989).†

99. D. A. Petti et al., *Power Burst Facility (PBF) Severe Fuel Damage Test 1-4 Test Results Report*, USNRC Report NUREG/CR-5163 (EGG-2542), April 1989.*

100. R. R. Hobbins, D. A. Petti, and D. L. Hagrman, "Fission Product Release from Fuel under Severe Accident Conditions," *Nucl. Technol.* 101, 270 (1993).†

101. Z. R. Martinson, D. A. Petti, and B. A. Cook, "PBF Severe Fuel Damage Test 1-1 Test Results Report," USNRC Report NUREG/CR-4684 (EGG-2463), Vol. 1, October 1986.*

102. Z. R. Martinson et al., "PBF Severe Fuel Damage Test 1-3 Test Results Report," USNRC Report NUREG/CR-5354 (EGG-2565), October 1989.*

103. K. O. Reil et al., "Results of the ACRR-DFR Experiments," *Proceedings of the International Topical Meeting on Thermal Reactor Safety, San Diego, California, February 2–6, 1986*, Vol. 3, American Nuclear Society, 1986.

104. R. D. Gasser et al., "Damaged Fuel Relocation Experiment DF-1: Results and Analyses," USNRC Report NUREG/CR-4668 (SAND86-1030), January 1990.*

105. D. W. Akers and R. K. McCardell, "Fission Product Partitioning in Core Materials," *Nucl. Technol.* 87, 264 (1989).†

106. R. R. Hobbins et al., "Insights on Severe Accident Chemistry from TMI-2," *Proceedings of the Symposium on Chemical Phenomena Associated with Radioactivity Released During Severe Nuclear Plant Accidents, Anaheim, California, September 8–12, 1986*, USNRC Conference Proceeding NUREG/CP-0078, 1987.*

107. S. Hagen and P. Hofmann, "Physical and Chemical Behavior of LWR Fuel Elements up to Very High Temperatures," KfK-4104, Kernforschungszentrum Karlsruhe, Federal Republic of Germany (June 1987).

108. P. Hofmann and M. E. Markiewicz, "Chemical Behavior of (Ag,In,Cd) Absorber Rods in Severe LWR Accidents," KfK-4670, Kernforschungszentrum Karlsruhe, Federal Republic of Germany (1990).

109. D. A. Petti, "Silver-Indium-Cadmium Control Rod Behavior in Severe Reactor Accidents," *Nucl. Technol.* 84, 128 (1989).†

110. P. Hofmann, S. Hagen, G. Schanz, and A. Skokan, "Reactor Core Materials Interactions at Very High Temperatures," *Nucl. Technol.* 87, 146 (1989).†

111. M. L. Carboneau, V. T. Berta, and M. S. Modro, "Experiment Analysis and Summary Report for OECD LOFT Project Fission Product Experiment LP-FP-2," Organization for Economic Cooperation and Development OECD LOFT-T-3806, Paris, France (June 1989).

112. P. D. Parsons and W. G. Burns, "PWR Degraded Core Analysis," Atomic Energy Authority Report ND-R 610, Chap. 3 (Ed. J. H. Gittus), United Kingdom (1987).

113. C. A. Alexander and J. S. Ogden, *J. Nucl. Mater.* 175, 197 (1990).†

114. S. R. Mulpuru, D. J. Wren, and R. K. Rondeau, *Aerosol Material Release Rates from Zircaloy-4 at Temperatures 2000 to 2200°C*, AECL report WNRE-770, 1988. Also, *ANS Trans.* 55, 434 (1988).†

115. B. R. Bowsher, *Prog. Nucl. Energy* 20, 199 (1987).†

116. B. R. Bowsher, "The Role of Boric Acid in the Phebus-FP Experiments," Atomic Energy Authority Report AEA RS 5166, United Kingdom (1991).

117. S. R. Kinnersly, C. G. Richards, and R. O'Mahoney, "Data for Use in UKAEA PWR Plant Studies," Atomic Energy Authority Report AEEW-M 1958, United Kingdom (1982).

118. R. M. Elrick and R. A. Sallach, *Proceedings of the International Meeting on LWR Severe Accident Evaluation, Cambridge, Massachusetts, August 28–September 1, 1983*, American Nuclear Society, 1983.

119. A. B. Anderson, A. M. Beard, P. J. Bennett, and C. G. Benson, Atomic Energy Authority Report AEA TRS 5091, United Kingdom (1991).

*Available for purchase from the National Technical Information Service, Springfield, VA 22161.
†Available in public technical libraries.

3.2 Experimental Programs on Release Phenomena

3.2.1 In-Reactor Fission Product Release Experiments

3.2.1.1 ACRR ST-1 and ST-2

The ST-1 and ST-2 source term experiments[1–5] were conducted in the ACRR reactor at Sandia National Laboratories during 1987–1988. These experiments were undertaken to measure fission product release rates in reducing conditions at temperatures above 2400 K. The test fuel consisted of four 15.2-cm-long segments of BR-3 fuel (47 MWd/kgU), which had been prepared by cutting the fuel rods and inert welding Zircaloy end caps onto them.

The experimental conditions were approximately the same for both tests except for the system pressure, which was 0.16 MPa in ST-1 and 1.9 MPa in ST-2. The fuel was fission-heated at a rate of about 1 K/s to a low-temperature plateau of about 1600 K, which was held for a period of time while instrumentation was adjusted. The heatup ramp was resumed at a rate of 1.3 to 1.6 K/s until test section temperatures exceeded 2400 K. The reactor power was then regulated to maintain the temperatures in the irradiated fuel at about 2450 K for 20 min, followed by reactor shutdown and dry cooling in flowing Ar/H_2. To maintain the same hydrogen partial pressure for the two tests at different pressure, the carrier gas was Ar 33 vol% H_2 in ST-1 and Ar 2.5 vol% in ST-2. The same molar flow rates were used, which gave linear velocities through the test section of 98 cm/s in ST-1 and 7 cm/s in ST-2.

The fission product gases and aerosols flowed upward out of the test section into a zirconia ceramic mixing plenum and then into one of seven time-sequenced filter samplers, consisting of a nozzle, thermal gradient tube with deposition wires, a Pt-10%Rh fibre filter, and a charcoal backup filter. The nozzle was located about 10 cm above the top of the irradiated fuel stack. Five evacuated grab sample bottles were used to collect gas from the recirculating Ar/H_2 coolant and provide data on noble gas releases. An optical line-of-sight was incorporated into the design of the experiment to provide an end-on view of the irradiated fuel during the experiment. Video and framing cameras were used to record images during the experiment and posttest. A portion of the light was also directed to an optical multichannel analyzer, where emission and absorption lines in the optical spectrum were used to obtain information on fission product species in the gas stream.

Table 3.1 summarizes the integral release and transport data for the ST-1 and ST-2 tests. A comparison of pretest and posttest axial gamma scans of the irradiated fuel was used to determine the total integral releases of Cs-137 and Eu-154. The seven filter samplers provided data on the time dependence and cumulative amount of fission products transported to the samplers. Cs, I, and Kr were released at similar rates, with the peak release rates occurring during the high-temperature heatup period. The peak release rates for Te, Ba, Sr, and Eu occurred at the end of the high-temperature heatup period. As expected for the test conditions, the volatile fission-product release fractions were high (71 to 99%). Significant release fractions of europium (15 to 20%) were also measured. Of the 15 to 20% europium integral release, 2 to 5% was collected at

Table 3.1 Summary of fission product releases from the ST-1 and ST-2 tests

Element	ST-1 release fractions		ST-2 release fractions	
	Integral release	Collected at filters	Integral release	Collected at filters
Cs	0.71	0.56	0.82	0.30
Ba		0.08 + 0.032[a]		0.04
I		0.38		0.23
Te		<0.002		<0.005
Kr	0.993			
Sr		0.05 + ≤0.0043[a]		0.03
Zr		≥0.0034[a]		
Eu	0.20	0.05	0.15	0.02
U		0.00011[a]		

[a]Includes amounts collected in water leachates.

the filters, where 4 to 8% of the barium and 3 to 5% of the strontium were also collected, indicating significant release fractions for these latter species. Tellurium and zirconium releases were very low, based on filter measurements. Significant amounts of uranium were collected in the filters, but fractional releases were low.

Posttest examinations of the fuel indicated that Zircaloy melting and Zr-UO_2 interactions had occurred, with relocation of molten material to the bottom of the test bundle. There was widespread liquefaction and foaming of the pre-irradiated fuel. Extensive production of metallic uranium has been suggested as the cause for foaming of the fuel.[5] Releases of Ba, Sr, and U could be explained by the volatility of these species at low oxygen potentials. The low tellurium releases suggest the formation of low-volatile tellurium compounds under these test conditions.

3.2.1.2 Source Term Experiments Project (STEP)

A series of four experiments were conducted at the Argonne National Laboratory (ANL) in the Transient Reactor Test (TREAT) Facility in an effort to provide data regarding the physical and chemical nature of fission product releases from LWR fuel during severe accidents.[6,7] These experiments were designed to characterize the components of the source term that may be released early in a severe accident. Of particular interest were the volatile fission products Cs, I, Te, and Rb.

The four STEP tests were planned to simulate some of the accident sequences in both PWR and BWR reactors (see Table 3.2). In STEP-1, conditions of a large-break loss-of-coolant accident (LOCA) followed by a failure of emergency core cooling injection for a PWR were simulated. In

Table 3.2 Planned and actual values of selected operating parameters for the STEP tests[a]

Test	Energy deposition[b] (MJ/kg)	Duration (min)	Pressure (MPa)	Initial heatup rate[c] (K/s)	Simulated accident scenario
STEP-1	3.4/3.4	20/20.6	0.31/0.32[d]	2.0/1.8	AD (PWR)—large coolant pipe break with failure of emergency core cooling; rapid depressurization and prompt core uncovery
STEP-2	4.5/2.9	30/20.5	0.14/0.16–1.24[e]	0.3,1.2[f]/2.1	TQUW (BWR)—transient event combined with failures of high-pressure emergency core cooling and long-term decay heat removal; automatic depressurization and temporary low pressure coolant injection results in very long time to core uncovery
STEP-3	3.2/3.2	20/21.4	8.27[g]/8.00	1.3/1.1	TMLB' (PWR)—transient with failure of main feedwater and auxiliary feedwater and failure to recover electric power; no depressurization, coolant loss by venting through relief valves, core uncovery in 1 h or more
STEP-4	3.2/3.6	20/23.8	8.27[g]/7.86	1.3/1.0	TMLB' (PWR)—like TMLB' above but with control rod simulant in test fuel

[a]The two values given are planned/actual.
[b]Peak fission energy only; does not include contribution from zirconium oxidation.
[c]Planned values correspond to the period before zirconium oxidation is expected to become a significant contributor to heatup rate. Actual values are best-estimate peak fuel heating rates from the initial temperature to 1500 K.
[d]Pressure perturbation to 0.45 MPa occurred 10 min into the test, and another to 0.42 MPa occurred after shutdown.
[e]A pressure rise began at 8 min into the test. At 0.97 MPa the reactor was manually shut down, and pressure continued to rise to 1.24 MPa, at which time steam supply was terminated.
[f]The initial heatup rate associated with the TQUW sequence was 0.3 K/s. The lowest value attainable given the reactor and test vehicle constraints was 1.2 K/s.
[g]The actual TMLB' pressure of 17.2 MPa was thought to be beyond the capability of the primary vessel; the chosen value of 8.27 MPa was thought to be sufficiently high to determine the effects of high pressure.

STEP-2, a transient with failure of the high-pressure emergency core cooling and long-term decay heat removal systems for a BWR were simulated. In STEP-3 and STEP-4, the conditions simulated were transients with failure of the feedwater systems and failure to recover electric power for a PWR at high pressure. A PWR control rod was included in STEP-4.

Four fuel rods previously irradiated in the Belgian BR-3 reactor were used in each test. Deposits on coupons from a sample tree located directly above the fuel rod bundle and from coupons, deposition plates, and impactor wires located in canisters adjacent to the test vessel were examined by scanning electron microscopy (SEM), electron microprobe, and other methods. The SEM images were used to determine aerosol size distributions and concentrations. An extensive release of fission products occurred for the low-pressure tests (STEP-1 and STEP-2). The relative quantities, morphologies, and chemical characteristics were determined for fission products Cs, I, Te, and Rb and the fuel rod materials Sn, Zr, and U. The measured elemental compositions of canister deposits collected during the STEP-1 and STEP-2 tests are presented in Table 3.3. A smaller release of fission products occurred in the high-pressure tests (STEP-3 and STEP-4) because of lower fuel

Table 3.3 Measured and calculated elemental compositions of canister deposits

Element	STEP-1			STEP-2		
	Measured (%)[a]		Calculated[c]	Measured (%)[b]		Calculated[c]
	5–11 min	11–22.7 min		11–16.5 min	15.5–21.1 min	
Cs	40[d]	40[d]	41	46	60	47
I	1.3	1.9	2.6	-	-	3.0
Rb	0.7	1.3	6.7	6.5	7.7	7.6
Se	1.3	0.4	1.0	-	-	1.1
Cd	1.0	0.8	0.41	-	-	0.47
Te	10	13	5.3	0.22	-	5.8
Ag	0.2	1.5	0.33	-	-	0.35
Sb	-	-	0.055	-	-	0.05
Ba	0.07	0.02	2.9	-	-	2.7
Mo	9.6	2.0	2.8	9.3	9.7	3.5
Sr	0.02	0.1	0.77	-	-	0.6
Ru	-	-	0.12	-	-	0.09
Fuel	-	-	6.2	0.12	0.1	2.6
Zr	0.05	0.1	0.41	15.5	1.3	0.39
Sn	36	40	27	3.1	3.2	23
Fe,Cr,Ni	-	-	2.2	2.0	3.2	2.0
Al	-	-	-	3.3	1.0	-
Si	-	-	-	9.1	11	-
Ca	-	-	-	4.8	3.3	-

[a]Analysis by spark source mass spectrometry at ORNL.
[b]Each is average of 5 SEM area scans.
[c]Modified CORSOR equations.
[d]Estimated from measured aerosol masses.

temperatures that resulted from natural convection flow induced under the high-pressure conditions.

3.2.1.3 Severe Fuel Damage Tests

Four SFD tests were performed in the PBF at the Idaho National Engineering Laboratory (INEL). These tests were designated SFD-ST (Ref. 8), SFD 1-1 (Ref. 9), SFD 1-3 (Ref. 10), and SFD 1-4 (Ref. 11). All four tests were fission-heated coolant boildowns of fuel rod bundles with a small, continuous inlet flow of coolant. The active length of the 32-position bundles was 0.91 m, and three Inconel spacer grids were used in each bundle. The objectives of the test series were to measure core degradation phenomena and fission product release under severe accident conditions. Fuel melting and relocation occurred in all four tests.

The experimental conditions of each of the tests are presented in Table 3.4. In the first two tests (SFD-ST and SFD 1-1), unirradiated fuel rods were given a short irradiation before the transient to provide measurable quantities of fission products. The last two tests used highly irradiated fuel rods, and test SFD 1-4 contained Ag-In-Cd control rods. Test SFD-ST was steam rich, whereas the remaining tests were steam-limited (Zircaloy-water reaction rate limited by steam supply rate). All four tests were conducted at high system pressure (4.7 to 6.9 MPa), and temperatures exceeded 2800 K in each.

On-line fission gas release measurements were made in each test, as well as measurements of integral releases of fission products. In test SFD 1-4, on-line measurements of aerosol concentration and time-resolved samples of the aerosol were obtained. Hydrogen generation was measured on line in all four tests. Fission product release fractions, extent of Zircaloy oxidation, and extent of fuel melting in the four tests are presented in Table 3.5.

3.2.1.4 LOFT-FP Tests

The LOFT experimental facility at INEL was a 1/50 scale model of a commercial PWR, designed to simulate the major components and system responses of a 4-loop PWR during a LOCA.[12] The experimental subsystems included the reactor vessel, an intact loop (simulating 3 intact loops), the broken loop, a blowdown suppression tank (BST) system, and ECCSs. The intact loop contained a U-tube steam generator, two primary coolant pumps in parallel, a pressurizer, Venturi flowmeter, and connecting piping. The broken loop consisted of a hot leg and a cold leg with aerosol filters, gamma spectrometers, and deposition coupons to measure aerosol and fission product release to the primary system. A unique aspect of these tests was that actual fission product decay heating of the core was used.

The Organization for Economic Cooperation and Development (OECD) LOFT Project was a collaborative program including a number of OECD countries, organized through the OECD Nuclear Energy Agency. Two fission product release tests were done: LOFT LP-FP-1 and LOFT LP-FP-2.

LOFT LP-FP-1. The objective of this test, conducted in 1984, was to determine the system thermal-hydraulic response for initial and boundary conditions corresponding to a large-break LOCA, leading to fission product release from the fuel rod gap. The Center Fuel Module (CFM) contained 24 1.7-m-long fuel rods (22 cold prepressurized to 2.41 MPa, 2 not prepressurized) and 11 guide tubes. The fuel was irradiated to burnup of 1.42 MWd/kgU at an average linear power of 35.7 kW/m and peak power of 52.2 kW/m. The transient portion of the test consisted of a simulated large-break LOCA, with decay heat causing 8 of the 22 prepressurized rods to fail about 325 s after blowdown (maximum fuel temperatures were about 1200 K). At 345 s, ECCS water injection was started from two accumulators (earlier than planned), one attached to each loop. The test was terminated about 2 min after the reflood.

The number of failed rods was less than intended because of the unplanned accumulator blowdowns. However, information was obtained on gap release to a high-temperature steam environment and fission product transport through and out of the primary coolant system during reflood.[13,14] The released gap inventory was 1.3 to 1.8% for Xe-133, 0.7 to 0.9% for I-131 and 1.2 to 1.5% for Cs-137. The noble gases were released before reflood, about half of the iodine was released before reflood, and most of the cesium was leached from the fuel after reflood.

LOFT LP-FP-2. This experiment has provided information on a wide range of severe accident phenomena, including core melt progression, hydrogen generation, fission product behavior, composition of melts, and the effects of reflood on a severely damaged core.[15] It was conducted on a large scale, providing a valuable link between smaller-scale integral experiments and the TMI-2 accident.[16] The experiment simulated the system thermal-hydraulics and core uncovery conditions during fission product release and transport that are likely to occur in a 4-loop PWR from rupture of a low-pressure injection system (LPIS) pipe as a result of a V-sequence accident. The break conditions were simulated by blanking off the cold leg of the broken loop and connecting an LPIS line to the end of the hot leg with direct discharge to the BST.

Table 3.4 PBF SFD test conditions

Test	Bundle description	Nominal inlet flow rate (g/s)	Steam production rate (g/s)	Approximately heating rate prior to rapid oxidation[a] (K/s)	Cooldown procedure	System pressure (MPa)	Burnup (MWd/kgU)	Time-resolved measurements	
								Fission product	Aerosols
SFD-ST	32 fresh rods	16	16	0.1 to 0.15	Reactor scram, 16-g/s reflood increasing to ~30 g/s after 4 min. Whole bundle at saturation temperature ~8 min after scram.	6.9	Trace	Yes	No
SFD 1-1	32 fresh rods	0.6	0.7–1.0	0.46 between 800 and 1300 K 2.9 between 1300 and 2000 K	Power reduction and argon assisted cooldown over 20 min prior to 17-g/s reflood.	6.8	Trace	Yes	No
SFD 1-3	26 irrad. rods 2 fresh rods 4 guide tubes	0.6	0.6–2.4	0.5 below 1200 K 1.9 above 1200 K	Power reduction and argon assisted cooldown over at least 50 min. No reflood.	6.85 4.7	35-42	Yes	No
SFD 1-4	26 irrad. rods 2 fresh rods 4 Ag-In-Cd control rods in guide tubes	0.6	0.6–1.3	0.4 between 800 and 1200 K 1.6 between 1200 and 1600 K	Power reduction and argon assisted cooldown over at least 50 min. No reflood.	6.95	29-42	Yes	Yes

[a]The heating rate was extremely rapid and driven by the metal-water reaction above ~1500 to 2000 K (depending on axial location) in SFD-ST and ~1600 K in the other three tests.

Table 3.5 PBF SFD test results

Element/ experimental condition	Release fraction			
	SFD-ST	SFD 1-1	SFD 1-3	SFD 1-4
Krypton, xenon	0.50	0.026–0.093	0.07–0.53	0.23–0.52
Iodine	0.51	0.12	0.18	0.24
Cesium	0.32	0.09	0.18	0.39–0.51
Tellurium	0.40	0.01	0.01–0.09	0.03
Barium	0.011	0.006	0.004	0.008
Strontium	0.00002		0.00024	0.0088
Antimony			0.00019	0.0013
Ruthenium	0.0003	0.0002	0.00003	0.00007
Cerium	0.000002	0.00009	0.00008	0.00013
Europium			0.00007	0.0008
Actinides			<0.0001	<0.00001
Zirconium oxidized, %	27	22	32	
Fuel melted, %	15	16	18	18
References	(8)	(9)	(10)	(11)

The CFM contained 100 1.7-m-long fuel rods (cold pressurized to 2.41 MPa) and 21 control guide tubes in an 11 by 11 array. Ag-In-Cd control rods were inserted into 11 of the guide tubes. During pretransient irradiation, a burnup of 0.43 MWd/kgU was achieved. The transient was initiated (at t = 0) by reactor scram and opening of the break lines. The core was allowed to uncover and heat up, resulting in failure of the control rods in the CFM. Fission products were detected in the sample lines at 1200 s, and rapid temperature escalations associated with Zircaloy oxidation started in the CFM at about 1450 s. ECCS was activated at 1777 s, about 4.5 min after the core temperatures exceeded 2100 K. Peak temperatures were estimated around 3100 K (Ref. 17), and posttest examinations indicated metallic and ceramic flow blockages. About 15% of the fuel was liquefied, and 49% of the Zircaloy was oxidized. The on-line data and posttest examinations indicate that the highest temperatures, the majority of Zircaloy oxidation (80%), fuel liquefaction, and fuel fission product releases[18] all occurred during the reflood.

Table 3.6 summarizes the integral release data for the period before and after reflood. The reflood event accounted for about 80% of the total released activity. The noble gases, cesium and iodine, showed similar total releases (12 to 16%), and tellurium was lower at about 3%. A surprising result was 9% barium release. The posttest deposition and aerosol sampling measurements indicated that iodine was primarily transported as silver iodide (AgI) and that cesium was transported as cesium hydroxide (CsOH).

3.2.1.5 Phebus-FP

The in-pile Phebus-FP program is led by the Institut de Protection et de Sûreté Nucleaire (IPSN) of the French Commissariat à l'Energie Atomique (CEA) and the Commission of the European Communities (CEC), with participation from numerous organizations around the world. The aim of the program is to investigate the main phenomena governing the release of fission products from degraded fuel, as well as fission product transport, deposition, retention, and chemistry in the core, the primary circuit, and in the containment building.[19]

The integrated test facility at the Research Center of Cadarache is based on a scaling factor of 5000, which represents the fission product inventory ratio between a commercial LWR reactor and the Phebus-FP fuel bundle (20 fuel rods, one Ag-In-Cd control rod, 0.8-m fissile length).[20] The thermal-hydraulic boundary conditions will be controlled to maintain representative conditions derived

Table 3.6 Measured release fractions for the LOFT-LP-FP-2 test

Fission product	Measured release fraction	
	Before reflood	Total after reflood
Xe	0.017	-
Kr	0.02	0.12
I	0.03–0.05	0.16
Cs	0.008–0.03	0.16
Te	0.0003–0.005	0.03
Ba	0.002–0.008	0.09

from basic LWR severe accident sequences. The test objectives for behavior of the bundle, the circuit, and the containment are independently established.

The Phebus-FP test matrix includes six tests, the first of which will be performed with trace irradiated fuel in mid-1993. The other five tests will use irradiated fuel with burnups ranging from 23 to 33 MWd/kgU, and one test per year is scheduled for the duration of the program. Currently, only the first two tests, FPT-0 and FPT-1, are well specified. The overall objectives are defined for the third test, FPT-2, but it is clear that the results of the first two tests may change any "a priori" definition of subsequent tests. The test matrix beyond FPT-1 is presently under discussion and revision, taking into account the technological and safety constraints of the facility, with consideration of phenomena requiring in-pile testing and, more specifically, code validation needs and current priorities in LWR source term evaluation.

The main characteristics of the bundle aspects for the first three tests are presented in Table 3.7. The priority is to maximize the fission-product release and the fuel rod degradation by reaching the melting temperature of the fuel.

The first test, FPT-0, will be performed under oxidizing, low-pressure conditions using PWR-typical fresh fuel after 9-d irradiation in the Phebus reactor.* The second test, FPT-1, will be performed under similar conditions with pre-irradiated fuel in order to study the burnup effects on core degradation and fission product release and transport. In FPT-2, it is currently intended to investigate the effects of a reducing low-pressure environment on the same phenomena. The last three tests could be devoted to study fission product release and speciation in the following core conditions: high pressures, fuel oxidation by air, solid debris beds and molten pools, and rapid cooling of degraded rods.

Finally the test matrix (which is periodically revised) could also include future areas in reactor safety research for advanced LWRs. Further discussion of the Phebus-FP program is presented in Sect. 4.3.6.

3.2.1.6 Full-Length High-Temperature (FLHT) Tests

Four tests on highly instrumented assemblies of full-length PWR fuel rods have been conducted by the Pacific Northwest Laboratory (PNL) under the U.S. Nuclear Regulatory Commission (NRC) Coolant Boilaway and Damage Progression Program. During these tests, the fuel rods were

*I. Shepherd and F. Serre, "Precalculations for the Bundle for the First PHEBUS-FP Test FPT0," IAEA Technical Committee Meeting, Aix-en-Provence, France, May 16–19, 1992.

Table 3.7 Comparison of bundle conditions for the first three Phebus-FP tests

	FPT-0	FPT-1	FPT-2
Fuel burnup	Fresh fuel	≈30 MWd/kgU	≈30 MWd/kgU
Preirradiation in the Phebus reactor, d	9	15	15
Pressure, MPa	0.2	0.2	0.2
Maximum fuel temperature, K	3120	3030[a]	3030[a]
Number of fresh fuel rods	20	2[b]	2[b]
Control rods (Ag-In-Cd)	1	1	1
Boric acid	No	Not defined	Not defined
H_2/H_2O ratio	Low	Low	High
Clad oxidation (fraction)	High	High	Low
Fuel dissolution (fraction)	Low	Low	High

[a]Melting of a few kilograms of UO_2 is expected.
[b]Total of 20 fuel rods.

subjected to coolant flow reductions while operating at low heat ratings in the NRU reactor at the Atomic Energy of Canada Limited (AECL) Chalk River Laboratories (CRL). These tests have provided well-characterized data for evaluating the effects of coolant boilaway and core damage progression and for investigating integral severe accident phenomena, including cladding temperature escalations, oxidation behavior, hydrogen generation, fuel liquefaction, molten material relocation, and fission product release.[21] The completed tests (designated FLHT-1, FLHT-2, FLHT-4 and FLHT-5) were done with bundle assemblies of 12 unirradiated PWR fuel rods (FLHT-1 and FLHT-2) or 10 unirradiated rods plus a pre-irradiated rod (28 MWd/kgU) and an instrument guide tube (FLHT-4 and FLHT-5). A further test is planned with a BWR assembly (FLHT-6). All of the fuel assemblies are full length (3.7 m long) and include extensive instrumentation for axial and radial temperature measurements.

The key findings from the FLHT tests have been related to core damage progression phenomena,[21] including the dynamics of oxidation-related temperature excursions moving up and down the fuel assemblies, hydrogen generation, melting, liquefaction and material relocation events. A significant difference in the behavior of preirradiated and unirradiated fuel rods was noted in the FLHT-4 and FLHT-5 tests, with the observation of extensive foaming in the preirradiated rod over a 2-m length.

Data on fission product releases during the FLHT-5 test are the most extensive from the FLHT program. In this test, the fuel was subjected to low coolant flow while operating at low fission power, causing coolant boilaway, rod dryout and overheating, severe fuel rod damage, hydrogen generation and fission-product release. An oxidation burn front progressed rapidly down the assembly, and then a slower burn front moved upward and consumed most of the uncovered bundle Zircaloy. The test was conducted for 60 min after the onset of rapid oxidation, and peak temperatures in excess of 2500 K were confirmed. Fission product release, transport, and deposition data were obtained from on-line gamma spectrometers and gross gamma monitors, combined with posttest examination and gamma scanning of the top of the fuel stack, the upper plenum, and deposition rods from the plenum region.[22]

Release rates for several isotopes of noble gases were measured during the test, and the total integral release was estimated at about 50% of the noble gas fission product inventory in the fuel. The axial deposition patterns in the plenum region were similar for iodine and cesium and showed local variations due to wall temperature differences. Tellurium deposition showed a different axial distribution than iodine or cesium. The total deposition in the plenum region was estimated as 0.7% of the iodine inventory, 0.9% for cesium, and 0.02% for tellurium.

3.2.1.7 TMI-2 Accident

The TMI-2 accident was basically a small-break LOCA that was terminated by coolant injection after molten fuel relocation to the lower plenum, but before lower head failure. A comprehensive accident scenario has been developed,[23] and inventories of core materials[24] and fission product partitioning in core materials[25] have been reported. Fission product release behavior during the accident has been analyzed.[26] The average burnup in the core was 3 MWd/kgU, temperatures exceeded 2800 K, and the system pressure varied between 5 and 15 MPa during the accident. Approximately 45% of the fuel melted, and 45% of the Zircaloy in the core was oxidized. About 23% of the fuel relocated as ceramic melt into the lower plenum. The release of fission products from the core is summarized in Table 3.8 (Ref. 27).

3.2.1.8 AECL-BTF Experiments

The principal experimental tool in Canada for performing in-reactor fuel safety experiments is the Blowdown Test Facility (BTF),[28] located in the NRU reactor at AECL's CRL. This facility was designed for performing SFD tests on instrumented fuel assemblies and measuring the fission product release, transport, and deposition using on-line gamma spectrometers and coolant grab samples combined with posttest analyses of deposition coupons and effluent

Table 3.8 Fission product releases from the core in the TMI-2 accident

Isotope	Fraction of core inventory released
Kr-85	0.54
I-129	0.55
Cs-137	0.55
Te-132	0.06
Sr-90	0.001[a]
Ru-106	0.005
Sb-125	0.016
Ce-144	0.0001
Eu-154	<0.001

[a]Leaching from damaged core after reflood increased strontium release to 0.032, 2 months after accident.

Source: Taken from Ref. 27.

samples. The test section is in a vertical orientation, and coolant flows downward over the fuel. The fuel is surrounded by a thermal shroud, which permits the facility to investigate high-temperature scenarios up to fuel melting conditions.

The first SFD experiment in the BTF was the BTF-107 experiment, performed in November 1990. A trefoil assembly of three CANDU-type fuel elements was subjected to a blowdown from full reactor power; during the test thermal-hydraulics data, fuel and cladding temperatures, and fission product release data were collected.[29] One of the fuel elements was pre-irradiated (5.5 MWd/kgU). During the early stages of the blowdown, the fuel remained well-cooled, but the temperature increased rapidly with the onset of dryout. An unexpected flow blockage occurred below the fuel assembly following a brief period in dryout, while the fuel elements were operating at about 45 kW/m. The degraded cooling conditions caused by the onset of this flow blockage produced surface fuel temperatures in excess of 2570 K before the termination of the experiment by a reactor shutdown and cold water rewet.[30]

Posttest examinations of the fuel assembly revealed that the flow blockage was caused by a significant relocation of material from the fuel elements. Metallographic sections through the bottom quarter of the fuel assembly confirmed the presence of extensive uranium/zirconium alloy formation, fuel melting, and relocation.

The on-line gamma-ray spectrometers were saturated at or near the time of the reactor trip by the large amounts of short-lived fission products released from the fuel. Although these spectrometers were not useful during the transient, extensive posttest measurements were made throughout the facility and on 11 time-sequenced coolant grab samples. On-line readings from gross-gamma monitors were combined with these posttest measurements to determine the kinetics of fission product release and integral fractional releases for a number of fission products.

A large fraction of the inventory of volatile fission products was released from the fuel during the test and was collected in the blowdown tank. The release fractions for iodine and cesium were between 55 and 68%. A lesser amount of noble gases was collected (33 to 37%). About 21% of the tellurium and 6% of the molybdenum was released. About 2% of the barium was released, and lesser amounts of other fission products were measured (Zr, La, Ce).

The kinetics of activity transport along the blowdown line indicated that the releases from the fuel were very rapid and occurred over a period of about 30 s. Large portions of the I, Cs, and Te releases were deposited on piping surfaces. Rewet water later washed this deposited activity into the blowdown tank. Very little activity remained on piping surfaces following sustained cooling after the test.

3.2.1.9 Risø Transient Fission Gas Release Projects

In 1980 the Risø National Laboratory in Denmark began a series of fission gas release projects.[31–33] The aim of these projects was to provide in-pile experimental information on fission-gas release, especially for power transients (increases) late in the irradiation life of the fuel.

The fuel samples were obtained from fuel rods irradiated in the Halden reactor (Norway) and in the Millstone-1 BWR (USA) with a burnup range of 14.5 to 49.9 MWd/kgU. Samples were prepared by sectioning the previously irradiated rods. These segments were used to refabricate short test rods with instrumented pressure transducers. Test design variables investigated during these programs were (1) filling gas composition and pressure, (2) diametrical gap, and (3) burnup.

Several power transient tests (bump tests) were performed at the DR3 reactor at Risø in water-cooled test rigs. The maximum power reached during the transients ranged between 33.7 and 46.6 kW/m.

In these projects, great emphasis was placed on postirradiation examination of the tested specimens. Very detailed analyses were performed, focusing mostly on the local fuel microstructure, radial distribution of retained fission products, and grain boundary concentrations. These measurements were performed using microgamma scanning, transmission and SEM, X-ray fluorescence, and electron probe microanalysis, in addition to standard PIE methods.

The results of the Risø projects have indicated that, during in-pile power transients, the grain boundary bubbles may have a controlling role in the gas release process. In addition, these tests have also shown the relative importance of mechanical restraint pressure, fuel geometry, initial pore structure, and burnup in the determination of the amount of gas release during transient conditions.

3.2.1.10 Rod Cluster LOCA Tests and Simulated Transient Accident Tests in TREAT

In addition to the STEP tests (Sect. 3.2.1.2), two other fission product release experiments were conducted in the TREAT reactor at ANL.

Seven-Rod Controlled LOCA Tests in TREAT. Two 7-rod fuel bundle experiments, FRF-1 and FRF-2, were performed in the TREAT reactor to explore fuel rod ballooning, rupture failure, and fission product release during the early phase of a severe accident. The fuel rods were nominally 0.69 m long and had a 1.43-cm cladding outside diameter (OD). The gas flowing upward through the bundle was 11.0 L/min steam plus 1.8 L/min helium at 0.13 MPa. The fuel heatup rate was 40 K/s, and the fuel rods remained within ~80% of the peak temperatures for only 4 min.

Two fuel rods in each test were monitored continuously for internal pressure. These data were used to calculate ballooning rate, volumetric void expansion, and cladding stress and strain at rupture. The center rod in each bundle was irradiated so that fission product release could be measured. Tables 3.9 and 3.10 summarize the results of the two tests. Details have been published.[34–36]

Metallographic examinations were made. One rod was sufficiently oxygen-embrittled that it broke during handling in the hot cell. Table 3.9 demonstrates that the fission product releases were characteristic of releases from the gap space of low-burnup fuel rods. Organic iodide production was high, probably because of the large surface/volume ratio.

Transient Heating of UO_2 in Steam or Water in TREAT. Twelve tests with Type 347 stainless steel or Zircaloy clad UO_2 were conducted in the TREAT reactor to explore fuel behavior and fission product release during transient heatup to the melting point of UO_2. The fuel pins contained 32 g of UO_2 and were sealed along with steam or water in a high-pressure stainless steel "primary vessel". A reactor transient with a 50-ms period (77 ms for Test 5) heated the fuel by internal fission heating. The heated water (steam in Test 5) was allowed to escape from the primary vessel by means of rupture discs or explosive-operated valves. The steam carried released fission products through a condenser, and helium gas carried the remaining gas-borne material through membrane filters and charcoal-loaded paper into a receiving vessel (collectively, later called the filter vessel) until pressure equilibrium was attained.

The operating conditions for seven of the tests are given in Table 3.11. The heat input was ~510 cal/g UO_2 (330 in Test 5) with 273 K as the reference temperature. Changes were made in the apparatus during the series of tests so that it is important to examine the reference reports[37–41] to

Table 3.9 Operating conditions in TREAT bundle tests

Test No.	Fuel rod fill pressure (MPa)	Typical maximum temperature (K)	Typical rupture temperature (K)	Center rod burnup (MWd/kg U)
FRF-1	0.79 to 1.48	1200	1200	0.65
FRF-2	0.45 to 0.52	1590	1530	2.8

Table 3.10 Fission product release in TREAT bundle tests

Test No.	Fission product release (%)						
	^{85}Kr	^{137}Cs	^{131}I	^{129}Te	^{140}Ba, ^{89}Sr	Ru, Ce, Zr	U
FRF-1	0.094[a]	0.056	0.189	~0.03	0.0009	0.0009	0.0002
FRF-2	0.48	0.288	0.115	$<15 \times 10^{-6}$	$\sim 2 \times 10^{-6}$	1.4×10^{-6}	16×10^{-6}

[a]Release of ^{133}Xe was 0.14% in FRF-1.

Table 3.11 Operating conditions for transient heating tests in TREAT

Test No.[a]	Burnup (MWd/kg U)	Initial UO_2 temperature (K)	Maximum UO_2 temperature (K)	Initial pressure (MPa)	Maximum pressure (MPa)	Metal-water reaction (%)
5	0.009	583	3075	6.89	6.89	22
7	0.019	343	>3475	0.23	1.24	24
8z	0.018	343	>3475	0.23	NM[b]	41
9	0.027	403	>3475	0.88	1.90	16
10z	0.032	403	>3475	0.88	>1.85	49
11z	0.014	393	3475	0.17	4.48	43
12z	0.011	393	3475	4.83	15.17	55

[a]The z designation indicates that Zircaloy cladding was used.
[b]NM = not measured.

understand the observed differences in fission product behavior.

The amounts of fission products were measured in the remaining fuel, cladding, vessel, condenser, or filters. Even though the UO_2 burnup was very low, the fission product release and transport behavior is consistent with what is now known from various high-burnup fuel heating tests. For example, much of the tellurium was trapped by the cladding, and the barium and strontium behave alike. The analysis of Ba, Sr, Cs, and Ce isotopes transported to the filter vessel was probably influenced by gaseous or highly volatile precursors formed during the test. Ruthenium was slightly more volatile than cerium, and cerium was slightly more volatile than zirconium. The volatile precursors of cerium might account for some of this difference. Some of the tests were paired for identical conditions except for the cladding. Iodine and tellurium releases from fuel and cladding were greater with stainless steel cladding, but barium and strontium releases were greater when Zircaloy cladding was used. There was no detectable effect of steam pressure on the release of either barium or strontium.

3.2.2 Ex-Reactor Fission Product Release Experiments

Under the sponsorship of the NRC, ORNL has performed six series of fission product release tests with highly irradiated, commercial LWR fuel since 1976. These tests have been called the "high burnup" (HBU),[42] "high temperature" (HT),[43] "BWR,"[44] "horizontal irradiated" (HI),[45] "horizontal simulant" (HS),* and "vertical irradiated" (VI)[46–50] tests. The HS, HI, and VI series tests used an improved induction heating technique that did not require inductive coupling to the fuel-sample Zircaloy cladding; this permitted production of a relatively isothermal test zone and also allowed much higher temperatures to be reached in the tests.

The HS series of tests used simulated PWR fuel provided by the SASCHA project (Sect. 3.2.2.1). The tests were done in steam at 1900 to 2700 K. Results for some structural materials and fission product simulants were obtained.

The major recent ORNL tests are the HI and VI experiments. Conditions for these tests and important test results are summarized in Tables 3.12 and 3.13. Both test series used highly irradiated Zircaloy-clad UO_2 fuel samples that were 15 to 20 cm long (100 to 200 g). In these tests, fuel specimens have been heated under atmospheric-pressure conditions at temperatures up to 1700 to 2700 K; times at test temperatures were varied from 2 to 60 min. Major differences in the VI and HI tests were that (1) the VI tests had the test sample oriented vertically (all other ORNL

*M. F. Osborne, J. L. Collins, and R. A. Lorenz, Martin Marietta Energy Systems, Inc., Oak Ridge National Laboratory, "Highlights Report for Fission Product Release Tests of Simulated LWR Fuel," ORNL/NRC/LTR-85/1, February 1985.

Table 3.12 ORNL HI-Series test conditions and results

Test characteristic	Test No.					
	HI-1	HI-2	HI-3	HI-4	HI-5	HI-6
Specimen source, reactor[a]	HBR	HBR	HBR	PB	Oco	Mont
Specimen length, mm	203	203	203	203	152	152
Specimen mass[b], g	168	166	167	306	133	170
Fuel burnup, MWd/kgU	28.1	28.1	25.2	10.1	38.3	40.3
In-pile gas release, %	0.3	0.3	0.3	10.2	4.1	2.0
Steam flow rate, g/h	0.81	0.76	0.31	0.29	0.03	1.7[c]
Test heatup rate, K/s	1.2	1.3	2.1	2.3	1.1	2.3
Test temperature, K	1675	2000	2275	2200	2025	2250
Effective time at test temperature[d], min	33.8	22.5	21.3	21.6	21.5	2.5
UO_2 grain size, μm						
Pretest	2.8	2.8	2.8	6.6	9.2	-
Posttest	3.4	3.9	4.3	6.6	8.9	-
Fuel-cladding interaction	None	Minor	Yes	Yes	Minor	Yes
Fission product release (% of inventory)	h					
Kr-85[e]		51.8	59.3	31.3	19.9	31.6
I-129	3.13	53.0	35.4	24.7	22.4	24.7
Cs-137	2.04	50.5	58.8	31.7	20.3	33.1
Ag-110m[f]	1.75	3.13	0.02	0.09	18.0	5.96
Sb-125[g]	-	1.55	0.001	0.01	0.33	0.06
	0.02					

[a]Reactors: HBR = H.B. Robinson 2, PB = Peach Bottom 2, Oco = Oconee 1, Mont = Monticello.
[b]Total of UO_2 and Zircaloy.
[c]Average value over test time (rate varied from 0.2 to 2.4 g/min during test).
[d]Includes estimates for heatup and cooldown effects.
[e]Includes Kr-85 released during reactor operation.
[f]Ag-110m data for tests HI-2 through HI-4 are probably low.
[g]Sb-125 data are probably low for all tests.

tests had horizontally oriented samples), (2) the fuel burnups in the VI tests were for the most part higher than those used in the HI tests, and (3) VI test temperatures (2300 to 2700 K) were higher than HI test temperatures (1675 to 2275 K). The VI-3 and VI-5 tests were performed at maximum test temperatures of ~2700 K; the test atmosphere (steam in VI-3 and hydrogen in VI-5) was varied so that the influence of atmosphere on high-temperature fission product release could be evaluated.

Measurements made in the HI and VI tests included: (1) test sample temperature vs time by optical pyrometry, (2) thermal gradient tube measurements downstream of the fuel sample to collect condensing vapors, (3) a package of graduated filters and impregnated charcoal cartridges to collect particulates and volatile iodine species, (4) a charcoal cold trap to collect and measure fission gases, and (5) radiation detector measurements to monitor fuel location and to provide on-line measurements of cesium species in the thermal gradient tubes and Kr-85 in the gas traps. In addition, all test components were sampled and analyzed (by gamma-ray spectrometry, neutron activation analysis, spark-source mass spectrometry, and emission spectrometry) after each test.

Some of the key findings include confirmation of the high release rates for noble gases, iodine, and cesium. A difference in transport behavior was noted for cesium in steam relative to hydrogen. Reactive vapor forms of cesium predominate in hydrogen conditions, and transportable aerosols were noted in steam conditions. The releases of tellurium and antimony appear to occur from the UO_2 as for a volatile fission product, but these elements are retained by metallic Zircaloy, so their release is delayed until cladding oxidation is nearly complete. Both europium and antimony showed a sensitivity to the oxygen potential at high temperatures. Antimony release rates were observed to increase in steam conditions relative to hydrogen at temperatures above 2300 K. Hydrogen-rich conditions caused higher releases of europium above 2400 K, compared with steam environments.

Table 3.13 ORNL VI-series test conditions and results

Parameter	Test No.				
	VI-1	VI-2	VI-3	VI-4	VI-5
Fuel specimen	Oconee	BR3	BR3	BR3	BR3
Burnup, MWd/kgU	40	44	44	47	42
In-pile Kr release, %	0.7	~2	~2	~5	~2
Test conditions					
Test temperature, K	2020, 2300[a]	2300	2000, 2700[a]	2440	2000, 2720[a]
Time at temperature, min	20, 20	60	20, 20	20	20, 20
Atmosphere	Steam	Steam	Steam	Hydrogen	Hydrogen
Fractional release, %					
Cs-137	63	67	100	96	100
Kr-85	57	31	100	85	100
I-129	45	40	69	87	[b]
Sb-125	33	68	99	6.4	18
Eu-154	0	0	~0.01	19	57
Ru-106	0	0	5.0	0	0

[a]Test was conducted in two phases at two different temperatures.
[b]Analysis incomplete.

These tests have provided useful information on the release of volatile and less-volatile fission products, on fission product chemical forms and behavior, and on fuel behavior. They have also provided a valuable data base for model and code development purposes.

3.2.2.1 SASCHA Experiments

Out-of-pile core melting experiments were conducted in the SASCHA facility at the Karlsruhe Nuclear Research Centre (KfK). The objectives of the experiments were to quantify the fission product release and activation-product release from overheated fuel rods and from a corium melt and to characterize the physical and chemical forms of the resulting aerosols. The test program started in 1973 and ended in 1984. A total of about 50 tests were performed. The experiments used slightly radioactive fuel rod segments (3 short rods each with 6 Zircaloy-clad UO_2 pellets, including 3 to 6 tracer nuclides) with simulated burnup (i.e., fissium) and representative additions of structural materials, including control rod materials. The effects of temperature, melt composition, and test atmosphere were investigated.[51–56]

The SASCHA program was divided into three successive parts: release experiments conducted in air, similar tests in steam, and simulations of core melt-concrete interactions. Investigations were focused on:

- the behavior of iodine and cesium during and after release from the fuel,
- the potential for AgI formation in the gas phase,
- the size distribution and chemical composition of aerosol particles,
- the influence of steam supply and degree of Zircaloy oxidation,
- determinations of fractional release-rate coefficients,
- fission product release during melt-concrete interactions, and
- estimates of integral values of radioactivity and aerosol mass release from the primary system.

The test samples were placed in a crucible inside an induction-heated furnace and heated to one or more temperature plateaus, each plateau lasting about 10 to 15 min. For a few tests, a heated aerosol transport line was attached above the crucible. The transport line was connected to four main components: a 4-L glass vessel, an automatic filter changer, an 8-stage cascade impactor, and a specific iodine filter. The release behavior of 18 representative fission and activation products was analyzed by gamma-ray spectrometry, as a function of temperature and time. Table 3.14 summarizes the test parameters for the corium

Table 3.14 Conditions for the SASCHA tests

Mass of test specimens, g	150–250
Simulated burnup, MWd/kgU	44
Fission product additives	I, Cs, Te, Cd, Sb, Ag, Ba, Mo, Ru, Zr, Ce, Nd
Additional activation products	Cr, Mn, Fe, Co, Sn, Np
Test temperatures in air, K	1770–3070
Test temperatures in steam, K	2170–2670
Test temperatures in Ar+5% H_2, K	2670
Test temperatures in Ar+5% steam, K	2670
Heatup rate, K/s	0.8–5.0
Gas flow rate, L/min	10–30
Environments	H_2O, Ar-H_2O, Ar-H_2, Air
Pressure	2 bar

melt tests. In addition, two melt-concrete interaction tests were done in air at 1-bar pressure.

The melt included Zircaloy cladding, absorber materials (Ag-In-Cd), Inconel, and stainless steel mixed with the fuel. The compositions of the mixture varied between:

- 35- to 60-wt% fissium (UO_2 with fission product simulant additives),
- 20- to 50-wt% stainless steel,
- 10- to 20-wt% Zircaloy, and
- 5-wt% Inconel or Ag-In-Cd (Ref. 51).

For the time interval of the SASCHA tests (15 to 40 min), almost complete release of the volatile fission products (I and Cs) was measured upon reaching temperatures around 1970 K. Lesser releases of tellurium and antimony were measured. The steam supply and the degree of clad oxidation were identified as essential parameters for the retention of tellurium, which was favored by limited steam supply and unoxidized clad. A similar effect was noted for antimony and silver, but less marked than for tellurium. The opposite effect was noted for barium and strontium. The steam supply did not affect the release of zirconium. The less volatile elements were released to a small percentage only from liquefied material at test temperatures between 2270 and 2670 K.

A set of fractional release-rate coefficients was derived from data in steam and in air. The rates in steam (Table 3.15) were compared to NUREG-0772 data. SASCHA-based release rates were generally lower by a factor of 2 to 3 for tellurium and antimony, and 2 to 3 orders of magnitude lower for Ba, Zr, and Ru, as a result of the reaction behavior of the clad. Release rates of silver were slightly higher than NUREG-0772 (factor of 2) below 2270 K. Releases in steam or air were not significantly different.

Table 3.15 Fractional release rate coefficients in steam at 2670 K—SASCHA corium melt tests

Element	k (min^{-1})	Element	k (min^{-1})
I, Cs, Cd	>0.5	Zr	10^{-5}
In	0.2	U	2×10^{-4}
Ag	0.14	Np	10^{-5}
Te	0.071	Fe	10^{-3}
Sb	0.043	Cr	10^{-3}
Ba	10^{-4}	Co	10^{-3}
Mo	10^{-4}	Mn	0.01
Ru	10^{-6}	Sn	0.014
Ce, Nd	10^{-5}		

In comparing results of the SASCHA tests with results of the ORNL-HS tests (see Sect. 3.2.2), it was noted that the cesium release rates were almost identical and silver also showed good agreement within a factor of 2. The tellurium behavior was the same at 1870 K, but the ORNL rates were higher by a factor of 3.5 to 7 at 2170 to 2270 K. The antimony and tellurium differences were explained by a higher

degree of clad oxidation in the ORNL tests. The ruthenium and europium release rates were within half an order of magnitude of the ORNL results.

The ORNL-HI tests produced release rates of I, Cs, Sb, and Ag that were lower than the SASCHA results by factors of 2 to 4. For temperatures below 2270 K, it was concluded that release rates based on fissium may overestimate the releases from highly irradiated UO_2. This was probably due to differences in microstructural evolution during annealing of the fissium compared with irradiated fuel containing fission gases.

3.2.2.2 HEVA-VERCORS

Fission product and structural material releases from PWR fuel specimens have been studied in out-of-reactor experiments by the French CEA at Grenoble.[57,*] The HEVA program, conducted between 1983 and 1989, consisted of eight tests in the temperature range 1800 to 2370 K. An induction furnace was used to heat Zircaloy-clad specimens of PWR fuel, and gamma spectrometry was used to measure the fission product releases from the fuel and transport to different locations in the apparatus. In most of the tests, aerosols were collected in a heated cascade impactor and in filters. Control rod materials were used in the last two tests (HEVA-07 with Ag-In-Cd exclusively and HEVA-08 with both control rods and fuel). Mixtures of steam/H_2 and pure H_2 have been used as the environments for HEVA tests.[58]

The VERCORS program is an ongoing extension of the HEVA tests using a modified apparatus with augmented instrumentation. To date, three tests have been completed in this program, up to a maximum temperature of 2300°C. Most of the tests in the HEVA-VERCORS program have used spent PWR fuel that was re-irradiated in the SILOE research reactor, after a period of decay following discharge from a power reactor. This permits the detection of short-lived fission products such as I, Te, Mo, Ba, and La.

Table 3.16 summarizes the HEVA-VERCORS test conditions. To date, open publication of test results is limited to the HEVA-04 test[59] and the HEVA-06 test.[58]

3.2.2.3 AECL Chalk River Experiments

Single-effect annealing experiments using irradiated fuel specimens have been conducted in the AECL out-of-pile program on severe accident fission-product release at the CRL. Tests have been conducted at temperatures between 600 and 2350 K in steam, air, and inert environments, covering a wide range of burnup (4.6 to 57.3 MWd/kgU) and linear powers (28 to 62 kW/m). The emphasis of the program has been on CANDU fuel, from both power reactors and the NRU research reactor. Some LWR fuel has also been tested for comparison.[60] In most experiments, the fuel was characterized both before and after the tests by ceramographic examination.

Six different types of furnaces have been used, depending on the temperature range and size of specimen to be heated. For all experiments, monitoring and control of the gas environment has been a priority; in particular, control of the oxygen potential to which the fuel is exposed. One of the key features of the AECL program has been on-line measurements of fuel oxidation kinetics simultaneous with fission product release measuremen[61] This feature has provided data for development of models for severe accident fission product release in oxidizing conditions.[62,63] Another key feature of these tests has been a direct measurement of the fission product release rates, using a gamma-ray spectrometer, which views the heated specimen through a collimated aperture. A second spectrometer is used to monitor activity in the exhaust gas swept out of the furnace.

The fuel specimens include UO_2 fragments (0.2 to 1.5 g each) that were extracted from irradiated fuel elements after discharge and subsequent cutting. These tests have provided information on fission product release from bare UO_2 without any Zircaloy barrier. The role of Zircaloy on fission product release has been investigated using fragments of UO_2 enclosed in Zircaloy foil bags, and short segments of Zircaloy-clad fuel elements with end caps fitted onto one or both ends of these samples to exclude the surrounding atmosphere from direct contact with the UO_2.

A series of isothermal and transient air oxidation tests aimed at quantifying the release rates of important fission products during and after air oxidation of the UO_2 were don at temperatures up to 2350 K (Refs. 64–70,†). Air oxidation of the UO_2 was observed to cause enhanced releases of Xe, Kr, I, and Cs, as well as degradation of the fuel itself. Very rapid releases of ruthenium were also observed in oxidizing conditions.[70,71] Xe, I, and Cs releases during temperature ramps in air were observed to begin at lower temperatures and occur at faster rates from fuel with interconnected porosity compared to fuel with an as-manufactured microstructure.†

*B. Andre and G. Ducros, "The HEVA-VERCORS Programme," Note Technique DTP/SECC No. 44/92, Centre d'Etudes Nucleaires de Grenoble, 1992.

†C. E. L. Hunt et al., "Xenon and Ruthenium Release from UO_2 in Air," *Proceedings of the ANS International Topical Meeting on Safety of Thermal Reactors, Portland, Oregon, July 21–25, 1991.*

Table 3.16 Summary of HEVA-VERCORS experimental conditions

	HVA 01	HVA 02	HVA 03	HVA 04	HVA 05	HVA 06	HVA 07	HVA 08	VERCRS 01	VERCRS 02	VERCRS 03
Test date	1983	1983	1986	1986	1987	1988	1988	1989	1989	1990	1992
Burnup (MWd/kgU)	19.4	19.4	27.7	36.7	36.7	36.7	No Fuel	36.7	42.9	38.3	38.3
Re-irradiation	No	No	No	Yes	Yes	Yes	No	Yes	Yes	Yes	Yes
H_2O flow, g/min	6	1.8	2.2	1.8	1.5	0	1.5	1.5	0.15	0.15–1.5	1.5
H_2 flow, g/min	0	0	0.03	0.03	0.03	0.012	0.03	0.03	0.003	0.003–.27	0.03
Heating rate, °C/s	1	1	1	1	1	2	1	1	1	1	1
Plateau temperature, C	1903	2143	2073	2273	2073	2373	2073	2073	2123	2153	2573
Hold time, min	15	15	30	7	96	30	30	12	17	13	15
Impactor temperature, °C	None	None	1073	873	523	523	523	523	873	873	873
Ag-In-Cd	None	None	None	None	None	None	Yes	Yes	None	None	None
Position and type of γ-detection:											
Fuel sample	None	None	Ge[a]	Ge[a]	Ge[a]	Ge[a]	Ge[a]	Ge[a]	Ge[a]	Ge[a]	Ge[a]
Impactor outlet	None	None	IC[b]	IC[b]	IC[b]	IC[b]	Ge[a],	Ge[a],	Ge[a], IC[b]	Ge[a], IC[b]	Ge[a], IC[b]
After condenser	None	None	None	None	None	None	IC[b]	IC[b]	None	Ge[a]	Ge[a]
							None	None			
Gas chromatograph	No	No	No	No	No	No	No	No	No	Yes	Yes

[a]Ge = germanium crystal gamma spectrometer
[b]IC = ionization chamber

Volatilization of the fuel matrix in oxidizing conditions was identified as an important release mechanism for low-volatile fission products in tests above 2000 K (Ref. 68). An extensive laboratory test series was undertaken to produce a data base for UO_2 volatilization kinetics as a function of temperature and oxygen potential.[72]

A significant increase in barium release rates from bare UO_2 fuel was observed at temperatures above 2220 K, in either inert or oxidizing conditions.[68] Because much lower release rates are measured for clad fuel, it is possible that barium may be released from the UO_2 at high temperatures but is retained by the cladding (as for tellurium and antimony).

Experiments on rod segments have shown that the presence of the Zircaloy sheath can either inhibit or delay the release of volatile fission products, compared to tests under the same conditions using bare UO_2 (Refs. 60 and 73). The delay is primarily associated with the time required to oxidize the Zircaloy cladding, after which the UO_2 begins to oxidize and cause enhanced release rates.

In addition to release from the fuel, deposition of fission products has been studied on various surfaces. The deposition in thermal gradients was measured on Inconel, Zircaloy, carbon steel, and stainless steel surfaces.[74] Aerosol characterization has also been done on individual tests.[75,76] Fine wire impactors, cascade impactors, and high-efficiency particle filters have been used to gain information on the size distribution and composition of aerosol species. This work has been done in cooperation with fission product transport studies being conducted at AECL's Whiteshell Laboratory.

3.2.2.4 Atomic Energy Authority Technology

During the last 10 to 15 years a wide range of experiments has been performed at Atomic Energy Authority (AEA) Harwell to provide data for the development of thermal reactor fuel modeling codes, which are used in reactor safety case assessments and for the licensing of Advanced Gas Reactor (AGR) and LWR systems. The experimental programs have addressed (1) the determination of fission product release and swelling behavior from irradiated fuel in various gaseous atmospheres; (2) volatilization rates of oxidized urania at high temperatures; (3) the effects of irradiation on the thermal and mechanical properties of thermal reactor fuel; (4) fuel melting point determinations as a function of composition, burnup, and stoichiometry; and (5) postirradiation examination and assessment of LWR and AGR fuel.

Out-of-pile studies have been performed in the temperature range 448 to 3273 K using controlled gas compositions and associated oxygen potentials in sweep gas mixtures including air, CO_2/O_2, CO_2/CO, $He/H_2/H_2O$ and Ar/H_2. These studies have been undertaken in several independent facilities. Large-scale tests, requiring fuel annealing temperatures up to 1870 K, have been performed in one of two large-capacity furnaces capable of heating up to 100 g of highly irradiated fuel either as single or multiple fragments at rates of ~5 K/s to 1873 K (Refs. 77 and 78). Condensable fission products are collected on thermal gradient tubes and composite filters for posttest quantitative radiochemical analyses. Continuous measurements of Kr-85 are made in the exhaust sweep gas. Both unclad fuels and stainless steel clad fuels have been studied in this apparatus. Ru-106, I-131, Cs-134, and Cs-137 have been the key radionuclides investigated. Highly irradiated UO_2 has been heated in air[78] to provide data on the release and plate-out behavior of these radionuclides, and these studies are currently being extended to investigate the effects of temperature and oxygen potential.

A separate controlled-atmosphere shielded thermobalance has been used to measure the kinetics of oxidation and concomitant release of Kr-85 (Ref. 79), again utilizing an on-line β scintillator counter. These data have been used to develop fuel oxidation models and methods for the prediction of time to form loose UO_2/U_3O_8 powder. Data collected during air oxidation studies do not show any systematic variation due to fuel manufacturing route, physical properties, or burnup between 11.7 and 26.7 MWd/kgU. Releases of Kr-85 were observed to follow closely the fuel oxidation kinetics over the temperature range 523 to 673 K.

Effects of temperature ramp rate and fuel burnup have been studied extensively[80,81] in a third facility. This is based primarily on a radio frequency induction furnace and capable of heating 3-mm-diam fuel samples at heating rates up to 200 K/s to peak temperatures exceeding 2273 K. An on-line β scintillator counter enables the continuous detection of fission gas release, while posttest ceramographic examination has enabled the analysis of intergranular and intragranular bubble swelling. This work has demonstrated that fission gas release varies both as a function of heating rate and burnup. Currently the work is being extended to investigate the effects of small changes in stoichiometry on fission gas release.

3.2.2.5 Japanese Studies

Out-of-pile annealing experiments have been conducted in Japan in a collaborative effort by the Nippon Nuclear Fuel

Development Company and other sponsors. The focus of this work has been to investigate fission gas release from doped and undoped fuels with controlled microstructures and stoichiometries.[79–86]

The effect of UO_2 grain size has been investigated using samples of undoped standard UO_2 (16 μm), undoped large-grained UO_2 (43 μm), Nb_2O_5-doped UO_2 (110 μm), and TiO_2-doped UO_2 (85 μm). The samples were irradiated in the Halden reactor to a burnup of 23 MWd/kgU. Postirradiation annealing was done at 2070 and 1870 K in He/2% H_2 mixtures with the dew point controlled to provide slightly oxidizing or reducing conditions. The release kinetics of Kr-85 were measured during the annealing. Posttest examinations of the fuel microstructures were compared to the as-fabricated and irradiated microstructures. Differences in bubble swelling were determined from these examinations.

The results of these experiments showed that for the undoped UO_2, the large-grained fuel produced about one-third to one-half as much gas release as for the smaller-grained UO_2. Both of the undoped fuels showed higher releases and greater swelling in the oxidizing anneal compared to the reducing conditions. The doped fuels produced higher gas releases and swelling than the undoped UO_2, and the doped fuel did not show a significant difference between oxidizing or reducing conditions. All of the annealing releases could be described by a transient burst-type release during heating, followed by a diffusional release at constant temperatures. The effective diffusion coefficient for krypton in the doped fuel was about 2 to 3 orders of magnitude higher than for the undoped fuel at 2070 K.

3.2.2.6 ANL Direct-Electric-Heating Tests

From 1972 to 1979, experiments were conducted at ANL using DEH to heat irradiated fuel specimens in rapid transient modes.[87,88] Tests were conducted to study the behavior of both unirradiated and irradiated LWR fuel during power-cooling mismatch (PCM) transients and LOCA conditions.

The DEH technique uses ohmic heating of the UO_2, produced by passing an electric current axially through the sintered UO_2. DEH is different from nuclear heating because the electrical conductivity of UO_2 increases with temperature, and thus most of the current flows through the hot central region of the fuel. However, ohmic heating of the UO_2 combined with surface heat removal by the surrounding coolant flow produces a radial temperature profile that approximates the profile for fission or decay-heated fuel.

Two separate versions of DEH equipment were developed. The first version was used for PCM tests, and the second was used for blowdown-reflood LOCA tests. Depending on the type of test, the pellet stack was surrounded by a loose quartz sleeve (unrestrained geometry) or in a tight-fitting boron nitride sleeve (restrained geometry). A linearly variable differential transformer (LVDT) was used to monitor axial expansion or slumping motion. An optical pyrometer was used to measure the surface temperatures of the UO_2. The current-control circuitry allowed power to be increased at preset rates to simulate various thermal transients. Centerline heating rates of 2 to 500 K/s could be produced.

Flowing helium was used to cool the surface of the pellet stack and carry away fission gases released from the fuel. Particulate filters and a liquid-nitrogen-cooled activated charcoal trap were used to collect the fission products. The trapped gases were recovered and analyzed during posttest heating of the charcoal trap.

For all tests, it was necessary to preheat the UO_2 to increase electrical conductivity. The most significant difference between the two apparatus designs was the type of preheater used. In the first version, a focused line heater was used to preheat one side of the pellet stack. This produced nonuniform heating and was replaced in the second design by a tungsten mesh heater surrounding the pellet stack.

The ANL DEH program consisted of 23 PCM-type tests and 2 LOCA-type tests.[88] All of the tests were of short duration—less than ~2 min after the preheating period. UO_2 melting was produced in some tests. Integral gas releases of xenon and krypton were measured, and posttest examination was used to determine melt radii, grain growth, and other microstructural changes. Retained fission gas was also measured as a function of radius using localized laser heating.

Simulations of the PCM conditions were used to develop an empirical correlation for gas release with transient heating rates for constrained and unconstrained fuel.[88] Mechanical constraint was found to reduce gas releases by preventing formation of microcracks. Microstructural aspects of swelling, melting, and microcracking were investigated in the DEH tests, and this information was used during development of the GRASS-SST code for calculating gas release (see Sect. 3.3).

3.2.3 Nonfission Product Core Material Release Experiments

3.2.3.1 ORNL-HS Tests

The ORNL HS-series of tests (simulant fuel) provided data on structural material releases and simulant fission products. The results are discussed in Sect. 3.2.2.

3.2.3.2 SASCHA

The SASCHA program at KfK provided data on both fission product and structural material releases. The results of this program are reviewed in Sect. 3.2.2.1.

3.2.3.3 AEA Technology

Ag-In-Cd Control Rod. A large number of experiments have been conducted at Winfrith to characterize the release rates and aerosol characteristics of the control rod components.[89–91] These have involved heating both stainless steel clad and unclad elements of Ag-In-Cd at temperatures up to 1970 K in an induction furnace facility. Typically the clad samples were 40 mm long and 8.75-mm diam to hold 24 g of alloy (8.66-mm diam). The aerosols were characterized in both steam and inert atmospheres. Mass balance experiments were conducted to determine the distribution of the control rod alloy constituents, and the work was supported by differential thermal analyses of silver-indium mixtures. Metallographic studies were undertaken to characterize the failure mode of the stainless steel cladding and the interaction of the molten alloy with Zircaloy. Time-dependent measurements of the released material were conducted to quantify the release rate, while various aerosol analysis methods were used to characterize the aerosol.

Over 50 separate experiments have been conducted. Key points of note include the enhanced release of indium in a steam atmosphere (through formation of a transient hydroxide species InOH),[92] with the stabilization of relatively large cadmium spheres and smaller indium-based material resulting in semi-independent transport behavior.

Boric Acid. Various experiments have been conducted to investigate the role of boric acid and the physical characteristics of the aerosol.[93,94] Most studies involved injecting aqueous solutions of boric acid (either 200 or 2000 ppm boron) at a controlled rate onto a 304 stainless steel core held at 1270 K. The transport and deposition of the resulting aerosol was studied through a system including pipework and a dilution chamber. Two types of aerosol were formed: (1) large (~20-μm volume equivalent diameter) deposits with complex crystalline features and (2) small, approximately spherical deposits of ~0.1-μm volume equivalent diameter that agglomerated to form deposits of typically 1 μm.

The first type was formed by flashing of the aqueous solution on contact with the hot steel surfaces, and the second category involved volatilization of boric acid; formation of this aerosol was favored by higher temperatures. Work was also conducted to characterize the interaction between boric acid and stainless steel; the degree of interaction increased with increasing temperature, and a variety of products was formed, including iron borates.

More recent experiments have considered alternative release methods under more typical conditions, including evaporation from a boric acid solution (simulating vaporization of the core coolant[95]).

Zircaloy. Zircaloy samples (≈20 g) have been heated to 2370 K in a steam/argon atmosphere in an induction furnace apparatus. Any released material was collected either along a thermal gradient tube or by a single-stage inertial impactor. Complementary mass spectrometric experiments were also conducted to measure the vapor pressure of the tin component of Zircaloy as functions of the temperature and degree of Zircaloy oxidation. The experiments demonstrated that the aerosol releases from both of these potential sources were small: ≤0.6% of the tin and $\leq 2 \times 10^{-4}$% of the zirconium inventories. Tin was released as a vapor, and the zirconium dioxide aerosol was generated mechanically and consisted of small flakes of ~0.1-μm geometric diameter.

Integral Experiments. A large number of experiments have been conducted in the Falcon facility to study the release of fission products in the presence of both control rod and boric acid.[96–100] While some release rate information was obtained from these studies, these generally confirmed the separate-effects findings discussed previously. Most of the results of the program are more relevant to fission product transport issues and are discussed accordingly in Chap. 4.

3.2.3.4 AECL Whiteshell Experiments

Experimental data on release rates of structural materials (fuel and cladding) have been obtained at the AECL Whiteshell Laboratory by heating clad-UO_2 pellets (of the same size and dimension used in a CANDU power reactor) in a flowing steam and argon atmosphere.[101,102] Data were obtained as a function of temperature (1770 to 2370 K), steam flow rate, and surface area exposed to

steam. Rates for U, Sn, Fe, and Cr are summarized, and data on aerosol size distributions have been measured.

3.2.4 References

1. M. D. Allen, H. D. Stockman, K. O. Reil, and J. W. Fisk, "Fission Product Release and Fuel Behavior of Irradiated Light Water Reactor Fuel under Severe Accident Conditions: The ACRR ST-1 Experiment," USNRC Report NUREG/CR-5345, September 1991.*

2. M. D. Allen, H.W. Stockman, K.O. Reil, and A.J. Grimley, "Fission Product Release and Fuel Behavior of Irradiated Light Water Reactor Fuel under Severe Accident Conditions: The ACRR ST-1 Experiment," *Nucl. Technol.* 92, 214–228 (1990).†

3. M. D. Allen et al., Sandia National Laboratories, "ACRR Fission Product Release Tests: ST-1 and ST-2," *Proceedings of the International ENS/ANS Conference on Thermal Reactor Safety, Avignon, France, October 2–7, 1988*, Vol. 5, and SAND88-0597C, 1988.*

4. L. N. Kmetyk, Sandia National Laboratories, "MELCOR 1.8.1 Assessment: ACRR Source Term Experiments ST-1/ST-2," SAND91-02833, April 1992.*

5. A. J. Grimley, Sandia National Laboratories, "A Thermodynamic Model of Fuel Disruption in ST-1," USNRC Report, NUREG/CR-5312 (SAND88-03324), February 1991.*

6. J. E. Herceg et al., "TREAT Light Water Reactor Source term Experiments Program," *Proceedings of the ANS Topical Meeting on Fission Product Behavior and Source Term Research, Snowbird, Utah, July 15–19, 1984*, Electric Power Research Institute, NP-4113-SR, July 1985.

7. L. Baker et al., "Source Term Experiments Project (STEP): A Summary," Electric Power Research Institute, NP-5753M, March 1988.

8. A. D. Knipe, S. A. Ploger, and D. J. Osetek, "PBF Severe Fuel Damage Scoping Test—Test Results Report," USNRC Report NUREG/CR-4683, March 1986.*

9. Z. R. Martinson, D. A. Petti, and B. A. Cook, "PBF Severe Fuel Damage Test 1-1 Test Results Report," USNRC Report NUREG/CR-4684 (EGG-2463), Vol. 1, October 1986.*

10. Z. R. Martinson et al., "PBF Severe Fuel Damage Test 1-3 Test Results Report," USNRC Report NUREG/CR-5354 (EGG-2565), October 1989.*

11. D. A. Petti et al., "Power Burst Facility (PBF) Severe Fuel Damage Test 1-4 Test Results Report," USNRC Report NUREG/CR-5163 (EGG-2542), April 1989.*

12. D. L. Reeder, Idaho National Engineering Laboratory, "LOFT System and Test Description," USNRC Report NUREG/CR-0247 (TREE-1208), July 1978.*

13. E. Schuster, W. Morell, and W. Kuhnlein, "Experimental Analysis and Summary Report for OECD LOFT LP-FP-1, Volume 4, Fission Product Behavior," Organization for Economic Cooperation and Development, OECD-LOFT-LP-FP-1, Paris, France (1990).

14. E. Schuster, "FP Release and Deposition in LOFT-PL-FP-1," *Proceedings of Open Forum on the OECD/LOFT Project, Achievements and Significant Results, Madrid, Spain, 1990 May 9–11*, Organization for Economic Cooperation and Development, Paris, France (1991).

15. M. L. Carboneau, V. T. Berta, and M. S. Modro, "Experiment Analysis and Summary Report for OECD LOFT Project Fission Product Experiment LP-FP-2," Organization for Economic Cooperation and Development, OECD-LOFT-T-3806, Paris, France (June 1989).

16. R. R. Hobbins and G. D. McPherson, "Summary of Results of the LOFT-PL-FP-2 Test and Their Relationship to Other Studies at the PBF and of the TMI-2 Accident," Organization for Economic Cooperation and Development, OECD-LOFT-T-3806, Paris, France (June 1989).

17. S. M. Jensen, D. W. Akers, and B. A. Pregger, "Post-irradiation Examination Data and Analysis for OECD LOFT Project Fission Product Experiment LP-FP-2, Volume 1," Organization for Economic Cooperation and Development OECD-LOFT-T-3810, Vol. 1, Paris, France (December 1989).

18. M. L. Carboneau et al., "OECD LOFT Project Fission Product Experiment LP-FP-2: Fission Product Data Report," Organization for Economic Cooperation and Development OECD-LOFT-T-3805, Paris, France (May 1987).

19. A. Arnaud and A. Markovina, "Objectives, Test Matrix and Representativity of the PHEBUS-FP Experimental Programme, The PHEBUS FP Project: Presentation of the Experimental Programme and Test Facility," W. Krischer and M.C. Rubenstein, Eds. (Elsevier, 1991).

20. P. Von der Hardt and A. Tattegrain, "The PHEBUS Fission Product Project," *J. Nucl. Mater.* 188 (1992).†

21. N. J. Lombardo and F. E. Panisko, "Principle Results of Severe Damage Tests on Full Length Nuclear Fuel Rods," p. 297 in *Proceedings of the ANS International Topical Meeting on the Safety of Thermal Reactors, Portland, Oregon, USA, July 1991,* American Nuclear Society, 1991.

22. D. D. Lanning et al., Pacific Northwest Laboratory, "Data Report: Full-Length High-Temperature Experiment 5," PNL-6540, April 1988.*

23. J. M. Broughton, P. Kuan, D. A. Petti, and E. L. Tolman, "A Scenario of the Three Mile Island Unit 2 Accident," *Nucl. Technol.* 87, 34 (1989).†

24. D. W. Akers and R. K. McCardell, "Core Materials Inventory and Behavior," *Nucl. Technol.* 87, 214 (1989).†

25. D. W. Akers and R. K. McCardell, "Fission Product Partitioning in Core Materials," *Nucl. Technol.* 87, 264 (1989).†

26. D. A. Petti, J. P. Adams, J. L. Anderson, and R. R. Hobbins, "Analysis of Fission Product Release Behavior from the Three Mile Island Unit 2 Core," *Nucl. Technol.* 87, 243 (1989).†

27. D. W. Akers et al., "Three Mile Island Unit 2 Fission Product Inventory Estimates," *Nucl. Technol.* 87, 205 (1989).†

28. J. A. Walsworth et al., "The Canadian In-Reactor Blowdown Test Facility (BTF) Program in Support of Reactor Safety," *Proceedings of the International Symposium on Research Reactor Safety Operations and Modifications, Chalk River, Ontario, Canada, October 23–27, 1989,* International Atomic Energy Agency, IAEA-SM-310/102, Austria (1990).

29. R. D. MacDonald et al., "An In-Reactor Loss-of-Coolant Test with Flow Blockage and Rewet," Presented at the ANS International Topical Meeting on Safety of Thermal Reactors, Portland, Oregon, July 21–25, 1991, Atomic Energy of Canada Limited Report AECL-10464, Canada (1991).

30. J. W. DeVaal et al., "Post-Test Simulations of BTF-107: An In-Reactor Loss-of-Coolant Test with Flow Blockage and Rewet," pp. 4-43 to 4-60 in *Proceedings of the 3rd International Conference on CANDU Fuel, Pembroke, Ontario, Canada, October 4–8, 1992,* also Atomic Energy of Canada Limited Report AECL-10758, Canada (1993).

31. P. Knudsen et al., "Fission Product Behavior in High Burnup Reactor Fuel Subjected to Slow Power Increases," *Nucl. Technol.* 72 (March 1986).†

32. P. Knudsen et al., "Fission Product Behavior in High-Burnup Water Reactor Fuel Subjected to Slow Power Increases," *Proceedings of the ANS Topical Meeting on LWR Fuel Performance, Williamsburg VA, April 17–20, 1988,* American Nuclear Society, 1988.

33. M. Morgensen, C. Bagger, C. T. Walker, "An Experimental Study of the Distribution of Retained Xenon in Transient-Tested UO_2," *J. Nucl. Mater.* 199, 85–101 (1993).†

34. R. A. Lorenz, D. O. Hobson, and G. W. Parker, Union Carbide Corporation Nucl. Div., Oak Ridge National Laboratory, "Final Report on the First Fuel Rod Failure Transient Test of a Zircaloy-Clad Fuel Rod Cluster in TREAT," ORNL-4635, March 1971.*

35. R. A. Lorenz, D. O. Hobson, and G. W. Parker, "Fuel Rod Failure Under Loss-of-Coolant Conditions in TREAT," *Nucl. Technol.* 11, 502 (1971).†

36. R. A. Lorenz and G. W. Parker, Union Carbide Corporation Nucl. Div., Oak Ridge National Laboratory, "Final Report on the Second Fuel Rod Failure Transient Test of a Zircaloy-Clad Fuel Rod Cluster in TREAT," ORNL-4710, January 1972.*

37. G. W. Parker, R. A. Lorenz, and J. G. Wilhelm, "Release of Fission Products from Reactor Fuels During Transient Accidents Simulated in TREAT," pp. 292–324 in *Proceedings of the International Symposium on Fission Product and Transport Under Accident Conditions, Oak Ridge, Tennessee, April 5–7, 1965*, USNRC Conference Proceedings CONF-650407, Vol. 1.*

38. G. W. Parker, R. A. Lorenz, and J. G. Wilhelm, Union Carbide Corporation Nucl. Div., Oak Ridge National Laboratory, "Simulated Transient Accidents in TREAT," pp. 39–68 in *Nuclear Safety Semiannual Progress Report for Period Ending June 30, 1965*, ORNL-3843, September 1965.*

39. G. W. Parker, R. A. Lorenz, and J. G. Wilhelm, Union Carbide Corporation Nucl. Div., Oak Ridge National Laboratory, "Simulated Transient Accidents in TREAT," pp. 8–20 in *Nuclear Safety Program Semiannual Progress Report for Period Ending Dec. 31, 1965*, ORNL-3915.*

40. G. W. Parker, R. A. Lorenz, and J. G. Wilhelm, Union Carbide Corporation Nucl. Div., Oak Ridge National Laboratory, "Simulated Transient Accidents in TREAT," pp. 8–20 in *Nuclear Safety Program Annual Progress Report for Period Ending Dec. 31, 1966*, ORNL-4071, March 1967.*

41. G. W. Parker and R. A. Lorenz, Union Carbide Corporation Nucl. Div., Oak Ridge National Laboratory, "Simulated Transient Accidents in TREAT," pp. 44–54 in *Nuclear Safety Program Annual Report for Period Ending Dec. 31, 1967*, ORNL-4228, April 1968.*

42. R. A. Lorenz et al., Union Carbide Corporation Nucl. Div., Oak Ridge National Laboratory, "Fission Product Release from Highly Irradiated LWR Fuel," USNRC Report NUREG/CR-0722 (ORNL/NUREG/TM-287/R2), February 1980.*

43. R. A. Lorenz et al., Union Carbide Corporation Nucl. Div., Oak Ridge National Laboratory, "Fission Product Release from Highly Irradiated LWR Fuel Heated to 1300–1600 C in Steam," USNRC Report NUREG/CR-1386 (ORNL/NUREG/TM-346), November 1980.*

44. R. A. Lorenz et al., Union Carbide Corporation Nucl. Div., Oak Ridge National Laboratory, "Fission Product Release from BWR Fuel Under LOCA Conditions," USNRC Report NUREG/CR-1773 (ORNL/NUREG/TM-388), July 1981.*

45. M. F. Osborne, J. L. Collins, and R. A. Lorenz, "Experimental Studies of Fission Product Release from Commercial LWR Fuel Under Accident Conditions," *Nucl. Technol.* 78(2), 157–169 (August 1987).†

46. M. F. Osborne, Martin Marietta Energy Systems, Inc., Oak Ridge National Laboratory, "Data Summary Report for Fission Product Release Test VI-1," USNRC Report NUREG/CR-5339 (ORNL/TM-11104), June 1989.*

47. M. F. Osborne et al., Martin Marietta Energy Systems, Inc., Oak Ridge National Laboratory, "Data Summary Report for Fission Product Release Test VI-2," USNRC Report NUREG/CR-5340 (ORNL/TM-11105), September 1989.*

48. M. F. Osborne et al., "Data Summary Report for Fission Product Release Test VI-3," USNRC Report NUREG/CR-5480 (ORNL/TM-11399), June 1990.*

49. M. F. Osborne et al., "Data Summary Report for Fission Product Release Test VI-4," USNRC Report NUREG/CR-5481 (ORNL/TM-11400), January 1991.*

50. M. F. Osborne et al., "Data Summary Report for Fission Product Release Test VI-5," USNRC Report NUREG/CR-5668 (ORNL/TM-11743) October 1991.*

51. H. Albrecht and H. Wild, "Review of the Main Results of the SASCHA Program on Fission Product Release Under Core Melt Conditions," *Proceedings of ANS Topical Meeting on Fission Product Behavior and Source Term Research, Snowbird (Utah), July 15–19, 1984*, Electric Power Research Institute, NP-4113-SR, July 1985.

52. H. Albrecht and H. Wild, "Investigation of Fission Product Release by Annealing and Melting of LWR Fuel Pins in Air and Steam," *Topical Meeting on Reactor Safety and Aspects of Fuel Behavior, Sun Valley (Idaho), August 2–6, 1981*, American Nuclear Society, 1981.

53. H. Albrecht, V. Matschoss, and H. Wild, "Experimental Investigation of Fission Product Release from LWR Fuel Rods at Temperatures Ranging from 1500 to 2800°C," *IAEA Specialists Meeting on Behavior of Defected Zirconium Alloy Clad Ceramic Fuel in Water Cooled Reactors, Chalk River (ON) Canada, September 17–20, 1979*, International Atomic Energy Agency, IAEA-IWGFPT/6, Austria (May 1980).

54. H. Albrecht, "Out-of-Pile Release Tests Under Core Melting Conditions," *OECD/NEA/CSNI/IAEA Meeting, Riso, Denmark, May 16–20, 1983*, International Atomic Energy Agency, IAEA-IWGFPT/6, Austria (1983).

55. H. Albrecht and H. Wild, "Behavior of I, Cs, Te, Ba, Ag, In and Cd During Release from Overheated PWR Cores," *International Meeting on Nuclear Reactor Safety, Cambridge (MA), USA, August 28–September 1, 1983*, American Nuclear Society, 1983.

56. H. Albrecht, "Release of Fission and Activation Products at LWR Core-Melt: Final Report of the SASCHA Program," report KFK 4264, Kernforschungszentrum Karlsruhe, Federal Republic of Germany (June 1987).

57. G. Le Marois and R. Warlop, "Source Term Experiment for Fission Product Transport Assessment: the HEVA Programme," *Proceedings of International Conference on Thermal Reactor Safety, Avignon, France, October 2–7, 1988*, Societe Francaise d' Energie Nucleaire, Paris, France (1988).

58. J. M. Dumas, G. Lhiaubet, G. Lemarois, and G. Ducros, "Fuel Behavior and Fission Product Release Under Realistic Hydrogen Conditions: Comparison Between HEVA 06 Test Results and VULCAIN Computations," ICHMT Seminar on Fission Product Transport Processes in Reactor Accidents, Dubrovnik, Yugoslavia, May 22–26, 1989, in *Fission Product Transport Processes in Reactor Accidents*, J. T.Rogers, Ed. (Hemisphere Publishing, 1990).

59. R. A. Lorenz, J. L. Collins, and A. P. Malinauskas, "Fission Product Source Terms for the Light Water Reactor Loss-of-Coolant Accident," *Nucl. Technol.* 46, 40 (1990).†

60. D. S. Cox et al., "Fission-Product Release Kinetics from CANDU and LWR Fuel During High-Temperature Steam Oxidation Experiments," *Proceedings of IAEA Technical Committee Meeting on Fission Gas Release and Fuel Rod Chemistry Released to Extended Burnup, Pembroke, Ontario, Canada, April 28–May 1, 1992*, International Atomic Energy Agency, IAEA-TEC DOC-647, Austria (April 1993).

61. D. S. Cox, R. F. O'Connor, and W. W. Smeltzer, "Measurement of Oxidation/Reduction Kinetics to 2100°C Using Non-Contact Solid-State Electrolytes," *Solid State Ionics*, 53–56, 238 (1992).†

62. B. J. Lewis and F. C. Iglesias, "A Model for Calculating Fission Gas Diffusion in Annealing Experiments," *J. Nucl. Mater.* 154, 228 (1988).†

63. B. J. Lewis, F. C. Iglesias, D. S. Cox, and E. Gheorghiu, "A Model for Fission Gas Release and Fuel Oxidation Behavior for Defected UO_2 Fuel Elements," *Nucl. Technol.* 92, 353 (1990).†

64. C. E. L. Hunt et al., "Fission Product Release During UO_2 Oxidation," p. 508 in *International Conference on CANDU Fuel, Chalk River Nuclear Laboratories, Chalk River, Ontario, Canada, October 6–8, 1986*, Canadian Nuclear Society, 1986.

65. F. C. Iglesias et al., "UO_2 Oxidation and Fission Product Release," *Proceedings of Workshop on Chemical Reactivity of Oxide Fuel and Fission Product Release, Berkeley, Gloucestershire, United Kingdom, April 7–9, 1987*, Central Electricity Generating Board (1987).

66. D. S. Cox et al., "Fission Product Release from UO_2 in Air During Temperature Ramps," *Proceedings of the Canadian Nuclear Society 8th Annual Conference, Saint John, New Brunswick, June 14–17, 1987*, Canadian Nuclear Society (1987).

67. C. E. L. Hunt, F. C. Iglesias, and D. S. Cox, "Measured Release Kinetics of Iodine and Cesium from UO_2 at High Temperatures under Reactor Accident Conditions," ICHMT Seminar on Fission Product Transport Processes in Reactor Accidents, Dubrovnik, Yugoslavia, May 22–26, 1989, in *Fission Product Transport Processes in Reactor Accidents*, J. T. Rogers, Ed. (Hemisphere Publishing, 1990), p. 163.

68. D. S. Cox et al., "Fission-Product Releases from UO_2 in Air and Inert Conditions at 1700–2350 K: Analysis of the MCE-1 Experiment," *Proceedings of the ANS International Topical Meeting on Safety of Thermal Reactors, Portland, Oregon, U.S.A., July 21–25, 1991*, also as Atomic Energy of Canada Limited Report, AECL-10438, Canada (1991).

69. C. E. L. Hunt et al., "UO_2 Oxidation in Air or Steam—Release or Retention of the Fission Products Ru, Ba, Ce, Eu, Sb, and Nb," *Proceedings of the 8th Annual CNS Conference, Saint John, New Brunswick, June 14–17, 1987*, Canadian Nuclear Society (1987).

70. F. C. Iglesias et al., "Measured Release Kinetics of Ruthenium from Uranium Oxides in Air and Steam," pp. 7282–1296 in *Proceedings of International ENS/ANS Conference on Thermal Reactor Safety, Avignon, France, October 2–7*, 1988, Societe Francaise d' Energie Nucleaire, Paris, France (1988).

71. F. C. Iglesias, C. E. L. Hunt, F. Garisto, and D. S. Cox, "Ruthenium Release Kinetics from Uranium Oxides," ICHMT Seminar on Fission Product Transport Processes in Reactor Accidents, Dubrovnik, Yugoslavia, May 22–26, 1989, in *Fission Product Transport Processes in Reactor Accidents*, J. T. Rogers, Ed. (Hemisphere Publishing, 1990), p. 187.

72. D. S. Cox et al., "High-Temperature Oxidation Behavior of UO_2 in Air and Steam," *Proceedings of the International Symposium on High-Temperature Oxidation and Sulphidation Processes, Hamilton, Ontario, Canada, August 26-30, 1990* (Pergamon Press, 1990).

73. D. S. Cox, Z. Liu, R. S. Dickson, and P. H. Elder, "Fission-Product Release During Post-Test Annealing of High-Burnup CANDU Fuel," *Third International Conference on CANDU Fuel, Pembroke, Ontario, Canada, October 4–8, 1992*, Canadian Nuclear Society (1992).

74. C. E. L. Hunt et al., "The Release and Transport of Fission Products During Oxidation of UO_2 in Air," 192nd *Proceedings of 192nd American Chemical Society National Meeting, Symposium on Chemical Phenomena Associated with Radioactivity Releases During Severe Nuclear Plant Accidents, Anaheim, California, September 7–12, 1986*, American Nuclear Society, USNRC Conference Proceedings NUREG/CP-0078, 1990.*

75. S. R. Mulpuru et al., "Characterization of Aerosol Particles Formed During Steam Oxidation of an Irradiated UO_2 Sample," Atomic Energy of Canada Limited Report, AECL-9847, Canada (1990).

76. S. R. Mulpuru and M. D. Pellow, "Experimental Study of Aerosol Extraction and Transport in a Sampling System for Nuclear Aerosols," *The Ninth Annual Meeting of the American Association of Aerosol Research, Philadelphia, June 18–22, 1990*, American Nuclear Society, 1990.

77. R. Williamson and S. A. Beetham, "Fission Product and U_3O_8 Particulate Emission Arising from the Oxidation of Irradiated Uranium Dioxide: Preliminary Studies," ICHMT Seminar on Fission Product Transport Processes in Reactor Accidents, Dubrovnik, Yugoslavia, May 22–26, 1989, in *Fission Product Transport Processes in Reactor Accidents*, J. T. Rogers, Ed. (Hemisphere Publishing, 1990).

78. R. Williamson and S. A. Beetham, "Fission Product Release During the Air Oxidation of Irradiated Uranium Dioxide," ICHMT Seminar on Fission Product Transport Processes in Reactor Accidents, Dubrovnik, Yugoslavia, May 22–26, 1989, in *Fission Product Transport Processes in Reactor Accidents*, J. T. Rogers, Ed. (Hemisphere Publishing, 1990).

79. M. J. Bennett, J. B. Price, and P. Wood, "Influence of Manufacturing Route and Burn-up on the Oxidation and Fission Gas Release Behavior of Irradiated Uranium Dioxide in Air at 175–400°C," *Proceedings of the Workshop on Chemical Reactivity of Oxide Fuel and Fission Product Release, Gloucestershire, United Kingdom, April 7–9, 1987*, Central Electricity Generating Board, United Kingdom (1987).

80. G. J. Small, "Fission Gas Release from Uranium Dioxide in High Temperature Transients," Atomic Energy Authority Report AERE R12956, United Kingdom (May 1988).

81. G. J. Small, "Fission Gas Release and Bubble Development in UO_2 During High Temperature Transients," *Proceedings of IAEA Committee Meeting on Water Reactor Fuel Element Computer Modelling in Steady State and Transient Accident Conditions, Preston, UK, September 1988,* International Atomic Energy Agency, IAEA-IWGFPT/32, Austria (1988).

82. K. Une, S. Kashibe, and K. Ito, "Fission Gas Behavior During Postirradiation Annealing of Large Grained UO_2 Fuels Irradiated to 23 GWd/t," *J. Nucl. Sci. Technol.* 30, 221 (1993).†

83. K. Une, I. Tanabe, and M. Oguma, *J. Nucl. Mater.* 150, 93 (1987).†

84. K. Une and S. Kashibe, *J. Nucl. Sci. Technol.* 27, 1002 (1990).†

85. S. Kashibe and K. Une, *J. Nucl. Sci. Technol.* 28, 1090 (1991).†

86. K. Une and S. Kashibe, *J. Nucl. Mater.* 189, 210 (1992).†

87. B. J. Wrona and E. Johanson, "Development of Direct-Electrical-Heating Apparatus to Study the Response of Nuclear Fuels to Applied Transients," *J. Nucl. Technol.* 29, 433 (1976).†

88. S. M. Gehl, "The Release of Fission Gas During Transient Heating of LWR Fuel," USNRC Report NUREG/CR-2777 (ANL-80-108), May 1982.*

89. J. P. Mitchell, A. L. Nichols, and J. A. Simpson, "The Characterization of Ag-In-Cd Control Rod Aerosols Generated at Temperatures Below 1900 K," p. 37 in *Proceedings of CSNI Specialist Meeting on Nuclear Aerosols in Reactor Safety, September 4–6, 1984,* Kernforochungszentrum Karlsruhe KfK 3800/ CSNI 95, Germany (1985).

90. B. R. Bowsher et al., "Silver, Indium-Cadmium Control Rod Behavior During a Severe Reactor Accident," Atomic Energy Authority Report AEEW-R, United Kingdom (1991).

91. A. M. Beard and P. J. Bennett, "Characterization of Control Rod Release Rates and Aerosol Behavior," Atomic Energy Authority Report AEA TRS 5064, United Kingdom (1991).

92. I. R. Beattie et al., "Metal Hydroxides and their Relevance to Vapor Transport in Severe Reactor Accidents," ICHMT Seminar on Fission Product Transport Processes in Reactor Accidents, Dubrovnik, Yugoslavia, May 22–26, 1989, in *Fission Product Transport Processes in Reactor Accidents,* J. T. Rogers, Ed. (Hemisphere Publishing, 1990), p. 137.

93. B. R. Bowsher, "The Role of Boric Acid in the PHEBUS-FP Experiments," Atomic Energy Authority Report AEA RS 5166, United Kingdom (1991).

94. A. B. Anderson, A. M. Beard, P. J. Bennett, and C. G. Benson, "Characterization of Boric Acid Aerosol Behavior and Interactions with Stainless Steel," Atomic Energy Authority Report AEA TRS 5091, United Kingdom (1991).

95. A. M. Beard, L. Codron, and A. Mason, "Evaluation of Different Methods of Introducing Boric Acid into the PHEBUS-FP Tests," Atomic Energy Authority Report AEA RS 5344, United Kingdom (1992).

96. C. G. Benson, B. R. Bowsher, and M. S. Newland, *Falcon Seminar, Winfrith Technology Centre, June 27–28, 1989,* Atomic Energy Authority Report AEEW-M 2612, United Kingdom (1989).

97. P. J. Bennett and B. R. Bowsher, *Falcon II Seminar, Winfrith Technology Centre, March 13–14, 1992,* Atomic Energy Authority Report AEA RS 5116, United Kingdom (1991).

98. P. J. Bennett, B. R. Bowsher, and D. A. Williams, *CSNI ISP 34 (Falcon): Proceedings of First Workshop, Winfrith Technology Centre, March 23–24, 1992,* Atomic Energy Authority, AEA RS 5321, United Kingdom (1992).

99. A. M. Beard et al., "Fission Product and Aerosol Behavior within the Containment," Commission of the European Communities Report EUR 12844 EN, Brussels (1990).

100. A. M. Beard et al., "Chemistry Studies in Support of PHEBUS-FP: Multicomponent Aerosol Behavior,"

Commission of the European Communities Report 14005, Vols. 1 and 2, Brussels (1992).

101. S. R. Mulpuru, D. J. Wren, and R. K. Rondeau, "Aerosol Material Release Rates from Zircaloy-4 at Temperatures 2000 to 2200°C," AECL report WNRE-770, 1988. Also, *Trans. Am. Nucl. Soc.* 55, 434 (1988).†

102. S. R. Mulpuru, F. B. Banks, and M. D. Pellow, "Aerosol Material Releases from a Zircaloy-4 Clad UO_2 Pellet at Temperatures up to 2000°C in a Flowing Argon Atmosphere," p. 245 in *Canadian Nuclear Society 9th Annual Conference Proceedings, Winnipeg, Mb, 1988*, Canadian Nuclear Society (1988).

*Available for purchase from the National Technical Information Service, Springfield, VA 22161.
†Available in public technical libraries.

3.3 Review of Main Computer Models/Codes

Computer codes for modeling in-vessel fission product (FP) release may be divided into two categories:

1. **System codes** that cover all aspects of severe accident phenomena, that is, in-vessel degraded core phenomena such as structure heatup, oxidation, fuel melting and relocation, and debris formation, reactor coolant system (RCS) thermal hydraulics, and ex-vessel phenomena.

   In most cases the associated FP release during the accident sequences is treated by means of models from:

2. **Special FP release codes.** These are stand-alone codes for the calculation of FP release to the RCS with input requirements for the governing core state (e.g., fuel rod temperatures). Some of the codes also treat fission product transport (see Chap. 4).

In terms of in-vessel FP release, the system codes are largely based on modeling features from the special FP release codes. Thus, a review of the governing system code models requires a review of the underlying FP release code models. The latter again can be split into two categories:

1. **empirical** models, based on an Arrhenius type of correlation for the release rate with the constants and exponents found by fitting experimental data, and

2. **mechanistic** models, which define one or more serially connected steps of release with certain regimes of FP release in the course of an accident:

   (i) from intact fuel rods, absorber rods, and structural materials,

   (ii) during fuel dissolution and molten material relocation,

   (iii) from debris beds,

   (iv) from molten pools, and

   (v) from fuel-coolant interactions.

Most codes address the first regime (see Fig. 3.1 for illustration), and only a few address at least parts of regimes (ii), (iii), (iv), and (v). Drawing a line between mechanistic and empirical types is not as straightforward in the case of codes as it is in the case of models. Codes, for example CORSOR-Booth and VICTORIA, may apply mechanistic models for certain species (e.g., xenon) and empirical correlations for others.

Some of the mechanistic models/codes concentrate on detailed modeling of a limited number of rate limiting processes; for example, the first three of the following processes of serially connected FP release steps up to release to the coolant (see Table 3.17):

- mass transport in fuel grains and to the grain surface (diffusion as atoms and diffusion within bubbles, due to temperature gradients, grain growth, liquefaction, and dissolution);
- pore network development due to bubble formation of noncondensable noble gases and volatile species, and gas expansion due to temperature;
- gaseous and surface transport through the pore network (due to concentration and pressure gradients);
- transport in the fuel/cladding gap;
- reaction of FPs (mostly tellurium) with the cladding (impact of steam/cladding and cladding/fuel surface interactions on FP reactions); and
- release through the breach into the coolant channel.

The information contained in the remainder of this chapter is as follows (with most of the information condensed in tables). Section 3.3.1 gives an overview of the most important severe accident analysis codes treating in-vessel FP release. Section 3.3.2 discusses the basic models underlying the FP release codes evaluated. Section 3.3.3 reviews

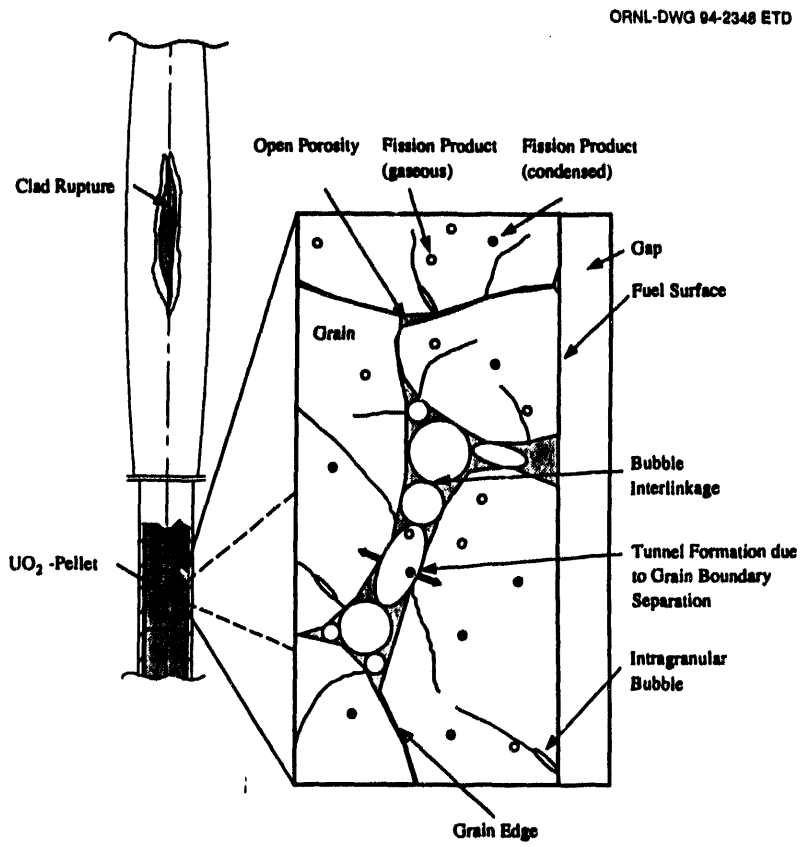

Figure 3.1 Illustration of fission product release mechanism regimes

the specific system code environments for models implemented from stand-alone FP release codes. Finally, a summary and conclusions are given in Sect. 3.3.4.

3.3.1 Codes Under Investigation

The review covers eight system codes—ATHLET/CD, KESS, ICARE-2 (and ESCADRE), ESTER, SCDAP/RELAP5, MELCOR, MAAP, and THALES—and seven FP-release codes—CORSOR and CORSOR-M, CORSOR-Booth, GRASS (FASTGRASS, PARAGRASS), VICTORIA, FREEDOM, MITRA, and FIPREM (including FPRATE).

Details concerning the code version considered, the developing organization, and the underlying documentation (Refs. 1–15)*,†,‡ are given in Table 3.18 (CORSOR and CORSOR-M are denoted together, ESTER is the European Source Term Code and contains ICARE-2 and VICTORIA; a more recent version also includes KESS and FPRATE).

In the course of LWR accidents, a number of phenomena starting from blowdown, boiloff, and early core heatup to the failure of fuel rods, melting, and debris (and molten pool) formation can lead to a corresponding release of FPs.

Table 3.17 gives an overview of the governing phenomena resulting in release and the corresponding release type,

*M. Ranamurthi and M. R. Kuhlman, "Final Report on Refinement of CORSOR—An Empirical In-Vessel Fission Product Release Model," Battelle, Columbus, Ohio, Oct. 1990.

†R. Prior and V. Hancart, "Application of the MAAP Code to the Optimization of Design Requirements for Severe Accident Mitigation Systems," pp. 251–254 in *Tagungsbericht "Jahrestagung Kerntechnik 1990," Nuernberg, 15–17, May 1990.*

‡M. Kajimota et al., "Development of THALES2, a Computer Code for Coupled Thermal-Hydraulics and Fission Product Transport Analysis for Severe Accidents at LWRs and its Application to Analysis for Severe Accidents at LWRs and its Application to Analysis of Fission Product Revaporization Phenomena," *Proceedings of the ANS International Topical Meeting on Safety of Thermal Nuclear Reactors, Portland, Oregon, July 21–25, 1991.*

Table 3.17 In-vessel fission product release

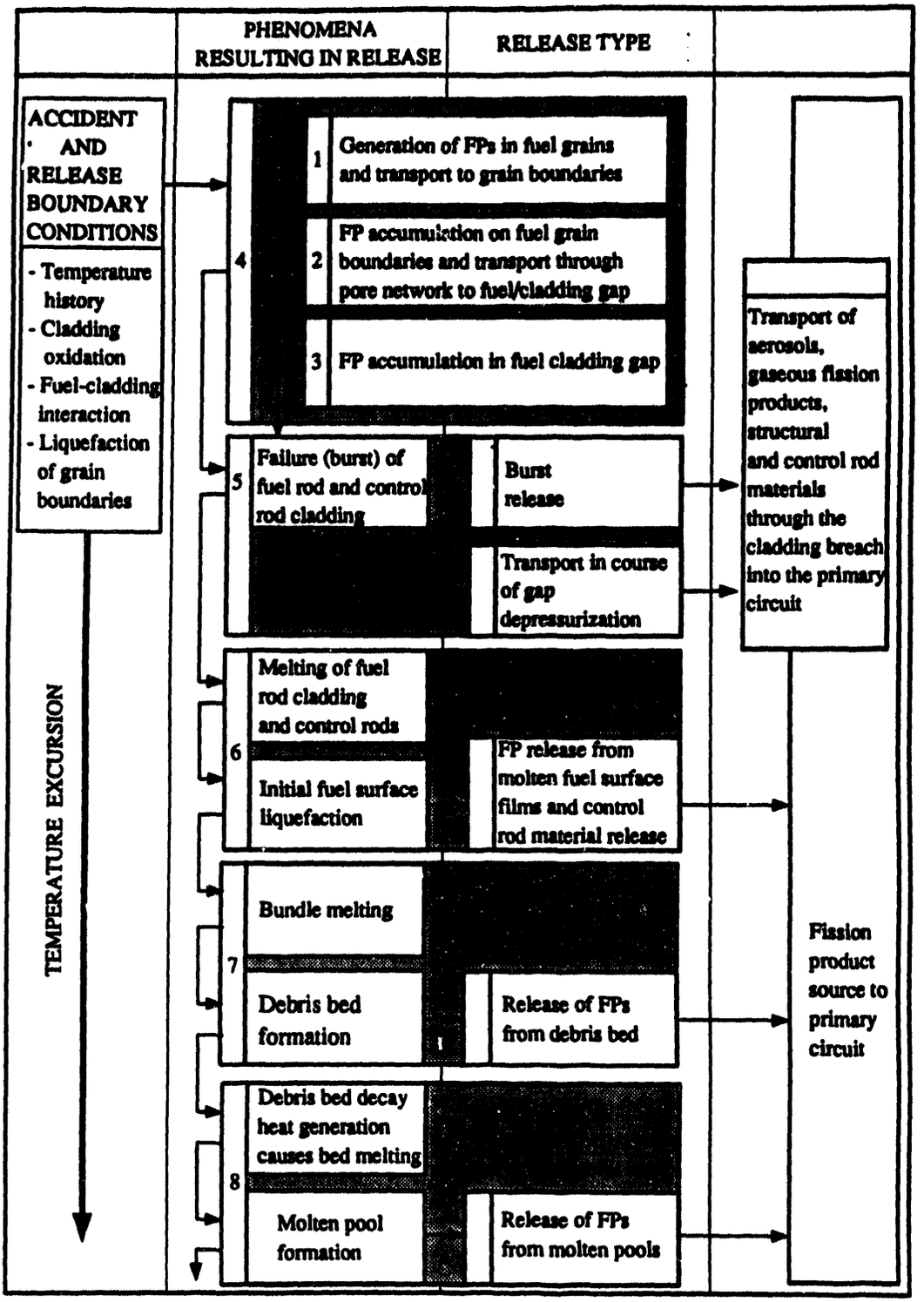

Table 3.18 Codes under investigation

Code name	Code type[a]	Code version, or year	Developing organization (country)	Documentation/ reference
ATHLET/CD	S	Mod 1.0, Cycle E	Gesellschaft f. Anlagen- und Reaktorsicherheit (GRS) mbH, Germany	/1/
CORSOR CORSOR-M	FP	1990	Nuclear Regulatory Commission, Battelle Columbus Laboratories, USA	/2/
CORSOR - Booth	FP	1990	Oak Ridge National Laboratory, Battelle Columbus Laboratories, USA	[b]
ESTER	S	1992	Joint Research Centre, Travedona, Italy	/4/
FAEREL	CRM	1985	AEA Technology, Dorchester, United Kingdom	/5/
FASTGRASS	FP	1992	Argonne National Lsboratory, USA	/6/
FIPREM	FP	1992	IKE, Institut für Kernenergetik and Energiesysteme, Universität Stuttgart, Germany	[c]
FREEDOM	FP	Ver. 1.2	Chalk River Laboratories, Chalk River, Ontario, Canada	/8/
ICARE-2 ESCADRE	S	Ver. 2 Mod 1	Institut de Protection et de Surete Nucleare, Caderache, France	/9/
KELLY	FPM	1984	University of Virginia, USA	/10/
KESS-III	S	1992	IKE, Institut für Kernenergetik and Energiesysteme, Universität Stuttgart, Germany	/11/
MAAP	S	3.0B and 4	FAUSKE and Associates, Westinghouse Energy Systems, Inc., USA	[d]
MELCOR	S	1.8.2	Sandia National Laboratories, USA	/13/
MITRA	FP	1992	Institut für Transurane, Karlsruhe, Germany	/14/
NUREG 0772	FPM	1981	Oak Ridge National Laboratory, Battelle Columbus Laboratories, Sandia National Laboratory, USA	/15/
SCDAP / RELAP5	S	Mod 3	Idaho National Engineering Laboratory, USA	/16/
THALES-2	S	1991	Japan Atomic Energy Research Institute, Japan	[e]
VICTORIA	FP	1992, Rev 1	Sandia National Laboratories, USA, Winfrith Technology Center, UK	/18/

[a]System code—S, FP release code—FP, FP release model—FPM, Control rod material release model—CRM.
[b]M. Ranamurthi and M. R. Kuhlman, "Final Report on Refinement of CORSOR—An Empirical In-Vessel Fission Product Release Model," Battelle, Columbus, Ohio, October 1990.
[c]C. Ronchi and C. T. Walker, "Determinations of Xenon Concentrations in Nuclear Fuels by Electron Microprobe Analysis," *J. Phys. D.: Appl. Phys.* 13, 2175 (1980).
[d]R. Prior and V. Hancart, "Application of the MAAP Code to the Optimization of Design Requirements for Severe Accident Mitigation Systems," pp. 251–254 in *Tagungsbericht "Jahrestagung Kerntechnik 1990," Nuernberg, 15–17, May 1990.*
[e]M. Kajimota et al., "Development of THALES2, a Computer Code for Coupled Thermal-Hydraulics and Fission Product Transport Analysis for Severe Accidents at LWRs and its Application to Analysis for Severe Accidents at LWRs and its Application to Analysis of Fission Product Revaporization Phenomena," *Proceedings of the ANS International Topical Meeting on Safety of Thermal Nuclear Reactors, Portland, Oregon, July 21–25, 1991.*

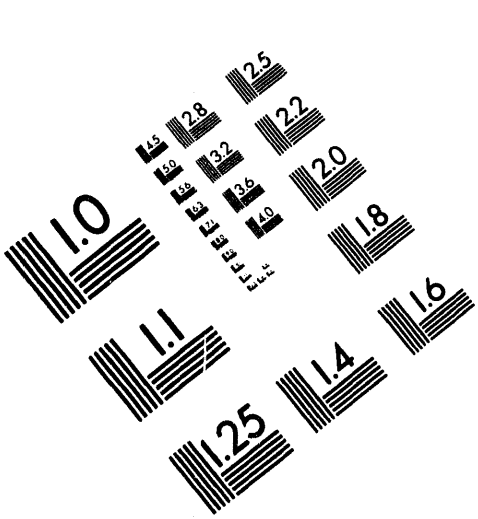

Association for Information and Image Management
1100 Wayne Avenue, Suite 1100
Silver Spring, Maryland 20910
301/587-8202

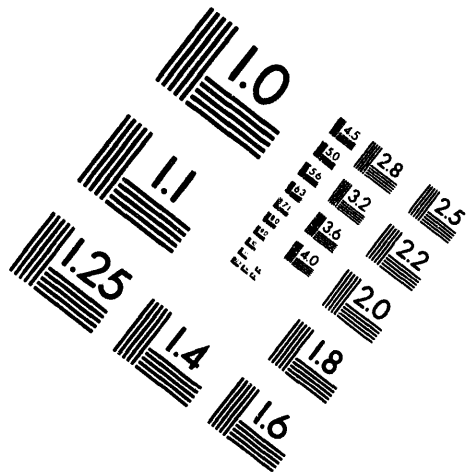

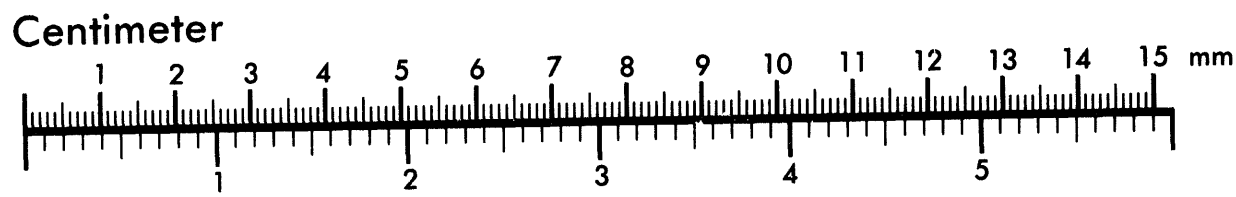

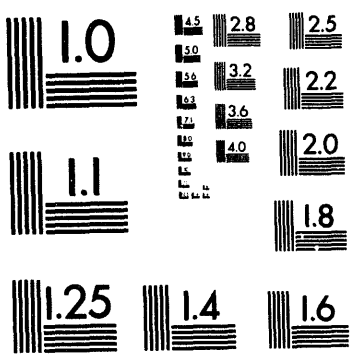

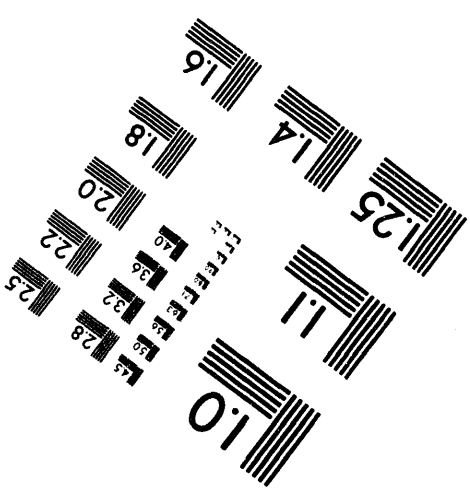

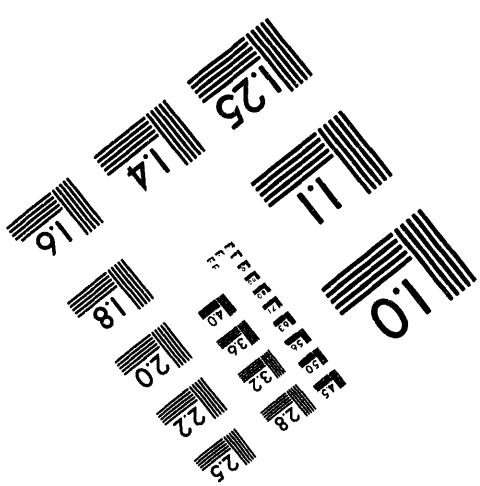

2 of 3

each denoted with numbers from (1): generation of FPs in fuel grains and diffusion to grain boundaries to (8): release of FPs from molten pools.

Tables 3.19 and 3.20 give an overview of the basic capabilities of the codes according to the two code categories: system codes and FP release codes. Table 3.19 includes the only pure structural material and control rod release code FAEREL. Table 3.20 includes two FP release models (the NUREG-0772 model[13] and the Kelly model,[9] described by means of a flow chart), on which several codes are based. Both the NUREG-0772 and Kelly models are based on the release rate equation developed by Albrecht-Wild,[16] where the major variable is a function of several parameters. In these models, the fraction of FPs remaining in the fuel is identified as an exponential function of the time multiplied by a variable. The NUREG-0772 model identifies the variable to be an exponential function of the temperature, using temperature range and species-dependent constants; the Kelly-Model is based on an Arrhenius type equation, considering an activation energy and the temperature for each species treated. CORSOR and CORSOR-M are based on these models to calculate the fractional release rate of FPs (see also Table 3.21). MAAP uses both release models and applies the Cubicciotti-model[17] to calculate the FP release as a function of fuel oxidation with a steam oxidation model.

The first line in Tables 3.19 and 3.20 gives the phenomena and release types modeled in the codes in terms of the numbers defined in Table 3.17. Depending on physical and chemical models, the codes treat the release of elements (as FPs and/or structural materials), their chemical compounds, and nuclides. Tables 3.19 and 3.20 give the number of elements physically treated (release groups) and chemically treated and a simple yes/no ranking whether chemical interactions (resulting in chemical compounds) are calculated. In general, the physical models for release are applied to release groups containing species with similar physical characteristics (e.g., volatility). Concerning the number of species treated chemically, it should be noted that certain elements are available as FPs and as structural material elements (with different governing release mechanisms) and that codes may treat nuclides resulting from transmutation.

Most of the system codes are able to simulate control rod and structural material release. The respective underlying FP release codes like CORSOR and CORSOR-M treat control rod and structural material release by means of separate sets of temperature-range-dependent empirical equations. System codes often extend FP release models to structural and control rod release by adapting the rate coefficients to reflect corresponding experimental results.

The initial conditions required for the release calculation—in most cases an initial inventory from ORIGEN calculations[18]—are given in the Tables 3.19 and 3.20.

Most of the system codes are based on CORSOR and CORSOR-M type rate equation models. The German codes ATHLET and KESS allow the optional use of FPRATE (CORSOR-M approach) or the mechanistic FIPREM-models. The French codes ICARE-2 and ESCADRE use CORSOR type rate equations extended to include the EMIS correlations (based on French HEVA-experiments[19]), the SASCHA-derived release rates (based on the German SASCHA experiments[20]) and the Petti-correlations[21–22] (control rod release). ESTER includes ICARE-2, KESS, and VICTORIA models. SCDAP/RELAP5 is based on the mechanistic FASTGRASS models for the volatiles Xe, Kr, Cs, I, and Te and treats the other FPs with CORSOR-M. MAAP uses correlations based on NUREG-0772 and the Kelly model and thus can be said to have CORSOR and CORSOR-M type of models. The Japanese code THALES-2* uses CORSOR-M. The structural material release code FAEREL uses a convective mass transfer approach for the release from the structure surface (structural materials start from the surface) into the bulk gas.

An outline of the basic FP release models and their modeling feature is presented in detail in Tables 3.21 and 3.22. In several cases, the capabilities of the FP release models in the environment of the system codes differ from the capabilities of the underlying FP release models as operated in the stand-alone FP release codes. For example, some system codes extend their applicability to the release from debris beds by applying the fuel rod grain release model from the underlying FP release code to the release from debris particles.

3.3.2 Basic Fission Product Release Models

The basic FP release codes have been identified in Table 3.20. The review of basic models focuses on the codes VICTORIA, GRASS (FASTGRASS, PARA-GRASS), CORSOR and CORSOR-M, CORSOR-Booth, FREEDOM, MITRA and FIPREM, on the NUREG-0772, and the Kelly models, and on the structural material release

*M. Kajimota et al., "Development of THALES2, a Computer Code for Coupled Thermal-Hydraulics and Fission Product Transport Analysis for Severe Accidents at LWRs and its Application to Analysis for Severe Accidents at LWRs and its Application to Analysis of Fission Product Revaporization Phenomena," *Proceedings of the ANS International Topical Meeting on Safety of Thermal Nuclear Reactors, Portland, Oregon, July 21–25, 1991.*

Table 3.19 Overview on codes, systems codes, and structural material release code FAEREL

System codes	ATHLET/CD	KESS-III	ESTER	ICARE-2 ESCADRE	SCDAP/ RELAP5	MELCOR	MAAP	THALES-2	FAEREL
Phenomena resulting in release/release type (see Table 3.17)	4–6	4–6	1–3, 4–6	4–6	1–3, 4–7	4–7	4–8	4–8	5, 6
Number of elements: –physically treated –chemically treated	24 groups 41 elements	25 groups 43 elements	21 groups 39 elements	21 groups 39 elements	16 groups 22 elements	14 groups 100 elements	12 groups 33 elements	7 groups 18 elements	7 elements 26 species
–chemical interactions	According to FP release models	According to FP release models	According to FP release models	According to FP release models	According to FP release models, own models see Table 3.25	According to FP release models, own models see Table 3.25	According to FP release models, own models see Table 3.25	According to FP release models, own models see Table 3.25	Own models see Table 3.25
Initial species inventory	ORIGEN	ORIGEN or user input	User input	User input	PARAGRASS, ORIGEN, or user input	ORIGEN or user input	ORIGEN or user input	User input	Code model
Basic FP release models	CORSOR-like empirical rate equation module FPRATE, or mechanistic FIPREM-models, see Table 3.20	CORSOR-like empirical rate equation module FPRATE, or mechanistic FIPREM-models, see Table 3.20	CORSOR, CORSOR-M, EMIS, SASCHA, Petti from ICARE-2, FPRATE, VICTORIA, see Table 3.20	CORSOR, CORSOR-M, EMIS, SASHA, Petti, see Table 3.20	Xe, Kr, Cs, I, Te, see FASTGRASS, other FP's see CORSOR-M, see Table 3.20	CORSOR - Booth, see Table 3.20	Rate equation models based on NUREG 0772 and Kelly model, Cubicciotti model for steam oxidized fuel, see Table 3.20	CORSOR, CORSOR-M, see Table 3.20	Convective mass transfer from material surface, see Table 3.20
Special capabilities of the system code FP release models differing from the underlying basic FP release code models	Different models can be chosen, e.g., depending on temperature range, details see Table 3.25	Different models can be chosen, e.g., depending on temperature range, details see Table 3.25	Different models can be chosen, e.g., depending on temperature range, details see Table 3.25	User defined corrections to default values in CORSOR-like correlations, details see Table 3.25	Special models for release from fragmented fuel rods and rubble beds, details see Table 3.25	Geometry correction factor for treatment of degraded fuel rods, details see Table 3.25	See Table 3.25	See Table 3.25	—

Table 3.20 Overview on codes and FP release codes/models

FP release codes	CORSOR, CORSOR-M	CORSOR Booth	FAST-GRASS	FIPREM	FREEDOM	MITRA	VICTORIA	FP Release Models: NUREG-0772 / KELLY
Phenomena resulting in release/release type (see Table 3.18)	4, 5	1, 2	1–3 6, 8	1–3, 4, 5	1, 2	1–3	1–8	
Number of elements:								
– physically treated	16 groups	12 groups	8 groups	24 groups	1 group	20 groups	26 groups	
– chemically treated	22 elements	18 elements	8 elements	200 chemical species	12 chemical species incl. isotopes	500 chemical species incl. isotopes	288 chemical species no isotopes	
– chemical interactions	N	N	Y	Y	N	Y	Y	
Initial species inventory	User input	User input	Code model for Kr, Xe, Cs, I Te, Ba, Sr	ORIGEN	Code model	KORIGEN (modified database) Decay chains from TOBIAS	Same as FAST-GRASS, others from ORIGEN	

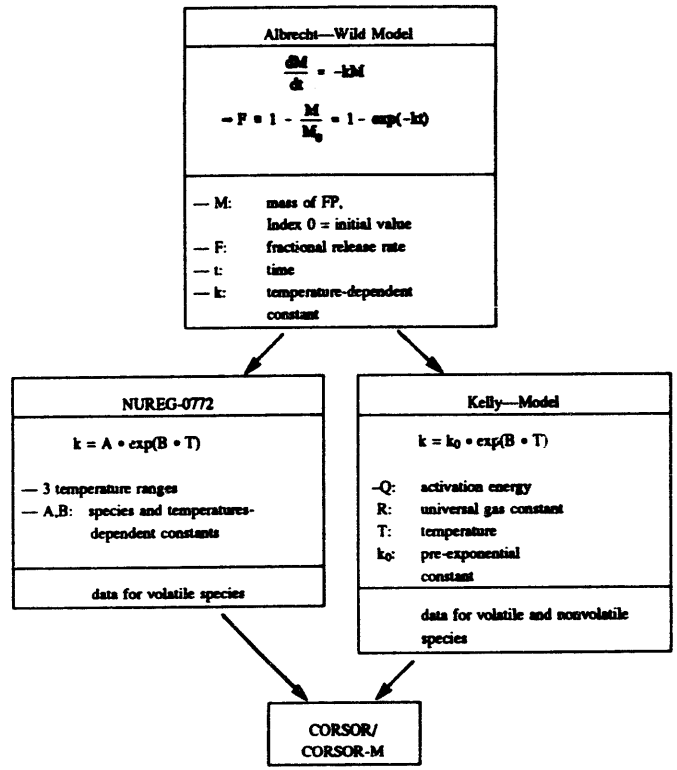

Table 3.21 Overview of modeling capabilities for VICTORIA, FASTGRASS, CORSOR-M, and CORSOR-Booth

Transport processes modeled during release	VICTORIA	FASTGRASS	CORSOR/CORSOR-M	CORSOR-Booth
1. Transport from within the fuel to its surface, i.e., transport of radionuclides to a free surface, subsequent transport through a porous structure	Intragranular transport within the fuel grains to the grain surface: mechanistic model (VICTORIA—FASTGRASS) for the diffusion of atoms and gas bubbles or Booth model (VICTORIA—CORSOR—Booth) Intergranular transport through the pore network: Diffusive and convective (due to permeable flow) transport to the gap Equilibrium chemistry controls vapor- and condensed-phase speciation	Mechanistic model for the release of Xe, I, Cs, Te, Ba and Sr. Intragranular: – atomic and bubble diffusion to grain surfaces, – grain growth and grain boundary sweeping, – liquefaction and dissolution Intergranular: – diffusive flow in the open porosity, – impact of grain boundary micro-cracking and grain face channel formation	Instantaneous release of a default value fission product fraction, if the cladding breaches (temperature criteria T_c = 900°C) Transient release starts when cladding has breached (T_c > 900°C) with the mass of the species released as an exponential function of a "fractional release rate coefficient" FRC and the time CORSOR: FRC is an exponential function of the temperature with species-dependent coefficients for different temperature ranges CORSOR-M: FRC is given by an Arrhenius-type equation with species-dependent constants Control Rod Release: Fraction of the inventory released given as constant for failure temperature (T_c = 1400°C) and as linear function of temperature above T_c	Quasi mechanistic model based on Booth diffusion approach for the release of Cs Intragranular: Booth diffusion model for Cs, correlations from experimental data for other FPs Intergranular: Mass transport in analogy to heat transfer
2. Transport within the fuel cladding gap, i.e., gas-phase mass transport from the fuel surface to the clad breach	Convective and diffusive porous flow model with: – Accumulation of species in cladding plenums, – accumulation due to condensation on inner cladding surface.	Not treated		
3. Transport through the clad breach into the coolant channel, i.e., gas-phase mass transport from the breach into the coolant	Mass transport resistance controlled release through a specified breach	Not treated		

Table 3.22 Overview of modeling capabilities for FREEDOM, MITRA, and FIPREM

Transport processes modeled during release	FREEDOM	MITRA	FIPREM
1. Transport from within the fuel to its surface, i.e., transport of radio nuclides to a free surface, subsequent transport through a porous structure	Mechanistic code with implicit coupling of FP transport and changes in fuel microstructure. Intragranular: FP diffusion and sweeping due to grain growth, implicit account for FP production, decay and capture, accumulation of FPs on grain face bubbles. Intergranular: Interlinkage of bubbles induces instantaneous venting of excess and newly arrived gases to open voids via cracks and surfaces.	Mechanistic code with separate models for intragranular and intergranular transport implicitly coupled to FP decay. Detailed reaction-rate equations including production, intragranular precipitation, radiation resolution, biased diffusion, grain growth sweeping, transmutations and capture, along with changes in fuel microstructure.	Mechanistic code with models for intragranular and intergranular transport: Intregranular: Similar to VICTORIA—FASTGRASS, (without model for microstructure changes) Intergranular: Similar to VICTORIA
2. Transport within the fuel cladding gap, i.e., gas-phase mass transport from the fuel surface to the clad breach	Not treated (separate modules outside of FREEDOM)	When a critical value of the percolation probability is attained, ejection of volatile species occurs. Calculations performed by the subprogram FUTURE. Assumption of viscous (Darcy) flow in pressurized channels. Calculation of open path (fuel/cladding gap thickness) in the presence of fuel swelling and clad ballooning.	Diffusive/convective transport along the gap and plenum, depending on gap size/gap closure
3. Transport through the clad breach into the coolant channel, i.e., gas-phase mass transport from the breach into the coolant	Not treated (separate modules outside of FREEDOM)	Not treated	Instantaneous release across clad or gas-phase mass transfer from cladding surface into the coolant channel similar to FAEREL

code FAEREL (see Table 3.19 and Sect. 3.3.2.4 for details). A further breakdown allows a classification into two groups of models: mechanistic diffusion models and Arrhenius type rate equation models.

Tables 3.21 and 3.22 give an overview of the modeling capabilities (VICTORIA, FASTGRASS, CORSOR and CORSOR-M, and CORSOR-Booth in Table 3.21 and FREEDOM, MITRA and FIPREM in Table 3.22). The models are discussed in broad terms related to the following major transport processes modeled during release:

(1) transport from within the fuel to its surface,

(2) transport within the fuel cladding gap, and

(3) transport through the clad breach into the coolant channel.

In the case of the rate equation models (CORSOR), single transport processes are not explicitly modeled. This is reflected by the down-the-line columns for the respective codes.

The major transport processes (1), (2), and (3) defined in Tables 3.21 and 3.22 form the background for the details of the transport models discussed in Sects. 3.3.2.1–3.3.2.3. In the case of the mechanistic codes a further breakdown into subprocesses like intragranular transport, intergranular transport, and chemical processes is convenient. Thus, the discussion of modeling details is carried out according to these subprocesses. In the case of empirical models, certain subprocesses are all considered in the integral release rates (see CORSOR).

Depending on whether the physical models result in partial differential equations (mechanistic approaches) or in relatively simple algebraic expressions (empirical models), the computational effort for solving the equations differs. Tables 3.23 and 3.24 give information about the computational background of the FP release codes in broad terms. Generally, the core is treated numerically on two computational domains: a coarse grid representing the core itself (mostly divided into radial rings and axial levels corresponding to the core nodalization of the system codes) and a fine grid for the representation of the single rods (only in the case of the detailed mechanistic models; no specific fine grid nodalization is required for the empirical models other than the nodalization of the system code). Tables 3.23 and 3.24 also give information on the computer storage capacity and running times needed. The information is given in terms of several machine-storage-independent key information about computational effort required by the numerical solution schemes.

3.3.2.1 Transport from within the Fuel to its Surface (according to Transport Process No. 1 in Tables 3.21 and 3.22)

VICTORIA. The transport process in both physical regions (intragranular and intergranular) is modeled based on the general transport equation (Fick's Second Law) applied to the atomic diffusion within the grains to the grain surface and open pores (intragranular) and the diffusive and porous flow in the open fuel porosity (intergranular). In both regions FPs are assumed to be in chemical equilibrium (i.e., under the high-temperature conditions during release, chemical equilibrium is assumed to be achieved instantaneously). The driving forces for release or condensation are the partial pressure differences between the FP chemical species equilibrium partial pressures and their (bulk gas) environmental partial pressures.

Applied to the intragranular (fuel grain) region, the general transport equation describes the diffusion of gas atoms (and gas bubbles in the VICTORIA-FASTGRASS version, see FASTGRASS) to the surface of the grains and to the open pores (similar to the Booth model). The buildup of bubbles is governed by capturing gas atoms or, vice versa, nucleation into gas atoms and leads to an enhancement of the passage from the grain surface to the fuel open porosity. Effects of grain growth, grain boundary sweeping, and the destruction of the UO_2-matrix due to liquefaction and dissolution are taken into account in the VICTORIA-FASTGRASS version. Applying the FASTGRASS model (VICTORIA-FASTGRASS-version) to intragranular processes, the general transport equation describes the intragranular transport of noble gases only, taking into account effects from

- the loss of gas atoms caused by bubble nucleation,
- the capture of gas atoms by bubbles,
- biased and random diffusion of gas atoms to grain boundaries,
- loss of gas atoms caused by grain boundary sweeping,
- gas atom generation caused by fission,
- the gain of gas atoms caused by fission-induced gas atom re-solution,
- equilibrium chemistry determining the speciation of the FPs in the solid matrix, and
- diffusive flow of FPs (elemental) within the grains to the grain boundaries.[15]

In addition, the FASTGRASS models for intergranular noble gas behavior are utilized. FP release from the grain

Table 3.23 Computational background for VICTORIA, FASTGRASS, CORSOR-M, and CORSOR-Booth

Computational background	VICTORIA	FASTGRASS	CORSOR/CORSOR-M	CORSOR-Booth
Coarse grid:				
Computational domain (Vessel interior)	Subdivision of core into groups of representative rods by user input or according to overlying system code. Each representative rod is treated separately.		Subdivision of core into radial rings and axial levels by user input, optionally according to the system code computational grid (representative rods and axial levels).	
Fine grid:				
Computational domain (Fuel rod geometry subdomains)	2-D-cylindrical (r,z) Eulerian mesh with arbitrary number of radial rings and axial levels: – several radial fuel zones, – fuel cladding gap, – cladding, – volumes for chemical interactions: – fuel grains, – fuel open porosity, – fuel/cladding gap (incl. cladding inner surface), – bulk gas, – structure surface.	Arbitrary number of radial rings and axial levels: – Volumes for chemical interactions, – fuel grains, – grain edges.	The diffusive transport models do not result into a set of partial differential equations. Consequently, no need for a computational grid within the rods.	
Numerical scheme	Numerical solution of coupled partial differential equations (PDE) by an explicit time-step scheme (Courant time step limit).	Numerical solution of PDE by an explicit time-step scheme (Courant time step limit).	Noniterative, algebraic calculation.	Time discretization of diffusive transport process. Solution by explicit time-step scheme.

Table 3.24 Computational background for FREEDOM, MITRA, and FIPREM

Computational background	FREEDOM	MITRA	FIPREM
Coarse grid:			
Computational domain (Vessel interior)	Subdivision of core into groups of representative rods by user input or according to overlying system code. Each representative rod is treated separately.		
Fine grid:			
Computational domain (Fuel rod geometry subdomains)	The PDE are solved on a moving, irregular mesh following actual changes of the fuel microstructure (e.g., grain radius and grain surface boundary layer).	2-D-cylindrical (r,z) Eulerian mesh with arbitrary number of radial rings and axial levels: – several radial fuel zones, – fuel cladding gap, – cladding, – volumes for chemical interactions: – fuel grains, – fuel open porosity, – fuel / cladding gap (incl. cladding inner surface), – bulk gas, – structure surface.	Per representative fuel rod: – Radial fuel zones (modelled as concentric shells, typically 5–10), – fuel grain zones (modelled as concentric spheres, typically 10), – gas section, – cladding section, – coolant channel section.
Numerical scheme	Numerical solution of PDE, second-order accurage, semi-implicit finite difference method.	Calculation of decay chains by iterative algebraic calculation for arbitrary timesteps. Gross volatile fission product inventory including swelling effects: Runge-Kutta numerical integration (by fuel performance code FUTURE, developed at Institut für Transurane, Karlsruhe). Transport equations are solved with a quasi-analytical method; numerical integration is not needed, so that solutions are evaluated as functions of time at prefixed macrostep sequences.	FPRATE: Algebraic calculation (see CORSOR-M), FIPREM: Finite-difference method for intragranular and intergranular transport (diffusion equation), FMITRA: [MITRA code (1989 version) integrated into FIPREM] transformation of transport equation into rate equations.

boundaries is scaled to the calculated noble gas release. The user can opt to apply the Booth model to the intragranular processes. Two processes are considered to be governing:

1. equilibrium chemistry determining the speciation of the FPs in the solid matrix, and
2. the actual movements of FPs within the grains by solid state diffusion through the lattice. The driving force is the concentration (or partial pressure) gradient between the interior and the surface of the fuel grains. The concentration on the grain surface yields a volumetric source term for the intergranular transport through the open fuel porosity. This source term is determined by applying the Booth model to subsequent time planes (for details concerning the Booth model see CORSOR-Booth).

Once the FPs have proceeded to the open pores, the further **intergranular** transport is governed by

1. equilibrium chemistry, which may change the species and compound concentrations, and
2. diffusive and convective transport (due to permeable flow) according to Fick's Second Law with gaseous species transported in the bulk of the pores and the condensed phase species by surface diffusion.

FASTGRASS. FASTGRASS is a code that predicts the release of Xe, I, Cs, Te, Ba, and Sr. The basic features of the code are very similar to what has been described for VICTORIA in its VICTORIA-FASTGRASS version. FASTGRASS is limited to the release of these six elements (chemistry model limitation) and six additional species used to tie up strontium and barium with the UO_2 matrix. The chemistry is based on data for the Gibbs free energy and takes the fuel oxide–metal ratio into account. The basic features as discussed for the VICTORIA-FASTGRASS version are in broad terms:

Intragranular

- atomic and bubble diffusion to grain surfaces (Arrhenius),
- grain growth and grain boundary sweeping, and
- liquefaction and dissolution.

Intergranular

- diffusive flow in the open fuel porosity,
- augmentation of pore transport due to grain boundary microcracking and grain face channel formation.

CORSOR/CORSOR-M. The codes CORSOR and CORSOR-M predict the release of FPs and control and structural material release by empirical rate equations. The rate equations are fit to experimental release data from high-burnup fuel samples, reflecting different temperature ranges with subsequent sets of rate constants. The release is calculated on a time-dependent basis for time steps Δt at constant temperature.

From general considerations it is clear that predictions are strictly valid only for conditions similar to those from the underlying experiments. Thus, the effects of burnup, microcracking due to rapid cooldown (quenching), debris bed, molten pool and fuel coolant interactions are not modeled although it should be possible in principle to correlate at least burnup impacts on release.

The calculation of transient release starts when the cladding has failed, exceeding the temperature of $T_c = 900°C$. The mass fraction FFP_i of the fission product i, released in each node of the grid during the time Δt, is given by:

$$FFP_i = FP_i \cdot \exp(-FRC_i \cdot \Delta t) \ ,$$

with

FP = initial mass of fission product,
FRC = fractional release rate coefficient.

The fractional release rate coefficient can be determined using two different models:

In the case of **CORSOR**:

$$FRC_i = A(i,j) \cdot \exp[B(i,j) \cdot T_i] \ ,$$

with

T = temperature,
A(i,j), B(i,j) = species-dependent constants for species i in temperature range j (three ranges) from experimental data.

In the case of **CORSOR-M**:

$$FRC_i = KO_i \cdot \exp[-Q_i/(R \cdot T_j)] \ ,$$

with

T = temperature,
Q_i = activation energy for species i from experimental data or from heat of vaporization for vaporizing species,

KO_i = pre-exponential factor from experimental data,
R = universal gas constant.

CORSOR-BOOTH. Concerning **intragranular** transport, the code applies a mechanistic model (Booth-Diffusion) to the release of cesium from spherical grains to the grain surface and empirical correlations for the other elements relating their release to those of cesium.

An apparent diffusion coefficient accounts for effects of UO_2 fuel inhomogeneity, closed porosity, grain boundaries, and fission gas bubbles or other internal traps. The diffusion coefficient is given by an Arrhenius-type of equation, with best-fit parameters derived from experimental data for the release of fission gases from fuel test samples. Different fuel burnup rates are taken into account by two sets of equations treating two ranges.

The **intergranular** transport of radionuclides within the open fuel porosity is treated by a single lumped model for both gas-phase diffusion and surface diffusion for condensed species. The release is governed by mass transfer resistances derived from heat transfer analogy considerations.

The release rate for each species is the sum of the diffusional and gas-phase mass transport rates of the species. The release for the species i is based on the release rate of cesium (best-fit parameters from experimental data), corrected by a species-dependent weighting factor, with

–Xe = Kr = I = Cs , Sr = Ba = Cs/20 , Te = Cs/40 , and Eu = Cs/10 for low oxidation ,

and

–Xe = Kr = I = Cs , Sr = Ba = Cs/300 , Te = Cs , and Eu = Cs/1000 for high oxidation .

For species with negligible equilibrium vapor pressures, the release is governed only by diffusive transport.

FREEDOM. FREEDOM is a highly mechanistic code with models for microstructure-dependent transient gas release (stable and radioactive FPs). The resulting transport equations are solved on an irregular moving numerical grid following the microstructural changes in the UO_2 matrix.

The **intragranular** transport is modeled by applying the general transport equation (Fick's Second Law). The transport processes from the grain interior to the grain boundaries or fuel surfaces are governed by FP diffusion and sweeping due to grain growth. The equations account implicitly for fission production, production by decay of precursors, losses by decay, and neutron capture. On the grain boundaries, the FPs accumulate in bubbles on the outside of the grains. At a given bubble radius, the bubbles are modeled to interlink, and **intergranular** transport starts by venting the FPs through the free voidage formed by the interlinked bubbles. Venting of excess, as well as newly arrived, FPs is assumed to be instantaneous once bubble interlinkage occurs. If the fuel melts, all of the FPs are released instantaneously.

MITRA. MITRA is a highly mechanistic code which, based on system-related parameters (e.g., type of reactor, temperature power history, neutron flux, etc.) and a set of integrals that describes the evolution of the fuel microscopic structure, solves analytically the system of fission product transport equations (Fick's Second Law).

The **intragranular** migration of radioactive nuclides is calculated by solving a system of reaction-rate equations containing source, sink, and loss terms; some of these are deduced from specific analytical solutions of the mass transport equations in different space domains. The following terms are considered:

- the fission birth rate (direct production of FPs),
- the birth rate from (up to 5) mothers (FP occurs due to radiative decay of mother nuclei: e.g., by α-decay),
- the loss of FPs due to decay of the FP itself,
- the neutron capture of FPs,
- the precipitation into intragranular sinks,
- the radiative re-solution of precipitated species,
- the loss due to atomic migration to the grain boundary, and
- the loss due to biased and random migration of bubbles to the grain boundary.

The transport equation is solved for grouped species that are linked by radiative decay and/or neutron capture using a quasi-analytical method.

The migration of precipitated (or reacted) species within the grains is solved by using the same quasi-analytical method. Additionally, loss terms are included that describe the biased migration of precipitates to the grain boundaries.

The calculated amounts of fission product nuclides are subdivided into three different inventories: in solution, precipitated within the grains, and in grain boundary pores.

The inventory evolution due to decay is calculated simultaneously.

The **intergranular** transport (migration through the open fuel porosity) is governed by face- and edge-bubble morphology. Transport depends on the gross pressure of volatile FPs.

FIPREM. FIPREM is a mechanistic code applying the basic models for intragranular and intergranular transport from FASTGRASS and VICTORIA, respectively.

The **intragranular** transport is governed by

- atomic and bubble diffusion according to Fick's Second Law from the grain interior to the grain surfaces (Arrhenius),
- changes in fuel morphology as input to the model,
- FP chemistry in either region (partial volumes) by means of an equilibrium model (however, transport properties are not influenced by compound formation), and
- liquefaction, dissolution, and relocation.

The **intergranular** transport is governed by diffusive transport according to Fick's Second Law for gaseous- and condensed-phase species.

3.3.2.2 Transport within the Fuel Cladding Gap (According to Transport Process No. 2 in Tables 3.21 and 3.22)

VICTORIA. VICTORIA applies a convective porous flow model for the transport within the fuel cladding gap similar to that for the intergranular flow through the fuel open porosity. Condensed-phase species transport in the gap is not allowed.

The open volume available for the transport (and accumulation) of gas-phase species is given by the total volume (identical to the volumes of the respective numerical grid cells) times a "volume correction term" accounting for (1) melting processes, (2) gap reduction due to pinching, and (3) cladding rupture, etc.

The degree of interconnectedness between adjacent cells in the numerical grid for the fuel rod is defined by an "interconnectedness term" with (1) reduced interconnection in case of fuel frothing expansion, and (2) complete interconnection (to outside cladding cells) in case of cladding breach.

FASTGRASS. Transport in the gap is not modeled by FASTGRASS.

CORSOR, CORSOR-M, and CORSOR-Booth. Due to the integral treatment of FP release from fuel rods, the transport in the gap is covered by the empirical model discussed in Sect. 3.3.2.1.

FREEDOM. The transport in the gap is not modeled by FREEDOM. Convection and diffusion will be treated separately in another model (under development).

MITRA. Diffusional transport of both condensed and gas/vapor phases is considered. By coupling MITRA with the chemical computer code CHEMIF, which is an enhanced version of the SOLGASMIX-PV program developed at ORNL, chemistry from interactions of the FPs with steam in the gap and with fuel and cladding surfaces can also be treated.

FIPREM. When the cladding gap is closed, a diffusional model treats the distribution and accumulation in the gap. Where the cladding gap is open, a convective transport model treats the FP transport.

3.3.2.3 Transport Through the Clad Breach into the Coolant Channel (According to Transport Process No. 3 in Tables 3.21 and 3.22)

VICTORIA. The transport of gas-phase species through a user-specified cladding breach is considered if a cladding failure criterion is met (temperature and minimum clad thickness criterion). If the cladding gap is open, the "volume correction term" accounts for the available new open transport volume, and the "interconnectedness term" accounts for the new interconnection of inner clad cells to outer clad cells.

FASTGRASS. The transport of FPs through the clad breach into the coolant channel is not modeled by FASTGRASS.

CORSOR, CORSOR-M, and CORSOR-Booth. CORSOR codes do not model the transport through the breach explicitly. In the case of the cladding breach, the gap inventory is assumed to belong to the bulk gas or an instantaneous release of a default amount of the original inventory of the fission products Cs, I, Kr, Xe, Te, Sb, Ba, and Sr is calculated.

FREEDOM. The transport through the clad breach into the coolant is not modeled. The release through the breach is treated in a separate model (under development).

MITRA. The transport of FPs through the clad breach into the coolant channel is not modeled.

FIPREM. Two approaches are available. If the clad breaches locally, either FPs are not retained at all or a gas-phase mass-transfer limitation model is used, similar to the approach adopted in the FAEREL code (see Sect. 3.3.2.4).

3.3.2.4 Structural Release Code FAEREL

As a code specifically for structural materials, the computer code FAEREL[4] plays a special role. The code incorporates mechanistic models for the vaporization and gas-phase mass transport of fission products, fuel, control and structural materials to predict their limiting release rates. The evaporation from and condensation onto surfaces is assumed to occur by simple one-dimensional convective mass transfer, depending on the species vapor pressure in the boundary layer at the solid surface and the vapor pressure in the bulk gas. The mass transfer can be evaluated by means of an analogy from heat transfer. In addition, a limited treatment of gas-phase chemistry in the prevailing steam-hydrogen mixture in the cooling channel is included. The code has been applied to predict the limiting releases of control rod constituents silver and indium (the constituent cadmium is assumed to release instantaneously, if the cladding breaches); spacer grid Inconel materials Fe, Cr, Ni; and the tin component from Zircaloy.

3.3.3 System Code Environments

The system codes are mostly based on modeling features from the special FP release codes (see Tables 3.19 and 3.20). Furthermore, most codes today are still based on the empirical FP release approaches (i.e., CORSOR-models). Nevertheless, the operation of these FP release code models in the system codes implies either certain restrictions or certain extents in application. In some system codes, different FP release code models are combined to cover a wider range of release phenomena, as for instance the release from rubble beds and molten fuel; others model extended chemical interactions. Table 3.25 shows the specific capabilities of the system codes in terms of those specifics going beyond the characteristics of the underlying FP release code models discussed in Tables 3.21 and 3.22.

3.3.4 Summary and Conclusions

The review of the main computer models and codes covers seven FP release codes, two stand-alone models, and eight system codes for integrated LWR (mostly PWR) accident analyses. Generally, the system codes are based on the FP release codes or corresponding models linked to or implemented into the system codes. Furthermore, most of the system codes (7 out of 8) are based on versions of CORSOR. Thus, the review of the governing code models could be restricted to the capabilities of the special FP release models, including certain capabilities of the system codes to extend the basic FP release code approach (i.e., application of fuel grain release models on debris particles).

The FP release codes fall into two categories: codes based on empirical correlations and mechanistic codes. Their simplicity and reliability has led to a widespread acceptance of the empirical models for FP release calculations. The reliability is mainly due to the direct reflection of experimental results with well-known boundary conditions in the empirical models. However, the restrictions in the validity of empirical models are apparent: with boundary conditions considerably different from the underlying experiments, predictions will lose accuracy. Here, the mechanistic approaches based on first-order principles are more general and should be expected to give more reasonable results. The disadvantages are—besides the considerable increase in computational effort—that the mechanistic models need boundary conditions on the microstructure level (local diffusion coefficients, grain growth rates, etc.) that are difficult to determine. Hence, the mechanistic codes represent a powerful tool with general applicability but complex, sometimes strongly user-dependent, input requirements. The empirical codes, on the other hand, reflect experimental data in the form of mechanistically based correlations, are fast running with less complex input requirements, and thus have gained more widespread acceptance.

3.3.5 References

1. K. Trambauer, A. Ball, and J. D. Schubert, "Entwicklung des Rechenprogramms ATHLETSA zur Analyse schwerer Storfalle," Zwischenbericht RS 828, Gesellschaft für Reaktorsicherheit, Marz (1992).

Table 3.25 Specific capabilities of the system codes

ATHLET/CD	KESS	ICARE-2, ESCADRE	SCDAP/RELAP5	MELCOR	MAAP	THALES-2
– In case of FPRATE different rate equations based on – NUREG-0772, – CORSOR, – CORSOR-M, – SASCHA, can be chosen, e.g., depending on temperature ranges – Structural material release based on CORSOR-like approach, – Fuel grain and fuel pellet release models of FIPREM integrated (intragranular and intergranular FP release; optional use)	No special models exceeding those in FIPREM and FIPRATE approach, exceeding feedback of reduced heat source to core models	– Different rate equations based on: CORSOR CORSOR-M SASCHA (Volatiles) EMIS (Volatiles) Petti (Volatiles) – For cladding breach release, the breach is computed by a thermo-mechanical module (ICARE-2) or user dependent for a given temperature, or temperature slope – The amount of FPs released instantaneously through the breach can be user-defined differing from CORSOR-M default values – User input values of additional or total FP release from liquid UO_2 (by default; no additional release)	– Axial diffusion transport of gas in fuel cladding gap – Instantaneous release of Xe, Kr, Cs, I from liquid UO_2 to the gap and subsequent to the clad breach – Instantaneous release of FPs accumulated on the grain boundaries (PARAGRASS calculation) during fuel fragmentation – Subsequent release from rubble beds is controlled by the intragranular release (PARAGRASS calculation) – Sn release from Zry and transport of Sn	– Deviations from the original intact fuel rod geometry are taken into account by a surface to volume correction factor Chemistry: The elemental release from CORSOR is instantaneously corrected to a compound form, i.e., $Cs + I \rightarrow CsI$, when released from the fuel	– Fission product release of volatile species is based on NUREG 0772 model – Kelly model for nonvolatile species – No limitation of release of high volatiles Cs and I – UO_2 and actinides are not released from the fuel – Structural material is assumed to be released from degraded rods (including control rods) – Impact of oxidation on FP release (e.g. Te, Sn) is taken into account Chemistry: Chemical equilibrium is assumed for all species considered	– No special models exceeding NUREG-0772, CORSOR, CORSOR-M Chemistry: The elemental release from CORSOR is instantaneously corrected to a compound form, i.e., $Cs + I \rightarrow CsI$, when released from the fuel

2. M. R. Kuhlmann, D. J. Lehmicke, and R. O. Meyer, Battelle Columbus Laboratories, "CORSOR User's Manual," USNRC Report NUREG/CR-4173, 1985.*

3. "Ester-European Source Term Evaluation Research," *Workshop 22–23, June 1992, Travedona, Italy,* EC-Joint Research Centre, Ispra, Italy (1992).

4. P. N. Clough, H. C. Starkie, and A. R. Taig, "Vaporization and Transport of Structural Constituents from LWR Degraded Cores," UKAEA Safety and Reliability Directorate, Culcheth, Warrington, United Kingdom, *Proceedings of an International Symposium on Source Term Evaluation for Accident Conditions, Columbus, Ohio, September 28–November 1, 1985,* International Atomic Energy Agency, Vienna, Austria (1986).

5. J. Rest and S. A. Zawadzki, Argonne National Laboratory, "FASTGRASS: A Mechanistic Model for the Prediction of Xe, I, Cs, Te, Ba, and Sr Release from Nuclear Fuel Under Normal- and Severe-Accident Conditions: User's Guide for Maintenance, Workstation, and Personal Computer Applications," USNRC Report NUREG/CR-5840 (ANL-92/3), 1992.*

6. K. D. Hocke, "Model for the Analysis of FP Release in LWR Severe Fuel Damage Conditions," p. 137 in *Proceedings of IAEA Technical Committee Meeting on Behavior of Core Materials and Fission Product Release in Accident Conditions in Light Water Reactors, Aix en Provence, France, March 1992,* International Atomic Energy Agency, IAEA-TECDOC-706 (June 1993).

7. L. D. MacDonald et al., "FREEDOM 1.2: A Transient Fission-Product Release Model for Radioactive and Stable Species," Atomic Energy of Canada Limited, AECL-9810 (May 1989).

8. R. Gonzalez, P. Chatelard, and F. Jacq, "ICARE 2 Version 2 MOD 0 and MOD 0.1, Description of Physical Models," CEA, Note Technique DRS/SEMAR 92/24, Institut de Protection et de Sûreté Nucleaire, France (1992).

9. J. L. Kelly, A. B. Reynolds, and M. E. McGrown, "Temperature Dependence of Fission Product Release Rates," *Nucl. Sci. Eng.* 88, 184–199 (1984).†

10. K. D. Hocke, M. Borger, and A. Schatz, "KESS III—A Program System for Simulation of Beyond Design Basis Accidents in LWRs," Institut for Kernenergetik und Energiesysteme, IKE 2-93, Uni Stuttgart (January 1991).

11. R. M. Summers et al., Sandia National Laboratories, "MELCOR 1.8.2: A Computer Code for Nuclear Reactor Severe Accident Source Term and Risk Assessment Analyses," USNRC Report NUREG/CR-5531, 1993.*

12. M. Gardani and C. Ronchi, "Transport and Release of Radioactive Fission Products in Nuclear Fuels: The New Analytical Approach of the MITRA Code," *Nucl. Sci. Eng.* 107, 315 (1991).†

13. U.S. Nuclear Regulatory Commission, "Technical Bases for Estimating Fission Product Behavior during LWR Accidents," Battelle Columbus Laboratories, Oak Ridge National Laboratory, Sandia National Laboratory, USNRC Report NUREG-0772, 1981.*

14. C. M. Allison et al., Idaho National Engineering Laboratory, "SCDAP/RELAP5/MOD2 Code Manual," Vol. 1-111, USNRC Report NUREG/CR-5273 (EGG-2555), 1989.*

15. T. J. Heames et al., Sandia National Laboratories, "VICTORIA: A Mechanistic Model of Radionuclide Behavior in the Reactor Coolant System under Severe Accident Conditions," USNRC Report NUREG/CR-5545 (SAND 90-0756) Rev. 1, 1992.*

16. H. Albrecht and H. Wild, "Investigation of Fission Product Release by Annealing and Melting LWR Fuel Pins in Air and Steam," *Proceedings of Topical Meeting on Reactor Safety Aspects of Fuel Behavior, Sun Valley, Idaho, August 2–6, 1981,* American Nuclear Society, 1981.

17. D. Cubicciotti, "A Model for Release of Fission Gases and Volatile Fission Products from Irradiated UO_2 in Steam Environment," *Nucl. Technol.* 53, 5 (1981).†

18. D. E. Bennet, Sandia National Laboratories, "Sandia-ORIGEN User's Manual," USNRC Report NUREG/CR-0987 (SAND 79-0299) 1979.*

19. J. M. Dumas, G. Lhiaubet, G. Lemarois, and G. Ducros, "Fuel Behavior and Fission Product Release under Realistic Hydrogen Conditions with Comparisons between HEVA 06 Test Results and Vulcain Computations," p. 153 in *Proceedings of ICHMT Seminar on Fission Product Transport Processes in Reactor Accidents, Dubrovnik, May 22–25, 1989*, J. T. Rogers, Ed. (Hemisphere, 1990).

20. H. Albrecht and H. Wild, "Review of the Main Results of the SASCHA Program on Fission Product Release Under Core Melt Conditions," *ANS Topical Meeting on Fission Product Behavior and Source Term Research, Snowbird, Utah, July 15–19, 1984*, Electric Power Research Institute, NP-4133-SR, July 1985.

21. D. A. Petti, "Silver-Indium-Cadmium Control Rod Behavior in Severe Reactor Accidents," *Nucl. Technol.* 84, 128 (1989).†

22. J. K. Hartwell et al., Sandia National Laboratories, "The Fission Product Behavior During the PBF-Severe Fuel Damage Test 1.1," USNRC Report NUREG/CR-4925, 1987.*

*Available for purchase from the National Technical Information Service, Springfield, VA 22161.
†Available in public technical libraries.

3.4 Comparison Between Experimental Results and Computer Code Calculations

The comparison of calculational results with experimental results is a frequently complex, but necessary, step in assessing a computer model or code. Experiments to measure fission product release involve heating irradiated fuel to high temperatures for known times and under specific environmental conditions (e.g., steam, hydrogen, air, or inert gas). The thermal-hydraulic conditions of the experiment must be provided to the fission product release model or code before a meaningful release calculation can be made. For stand-alone models or codes, the temperature–time history and environmental conditions can be specified. For a model or code embedded in a systems code, the thermal-hydraulic conditions must be calculated from the initial and boundary conditions of the experiment. In either case, it is unreasonable to expect agreement between calculational and experimental values of fission product release if the thermal-hydraulic conditions in the calculation do not match those of the experiment. Conversely, agreement of fission product release calculational results with experimental results may not be meaningful if experimental conditions are significantly different from those represented in the calculation.

The information considered in this section is taken from published reports of the comparisons of calculated and measured fission product releases from fuel. Most of these comparisons involve the volatile fission products, for example, noble gases, iodine, and cesium. Fewer comparisons are available for the less volatile fission products, such as strontium and barium, due to both the difficulty of measuring the releases of these materials and the more limited modeling. This section is organized by comparisons of experimental data with specific code calculations and is concluded by a discussion of the insights provided by the detailed comparisons. A list of the experiments and code calculations discussed is provided in Table 3.26. The first four experiments utilized trace-irradiated or very low burnup fuel that (because of its unique microstructure) provides a challenge to fission product release codes.

Test SFD-ST. Test SFD-ST contained 32 0.9-m-long fuel rods trace-irradiated to 0.89 MWd/kgU, heated in steam to temperatures of at least 2800 K, and cooled by water addition.[1] Approximately 75% of the Zircaloy cladding in the fuel bundle was oxidized, and evidence of hyperstoichiometric uranium dioxide was found. Approximately 15% of the fuel was liquefied in the experiment.

Fission product release in SFD-ST was analyzed with the NUREG-0772 model (precursor to the CORSOR code)[1] and FASTGRASS.[1,2] Bundle temperatures as a function of time were provided for these fission product release calculations based on best-estimate experimental values and SCDAP code calculations. As can be seen in Fig. 3.2, the NUREG-0772 model greatly overpredicts the fractional release rate for noble gas compared with measurement. This result is not surprising because the NUREG-0772 model (as well as its successors CORSOR and CORSOR-M) is based on measurements of fission product release from fuels with moderate-to-high burnups and from fuels containing fission product stimulants.[3] The explanation for the low rate of fission product release measured in trace-irradiated fuel resides in the microstructure of this material.[1,4,5] In trace-irradiated fuel, fission products must first diffuse to grain boundaries before they can be released in a heatup transient. However, in highly burned fuel, some fission products have already diffused to grain boundaries before the transient and, therefore, are more readily released during the transient. Furthermore, grain boundary tunnels that form during irradiation at burnups exceeding about 5 MWd/kgU enhance transient releases from high-burnup fuel.

Table 3.26 Experiments and code calculations described in Sect. 3.4

Experiment	Code calculations
SFD-ST	NUREG-0772 model, FASTGRASS
SFD 1-1	CORSOR, FASTGRASS, MELCOR, MAAP
LOFT LP-FP-1	FASTGRASS-VFP
LOFT LP-FP-2	CORSOR, SCDAP/RELAP5, FASTGRASS, MELCOR (CORSOR-M)
SFD 1-3	SCDAP/RELAP5 (PARAGRASS)
SFD 1-4	CORSOR, FASTGRASS, BOOTH, MELCOR, MAAP, ICARE2
HI-1	CORSOR-M
HI-2	FASTGRASS-VFP, CORSOR-M
HI-3	FASTGRASS-VFP, VICTORIA, CORSOR-M
HI-4	FASTGRASS, CORSOR-M
HI-5	CORSOR-M
VI-1	VICTORIA
VI-2	VICTORIA
VI-3	CORSOR-M, VICTORIA
VI-4	VICTORIA
VI-5	CORSOR-M
ST-1	CORSOR, VICTORIA, MELCOR
ST-2	CORSOR, VICTORIA, MELCOR
HEVA 04	CORSOR, CORSOR-M
HEVA 06	CORSOR, CORSOR-M

Also shown in Fig. 3.2 are two curves calculated with FASTGRASS. One curve utilizes nominal grain growth kinetics for stoichiometric fuel, and the other employs grain growth kinetics enhanced by fuel oxidation (hyperstoichiometric fuel). Enhanced grain growth (appreciable grain growth was observed) provides a larger noble gas release rate (in agreement with the experimental data at high temperatures) due to grain boundary sweeping of fission products from the interior of the grains. Most of the fission product release in the SFD-ST experiment occurred after fuel liquefaction and during the cooldown following water addition. Integral fission product releases were calculated by assuming that most of the fission products predicted by FASTGRASS to be on the grain boundaries were released. Two sets of calculated values, one reported by INEL[1] and one reported by Rest and Zawadzki[2] are provided in Table 3.27 along with the measured values.

Mechanisms that could have opened grain boundaries to the surface to facilitate fission product release include fuel liquefaction (15% observed) and microcracking (observed over about 20% of the fuel bundle). Tellurium release was of the same order as iodine. This is the expected result in experiments such as this where the Zircaloy oxidation in many regions is nearly complete.[6,7] It is clear that successful modeling of fission product release from trace-irradiated fuel requires significant sophistication and detail in the mechanisms of fuel microstructural changes under accident conditions.

Test SFD 1-1. Test SFD 1-1 contained 32 0.9-m-long fuel rods trace-irradiated to 0.79 MWd/kgU, heated in steam to temperatures of at least 2800 K, and slowly cooled by power reductions.[8] Approximately 26% of the Zircaloy

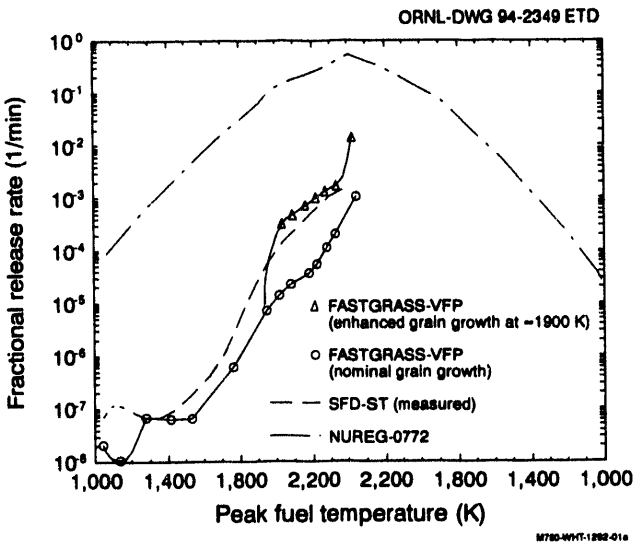

Figure 3.2 FASTGRASS-VFP predictions of noble gas release rates during SFD-ST experiment

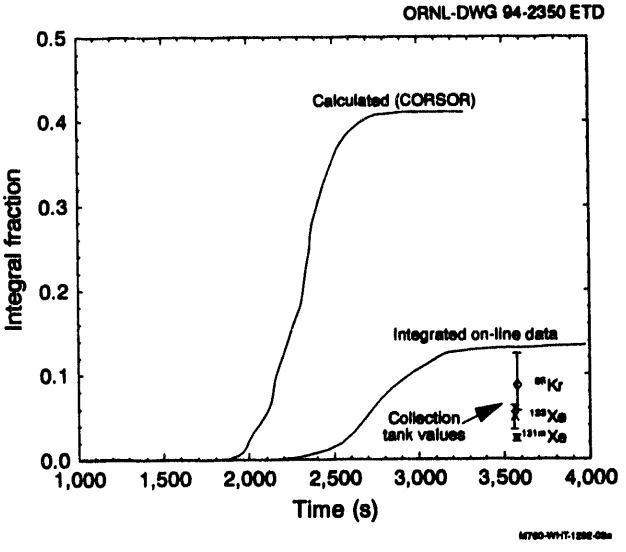

Figure 3.3 Test SFD 1-1 noble gas integral release comparison

cladding in the fuel bundle was oxidized, and ~16% of the fuel was liquefied in the experiment.

Fission product release in the SFD 1-1 test was analyzed with CORSOR (Ref. 8), FASTGRASS (Ref. 2), MELCOR (Ref. 9), and MAAP (Ref. 10). The noble gas release fraction calculated by CORSOR greatly exceeds the measurement, as shown in Fig. 3.3, for this trace-irradiated fuel for the same reasons as discussed in conjunction with SFD-ST. Spatial and axial temperatures as a function of time were provided to FASTGRASS, derived from calculations of SCDAP code, adjusted to experimental best-estimate values. FASTGRASS-calculated fission gas release rates with and without the effects of fuel liquefaction are shown in comparison to measured values in Fig. 3.4. Clearly, the inclusion of fuel liquefaction effects in the FASTGRASS code improves the prediction relative to the measurements in this experiment in which 16% of the fuel was observed to have been liquefied. Integral releases calculated with FASTGRASS, assuming one of the ten fuel nodes to go into total fuel liquefaction (monotectic melting at 2600 K) and four of the remaining nodes to have grain boundary liquefaction (eutectic melting at 2150 K), are presented in Table 3.28 along with measured values. The column titled FASTGRASS-Total includes the release due to liquefaction broken out in the adjacent column. It is apparent that the agreement with experiment would be even better if the full 16% liquefaction observed had been used in the calculation, but at the time the liquefaction was thought to be only 7%.

Table 3.27 Measured releases from SFD-ST compared with FASTGRASS calculations

Fission product	Fraction released		
	FASTGRASS-INEL (Ref. 1)	FASTGRASS-Rest (Ref. 2)	Measured
Xe	0.46	0.50	~0.5
Cs	0.46	0.39	0.32
I	0.48	0.39	0.51
Te	0.48		0.40

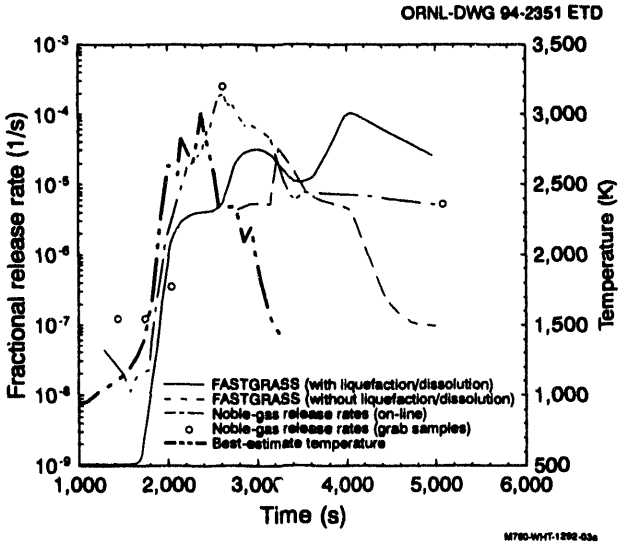

Figure 3.4 FASTGRASS-calculated noble gas release rates for SFD 1-1 with and without effects of liquefaction

Total liquefaction of fuel nodes enhances calculated values of fission product release in both trace-irradiated and high-burnup fuel. In trace-irradiated fuel, such as used in SFD 1-1, liquefaction of grain boundaries also increases calculated values of fission product release by enhancing fission product mobility in grain boundaries. As will be seen later in the analysis of the HI-4 test, this is not the case for high-burnup fuel with grain boundary tunnels that permit rapid fission product mobility in the solid state.

The tellurium release is much smaller in SFD 1-1 than in SFD-ST because the oxidation of Zircaloy is much less. The calculation of the release of barium by FASTGRASS is in good agreement with the measurement. As indicated in Table 3.28, most of the fission product release is predicted to be associated with fuel liquefaction in this trace-irradiated experiment. This prediction is in agreement with the experimental observation that fission product release was very small until late in the test when very high temperatures (2200 to 2800 K) were reached where fuel liquefaction could take place. The grain growth kinetics used in the FASTGRASS calculation were driven by temperature only in concert with the lower level of oxidation in this experiment. The initial grain size was taken as 8 μm, and the calculated final grain size of 12 μm is in good agreement with 10- to 12-μm grain size found in the postirradiation examination.

MELCOR is a systems code that uses the CORSOR or CORSOR-M models to calculate fission product release as a function of time at temperature. Madni[9] demonstrates that MELCOR (version 1.7.1) closely reproduced the experimental thermal-hydraulic conditions in the SFD 1-1 test, based on good agreement between calculated and measured fuel and cladding temperatures and hydrogen production. However, he states that the fission product release calculated for the SFD 1-1 experiment was an order of magnitude greater than that measured. It is suggested that the CORSOR and CORSOR-M models may not be appropriate for calculating fission product release from trace-irradiated fuels due to the unique microstructure of these fuels.

Fission product release in the MAAP code is calculated as a function of fuel oxidation using the steam oxidation model of Cubicciotti.[11] This model has been used to analyze fission product release from the SFD 1-1 test by Suh and Hammersley.[10] The overall heat transfer coefficient to

Table 3.28 Measured releases from SFD 1-1 compared with FASTGRASS calculations

Fission product	Fraction released		
	FASTGRASS-Liquefaction	FASTGRASS-Total	Measured
Noble gas	0.039	0.044	0.026–0.093
I	0.040	0.046	0.12
Cs	0.043	0.049	0.09
Te	0.0013	0.0015	0.01
Ba	0.008	0.009	0.006

the heat sink in the model was adjusted to obtain reasonable agreement with the measured heat loss. Figure 3.5 indicates that the steam oxidation model overpredicts the noble gas release rate during the bundle heatup period by as much as 5 orders of magnitude. The model underpredicts the release rate during the cooldown period by as much as 6 orders of magnitude. Alternate fission product release models, termed ARSAP 9-μm and ARSAP no-grain correlations, show better agreement with the measured release rate in Fig. 3.5; however, they have not been incorporated into the MAAP code. The 9-μm correlation refers to an effective fuel grain size of 9 μm, and the no-grain correlation has no grain size dependence. These are bulk mass transfer models with unique coefficients for each fission product element. The grain size-dependent correlation does not permit the fractional release rate to increase at temperatures above fuel liquefaction. Integral

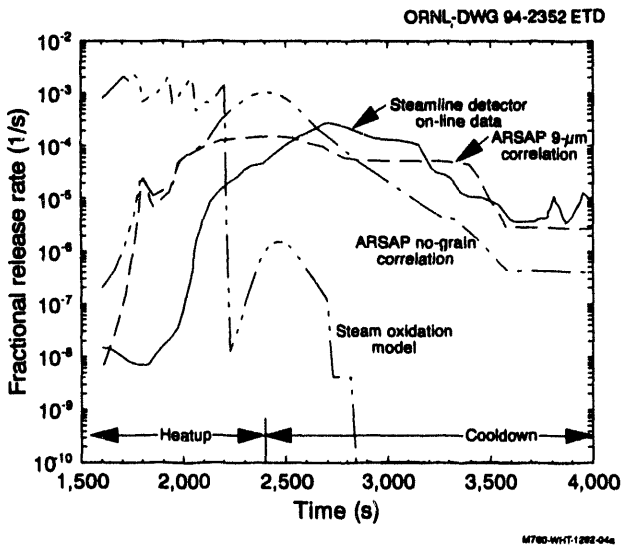

Figure 3.5 Comparative performance of predictive correlations for noble gas release rate during STD 1-1 test

releases calculated with these models are shown along with the measurements in Table 3.29.

The steam oxidation model strongly overpredicts the integral releases of the volatile fission products measured in the SFD 1-1 test, whereas the alternative models give values closer to the measurements.

LOFT LP-FP-1. The LP-FP-1 test[12] contained 22 prepressurized 1.7-m-long fuel rods irradiated to an average burnup of 1.42 MWd/kgU within an 11 by 11 rod bundle. The average linear heat generation rate was 35.7 kW/m, and the maximum was 52.2 kW/m. The transient portion of the test consisted of a simulated large-break LOCA, followed by ECCS injection. Fuel rod temperatures rose to ~1150 K during the LOCA, driven by decay heat, causing 8 of the 22 pressurized rods to rupture. ECCS water injection was started 20 s after the first rod failed, and the experiment was terminated 2 min after the core was reflooded.

The fission product inventory in the fuel-cladding gap before the transient was determined by extrapolation of data from postirradiation examination measurements of intact rods and has an uncertainty on the order of 50% (Appendix A of Ref. 12). Similarly, measurements of fission product release were also extrapolated to determine total release fractions and are considered to have uncertainty in this same range. Three sets of values of gap inventory and releases from ruptured fuel rods, based on measurements, are presented in Table 3.30, along with values of gap inventory calculated with FASTGRASS-VFP (Appendix C, Ref. 12).

As pointed out in Appendix A of Ref. 12, due to the large uncertainties, the releases measured should be considered

Table 3.29 Measured releases from SFD 1-1 compared with MAAP modeling calculations

Fission product	Fraction released			
	Steam oxidation	ARSA No-Grain	ARSAP 9-μm	Measured
Noble gas	0.93	0.38	0.13	0.026–0.093
I	0.93	0.33	0.13	0.12
Cs	0.93	0.39	0.12	0.09

Table 3.30 Measured gap inventory and releases from LP-FP-1 compared with FASTGRASS-VFP calculations (Ref. 12)

	Fraction released				
Fission product	Measured gap inventory	Calculated gap inventory	Measured release values		
			Main report	Appendix A	Appendix B
Xe-133	0.0067	0.0263	0.013	0.018	0.017
I-131	0.0046	0.0256	0.0072	0.011	0.0087
Cs-137	0.0085	0.0261	0.0021	0.012	0.015

to be the full gap inventory. The main report values for measured release are smaller than those derived in Appendixes A and B because releases due to leaching after reflood are not included. Virtually all of the noble gas release occurs before reflood, about half of the iodine release occurs before reflood, but virtually all of the cesium release occurs due to leaching of exposed fuel and cladding surfaces within ruptured rods after reflood. The values of gap inventory calculated by FASTGRASS-VFP are about a factor of 3 to 5 greater than the values derived from postirradiation examination measurements and 2 to 3 times greater than the measured releases. This overprediction is thought to be due to the use of fuel centerline temperatures some 300 K higher than measured during the irradiation preceding the transient testing (Appendix C of Ref. 12).

LOFT LP-FP-2. The LP-FP-2 test[13] contained 100 1.7-m-long fuel rods irradiated to a burnup of 0.45 MWd/kgU. The experiment simulated the system thermal-hydraulics and core uncovery conditions during fission product release and transport that are expected to occur in a four-loop PWR from rupture of a LPIS pipe as a result of a V-sequence accident. Temperatures as high as 3100 K were reached, and ~49% of the Zircaloy cladding in the fuel bundle was oxidized. Approximately 15% of the fuel was liquefied. The high-temperature transient was terminated by reflooding. Evidence from the postirradiation examination of the bundle,[14] in conjunction with thermocouple measurements, hydrogen distribution after the test, and fission product release and distribution measurements indicates that the highest temperatures and the vast majority of the Zircaloy oxidation, fuel liquefaction, and fission product release occurred during the reflood.

Fission product release in the LP-FP-2 experiment was analyzed with the CORSOR, SCDAP/RELAP5, and FASTGRASS codes[13] and MELCOR (CORSOR-M) (Ref. 15). Temperature histories calculated by the SCDAP/RELAP5 code were used as input to the fission product release codes. The results presented in Fig. 3.6 show that, in the heatup transient before reflood, CORSOR overpredicts noble gas releases for this low-burnup fuel; FASTGRASS with fuel liquefaction limited to grain boundaries in one-third[2] to one-half[3] of the six axial nodes in the core model provides reasonable agreement with measured values for xenon. It is interesting to note that the SCDAP/RELAP5 (PARAGRASS) calculation without liquefaction calculates noble gas release comparable with the iodine and cesium releases measured after reflood. The FASTGRASS and SCDAP/RELAP5 calculations were sensitive to the initial fuel grain size (smaller initial grain

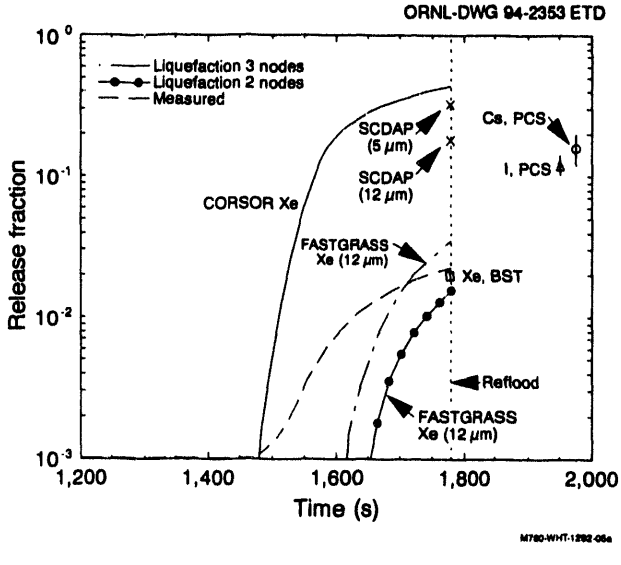

Figure 3.6 Comparison of CORSOR, SCDAP, and FASTGRASS calculated cumulative noble gas releases with data from LP-FP-2

size produced larger releases). A grain size of 12 μm was used based on preliminary postirradiation results. Final postirradiation examination results indicate a starting grain size of 14 μm and grain growth to 27 μm in the hottest regions. Integral fission product release measurements up to reflood and after reflood are provided in Table 3.31 along with FASTGRASS and MELCOR (CORSOR-M) calculations for releases up to reflood.

The FASTGRASS values in Table 3.31 were calculated assuming grain boundary liquefaction in one-third of the nodes. The releases measured before reflood are from the blowdown suppression tank and deposition in the sample lines, the LPIS line, and the upper plenum. The relatively large measurements of barium release are interesting to note. The FASTGRASS calculations of the releases of Xe, I, Cs, and Te are in reasonable agreement with values measured before reflood. The releases of xenon, iodine, and cesium calculated by MELCOR (CORSOR-M) are a factor of 2 to 5 greater than measured before reflood and somewhat less than measured after reflood. The tellurium release is significantly overcalculated and the barium release is significantly undercalculated by MELCOR (CORSOR-M).

Test SFD 1-3. From this point onward, analyses of experiments utilizing highly irradiated fuel are discussed. Test SFD 1-3[16] contained 26 0.9-m-long fuel rods irradiated to a burnup of 38 MWd/kgU, two fresh instrumented rods, and four empty Zircaloy guide tubes.[16] The bundle was heated in steam to temperatures as high as 2800 K, resulting in 22% of the Zircaloy being oxidized and 18% of the fuel being liquefied. A depressurization during the high-temperature portion of the experiment (due to a malfunctioning isolation valve) caused the gas flow from the bundle to stagnate for a period, disrupting information on fission product release rate measurements. Fission product release was calculated with the SCDAP/RELAP5 code, containing the PARAGRASS fission product release module. Results of these posttest calculations compare favorably with measurements as is shown in Table 3.32.

Table 3.31 Measured releases from LP-FP-2 compared with FASTGRASS calculations

Fission product	Fraction released			
	Before reflood			Total after reflood
	FASTGRASS	MELCOR (CORSOR-M)	Measured	Measured
Xe	0.016	0.107	0.017	—
Kr			0.02	0.12
I	0.014	0.107	0.03–0.05	0.16
Cs	0.014	0.107	0.008–0.03	0.16
Te	0.0003	0.066	0.0003–0.005	0.03
Ba		0.00007	0.002–0.008	0.09

Table 3.32 Measured releases from SFD 1-3 compared with PARAGRASS calculations

Fission product	Fraction released	
	Calculated	Measured
Kr-85	0.17	0.20 ± 10%
Cs-137	0.17	0.18 ± 9%
I-131	0.17	0.18 ± 10%

The brief discussion of these results[16] states that the calculated releases are dominated by effects of fuel liquefaction (16% calculated).

Test SFD 1-4. Test SFD 1-4 comprised 26 0.9-m-long fuel rods irradiated to a burnup of 36 MWd/kgU, two fresh instrumented rods, and four silver-indium-cadmium control rods.[17] Temperatures in excess of 2800 K were reached, resulting in hydrogen generation equivalent to the full oxidation of 32% of the Zircaloy and liquefaction of 18% of the fuel. Fission product release for this experiment has been analyzed using CORSOR, FASTGRASS, and Booth diffusion,[17,18] FASTGRASS (Ref. 2), MELCOR,* MAAP (Ref. 10), and ICARE2 (Ref. 19).

Results of calculations of noble gas release rates with the first three models are in reasonable agreement with measurements during the heatup phase (<2000 s) of the SFD 1-4 test as shown in Fig. 3.7 from Ref. 18. The best agreement on heatup was obtained with the Booth model that used a diffusion coefficient derived from out-of-pile fission product release tests conducted at ORNL on similar high-burnup fuel from the BR-3 reactor. The agreement suggests that for releases from high-burnup fuel on heatup, very little difference should be expected between in-pile and out-of-pile experiments.

Release rates on heatup for long-lived species as calculated by FASTGRASS were greater than for short-lived species. These results generally agree with the integral release measurements that show increased releases for long-lived and stable isotopes,[20] suggesting that fuel microstructure does affect fission product release to some extent in high-burnup fuel (grain boundaries contain a greater fraction of long-lived isotopes than short-lived isotopes). However, as illustrated in Fig. 3.7, these differences diminished once high temperatures and significant fuel liquefaction occurred (2050 to 2800 s). Each model overpredicted the measured release rates by factors of 2 to 5 during this high-temperature portion of the test. All models failed to account for the sustained releases measured during the cooldown portion of the test (>2800 s).

Integral releases calculated by CORSOR and FASTGRASS are compared with measurements in Table 3.33. Volatile fission product release is overpredicted by CORSOR due to the overprediction in release rate in the

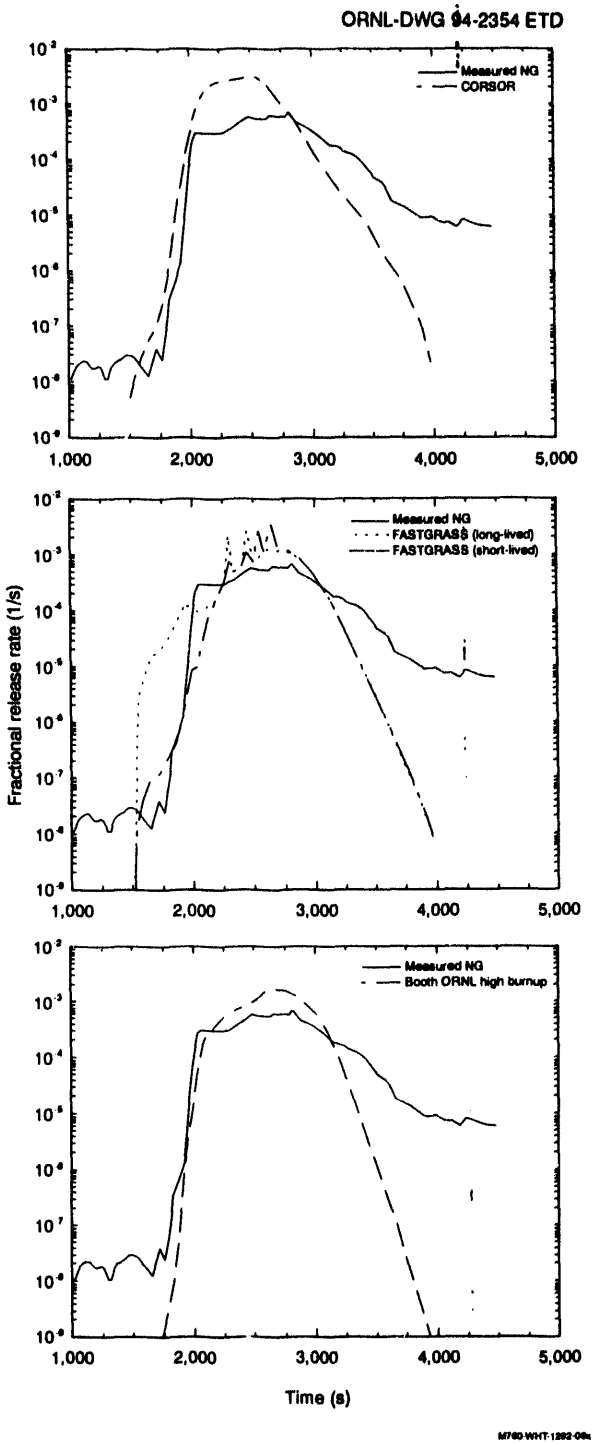

Figure 3.7 Comparison of noble gas release model results with online SFD 1-4 release rate data

period of peak temperatures during the test. The FASTGRASS code predicts the integral releases of the volatile fission products quite well, but badly overpredicts the release of the less volatile fission products barium and strontium and underpredicts the tellurium release.

*I. K. Madni, "MELCOR Modeling of the PBF Severe Fuel Damage Test 1-4," *Proceedings of the International Conference on PSAM, Beverly Hills, California, February 1991.*

Table 3.33 Measured releases from SFD 1-4 compared with FASTGRASS and CORSOR calculations

Fission product	Fraction released			
	CORSOR	FASTGRASS liquefaction	FASTGRASS total	Measured
Noble gas	0.83	0.15	0.42	0.23–0.52
I	0.83	0.15	0.42	0.24
Cs	0.83	0.13	0.35	0.51
Te	0.16	0.001	0.003	0.03
Ba		0.04	0.12	0.007
Sr		0.05	0.14	0.009

FASTGRASS predicts that about one-third of the fission product release is due to fuel liquefaction. The liquefaction modeled here is the same scheme as used previously in the analysis of SFD 1-1: one node in ten is assumed to be totally liquefied, and four nodes are assumed to experience grain boundary liquefaction.

For the SFD 1-4 test, MELCOR (version 1.8) calculates appropriate thermal-hydraulic conditions according to the good agreements in fuel and cladding temperatures and hydrogen generation between calculation and measurement.* Fission product releases calculated by the CORSOR model in MELCOR are compared with measurements in Table 3.34. The reason for the lower release fractions from CORSOR calculated with the MELCOR code is not known, but a sensitivity study[17] showed that a 15% reduction in bundle temperatures reduced the CORSOR-calculated release fraction by 20%. The good agreement of the calculated and measured tellurium release is probably a consequence of proper modeling of Zircaloy oxidation by MELCOR.

Suh and Hammersley[10] analyzed fission product release from SFD 1-4 using the MAAP steam oxidation model and two versions of a bulk mass transfer release model. Figure 3.8(a) shows that the steam oxidation model predicts a significantly premature release (~67%) of noble gases by 2000 s, at which time other correlations barely start to predict any release and the measured release rate is rising rapidly from very low values. The bulk mass transfer release model (ARSAP 9-μm correlation) is in good agreement to the measured release rate [Fig. 3.8(b)]. It can be seen in Table 3.35 that the steam oxidation model greatly overpredicts the integral releases measured for the volatile fission products, and the 9-μm ARSAP correlation predicts values in good agreement with measurement. The bulk mass transfer models (the ARSAP correlations) have not been incorporated into the MAAP code. The steam oxidation model is currently the resident fission product release methodology in the MAAP code.

Table 3.34 Measured releases from SFD 1-4 compared with MELCOR (CORSOR) calculations

Element	SFD 1-4 Test	MELCOR (CORSOR)
Noble gas	0.23 - 0.52	0.57
Cesium	0.51 ± 15%	0.57
Iodine	0.24 ± 19%	0.57
Tellurium	0.03 ± 37%	0.03

Mezza et al.[19] used experimental results from SFD 1-4 to test the ICARE2 code. They found satisfactory agreement between calculations with ICARE2 V2-Mod1 and experimental results of cladding and gas temperatures, the occurrence of steam starvation, and material relocation. The results of three fission product release models available in

*I. K. Madni, "MELCOR Modeling of the PBF Severe Fuel Damage Test 1-4," *Proceedings of the International Conference on PSAM, Beverly Hills, California, February 1991.*

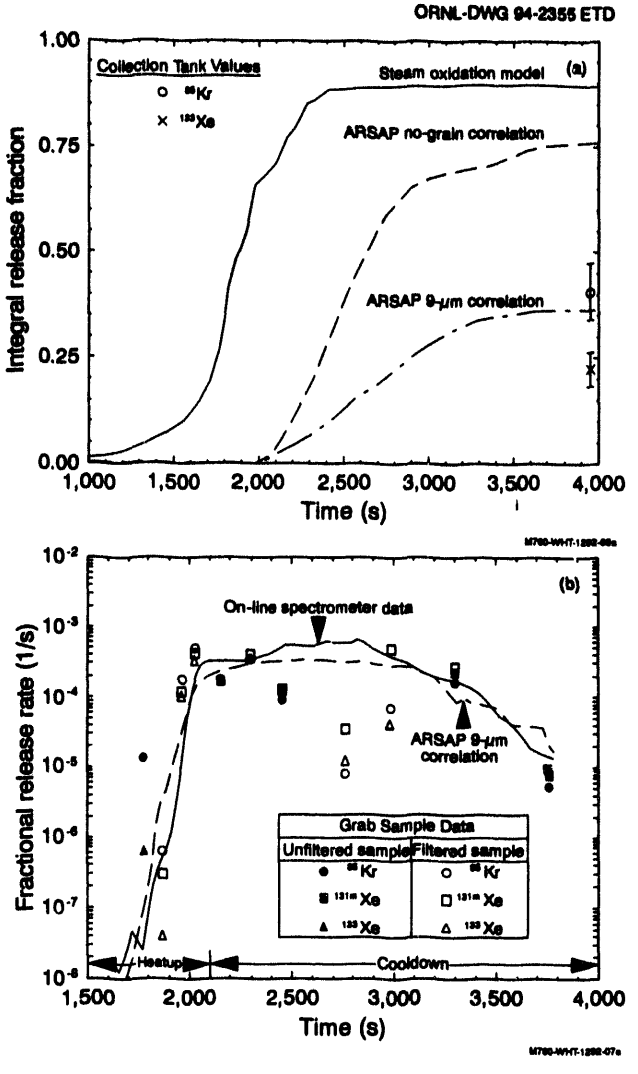

Figure 3.8 (*a*) Comparative performance of predictive correlations for noble gas integral release during SFD 1-4 test and (*b*) comparison between predictive models and the experimental data for noble gas release during SFD 1-4 test

this version of ICARE2 have been compared with experimental measurements. These models are CORSOR-M, EMIS (a CORSOR-like model validated with the French HEVA experiments[21]), and SASCHA (a CORSOR-like model from the German FPRATE module).[22]

The comparison with experimental data of noble gas fractional release rate in Fig. 3.9 shows a large overestimation by the three models during the high-temperature portion of the SFD 1-4 test and an underestimation during the cooldown portion of the test. The comparison with experimental data of integral releases is shown for several species in Table 3.36. The calculated behavior highlights a general satisfactory prediction for cesium release, but an overestimation of iodine and, to some degree, noble gas releases. For tellurium, CORSOR-M suggests too large a release; the two other models are in good agreement with experimental data. For less volatile fission products, such as barium and strontium for which the experimental releases are very small, the values obtained with CORSOR-M are satisfactory; however, the SASCHA and EMIS models overestimate the releases.

In addition to comparisons of code calculations of fission product releases with measurements from the SFD 1-4 test, one set of comparisons involving the release of control materials is available. Petti[23] analyzed the releases of silver, indium, and cadmium from the SFD 1-4 test. He compared calculations from CORSOR and VAPOR (a model of control rod behavior under severe accident conditions described in Ref. 23) with experimental data. These results are provided in Table 3.37 and indicate that CORSOR overpredicts the releases of silver and indium by 3 orders of magnitude and overpredicts the release of cadmium by 1 order of magnitude. A key phenomenon is the relocation of molten control rod materials to cooler regions lower in the test bundle. Such relocation freezes the molten control rod materials and limits the releases of their vapors. CORSOR is based on releases measured in experiments in

Table 3.35 Measured releases from SFD 1-4 compared with MAAP modeling calculations

Fission product	Fraction released			
	Steam oxidation	ARSAP no-grain	ARSAP 9-μm	Measured
Noble gas	0.89	0.76	0.37	0.23-0.52
I	0.89	0.67	0.41	0.24
Cs	0.89	0.81	0.40	0.51

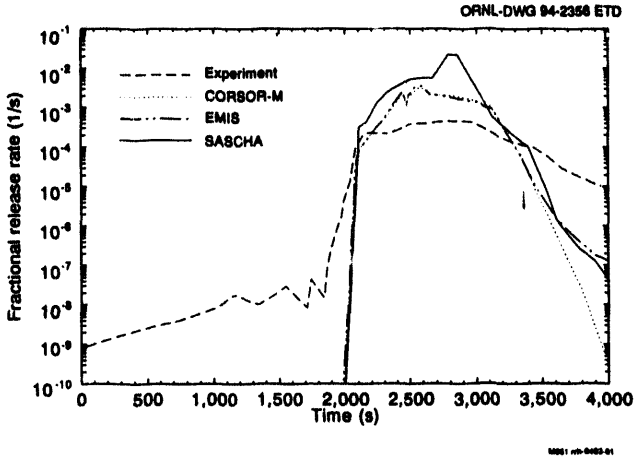

Figure 3.9 ICARE-Mod 1 noble gas release rates calculated with three different models compared with experimental data from SFD 1-4

which the melt was contained in a crucible and could not relocate; thus, CORSOR overpredicts control material releases in SFD 1-4 in which these materials relocated. The VAPOR code takes into account relocation of molten control materials with or without reheating by subsequent relocations of hotter core melts. VAPOR with the latter capability is able to match fairly well the experimental data on cadmium, but it underpredicts the silver and indium releases by 2 orders of magnitude. Petti suggests that the silver and indium releases may have been dominated by entrainment of the molten control alloy in the flow following early failure by bursting of a defective (water-logged) instrumented control rod, although the release of cadmium may have been dominated by vaporization from the other three control rods that failed later at higher temperature.

ORNL HI Tests. The HI tests[24] were a series of six out-of-pile fission product release tests conducted at ORNL by heating single, irradiated, fuel rod segments in a horizontal

Table 3.36 Measured releases from SFD 1-4 compared with ICARE2 modeling calculations

Element	Fraction released			
	SFD 1-4 Test	CORSOR-M	EMIS	SASCHA
Noble gas	0.23 - 0.52	0.57	0.55	0.69
Cesium	0.51 ± 15%	0.58	0.56	0.54
Iodine	0.24 ± 19%	0.56	0.54	0.68
Tellurium	0.03 ± 37%	0.07	0.04	0.04
Barium	0.007 ± 46%	0.01	0.04	0.05
Strontium	0.009 ± 28%	<0.01	0.02	0.05

Table 3.37 Measured releases of control materials from SFD 1-4 compared with CORSOR and VAPOR calculations

Measured element	Fraction released			
	Measured total	CORSOR	VAPOR without reheat	VAPOR with reheat
Silver	2.69×10^{-4}	0.57	1.89×10^{-6}	5.98×10^{-6}
Indium	8.79×10^{-4}	0.44	3.04×10^{-6}	9.57×10^{-6}
Cadmium	6.18×10^{-2}	0.70	1.18×10^{-2}	9.85×10^{-2}

geometry in flowing steam. The fuel segments varied in length from 15 to 20 cm, and the burnups were in the range 10 to 40 MWd/kgU. Heating ramps in the range of 1 to 2 K/s were used to reach isothermal holds that were mainly in the range of 1973 to 2273 K for usually about 20 min before cooling in flowing gas in the absence of heat input. Pertinent characteristics and fission product releases for the HI tests are summarized in Table 3.38, abstracted from Ref. 20.

Analyses of fission product release from the HI tests have been performed with FASTGRASS (Ref. 2) and with VICTORIA (Ref. 25). A thermally and mechanically coupled model, consisting of FASTGRASS and the LIFE-LWR fuel behavior code, was used to assess the state of the fuel after steady-state irradiation and before transient testing.[2] Rest has used the HI data to investigate the effects of grain boundary sweeping and the liquefaction of grain boundaries on modeling fission product release.[2] The increase in fission product release due to grain growth in stoichiometric fuel vs no grain growth is shown in Fig. 3.10 to provide much better agreement with data from test HI-3. The holding temperature in the HI-3 test was 2273 ± 50 K. The grain growth predictions with FASTGRASS were consistent with metallographic measurements of grain growth in the fuel. Test HI-2 was heated in steam at approximately half the heatup rate and with approximately twice the steam mass flow rate compared with test HI-3. As a result, the cladding was essentially completely oxidized and extensively fractured. Figure 3.11, showing HI-2 results, demonstrates that utilizing oxidation-enhanced grain growth kinetics for hyperstoichiometric fuel provides release results in good agreement with the experimental results for this test run at a maximum temperature of 1973 ± 50 K. In contrast, the results with grain growth kinetics appropriate for stoichiometric fuel provide much lower fission product releases.

Test HI-4 was conducted under conditions nearly identical to HI-3, but had lower fission product releases. Post-irradiation examination indicated more fuel-cladding interaction, including grain boundary liquefaction, in test HI-4 than in test HI-3 and no grain growth. Figure 3.12 shows that FASTGRASS predictions of fission gas release invoking the grain boundary liquefaction model provide good agreement with the experimental data, whereas the data are strongly overpredicted without the effects of grain boundary liquefaction. Grain growth with the grain boundary liquefaction model is predicted to be less than 10%, which is in reasonable agreement with the no growth

Table 3.38 Data for the HI test series

Characteristic/parameter	Test number					
	HI-1	HI-2	HI-3	HI-4	HI-5	HI-6
Fuel burnup (MWd/kgU)	28.1	28.1	25.2	10.1	38.3	40.3
In-pile gas release (%)	0.3	0.3	0.3	10.2	4.1	2.0
Steam flow rate (g/min)	0.81	0.76	0.31	0.29	0.30	1.7
Test heatup rate (K/s)	1.2	1.3	2.1	2.3	1.1	2.3
Test temperature (K)	1673	1973	2273	2200	2023	2250
Time at temperature (min)	33.8	22.5	21.3	21.6	21.5	2.5
UO_2 grain size (μm)						
Pretest	2.8	2.8	2.8	6.6	9.2	
Posttest	3.4	3.9	4.3	6.6	8.9	
Fuel-cladding interaction	None	Minor	Yes	Yes	Minor	Yes
Fission product release (%)						
Kr	3.13	51.8	59.3	31.3	19.9	31.6
I	2.04	53.0	35.4	24.7	22.4	24.7
Cs	1.75	50.5	58.8	31.7	20.3	33.1

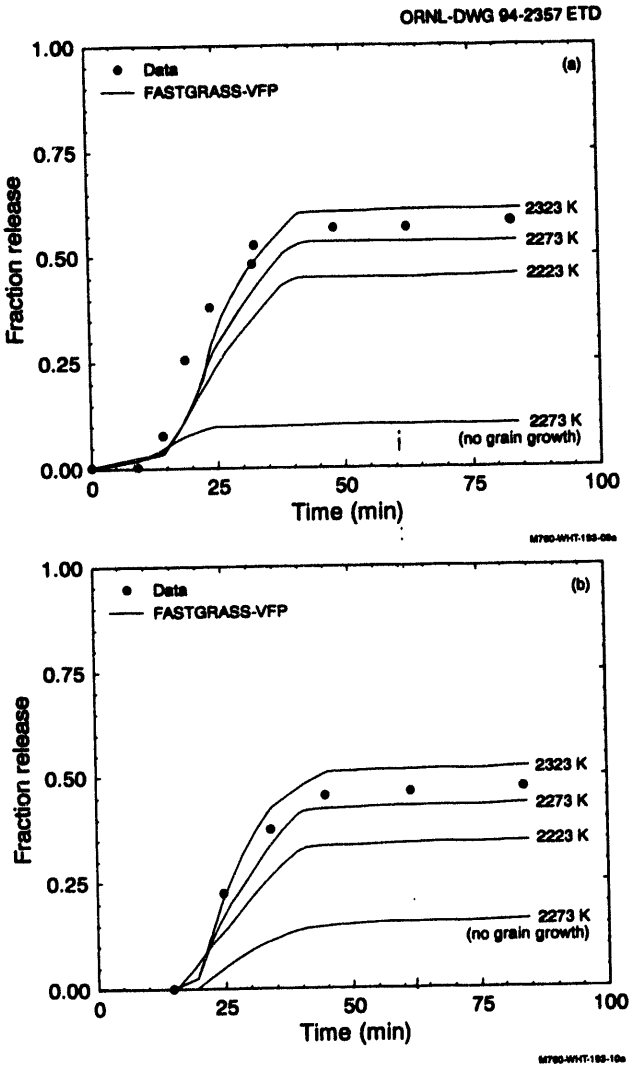

Figure 3.10 FASTGRASS-VFP predictions of (*a*) noble gas and (*b*) cesium release during ORNL test HI-3

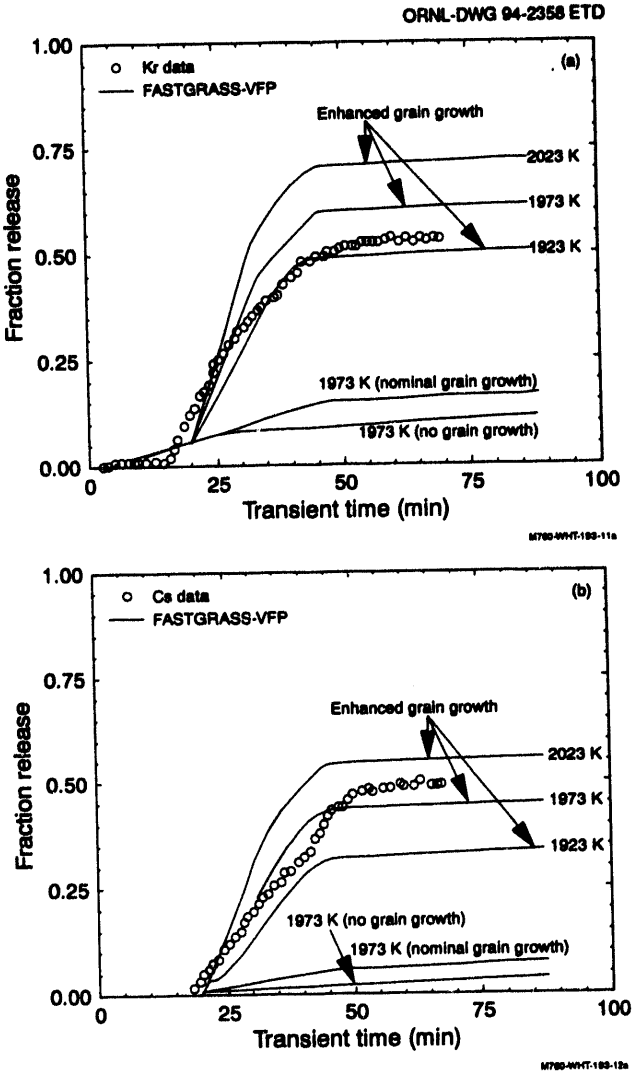

Figure 3.11 FASTGRASS-VFP predictions of (*a*) noble gas and (*b*) cesium release during ORNL test HI-2

observation. Fuel liquefaction along grain boundaries tends to inhibit fission product release in high-burnup fuel by two mechanisms: (1) limiting grain boundary sweeping of intragranular fission products and (2) reducing mobility of fission products in grain boundaries due to liquid filling of tunnels. In trace-irradiated fuel, grain boundary liquefaction increases fission product mobility by transforming pathways from solid to liquid.

Domagala et al.[25] have applied VICTORIA, containing improved models for calculating fission product release from intact fuel, to the analysis of the HI-3 test. The improved transport model, called TRANIF, includes a two-node diffusive flow formulation (which replaces the simple Booth diffusion model) and physically based models to calculate grain growth, grain boundary sweeping, and intergranular bubble behavior. Calculation of the fission gas distribution in the fuel before the HI-3 test was done by running a simulation of the steady-state irradiation with a stand-alone version of TRANIF. The results of the calculation of fission product release for krypton and cesium relative to HI-3 experimental data are presented in Fig. 3.13. It can be seen that the agreement between calculation and experiment for krypton release is excellent. The release of cesium is overpredicted by VICTORIA with the TRANIF improvements because, according to the authors,[25] in contrast to the noble gases, physical trapping mechanisms have not been included for nonrare gas fission products. A 50% increase in grain size during the HI-3 experiment is calculated. This result is in agreement with postirradiation measurements.

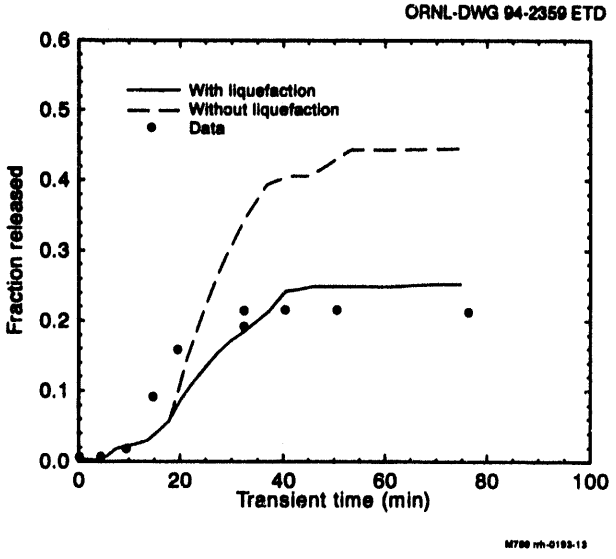

Figure 3.12 FASTGRASS predictions of noble gas release during ORNL test HI-4 with and without effects of fuel liquefaction

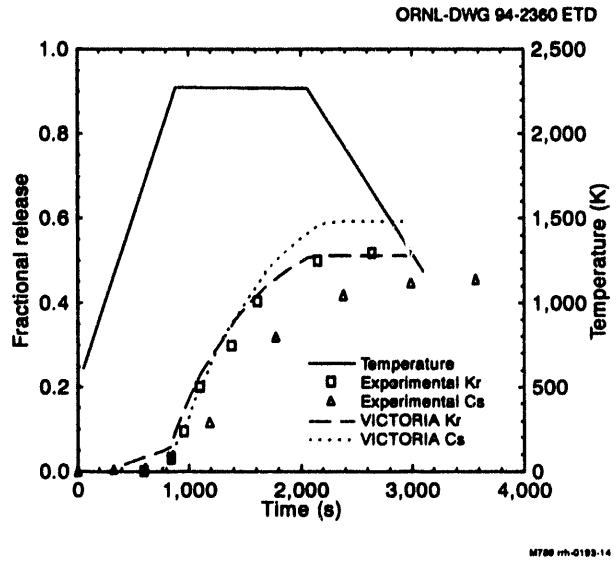

Figure 3.13 Comparison of krypton and cesium release from fuel in HI-3 test as calculated by VICTORIA with experimental data

ORNL VI Tests. Five tests have been performed in the VI test series at ORNL that are similar to the HI tests described earlier except that the irradiated fuel rod segment and the gas flow path are oriented vertically during heating. Fuel with burnups of 40 to 47 MWd/kgU have been heated to temperatures in the range 2000 to 2700 K in either steam or hydrogen. Pertinent characteristics and fission product releases for the VI tests are summarized in Table 3.39, extracted from Refs. 26–30.

Analyses of VI tests have been performed with VICTORIA. Domagala et al.[25] have applied VICTORIA with the TRANIF fission product transport model to the analysis of the VI-3 test. This test heated 43 MWd/kgU fuel in steam to 2700 K for 20 min after a hold for 20 min at 2000 K. The calculated releases of krypton and cesium are compared with measured releases in Fig. 3.14. As in the case of the HI-3 analysis, the krypton release is fairly well predicted with the cesium release lagging behind early in the test (because krypton is initially released from grain boundaries while cesium must diffuse through the grain) and then rising above the krypton release late in the test due to lack of intragranular and intergranular bubble trapping mechanisms for nonrare gases in the TRANIF model. In both the HI-3 and VI-3 analyses, the dominant fission gas release mechanism was reported to be grain growth/grain boundary sweeping. The importance of grain growth/grain boundary sweeping in effecting fission product release is illustrated in Fig. 3.15 for krypton in Test VI-3. In this case, this mechanism accounts for 90% of the calculated fission product release.

Williams and Bond[31] have analyzed four of the VI tests with VICTORIA 90 mod 1. This code currently only has the capability to model intact fuel pellet stacks, though the cladding may be either intact, fully or partially oxidized, ruptured, or partially or completely removed. Calculation of noble gas release from test VI-3, using several different time steps and plotted in Fig. 3.16, shows little time step sensitivity, but shows considerable underprediction of release relative to experimental measurement early in the test at temperatures less than about 2400 K.

Test VI-1 heated 40 MWd/kgU fuel in steam to two ascending isothermal holds, 20 min at 2020 K and 20 min at 2300 K. The calculated results for cesium and iodine plotted in Fig. 3.17 show reasonable agreement with experimental release measurements. The experimenters[26] report that the iodine-129 measurement technique provided a minimum value for iodine release, and they believe the true release value was significantly higher, probably similar to that of cesium. One would not normally expect to calculate an iodine release that is significantly lower than the cesium release, but Williams and Bond[30] did not comment on this anomaly.

In test VI-2, 44 MWd/kgU fuel was heated in steam to 1200 K and held for 5 min and then heated to 2300 K and

Table 3.39 Data for the VI test series

Characteristic/parameter	Test number				
	VI-1	VI-2	VI-3	VI-4	VI-5
Fuel burnup (MWd/kgU)	40	44	42	47	42
Reactive atmosphere	H_2O	H_2O	H_2O	H_2	H_2
Hold temperatures (K)	2020 (20)	1200 (5)	2000 (20)	1600 (20)	2015 (20)
and times (min)	2300 (20)	2300 (60)	2700 (20)	2400 (20)	2740 (20)
Fission product release (%)					
Kr	47	31	100	85	100
I	45	40	69	87	
Cs	63	63	99	95	100

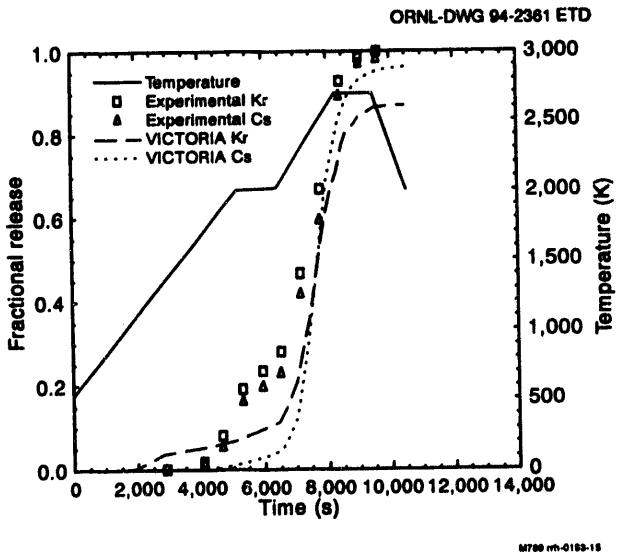

Figure 3.14 Comparison of krypton and cesium release from fuel in VI-3 test as calculated by VICTORIA with experimental data

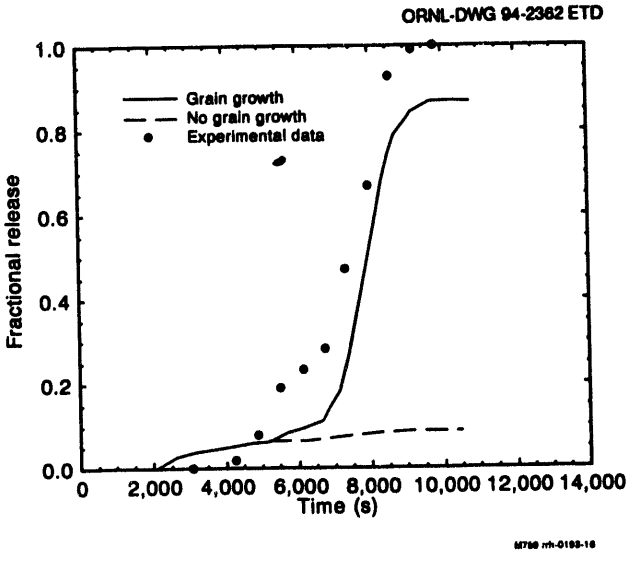

Figure 3.15 Krypton release from fuel for VI-3 test as calculated by VICTORIA with and without grain growth

held for 60 min. The calculated data shown in Fig. 3.18 greatly overpredict the releases of krypton and cesium relative to the experimental data. No explanation has been offered for the overprediction of the releases from the VI-2 test.

Test VI-4 heated 47 MWd/kgU fuel in hydrogen to about 1600 K for a 20-min hold and then up to 2400 K for a 20-min hold. The calculated releases of krypton and cesium are in reasonable agreement with the experimental data plotted in Fig. 3.19.

Experimental measurements of release rate coefficients of cesium from the HI and VI tests have been compared with CORSOR-M calculations by Osborne et al.[28,30] As shown in Fig. 3.20, CORSOR-M overpredicts the HI measurements in all but one case where oxidation of the UO_2 is thought to have enhanced the release. The overprediction ranges from a factor of 1.5 to 5 and tends to increase at higher temperatures. Figure 3.21 demonstrates that CORSOR-M overpredicts the VI release rate coefficients by factors ranging from 2 to 27. The overprediction tends to increase at higher temperatures and after long times at elevated temperature.

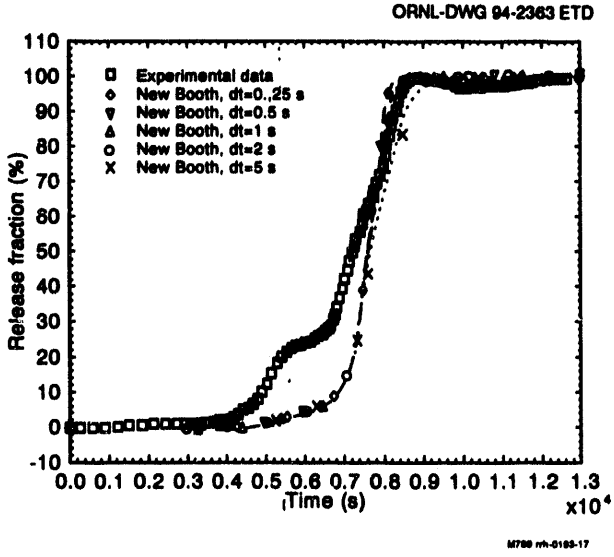

Figure 3.16 ORNL VI-3: noble gas fractional release measurements and VICTORIA calculations

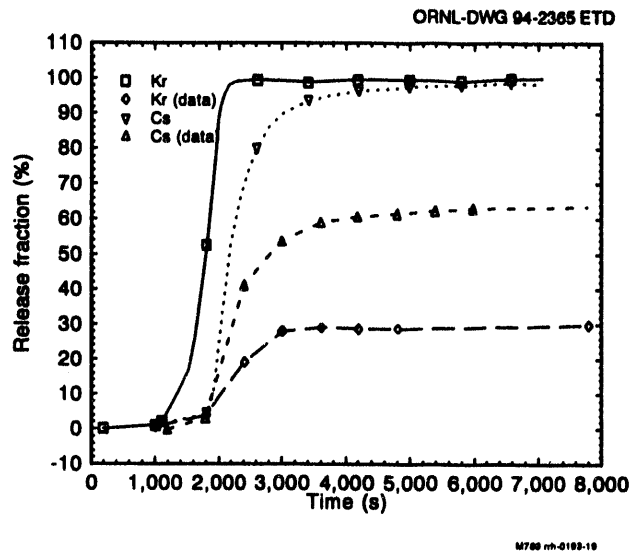

Figure 3.18 ORNL VI-2: fractional release measurements and VICTORIA calculations

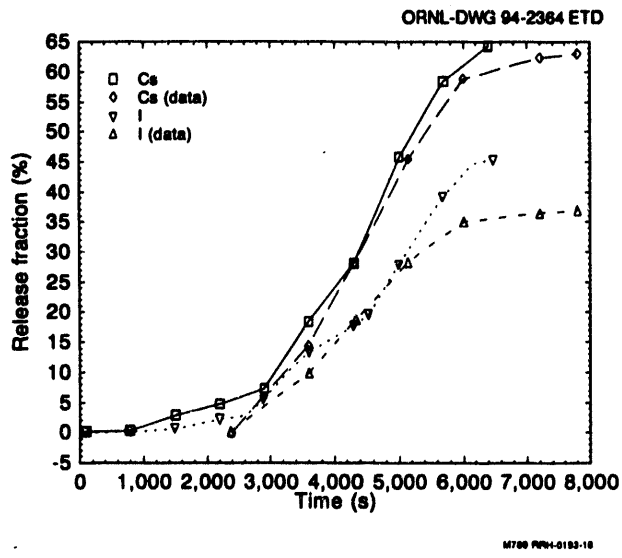

Figure 3.17 ORNL VI-1: fractional release measurements and VICTORIA calculations

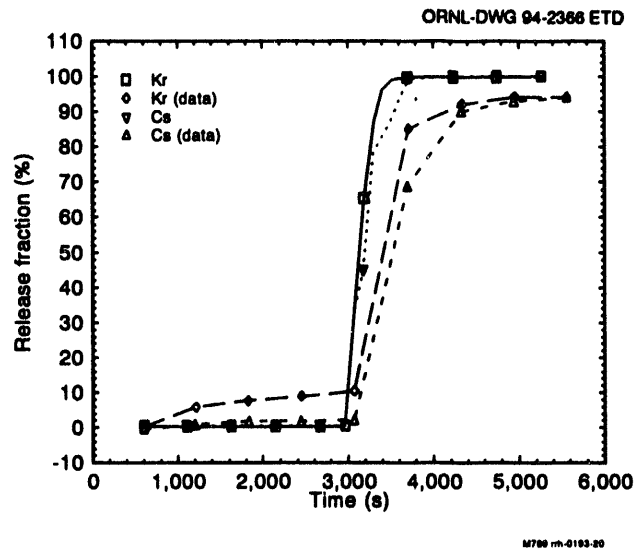

Figure 3.19 ORNL VI-4: fractional release measurements and VICTORIA calculations

ACRR ST-1 and ST-2. The ST-1 (Ref. 32) and ST-2 (Ref. 33) tests were conducted in-pile in the ACRR on four 15-cm-long fuel rod segments irradiated to 47 GWd/TU. The rods were heated in a mixture of flowing hydrogen and argon to ~2450 K and held at this temperature for 20 min. In ST-1 the system pressure was 0.16 MPa, and the linear gas velocity was about 98 cm/s; in ST-2 the system pressure was 1.9 MPa, and the linear velocity was about 7 cm/s. The hydrogen concentration in the mixture was reduced in ST-2 to maintain the same partial pressure of hydrogen in the two tests. In these tests the Zircaloy cladding melted, interacted with the fuel, and relocated to the bottom of the test bundle. The fuel-cladding interaction caused widespread liquefaction and foaming of the fuel.

Integral release measurements from these experiments are only available for cesium and europium, and in the case of

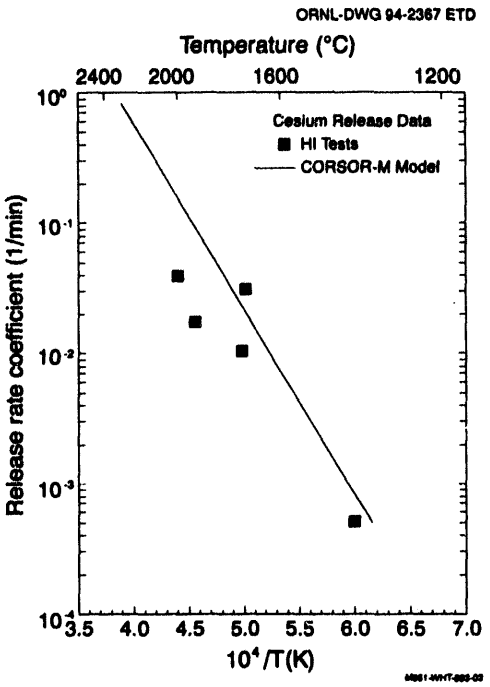

Figure 3.20 Comparison of release rate coefficients from all HI tests with CORSOR-M

ST-1, krypton. Experimental values for iodine, barium, strontium, and tellurium represent a lower bound because the measurements were made on filters downstream from the fuel, allowing deposition during transport to the filters. For example, the filters contained 56% and 30% of the cesium inventory in the ST-1 and ST-2 test, respectively; the cesium releases measured were 71% and 82%, respectively. Similarly, the europium measured at the filters was 5% and 2% of the inventory in the ST-1 and ST-2 tests, respectively, and the measured releases were 20% and 15%, respectively.

CORSOR, VICTORIA, AND MELCOR (CORSOR) have been used to calculate releases from the ST-1 and ST-2 tests.[32–34] Calculations with the MELCOR (CORSOR) code are compared with measurements in Table 3.40 for ST-1 and Table 3.41 for ST-2. Results for three different versions of CORSOR used within MELCOR are presented in these two tables under the headings CORSOR, CORSOR-M, and CORSOR-Booth. Results are also presented for a model with enhanced surface-to-volume ratio in Ref. 34 for CORSOR and CORSOR-M that tend to be a little greater than the results reported here, but do not lead to new insights. CORSOR and CORSOR-M calculate quite high releases of noble gases, iodine, and cesium, in good agreement with measurements (recall that the iodine measurement is a lower bound). The releases calculated by CORSOR-Booth for these same materials are significantly lower than the measured values. The release of tellurium is greatly overcalculated by CORSOR-M, overcalculated by CORSOR-Booth, and reasonably calculated by CORSOR. Tellurium was measured to be distributed evenly along the fuel after the tests, indicating holdup in the residual molten Zircaloy cladding. The barium and strontium releases are probably underpredicted in these tests under reducing conditions by all three versions of CORSOR, but especially CORSOR-M. If barium and strontium exhibited transport behavior similar to europium in these tests, the releases of these two materials are probably in the neighborhood of 30% in each test.

Two calculations for integral fission product releases were made with VICTORIA for each test. In one calculation, transport within open porosity in the fuel was treated in a manner suitable for intact rods, but with the cladding removed. In the second calculation, gas transport within the open porosity was enhanced by allowing greater interlinkage between intergranular pores to simulate the foamed condition of the fuel. The VICTORIA-calculated results and measurements are presented in Table 3.42. The releases calculated for noble gases, iodine, and cesium are in reasonable agreement with the measurements. The VICTORIA-calculated barium release of 25% for ST-1 is in the region expected for barium release, given the measurement downstream on the filter and the deposition during transport indicated by the measurements of europium. VICTORIA had predicted more than a tenfold decrease in barium release for the higher pressure ST-2 test relative to the ST-1 test, based on a model that calculates a suppression of gas-phase mass transport at higher pressure; however, the releases measured in the two tests differ by only a factor of 2. The calculated cesium release is in fairly good agreement with the measurements in the two tests. Clearly, there is a limit to analyzing fission product releases successfully from severely disrupted fuel with a code designed to model intact fuel. High-burnup fuel taken to high temperatures will release most of its inventory of highly volatile products even if the fuel remains intact. The VICTORIA code accounted for the effect of the reducing conditions in the ST-1 test on the chemical form of barium (more volatile Ba rather than less volatile BaO) to predict successfully a substantial release of this normally low-volatile material. However, the code grossly underpredicted the release of barium in the higher pressure ST-2 test.

Release rates were derived from time-resolved measurements of materials trapped in the filters downstream from the heated bundle. Release rates measured for cesium are in the vicinity of those calculated by CORSOR-M for both ST-1 and ST-2 as shown in Fig. 3.22, although they tend to decrease with time during the high-temperature hold at 2450 K as the inventory becomes depleted. As illustrated

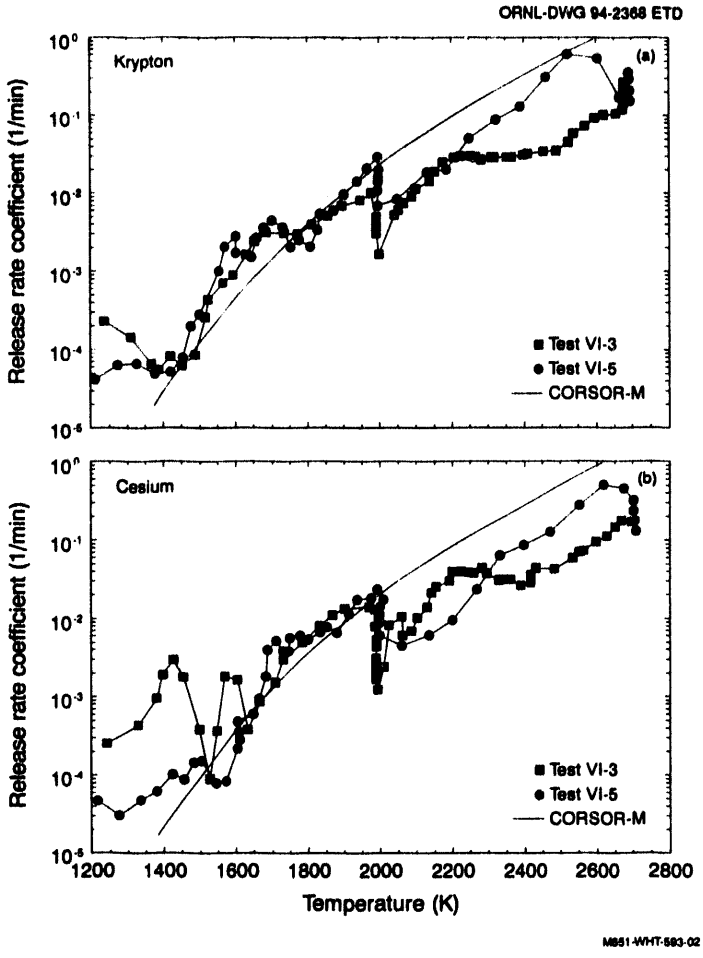

Figure 3.21 Comparison of release rate coefficients for krypton (*a*) and cesium (*b*) vs temperature in tests VI-3 (steam) and VI-5 (hydrogen) with CORSOR-M

Table 3.40 Measured release from ST-1 compared with MELCOR calculations using CORSOR, CORSOR-M, and CORSOR-Booth

Fission Product	Fraction released			
	CORSOR	CORSOR-M	CORSOR-Booth	Measured
Krypton	0.98	0.99	0.56	0.99
Iodine	0.98	0.99	0.56	0.38
Cesium	0.98	0.99	0.56	0.71
Tellurium	0.0031	0.15	0.022	0.002
Barium	0.11	0.0048	0.043	0.08
Stontium	0.041	0.0048	0.043	0.05
Europium	0.00014	0	0.084	0.20

Table 3.41 Measured releases from ST-2 compared with MELCOR calculations using CORSOR, CORSOR-M, and CORSOR-Booth

Fission Product	Fraction released			
	CORSOR	CORSOR-M	CORSOR-Booth	Measured
Krypton	0.98	0.99	0.56	
Iodine	0.98	0.98	0.56	0.23
Cesium	0.98	0.98	0.56	0.82
Tellurium	0.0033	0.16	0.022	0.005
Barium	0.11	0.0051	0.044	0.04
Stontium	0.042	0.0051	0.044	0.03
Europium	0.00015	0	0.086	0.15

Table 3.42 Measured releases from ST-1 and ST-2 compared with VICTORIA calculations

Fission product	Transport efficiency	Fraction released			
		ST-1		ST-2	
		Calculated	Measured	Calculated	Measured
Cesium	low	0.94	0.71	0.65	0.82
	high	0.94		0.74	
Iodine	low	0.81	0.38	0.74	0.23
	high	0.81		0.74	
Barium	low	0.27	0.08	0.014	0.04
	high	0.39		0.029	
Europium	low		0.20		0.15
	high				
Xenon	low	1.00		0.98	
	high	1.00		0.98	

in Fig. 3.23, the release rates for barium remain above those calculated with CORSOR-M at all temperatures and show relatively less drop at the high temperature hold, probably due to a smaller depletion of its inventory. CORSOR-M models the release of barium in the form of BaO (the form normally existing in the fuel and under accident conditions involving steam-hydrogen mixtures), so it underpredicts the rate of release of more volatile elemental barium. Release rate measurements for iodine in ST-1 plotted in Fig. 3.24 show similar behavior to that described for cesium. Release rate measurements for strontium in Fig. 3.25 and europium in Fig. 3.26 show similar behavior to that discussed for barium and for similar reasons.

HEVA Tests. In this test series, conducted in the HEVA loop at Grenoble by CEA, previously irradiated fuel rod segments (composed of three pellets) are re-irradiated and then heated in flowing gas to measure the fission product release and deposition. Test HEVA 06 was conducted by heating in a flowing steam/hydrogen mixture for 50 min at 1573 K to convert two-thirds of the cladding to ZrO_2, replacing the steam with helium, heating at 1.5 K/s to

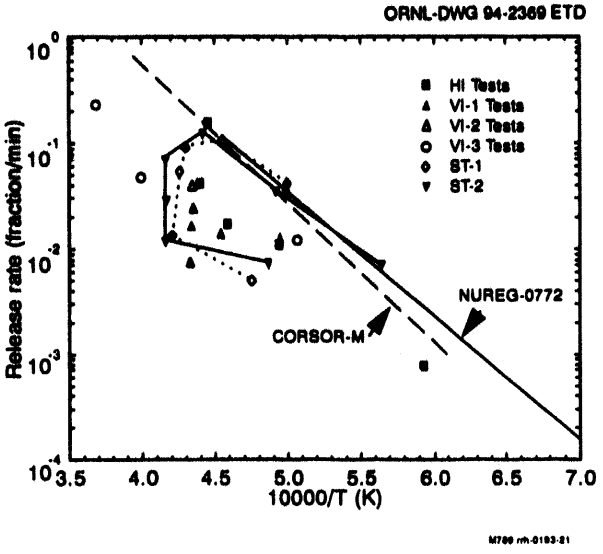

Figure 3.22 Comparison of fractional release rates for cesium measured in ST-1 and ST-2 with previously published data

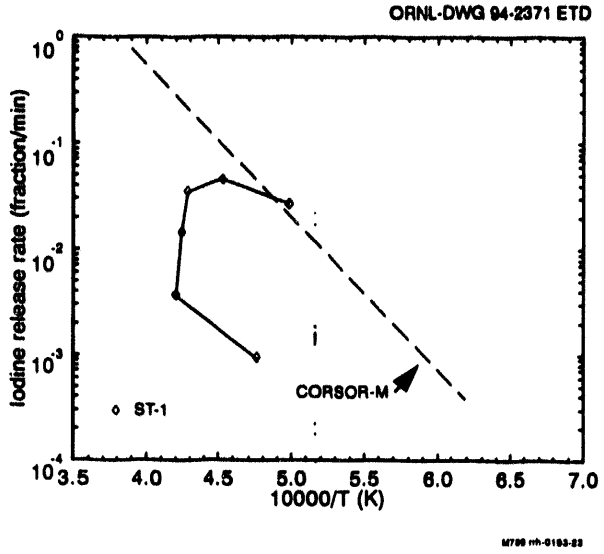

Figure 3.24 Comparison of fractional release rate of iodine measured in ST-1 with the CORSOR-M model

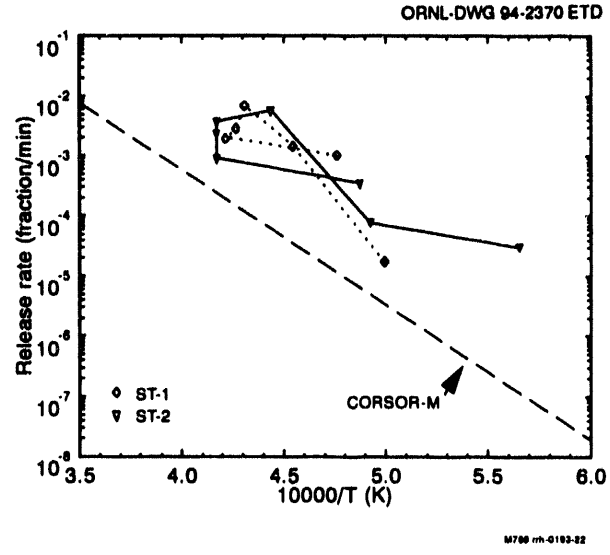

Figure 3.23 Comparison of fractional release rates for barium measured in ST-1 and ST-2 with the CORSOR-M model

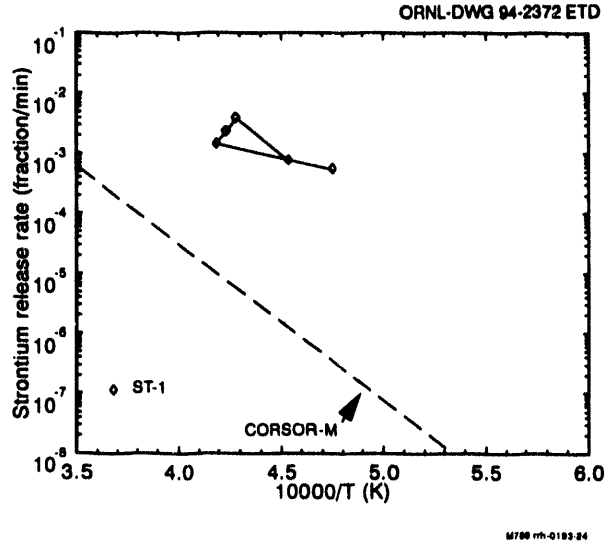

Figure 3.25 Comparison of fractional release rate of strontium measured in ST-1 with the CORSOR-M model

2373 K, and holding for 30 min at 2373 in a flowing helium/hydrogen mixture.[21] Postirradiation examination revealed molten metallic Zircaloy inside UO_2 cracks and outside the original cladding. Fuel swelling (average radial expansion) of 9.4% was measured. Fractional release rates of fission products during the HEVA tests are determined by measuring the depletion of various radioisotopes with a gamma spectrometer sighted on the lowest pellet in the three pellet stack. Release rates measured in HEVA 06 under reducing conditions are compared with results measured in HEVA 04 under oxidizing conditions and with calculations using the CORSOR and CORSOR-M models (these models do not distinguish between oxidizing and reducing conditions) in Table 3.43.

The results in Table 3.43 indicate that the CORSOR models overpredicted the measured release rates of cesium

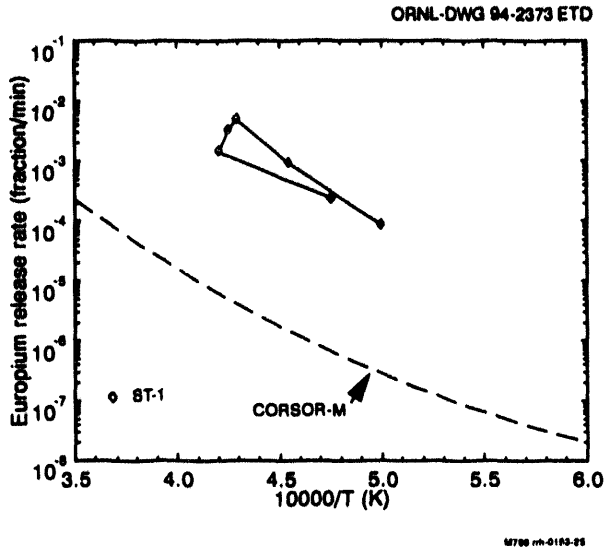

Figure 3.26 Comparison of fractional release of europium measured in ST-1 with the CORSOR-M model

and iodine by a factor of 6 under oxidizing conditions and a factor of 24 under reducing conditions. Dumas et al.[21] state that the release rates measured for iodine and cesium in HEVA 06 decreased with increasing inventory depletion. This observation is in agreement with results from the ST-1 and ST-2 tests in Figs. 3.22 and 3.24 and with observations from the VI tests.[26–30] This effect is not modeled in CORSOR or CORSOR-M.

The models underpredicted the release rate of tellurium by a factor of 10 under oxidizing conditions but were in good agreement with measurement under reducing conditions. These experimental results are in good agreement with previous observations that the release rate of tellurium is similar to those of cesium and iodine under highly oxidizing conditions, but is much reduced when metallic zirconium is available.[6,7] Release rates modeled as a function of temperature only (CORSOR and CORSOR-M) will miss this effect.

The CORSOR model was in good agreement with the measured release rate of barium under oxidizing conditions whereas the CORSOR-M model underpredicted this result by about a factor of 20. The HEVA 04 result seems high relative to integral release measurements from the PBF SFD tests and the TMI-2 accident.[20] Both models underpredicted the experimental result for barium release rate under reducing conditions by factors of 2 (CORSOR) and 50 (CORSOR-M). These results are in agreement with the results of the ST-1 and ST-2 tests and reflect the increased volatility of metallic barium under reducing conditions.

Discussion. Despite the large number of comparisons of code calculational results with experimental results listed in Table 3.26 and discussed in this section, it is difficult to assess the robustness of calculations of fission product release that have been reported because none of these calculations have been blind. A number of the codes have options such as grain growth, accelerated grain boundary sweeping, fuel liquefaction, and grain boundary liquefaction that, when employed under appropriate conditions, are able to match measured fission product releases fairly well. However, there are also instances in which calculations match experimental data that are likely to be in error, such as iodine release measurements that are significantly lower than cesium release measurements. Given severe accident scenarios in which high temperatures ($T > 2700$ K) are reached, large fractional releases of the noble gases and the volatile fission products occur from high-burnup fuels and are calculated by the codes. However, the calculated timing of the releases during heatup is more difficult to match with the experiment. In addition, calculations of the

Table 3.43 Measured release rates from HEVA 04 and HEVA 06 compared with CORSOR calculations

Fission product	Fractional release rate (L/min)			
	CORSOR model	CORSOR-M model	HEVA 04 results	HEVA 06 results
	(2373 K)	(2373 K)	(2273 K)	(2353 K)
Cesium	0.24	0.27	0.042	0.013
Iodine	0.24	0.27	0.037	0.012
Tellurium	0.0042	0.0042	0.037	0.0039
Barium	0.0047	0.00017	0.004	0.010

releases of the less volatile fission products such as barium and strontium are generally overpredicted.

The simplest models, such as CORSOR, CORSOR-M, and the Cubicciotti oxidation model, tend to overpredict fission product release data, especially for fresh fuel. More sophisticated codes such as FASTGRASS and VICTORIA incorporate physical and chemical phenomena that are capable of producing better agreement with experimental results, but these codes appear to require very careful application to achieve useful results. The state of cladding oxidation influences tellurium release. Relatively simple models taking this effect into account achieve reasonable results. Fuel liquefaction (bulk and grain boundary) affects fission product release in fresh and irradiated fuels calculated by the FASTGRASS codes in complex and subtle ways. Significant fission product release has been measured during cooldown, but this effect is not modeled in the codes. A hydrogen (reducing) environment affects the chemical speciation and, therefore, release of fission products such as barium, strontium, and europium. These chemical effects are modeled in codes such as FASTGRASS and VICTORIA. Clearly, the performance of blind calculations for future fission product release experiments, such as the Phebus-FP tests, would be most instructive.

Finally, the release of silver, indium, and cadmium control materials is significantly overpredicted by models that do not take into account the relocation of molten materials to cooler regions lower in the core.

3.4.1 References

1. A. D. Knipe, S. A. Ploger, and D. J. Osetek, "PBF Severe Fuel Damage Scoping Test—Test Results Report," USNRC Report NUREG/CR-4683, March 1986.*

2. J. Rest and S. A. Zawadzki, "FASTGRASS: A Mechanistic Model for the Prediction of Xe, I, Cs, Te, Ba, and Sr Release from Nuclear Fuel under Normal and Severe Accident Conditions," USNRC Report NUREG/CR-5840 (ANL-92/3), May 1992.*

3. U. S. Nuclear Regulatory Commission, "Technical Bases for Estimating Fission Product Behavior During LWR Accidents," USNRC Report NUREG-0772, June 1981.*

4. D. J. Osetek, J. K. Hartwell, and A. W. Cronenberg, "Fuel Morphology Effects on Fission Product Release," *Proceedings of the International Topical Meeting on Thermal Reactor Safety, San Diego, California, February 2–6, 1986*, Vol. 5, American Nuclear Society, 1986.

5. R. R. Hobbins, D. J. Osetek, and D. L. Hagrman, "In-Vessel Release of Radionuclides and Generation of Aerosols," *Proceedings of Symposium on Source Term Evaluation for Accident Conditions, Columbus, Ohio, September 28–November 1, 1985*, International Atomic Energy Agency, Vienna, Austria, 1986.

6. R. A. Lorenz, E. C. Beahm, and R. P. Wichner, "Review of Tellurium Release Rates from LWR Fuel Elements under Accident Conditions," p. 4.4-1 in *Proceedings of the International Meeting on Light Water Reactor Severe Accident Evaluation,"* Vol. 1, *Cambridge, Massachusetts, August 28–September 1, 1983*, American Nuclear Society, 1983.

7. J. L. Collins, M. F. Osborne, and R. A. Lorenz, "Fission Product Tellurium Release Behavior Under Severe Light Water Reactor Accident Conditions," *Nucl. Technol.* 77, 18 (1987).*

8. Z. R. Martinson, D. A. Petti, and B. A. Cook, "PBF Severe Fuel Damage Test 1-1 Test Results Report," USNRC Report NUREG/CR-4684 (EGG-2463), Vol. 1, October 1986.*

9. I. K. Madni, "MELCOR Simulation of the PBF Severe Fuel Damage Test 1-1," *Heat Transfer—Philadelphia, 1989, AIChE Symposium* Series No. 269, 85, 122–127 (1989).†

10. K. Y. Suh and R. J. Hammersley, "Modeling of Fission Product Release and Transport for Severe Fuel Damage Analyses," *Nucl. Sci. Eng.* 109, 26–38 (1991).

11. D. Cubicciotti, "A Model for Release of Fission Gases and Volatile Fission Products from Irradiated UO_2 in Steam Environment," *Nucl. Technol.* 53, 5 (1981).†

12. E. Schuster, W. Morell, and W. Kuhnlein, "Experiment Analysis Summary Report (EASR) of OECD LOFT LP-FP-1, Volume 4, Fission Product Behavior," Organization for Economic Cooperation and Development LOFT-LP-FP-1, Paris, France (April 1989).

13. M. L. Carboneau, V. T. Berta, and M. S. Modro, "Experiment Analysis and Summary Report for OECD LOFT Project Fission Product Experiment LP-FP-2,"

Organization for Economic Cooperation and Development LOFT-T-3806, Paris, France (June 1989).

14. S. M. Jensen, D. W. Akers, and B. A. Pregger, "Postirradiation Examination Data and Analysis for OECD LOFT Fission Product Experiment LP-FP-2 Volume 1," Organization for Economic Cooperation and Development LOFT-T-3810, Vol. 1, Paris, France (December 1989).

15. L. N. Kmetyk, Sandia National Laboratories, "MELCOR 1.8.1 Assessment: LOFT Integral Experiment LP-FP-2," SAND92-1373, December 1992.*

16. Z. R. Martinson et al., "PBF Severe Fuel Damage Test 1-3 Test Results Report," USNRC Report NUREG/CR-5354 (EGG-2565), October 1989.*

17. D. A. Petti et al., "Power Burst Facility (PBF) Severe Fuel Damage Test 1-4 Test Results Report," USNRC Report NUREG/CR-5163 (EGG-2542), April 1989.*

18. D. A. Petti et al., "Results from the Power Burst Facility Severe Fuel Damage Test 1-4: A Simulated Fuel Damage Accident with Irradiated Fuel Rods and Control Rods," *Nucl. Technol.* 94, 313 (1991).†

19. M. Mezza, P. Chatelard, and R. Gonzalez, "Validation Results of ICARE2 Code on the PBF SFD 1-4 Experiment," Proceedings of *IAEA Technical Committee Meeting on Behavior of Core Materials and Fission Product Release in Accident Conditions in Light Water Reactors, Aix en Provence, France, March 1992*, International Atomic Energy Agency, IAEA-TECDOC-706 (June 1993).

20. R. R. Hobbins, D. A. Petti, and D. L. Hagrman, "Fission Product Release from Fuel under Severe Accident Conditions," *Nucl. Technol.* 101, 270 (1993).†

21. J. M. Dumas, G. Lhiaubet, G. Lemarois, and G. Ducros, "Fuel Behavior and Fission Product Release under Realistic Hydrogen Conditions with Comparisons between HEVA 06 Test Results and Vulcain Computations," p. 153 in *Proceedings of the ICHMT Seminar on Fission Product Transport Processes in Reactor Accidents, Dubrovnik, May 22–25, 1989*, J. T. Rogers, Ed. (Hemisphere, 1990).

22. K. D. Hocke, "Model for the Analysis of FP Release in LWR Severe Fuel Damage Conditions," *Proceedings of IAEA Technical Committee Meeting on Behavior of Core Materials and Fission Product Release in Accident Conditions in Light Water Reactors, Aix-en-Provence, France, March 1992*, International Atomic Energy Agency, IAEA-TECDOC-706 (June 1993).

23. D. A. Petti, "Silver-Indium-Cadmium Control Rod Behavior in Severe Reactor Accidents," *Nucl. Technol.* 84, 128 (1989).†

24. M. F. Osborne, J. L. Collins, and R. A. Lorenz, "Experimental Studies of Fission Product Release from Commercial Light Water Reactor Fuel Under Accident Conditions," *Nucl. Technol.* 78, 157 (1987).†

25. P. E. Domagala, J. Rest, and S. A. Zawadzki, "Assessment of Improved Fission Product Transport Models in VICTORIA Against ORNL HI and VI Tests," *Heat Transfer—Minneapolis 1991, AIChE Symposium Series*, No. 283, 87, 182–189 (1991).†

26. M. F. Osborne et al., Martin Marietta Energy Systems, Inc., Oak Ridge National Laboratory, "Data Summary Report for Fission Product Release Test VI-1," USNRC Report NUREG/CR-5339 (ORNL/TM-11104), June 1989.*

27. M. F. Osborne et al., Martin Marietta Energy Systems, Inc., Oak Ridge National Laboratory, "Data Summary Report for Fission Product Release Test VI-2," USNRC Report NUREG/CR-5340 (ORNL/TM-11105), September 1989.*

28. M. F. Osborne et al., Martin Marietta Energy Systems, Inc., "Oak Ridge National Laboratory, "Data Summary Report for Fission Product Release Test VI-3," USNRC Report NUREG/CR-5480 (ORNL/TM-11399), June 1990.*

29. M. F. Osborne et al., Martin Marietta Energy Systems, Inc., Oak Ridge National Laboratory, "Data Summary Report for Fission Product Release Test VI-4," USNRC Report NUREG/CR-5481 (ORNL/TM-11400), January 1991.*

30. M. F. Osborne et al., Martin Marietta Energy Systems, Inc., Oak Ridge National Laboratory, "Data Summary Report for Fission Product Release Test VI-5,"

USNRC Report NUREG/CR-5668 (ORNL/TM-11743), October 1991.*

31. D. A. Williams and H. S. Bond, "Analysis of the ORNL VI Experiments Using VICTORIA," Atomic Energy Authority—Winfrith, AEA-RS- 5139, United Kingdom (June 1991).

32. M. D. Allen, H. W. Stockman, K. O. Reil, and J. W. Fisk, Sandia National Laboratories, "Fission Product Release and Fuel Behavior of Irradiated Light Water Reactor Fuel Under Severe Accident Conditions, The ACRR ST-1 Experiment," USNRC Report NUREG/CR-5345 (SAND89-0308), November 1991.*

33. M. D. Allen et al., "ACRR Fission Product Release Tests ST-1 and ST-2," *Proceedings of the International ENS/ANS Conference on Thermal Reactor Safety, Avignon, France, October 2–7, 1988*, Societé d' Energie Nucleaire, Paris, France (1988).

34. L. N. Kmetyk, Sandia National Laboratories, "MELCOR 1.8.1 Assessment: ACRR Source Term Experiments ST-1/ST-2," SAND91-2833, April 1992.*

*Available for purchase from the National Technical Information Service, Springfield, VA 22161.
†Available in public technical libraries.

3.5 Conclusions and Recommendations

The current state-of-the-art understanding of in-vessel fission product/core material release is well developed for most aspects of release behavior, particularly for the noble gases and volatile fission products (I and Cs). The dominant phenomena have been recognized and are understood to the level that has permitted development of both empirical and some fundamental/mechanistic models for predicting the rates of fission product release. The existing experimental data are mostly adequate for continued development and improvement of the empirical models. On the other hand, continued development and validation of the mechanistic models require data from further well-characterized, separate-effect and integral experiments.

Several weaknesses have been identified in the current understanding of fission product release. These weaknesses have variable impact on fission product releases from the fuel. The two most important weaknesses identified with respect to potential source terms were (1) long-term releases of less volatile fission products from molten fuel and (2) releases at high temperature in air/high oxygen potential conditions (i.e., postvessel failure scenario). Other potentially important weaknesses include the effects of quenching/reflood, releases from debris beds, and the effects of UO_2 liquefaction.

A general overview is given below, based on the subsections of Chap. 3. Specific weaknesses in the current state of the art are identified, and recommendations are provided for future undertakings.

3.5.1 In-Vessel Release Phenomena

A physically based description of fission product release behavior requires a knowledge of the concentration, chemical form, spatial distribution, and mobility of fission products within the fuel. A detailed model of the fuel morphology and its evolution is also required.

The concentration of fission products in the fuel is considered to be well established. Concentrations can be calculated to the required level of accuracy using time-dependent irradiation data in a nuclear production/capture/decay code.

The chemical form of fission products can be predicted as a function of burnup, temperature, and oxygen potential, based on thermodynamic data, although uncertainties exist for some of the data. The chemical form is important for the determination of volatility and hence release rates for some fission products (e.g., Mo, Cs), which can form a variety of different compounds in the fuel. Also, once released from the fuel, the chemical form of the gaseous species will determine its subsequent transport and deposition. The spatial distribution of fission products within the fuel (i.e., intragranular bubbles, grain boundaries, gap, etc.) has also been studied, but limited quantitative data have been produced (except for gap inventories) because of the difficulty in performing such measurements.

The individual processes that contribute to fission product release from the UO_2 matrix have been identified. The main processes include atomic diffusion, intragranular bubble migration, grain-boundary sweeping, intergranular bubble coalescence, microcracking, liquefaction, and matrix volatilization. Physically based descriptions have been developed for all of these processes; however, there is still considerable uncertainty regarding the dominant processes controlling release behavior during the various stages of transient heating and core damage progression.

Fission product transport in the fuel-rod gap is also understood qualitatively, and models exist for describing behavior of defected fuel in intact geometries.

The individual phenomena controlling the release rates of most nonfission product materials are generally well understood. Ag-In-Cd control rod material releases depend on the timing of the failure of the stainless steel cladding, which varies between high- and low-pressure accident scenarios. Releases of tin from Zircaloy are known to be influenced by cladding oxidation that raises the tin activity, leading to a higher vapor pressure and more rapid releases. Boric acid aerosols can be formed by flashing of borated reactor coolant. Uranium-bearing aerosols may be produced by volatilization of exposed UO_2 at high oxygen potentials via formation of gaseous UO_3 or other volatile uranium species.

3.5.2 Experimental Programs on In-Vessel Release Phenomena

An extensive experimental data base of integral and kinetic release measurements is available to support both phenomenological understanding and the development of models or codes for describing release behavior. The data base includes information derived from small-scale, single-effect, out-of-reactor tests; large-scale, multiple-effect, in-reactor tests; and the TMI-2 accident. Experiments have been conducted under a variety of conditions representative of conditions expected to arise in reactor accidents. The data base, however, is not sufficiently complete that it can be used to formulate empirical release correlations that could be used confidently for the range of accidents of interest. Furthermore, the data base is mostly focused on cesium. More scattered data are available for noble gases or iodine. Release data are scarce for tellurium and the lower volatility radionuclides.

In general, the experimental data base indicates that cesium, iodine, and the noble gases show the highest release rates for most conditions and that the rates are similar for these species. Oxidizing conditions can produce significant releases of ruthenium and molybdenum. Reducing conditions cause increased europium and barium releases. Tellurium and antimony releases are shown to increase when the cladding is oxidized.

Some weaknesses have been identified in the existing experimental data base. The release rates from molten fuel, particularly for the less-volatile fission products, are not available. Only limited release data are currently available for postvessel failure conditions involving air/oxygen-rich conditions at high temperatures. The fission product source term from the fuel/debris under these conditions would be significantly different from steam/H_2 mixtures because of the high oxygen potential and increased volatility of many fission products, actinides, and other core materials. Data on releases from debris beds are lacking, and the effect on releases of UO_2 dissolution by Zircaloy have not been quantified. Irradiated fuel behavior in hydrogen-rich conditions at high temperatures is not well understood with respect to UO_2 "foaming" and its potential effect on fission product release. Data on fission product release under quenching/reflood conditions is inadequate for model development. Finally, the existing data base is not adequate for the wide range of burnup, including both low- and high-burnup fuels. By addressing these weaknesses, a more complete basis for quantifying releases from intact or degraded geometries would be available.

The data base for nonfission product material releases has some uncertainties but is generally adequate.

3.5.3 Release Modeling and Codes

Two types of models have been developed for calculating the release rates of fission products or core materials during severe accident conditions: empirical models and mechanistic models. The empirical models are based on correlations between experimental conditions and release rates and have achieved widespread use because of their simplicity and functional reliability. This simplicity, however, tends to produce inaccurate results for calculations done under boundary conditions that differ from those on which the correlations are based.

Mechanistic models, on the other hand, are based on fundamental principles and, in most cases, include microstructural information in the calculations. These models embody the understanding of individual release phenomena and, when implemented correctly, are regarded as powerful tools with general applicability. For certain cases, it can be shown that the mechanistic calculations give better agreement with data than do empirical calculations. However, the mechanistic models require a significant computational effort and demand boundary conditions and constitutive laws to be defined at a microstructural level. The mechanistic models must be linked to system codes to have adequately defined fuel morphology and cladding conditions, without which the user is faced with complex input requirements.

Many of the mechanistic codes are still under development. In some cases, the existing mechanistic models appear to be leading the experimental data base. The most obvious area in which the mechanistic codes require data is in the

spatial distribution of fission products within the fuel (e.g., the grain boundary inventory of fission products, which is calculated by all of the mechanistic codes). Other needs include data for the development of mechanistic fission product release models under quenching/reflood conditions. On the other hand, empirical models seem to be lagging the experimental data base. They should be extended to include data on the effect of burnup, fuel oxidation, and perhaps other phenomena such as liquefaction, quenching/reflood, and fuel morphology considerations.

Code validation is currently an area requiring some attention. This applies primarily to both verification of model implementations within codes and validation by comparison to experimental data. Clearly identified versions of mechanistic codes with documented validation are lacking.

3.5.4 Comparisons between Experimental Results and Code Calculations

Measured data from both in-reactor and out-of-reactor fission product release experiments have been compared with computer code calculations using both mechanistic and empirical models. The number of documented comparisons is considerable, but none of the calculations have been blind; thus, no conclusions can be drawn about the validity or robustness of the various models over a wide range of conditions. Very few comparisons are available for fission products other than the noble gases or iodine and cesium.

In general, the simple empirical models tended to overpredict the measured volatile fission product release data; however, this is not surprising given that the majority of comparisons were based on experiments with trace-irradiated or low-burnup fuel. The releases of barium and strontium tended to be overpredicted. The releases of control rod materials were overpredicted by models that did not take into account relocation of melts to cooler regions lower in the core.

The mechanistic models were able to match some measured integral release data fairly well for open calculations that permitted tuning of model parameters. Release rates were more difficult to reproduce. It should be noted, however, that the mechanistic codes require detailed fuel conditions to achieve useful results.

3.5.5 Recommendations

The existing experimental data, combined with planned experiments in the near future, generally appear to be adequate for the needs of understanding most aspects of release phenomena and model development. However, specific studies involving a mixture of single-effect and integral experiments should be conducted to address the need for data in the following areas: high-temperature releases of low-volatile fission products from molten fuel, high-temperature air/high oxygen potential conditions, quenching/reflood, release from debris beds, and release during liquefaction of UO_2. The mechanistic models should also be further developed to include more fundamental descriptions of these processes.

Model development and validation efforts should be continued for both empirical and mechanistic codes. The empirical models should be updated to include recent data and extended to include some simple additional features such as burnup, fuel oxidation and perhaps other phenomena such as liquefaction, quenching/reflood, and fuel morphology considerations.

International Standard Problems (ISPs), preferably blind or semiblind single-effect and integral tests, should be encouraged as a forum for code validation. However, well-defined thermal-hydraulic boundary conditions are necessary in the experiments to enable blind predictions to be judged and interpreted. As such, these exercises would be valuable for assessing the true capabilities of existing codes and to highlight areas for improvement. In addition, ISPs encourage a wider exchange between modelers and experimentalists; this in turn should promote a more objective assessment of analytical tools and improve the validation efforts.

4 Primary System Fission Product Transport

4.1 Introduction

Following release from the fuel, fission products would be transported through some portion of the reactor coolant system (RCS) before being emitted to the containment (or environment in the event of containment failure or an accident sequence that bypasses the containment building). Processes within the RCS will determine the magnitude, nature, and timing of this radioactive emission.

The RCS can attenuate the extent of the release by removing a significant fraction of fission products through a variety of aerosol and vapor removal mechanisms. Extensive experimental and code development studies undertaken over the last 10 years have demonstrated that significant attenuation can occur within the primary system and that analyses conducted prior to this time (which consciously assumed no retention) were oversimplified.

More recently there has been a growing appreciation of the role that the primary circuit can play as a reaction chamber in defining the timing and physical and chemical forms of the radioactive emission. Parametric code studies conducted by Longworth et al. concluded that "the major uncertainty in quantifying the behavior of the source term in the containment was identified with chemistry aspects of the initial source to the containment."* The role of the primary circuit as a reaction chamber has also been emphasized by recent plant analyses[1] that indicate the potential importance of revaporization (whereby fission products that have been initially deposited in the circuit are released because of decay heating of the surfaces when the containment may no longer be intact).

The discussion that follows in this chapter considers the main physical and chemical phenomena that occur within the primary circuit during a severe accident. These phenomena are summarized as follows in an approximately chronological order (i.e., from release from fuel to transport to the containment):

1. Vapor-phase phenomena
   - Thermodynamics and speciation
   - Vapor condensation
   - Vapor/surface and vapor/aerosol reactions
2. Aerosol Nucleation and Characterization
   - Nucleation
   - Growth (final particle size distribution)
3. Aerosol Transport and Relocation
   - Transport and Deposition
   - Resuspension
   - Revaporization

Section 4.2 provides a detailed analysis of these phenomena. Initially, the basic principles of each topic are reviewed, followed by a detailed description of the status of experimental and modeling work in the area. Each subsection concludes with a discussion of the main uncertainties associated with the individual phenomenon. All the major experimental programs examining these phenomena are considered in Sect. 4.3, both in terms of basic input to models (small-scale, separate-effects studies) and examination of the coupling between models and the validity of the source term codes (large-scale, integral studies). Emphasis is placed on those experiments that have been compared with code predictions.

Substantial efforts have been made to model the transport phenomena based on either application of empirical models or a more mechanistic approach. Modeling within both system codes and codes dedicated to fission product transport issues is reviewed in Sect. 4.4. Despite extensive experimental and code development programs, there have been relatively few comparisons of experimental data against code predictions. Such comparisons, building on the results from earlier subsections within the chapter, are discussed in Sect. 4.5. The main conclusions from the entire chapter are summarized in Sect. 4.6.

4.1.1 Reference

1. L. M. C. Dutton, "Fission Product Behavior and Consequence Analysis Following Severe Accidents at PWRs," NNC, Commission of European Communities Report ETNU-0001/UK, United Kingdom, 1991.

4.2 Physical and Chemical Phenomena

Predictions of the transport and deposition of radionuclides in the RCS are essential elements of severe reactor accident analyses. The physical and chemical phenomena that affect transport of radionuclides during reactor accidents take place in environments that are well outside conventional experience. Temperatures of surfaces in the RCS can range

*J. P. Longworth et al., The Sensitivity of PWR Severe Accident Source Terms to Uncertainties in the Mass, Size Distribution and Chemistry of Aerosols Produced from a Degrading Core, CEGB, NNC, and UKAEA, UK, to be published by Nuclear Electric, 1993.

from the reactor operating temperature (~600 K) to the melting point of steel (~1800 K). Even higher temperatures can occur in the gas phase. Pressures of steam and hydrogen can exceed 100 bars. An intense radiation field will exist producing dose rates of about 10^5 Gy/h.

The combination of extreme conditions expected to be present in the RCS under accident conditions is quite difficult to reproduce in the laboratory. Completely prototypic data concerning the behavior of radionuclides are scarce. Predictions of the transport and deposition of radionuclides must be made by extrapolating what data are available to the harsh environments hypothesized to develop in the RCS. There must be, then, an adequate understanding of the physical and chemical processes and phenomena that will affect radionuclide transport and deposition.

In this section, the basic principles of the physical and chemical phenomena affecting radionuclide transport and deposition in the RCS are described briefly. The status of experimental and theoretical understanding of these phenomena is assessed. The major areas of remaining uncertainty are discussed. The presentation of the material follows the outline given in Sect. 4.1. The discussions begin with the behavior of condensible vapors. The formation and growth of aerosols are presented next. Finally, aerosol deposition and resuspension phenomena are described.

4.2.1 Vapor-Phase Phenomena

Nearly all of the radioactive and nonradioactive materials escaping the reactor core during a severe accident are released by vaporization rather than by mechanical processes. Some condensation of vapors may begin within the core region. In fact, condensation within the thermal boundary layers around degrading core materials may enhance the vaporization process.[1] Nevertheless, substantial amounts of condensible vapor are expected to emerge from the core region into the balance of the RCS. In particular, the radiologically important elements cesium and iodine are expected to be in vapor form when they emerge from the core region. Were these vapors to remain gaseous and neither react nor condense on surfaces, they, like the noble gases (xenon and krypton), would pass through the RCS. Once they escaped the RCS they could become a part of the source term of radioactive material released from a nuclear power plant during an accident. However, chemical conditions in the balance of the RCS are expected to be quite different than in the core. Temperatures are expected to be lower, and oxygen potentials may be higher. Because of these changes in chemical conditions, it is possible for vapors to deposit on surfaces in the RCS. Deposition may be by simple condensation, or it may be by chemical reaction. Surfaces available for deposition may be structural surfaces or the surfaces of aerosol particles. Deposition on structural surfaces removes material that could have contributed to the severe accident source term. This, however, may be only a temporary removal. Continued heating of the surface by convection or by decay heat generated within the surface deposits may cause volatile species to revaporize later in the course of an accident and again become a part of the source term. Vapor deposition on aerosol surfaces by condensation or chemical reaction does not necessarily remove material from the potential source term. The deposition of vapors on aerosols does affect the properties of the aerosols and their ability to negotiate passage through the RCS.

Analyses of vapor behavior in the RCS usually begin with a definition of the thermodynamic driving forces for condensation or chemical reaction of the vapors. Then, the kinetic barriers that retard the approach to chemical equilibrium within the RCS are evaluated to determine the extent of vapor condensation and reaction. This approach has been selected in preference to an empirical determination of vapor deposition. Prototypic conditions for vapor deposition are too difficult to reproduce in laboratory settings to provide a useful empirical data base, and conditions expected to arise in the RCS vary too much to explore adequately by empirical methods.

This modern approach to the prediction of vapor behavior in the RCS under accident conditions is described further in the following subsections. The discussions begins with the thermodynamic driving forces for vapor deposition. Then, the rates of vapor deposition on structural surface and aerosol surfaces are described.

4.2.1.1 Thermodynamics and Speciation

4.2.1.1.1 Basic Principles

The thermodynamic driving force for vapor deposition in the RCS is the difference between prevailing conditions and the conditions of chemical equilibrium between the gas phase and the condensed phase. Quantitative definition of the equilibrium state is obtained by determining the equilibrium partial pressures of the various vapor species in the gas phase. This determination requires knowing what vapor species can form and what condensed phases will exist.

Early attempts to predict vapor pressures in the RCS considered only very few vapor species such as CsOH(g), CsI(g), and Te(g).[2] Condensed phases considered were simply CsOH(s,l), CsI(s,l), Te(s), and a nonvolatile product of the tellurium vapor reaction with structural surfaces. The environment of the RCS during a severe accident is more chemically complex than this simple prescription suggests.

Because of the chemical reactivity of this environment, many diverse condensed and vapor phase species can form. The vaporization of barium oxide provides an example (see Fig. 4.1). The parent species BaO(s) can undergo unary vaporization to BaO(g). In steam, especially the high-pressure steam expected to exist in the RCS, BaO(s) can also vaporize as $Ba(OH)_2(g)$. With increasing partial pressures of hydrogen, other vapor species such as BaOH(g), $Ba_2O(g)$, Ba(g), $Ba_2(g)$, and BaH(g) can form. The presence of other condensible vapors can lead to vaporization of barium. Formation of $BaMoO_4(g)$ shown in Fig. 4.1, is an example of such vapor speciation. The apparent vapor pressure of barium in the RCS is the sum of the partial pressures of the various molecular barium species weighted by the number of barium atoms in each species. Clearly, as the number of vapor species considered increases, the predicted volatility of barium increases; this is also true for other radionuclides. The apparent volatility increases with gas phase speciation. Cesium hydroxide transports farther along thermal gradient tubes in the presence of tellurium or cesium iodide vapors than when it is the only vapor present.[3,4] Speciation in the gas phase has been invoked to explain these observations and the effects of steam partial pressure on the transport of indium from control rod alloys.[5]

On the other hand, condensed barium oxide can react with other surface materials to form more stable, less volatile condensed phases such as $BaFe_2O_4(s)$, $BaB_2O_4(l)$, or BaTe(s). Neglect of these condensed phase species would lead to overly large predictions of the apparent volatility of barium in the RCS. Furthermore, condensed phase barium species can form solid or liquid solutions with other condensed phase species, which reduces the chemical activity of the barium species. The volatility of barium is then reduced. Reactions that transform radionuclides from the volatile forms evolved out of the core significantly affect the magnitude of release from the RCS.

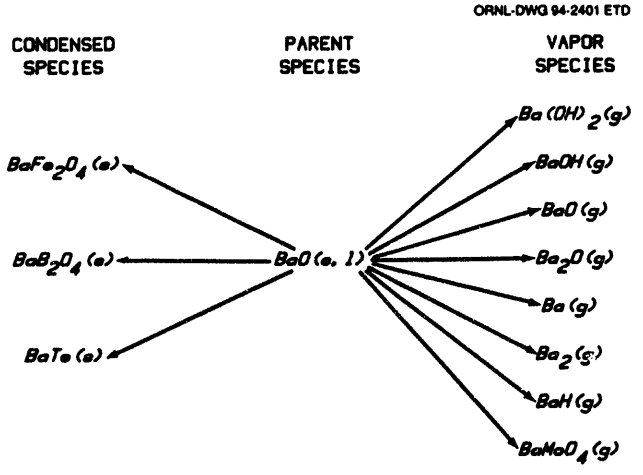

Figure 4.1 Schematic representation of barium speciation

The availability of substantial quantities of nonradioactive species in the RCS provides opportunities for chemical transformations of radionuclides. The nonradioactive materials expected to be abundant in the RCS include tin from the zircaloy cladding on fuel, cadmium and indium from control rods, uranium oxide, and vapors generated when structural steel in the core region is heated. Boric acid is present in the coolant of pressurized-water reactors at concentrations of 800 to 3000 ppm. Residues of boric oxide will be left on surfaces throughout the RCS when coolant has been boiled away at the start of an accident. Boric acid will vaporize from water in the lower plenum of the reactor vessel throughout the core degradation process.[6] As a result, there will be hundreds of moles of boric acid and boric oxide on surfaces and in the vapor available to react with radioactive and nonradioactive vapors. Reactions with CsOH and CsI to form cesium borates that have low vapor pressures are examples of the effects boric acid might have on severe reactor accident source terms.

Analysis of vapor deposition, then, begins with the solution of a thermodynamic problem involving the gas phase and the condensed phase. The equilibrium vapor pressures are compared with the prevailing vapor pressures to determine the driving force for deposition. The prevailing vapor pressures in the gas phase are also found by assuming that the gas phase is chemically equilibrated. Several kinetic analyses of gas phase reactions have shown that the assumption of chemical equilibrium is adequate for most purposes of reactor accident analyses.[7,8]

Techniques for solving the chemical equilibrium problems are relatively well established. Typically, optimization methods[9] or equilibrium constant methods[10] are employed. To carry out the solutions, it is necessary to know what species are present in both the gas phase and the condensed phase. Then, thermodynamic data for these species are needed. As more nonradioactive species that have evolved from the core are included, the thermodynamic data bases needed for the analyses have become enormous. For instance, the VICTORIA[11] model of transport in the RCS considers over 280 chemical species involving 26 elements.

Consideration of greater diversity in speciation has changed views on the predominant radionuclide vapors in the RCS. Certainly, tellurium has been found to be so reactive that neither Te(g) nor $Te_2(g)$ is expected to be a major gas phase species. Instead, tellurium may be present as SnTe(g), $Ag_2Te(g)$, or as metal tellurates or tellurites.

Similarly, cesium hydroxide can readily react in the gas phase to form substantially less volatile species such as $CsBO_2$, Cs_2MoO_4, Cs_2MnO_4, Cs_2ZrO_3, and various cesium uranates. Chemical kinetic studies done in chemically simple systems that did not allow for reactions of these types may have yielded results of generic interest but that are not directly applicable to the analyses of vapor behavior in the RCS. Computer codes that consider only chemically simple systems cannot accurately predict radionuclide behavior in the RCS.

4.2.1.1.2 Status

A substantial data base exists of thermodynamic properties for species pertinent to the analysis of vapor behavior in the RCS. Most of this data base has been generated for purposes other than the analysis of reactor accidents. Much of the data was generated as part of research on rocket propulsion,[12] and there is a continuing generation of pertinent data. Within the reactor safety community, mass spectrometry,[13,14] matrix isolation infrared spectroscopy,[14] and even classic transpiration techniques[15,16] are being used to identify and characterize important vapor and condensed phase species. Auger spectroscopy and electron spectroscopy for chemical analysis are being used to identify condensed phase species. Differential scanning calorimetry, drop calorimetry and thermogravimetric analyses are being used to characterize thermodynamic properties of condensed species.[17]

Because of the diverse sources of thermodynamic data, there are potential problems of thermodynamic consistency in the data bases. Efforts are under way to compile a consistent thermodynamic data base for use in reactor accident analysis.[18–20]

4.2.1.1.3 Remaining Areas of Uncertainty

The principal uncertainty regarding the thermodynamics of vapor species is completeness. Experimental studies of vapors have not ventured extensively into regimes where there are simultaneously high temperatures and high partial pressures of steam and hydrogen. High concentrations of steam may stabilize vapor phase hydroxides and hydrates that have been undetectable at the lower steam concentrations in experimental studies to date.[21] Similarly, high partial pressures of hydrogen may create important hydrides not included in available data bases.

Much of the speciation data available to the reactor safety community has come from the study of chemically simple systems. The data base on vapor species involving two or more elements [such as $BaMoO_4$(g), cited previously] is not well developed.

The vapor phase in the RCS will be exposed to an intense radiation field that will produce high concentrations of gas phase ions. Models of vapor behavior in the RCS have generally ignored ion formation. Yet, there is evidence that at high steam concentrations vapor phase ions may be stabilized as hydrates such as $Cs^+ \cdot (H_2O)_n$ (n = 1 to 6) or $I^- \cdot (H_2O)_n$ (n = 1 to 4) (Refs. 22–24). Some analyses also suggest that these ions may affect aerosol behavior as well as vapor behavior in the RCS.[25]

Errors that can arise because dominant vapor species are neglected in analyses can be profound. Consequently, experts on high-temperature chemistry have recommended including estimated properties of hypothesized species in the analyses of vapor behavior.[26]

Condensed phases have received less attention than have vapor phase species. There has, of course, been some characterization of the duplex oxide film that will form on stainless steel surfaces within the RCS (see, for example, Ref. 27 and 28). Interactions of selected vapor species with these surfaces have been studied as are discussed subsequently. Interactions of nonradioactive species with these surfaces have not been characterized extensively. A notable issue for pressurized water reactors especially is the interaction of boric acid or boric oxide with the oxides on stainless steel as well as with radionuclides.[28,29]

An essential problem with developing further understanding of condensed phase species seems to be diversity. Without guidance from experimental studies using prototypic combinations of materials, there are too many possible combinations of condensed phases to address tractably. The forthcoming Phebus-FP tests (see Sect. 4.3) may yield results that will guide the refinement of the thermodynamic data base.

Thermodynamic data now available for both condensed phase and vapor phase species are known only to a finite accuracy. For instance, the thermodynamic properties of the important vapor species $Ba(OH)_2$ (g) are uncertain by ±9000 cal/mole.[30] This means the vapor pressure of $Ba(OH)_2$ at 1500 K is uncertain by a factor of about 20. Similar and even larger uncertainties exist in thermodynamic data for most of the chemical species considered in the analyses of radionuclide behavior in the RCS. Resources necessary to reduce uncertainties in the thermodynamic data base would be used most efficiently if prototypic data indicated what species were indeed most important for accident analyses.

4.2.1.2 Vapor Deposition on Structural Surfaces

4.2.1.2.1 Basic Principles

Once the driving force for vapor deposition is defined, the kinetic barriers that inhibit deposition must be evaluated to calculate the extent of deposition. The rate at which a vapor deposits on a structural surface can be formally described by

$$\frac{1}{A}\frac{dN(i)}{dt} = \frac{V_d(i)}{RT}\left[\frac{P(i) - P_{eq}(i)}{1 - P_{eq}(i)/P}\right], \qquad (4.1)$$

where

- $N(i)$ = moles of deposited vapor species i,
- A = surface area,
- t = time,
- R = universal gas constant,
- T = absolute temperature,
- $P(i)$ = existing partial pressure of the i^{th} vapor species,
- $P_{eq}(i)$ = equilibrium partial pressure of the i^{th} vapor species,
- P = total pressure,
- $V_d(i)$ = vapor deposition velocity for the i^{th} vapor species.

This formal definition is equally applicable whether deposition is caused by simple condensation on the surface or chemical reaction of a vapor with the surface. Note that this formal definition of the deposition velocity can also be used to describe revaporization.

The vapor deposition velocity is not a constant but rather a mass transport coefficient that describes all the principal barriers to deposition. These barriers can be categorized as

- gas phase mass transport to a surface,
- chemical kinetics of reaction at the surface, and
- mass transport within the surface layer.

Consequently, vapor deposition velocities can have quite complicated functional dependencies on chemical and physical conditions. They are, however, usually known only as functions of temperature, pressure, and flow velocity.

For vapor fluxes to structural surfaces typically encountered in reactor accident analyses, gas phase mass transport can usually be described adequately by simple analogies to convective heat transport to the surfaces.[31] The only major impediments to doing this are

- definition of the thermal hydraulic regimes in the RCS and
- estimation of diffusion coefficients in the gas phase.

Definition of the appropriate thermal-hydraulic regime is not a trivial task for so complex a system as the RCS. Most of the available mass transport and heat transport correlations are for far simpler configurations and do not account for complexities such as ratcheting safety relief valves or bursts of steam flow as core debris falls into water. A particular complexity can be countercurrent natural circulation flows in the RCS.[32]

Diffusion coefficients for the exotic vapor species of interest in reactor accident analyses have not been measured. Estimates of these diffusion coefficients are usually derived from the Chapman-Enskog first-order solution to the Boltzmann gas kinetics equation.[33] These estimates indicate that diffusion coefficients are proportional to $T^{1.5}/P$. Thus, it is expected that the importance of gas phase mass transport as a kinetic barrier increases with increasing system pressure.

Chemical reaction kinetics are believed to limit the rate of deposition of species such as CsOH(g) on stainless steel.[34,35] Deposition of CsOH was found to take place in two ways. At low temperatures, the predominant mode of deposition was as a water soluble surface species. This species is often thought to be CsOH but is often found to be associated with other elements. At elevated temperatures (>1100 K), the dominant mode of CsOH deposition yields a water insoluble product bound within the oxide formed by steam oxidation of stainless steel. Indeed, similar bound deposits of cesium have been found on lead screws from the Three Mile Island reactor.[36] Deposition velocities for CsOH in both modes have been empirically correlated with temperature using an Arrhenius-type expression

$$V_d(i) = A(i)\exp[-E(i)/RT], \qquad (4.2)$$

where A(i) and E(i) are parameters found by fitting the expression to deposition data. For instance, Bowsher et

al.[37] correlated the deposition velocity data for cesium hydroxide on stainless steel to form an insoluble product with the expression

$$V_d(\text{cm/s}) = 1.05\exp(-4270)[\pm 2320/T] \quad . \quad (4.3)$$

Sallach and Elrick[34] obtained for the same process:

$$V_d(\text{cm/s}) = 7\exp(-7197/T) \quad . \quad (4.4)$$

Deposition velocities would be expected to be more complex than these simple temperature-dependent expressions suggest. Certainly, they do depend on the surface material as well as the vapor species. Sebathier[38] found that at 973 K the deposition velocity of CsOH on Inconel 600 was about a factor of 3 less than the deposition velocity on stainless steel.

The dominant vapor species of an element need not be responsible for most of the deposition. For instance, Elrick et al.[39] rationalized their observations concerning the interactions of SnTe(g) with stainless steel by hypothesizing the reaction

$$SnTe(g) + H_2O \Leftrightarrow SnO(g) + Te(g) + H_2 \quad . \quad (4.5)$$

They then argued that Te(g) reacted with the metal to form iron and nickel tellurides while SnO(g) deposited in the grain boundaries of the steel.[40,41] A similar gas phase dissociation has been suggested to explain decomposition of CsI on Inconel and stainless steel. In the gas phase, there is an equilibrium:

$$CsI + H_2O \Leftrightarrow CsOH + HI \quad . \quad (4.6)$$

The reaction proceeds to the right only a small extent even at 1200 K. But, the product CsOH(g) can deposit on stainless steel surfaces to form a low-volatility product, leaving HI free to pass out of the system. On the other hand, HI can react to form other iodides such as CdI_2, AgI, or FeI_2.[42]

More extensive deposition of CsOH and apparent decomposition of CsI can occur in pressurized-water reactors if structural surfaces are coated with boric oxide left after boiloff of the coolant. Extensive studies of the interaction[43–46] have shown that reactions of the type

$$CsOH + HBO_2 \Leftrightarrow CsBO_2 + H_2O \quad (4.7)$$

and

$$CsI + HBO_2 \cdot nB_2O_3 \Leftrightarrow CsBO_2 \cdot nB_2O_3 + HI \quad (4.8)$$

are possible. Cesium borates formed by these reactions are less volatile than either cesium hydroxide or cesium iodine and would be expected to condense on surfaces more readily. However, other reactions may consume boric oxide before it can react with cesium species. CdO forms stable borates. Surface deposits of boric oxide and tin oxide have also been shown to enhance the rates of corrosion of stainless steel in steam.[28] Evidence exists of strong interactions between boric oxide and the iron oxides found on the surfaces of oxidized stainless steel.[29]

Vapors deposited on surfaces may not be in the most thermodynamically stable form initially. The deposited material can continue to evolve chemically on the surface. For instance, cesium hydroxide can diffuse into the oxides on stainless steel surfaces to form a less volatile species. This less volatile material may be cesium silicate[34] or cesium chromite.[47] Evolutions of tellurium deposited on stainless steel to more stable chemical forms are thought to occur.[27,48] Similar transformations of other deposited radionuclides can be imagined to occur as results of chemical interactions with surface oxides or with other deposited materials. Formation of solid or molten solutions can be quite important. Chemical activities and, consequently, volatilities of radionuclides can be quite low in these solutions.[49]

4.2.1.2.2 Status

Fairly extensive laboratory studies of the kinetics of deposition of CsOH(g), CsI(g), Te(g), and SnTe(g) on stainless steel and Inconel 600 have been conducted.[3,34,35,40,41,48,50] Tests have also been made of HI(g) and I_2(g) interactions with control rod materials and steel[4,51,52] that establish HI and I_2 to be quite reactive. That is, the decomposition of cesium iodine does not necessarily mean that iodine in a gaseous form will emerge from the RCS; on the other hand, experimental studies have observed this to happen.[40,41] Analyses including descriptions of the thermodynamics and kinetics of HI(g) and I(g) reactions with materials in the RCS under the prevailing chemical conditions are necessary to adjudicate what will happen in reactor accidents. Retention of iodine in the RCS as CsI or some other iodide would create an inventory of radioactive iodine susceptible to revaporization later in a reactor accident.

Tests of vapor deposition kinetics that have been done include both isothermal tests and tests in thermal gradient tubes. Tests done in thermal gradient tubes appear particularly useful for identification of condensation rates of dominant vapor species. Isothermal tests are better suited for study of kinetically slow processes involving chemical reactions with surfaces. These deposition data, as well as

models of gas phase mass transport, have been incorporated into models of vapor transport in the RCS. Further laboratory-scale tests are under way in the Falcon program in the United Kingdom and the DEVAP program in France, as described in Sect. 4.3.

Large-scale tests such as the LACE and Marviken-V tests have not involved high-enough piping system temperatures to demonstrate the full impact that chemical phenomena and vapor deposition can have on radionuclide retention in the RCS.

4.2.1.2.3 Remaining Uncertainties

Uncertainties regarding thermal hydraulic conditions in the RCS and the consequent uncertainties in mass transport rates have been discussed previously. Uncertainties in properties of the vapor species also affect transport. Uncertainties in the diffusion coefficients arise because diffusion coefficients of species of interest have not been measured. The Chapman-Enskog theory that is used to estimate these diffusion coefficients is often not applicable for expected conditions in the RCS during severe accidents. The Chapman-Enskog theory was developed for monatomic, nonpolar species at a total pressure of less than 10 bars. The theory is being used to estimate diffusion coefficients of species that are often polyatomic, quite polar, and in environments with pressures in excess of 100 bars. Uncertainties of at least a factor of three can be expected in estimates of the diffusion coefficients of high-temperature vapor species.[53] Reports indicate that even at low pressures estimates of the diffusion coefficients are not adequate to reconcile model predictions with data.[54]

The data base on the deposition kinetics of CsOH, CsI, Te, SnTe, HI, I_2 and the like suffers from the difficulty that these vapor species may not be dominant vapor species in the RCS. That is, consideration of nonradioactive vapors that may be present along with radionuclides shows that other vapor species can form. Cesium uranates, cesium stannates, cesium borate, cesium zirconates, silver iodide, barium iodide, cadmium iodide, and silver telluride may be dominant species in the RCS. Deposition kinetics of these species have not been determined. Unlike estimation of the thermodynamic properties of vapor species, estimation of the deposition kinetics for vapor species is not feasible if deposition rates are controlled by factors other than mass transport. Significant progress in the understanding of vapor deposition kinetics is unlikely to occur until there is a much better understanding of the vapors present and the reaction products that can form. Again, guidance from prototypic tests would facilitate needed improvements to the models.

Experimental studies of the long-term chemical evolution of deposited radionuclides are scarce. In the absence of experimental guidance, it is difficult to predict the formation of metastable deposited species and the evolution of these species to more stable chemical forms. Indeed, only limited consideration of these processes are found in existing accident analysis codes. Yet, continued chemical evolution may have a significant bearing on subsequent revaporization or resuspension of deposited radionuclides.

4.2.1.3 Vapor Deposition on Aerosols

4.2.1.3.1 Basic Principles

Based on considerations of the available surface areas alone, vapor deposition on aerosol surfaces should be far more extensive than deposition on structural surfaces in the RCS. The relative extents of vapor deposition on structural surfaces and aerosol surfaces is not an academic point in the analysis of reactor accidents. Radionuclide vapors deposited on structural surfaces are lost from the potential source term at least temporarily, whereas radioactive vapors deposited on aerosols may not be removed from the potential source term.

The extent of vapor deposition on aerosol surfaces is not just a matter of the available surface area. Throughout much of the RCS, aerosol surfaces will be hotter than structural surfaces. Vapor pressures in equilibrium with these aerosol surfaces may be essentially equal to ambient partial pressures, so no net deposition occurs. For very small aerosol particles (<0.1 μm), surface curvature effects (Kelvin effect) raise the equilibrium vapor pressures significantly above values that would be calculated for bulk materials.

If vapor deposition on aerosol particles can occur, the rates of deposition are governed by the same kinetic effects that limit deposition on structural surfaces, i.e., gas phase mass transport, chemical kinetics, and condensed phase mass transport. Another effect to consider is the disposition of heat liberated by the condensation or chemical reaction of vapors with the aerosol. Because of their small masses, aerosol particles have more limited capabilities to conduct away this heat than do structures within the RCS. The rate of heat removal from the aerosol particles can limit the rate of vapor deposition.

Gas phase mass transport of vapors to aerosol particles can be predicted using conventional correlations if the aerosol particles are large in comparison to the mean free path for vapor molecule motion in the gas phase. Mass transport to particles that are much smaller than the mean free path can

be calculated using gas kinetic theory. Thus, neglecting heat transfer effects, the molar rate of vapor deposition on very small particles (free molecular limit) is

$$\left.\frac{dN(i)}{dt}\right|_{fm} = \frac{\pi r_p^2}{RT}\left[P(i) - P_{eq}(i)\right]\left[\frac{8kT}{\pi m_v}\right]^{1/2}, \quad (4.9)$$

whereas for very large particles (continuum limit) the rate is

$$\left.\frac{dN(i)}{dt}\right|_{c} = \frac{4\pi D_o T^{1.5} r_p}{PRT}\left[P(i) - P_{eq}(i)\right], \quad (4.10)$$

where

r_p = radius of the aerosol particle,
k = Boltzmann's constant,
m_v = mass of a vapor molecule,
$D_o T^{1.5}/P$ = vapor diffusion coefficient.

The rate of vapor deposition on aerosol particles between these limits is an active area of research. Williams and Loyalka[55] have suggested an approximate expression for deposition rates in the transition regime:

$$\left.\frac{dN(i)}{dt}\right|_{trans} = \left.\frac{dN(i)}{dt}\right|_{c} \left\{1 + \frac{\bar{l}}{r_p}\frac{1.333\left.\frac{dN(i)}{dt}\right|_{c}\Big/\left.\frac{dN(i)}{dt}\right|_{fm} + 1.016}{1.333\frac{\bar{l}}{r_p} + 1}\right\}^{-1}, \quad (4.11)$$

where $\bar{l}$ is the mean free path of molecular motion. These rate expressions indicate that vapor deposition on particles varies in complicated ways with temperature, pressure, and particle size. Further complications in the description of vapor deposition rates arise when account is taken of the heat released by condensation or reaction. Chemical kinetic processes, if rate limiting, can also complicate description of vapor deposition.

4.2.1.3.2 Status

That vapors might deposit on aerosols is suggested both by equilibrium thermodynamic calculations and experiments with supported materials.[42,56,57] These experiments have established that reactions between CsOH(g) and iron oxide aerosols can be quite exothermic.[42,56] Reactions of HI(g) and I_2(g) with cadmium and silver aerosols can be rapid.[42,47] Tests do not show if mass transport effects might be rate limiting for reactions with suspended materials or if heat loads produced by reactions will limit the rates of reaction. Experimental studies of vapor deposition on suspended particles of prototypic materials have not been conducted. Models employed to predict vapor deposition on particles use very approximate treatments. Frequently, kinetic effects are neglected, and the heat transfer limitations on deposition are usually ignored.

4.2.1.3.3 Remaining Uncertainties

The uncertainty of concern is the partitioning of depositing vapors between structural surfaces and aerosol surfaces. This partitioning directly affects the magnitude and timing of radionuclide release from the RCS. Analyses done to date do not appear to have the technical sophistication to provide resolution of the issue. Experimental studies with supported aerosol materials confirm only that reactions can occur and that the reactions can be quite exothermic.[56] The applicability of deposition rates obtained in experiments with supported aerosol materials to deposition on suspended aerosols has not been established. Design of experiments with suspended materials is complicated by the uncertainties in particle shape, size distribution, and composition needed to obtain prototypic results.

4.2.2 Aerosol Formation and Growth

Eventually, all the vapors evolved from the core save the noble gases and iodine gas will either deposit on structural surfaces or contribute to the formation and growth of aerosols. Interest in the behavior of aerosols in the RCS stems from the deposition of these radioactive particles in the RCS and the consequent reduction in the radiological source term that can be released from the nuclear power plant during an accident. The behavior of an aerosol in the RCS is almost entirely dependent on the size distribution of the aerosol particles. In the following subsection, the formation of aerosol and the growth of aerosol particles are discussed. Deposition of aerosols is discussed in the final portion of Sect. 4.2.

4.2.2.1 Basic Principles of Aerosol Formation and Growth

Aerosols can form when vapors are cooled sufficiently to reach critical levels of supersaturation. An extensive, heuristic theory of nucleation of conventional, pure vapors has been developed. This theory has been reviewed recently.[58] Nucleation directly from the vapor is usually predicted to proceed at readily detectable rates when the ambient partial pressure of the condensible vapor exceeds the equilibrium partial pressure by about a factor of four. Nucleation on ions can occur at lower supersaturation ratios. Hence, nucleation is then likely to occur in preference to condensation of vapor on surfaces when the vapors pass

quickly through large temperature gradients and the supersaturation of the vapor suddenly becomes large. The temperature change experienced by vapors as they emerge from the reactor core into the balance of the RCS is likely to produce nucleation. Nucleation is also possible when vapors can react to form a much less volatile product. The reaction of CsOH(g) with HBO_2(g) is a well-known example of a gas phase reaction that can lead to nucleation.

Quantitative prediction of nucleation in the RCS is a difficult problem. First is a numerical difficulty. Coupling the kinetic expressions for nucleation with competitive condensation and aerosol coagulation processes produces a numerically stiff set of differential equations. The second difficulty is that the existing theories of nucleation of pure vapors are difficult to extend to condensation from multicomponent vapors. Existing theories of nucleation predict nucleation rates that are extremely sensitive to the surface free-energy of the embryonic particle nuclei. For a pure vapor nucleating to form liquid droplets, the steady state homogeneous nucleation rate is given by

$$J = \left(\frac{P_v(sat)}{RT}\right)^2 \left(\frac{2\sigma_l M}{\pi N_A}\right)^{1/2} \frac{S^2}{\rho_l} \exp\left[\frac{-16}{3} \frac{\pi \sigma_l^3 M^2}{k R^2 \rho_l^2 T^3 [\ln(S)]^2}\right], \quad (4.12)$$

where

- J = nucleation rate (nuclei per unit volume per unit time),
- $P_v(sat)$ = saturation partial pressure of the vapor,
- σ_l = surface free-energy,
- M = molecular weight of vapor,
- N_A = Avogadro's number,
- S = $P_v/P_v(sat)$,
- P_v = vapor partial pressure,
- ρ_l = density of the liquid,
- k = Boltzmann's constant.[59]

Note that the dependences involve the exponential of the third power of the surface free-energy. Many other formulae predict the rates of homogeneous nucleation as well. All involve a very strong dependence on the surface free-energy. Whether the surface energy of macroscopic quantities of the condensed material is the appropriate value to use in these nucleation rate expressions is not known. Even if it is the right value, it is quite difficult to estimate the surface free-energies of mixtures produced by nucleation from multicomponent vapors.

Once aerosols nucleate, they grow by condensation of vapor or by coagulation. The issues of vapor condensation on extremely fine aerosol particles are discussed in Sect. 4.2.1.3. Coagulation of aerosols is an entirely physical process. When relative movements of aerosols bring particles into contact, they bind together as a result of surface free-energy or Van der Waals forces. Relative movements between aerosol particles can be produced by

- Brownian motion,
- gravitational settling, and
- turbulence.

These mechanisms of coagulation have been studied extensively within the reactor safety community in connection with aerosol behavior in reactor containment.*,[55] This technology has been adopted and adapted for the prediction of aerosol growth in the RCS.

There is a fourth factor that can affect coagulation of aerosol particles. Aerosols in the RCS will be radioactive and subjected to an intense radiation field. The particles can become electrostatically charged. Depending on the relative signs of the charges on particles, these electrostatic interactions can create a force that enhances or inhibits coagulation.

An assumption has been that the bombardment of charged aerosol particles by ions produced by the intense radiation field would discharge the aerosol particles. For this reason, Coulombic terms have been omitted from the expressions for aerosol coagulation. The arguments justifying omission of the Coulombic terms were usually based on the assumption that the mobilities of positive and negative ions in the atmosphere are the same. Recently, there have been suggestions that ion hydration in high-pressure steam may affect the mobilities of positive and negative ions differently.[25] Considering electrostatic forces in the predictions of aerosol growth may be necessary.

4.2.2.2 Status

To date, only the RAFT code attempts to explicitly model the homogeneous nucleation of vapors in the RCS.[60] Other models such as VICTORIA[11] simply inject particles to the extent needed to relieve supersaturation and maintain that coagulation proceeds on such a rapid time-scale that details of the kinetics of nucleation are erased quickly. There is neither proof of the need for detailed nucleation models nor proof of the adequacy of approximate techniques adopted to avoid explicit modeling of nucleation.

Primary

Nearly all models of aerosol growth in the RCS have adopted the methods for solution of the aerosol dynamic equations developed from studies of aerosol behavior in the reactor containment. The sectional methods, rather than moments methods, are nearly always used.[55] (An exception is the MAAP[61] code, which uses a linearized, self-preserving distribution to approximately solve the aerosol dynamic equation.) The adopted methods of solution are based on the assumption that the aerosol is homogeneously concentrated within a calculation node. The aerosol is assumed to be uncharged. Validation of the models has been derived from low-pressure tests with nonradioactive aerosols to validate models of aerosol behavior in reactor containments.*

Most models of aerosol behavior in reactor containment use a multicomponent aerosol size distribution. That is, aerosols of different sizes can have different compositions. Interestingly, models of aerosol behavior in the RCS typically either do not have this capability or it is not used in the analyses. The rationale for this is that running times for multicomponent aerosol models are too lengthy. Advances in numerical methods might eliminate this deficiency in existing models. The issue for analyses of behavior in the RCS may not be as crucial as it is for analyses of behavior in the reactor containment. Multicomponent effects are most pronounced when a fresh aerosol of one composition and size is injected into an aged aerosol of different composition.[62] Opportunities for this to happen in the RCS are not as common as in the containment. However, consideration of natural circulation currents within the RCS may raise the importance of having multicomponent aerosol models.

4.2.2.3 Remaining Uncertainties

The uncertainties in the application of homogeneous nucleation theory to multicomponent vapors have been discussed previously. The need to explicitly model nucleation is debated because inclusion of the necessary models can complicate and slow the computer codes. With respect to nucleation, it is known from some in-pile radionuclide release tests such as the STEP tests[63] and out-of-pile tests[64] that aerosol particles can be formed composed of a single, essentially pure phase and that particles can be found that are multiphase mixtures or solid solutions. A satisfactory explanation of this observation has not been made, though it may be related to nucleation processes. The suggestion has also been made that pressure affects the size distributions of aerosols in ways that mandate explicit modeling of the nucleation process.† The pressure effect on aerosol size distribution may not, however, be related to nucleation but may be indicative of the pressure dependence of aerosol coagulation.

Uncertainties concerning the effects of aerosol charging and electrostatic interactions on coagulation of particles have been discussed previously. Other uncertainties exist in the classic models of coagulation. Among these uncertainties are debates over the numerical coefficients in the expression for coagulation by gravitational settling[65] and uncertainties in how expressions for coagulation by different, simultaneous mechanisms should be summed.[66]

The equations for aerosol coagulation have been derived for spherical aerosol particles. Except for particles that are liquid, aerosol particles will not, in general, be spherical; this is especially true if vapors react to form rather refractory species as discussed in Sect. 4.2.1. Simple correction factors are incorporated into the equations to account for nonspherical particles. Most commonly used are the dynamic shape factor, χ, that affects aerosol settling and the collision shape factor, γ, that affects the interception of particles. Brockmann[67] has reviewed the state of understanding of shape factors for nuclear aerosols. He concludes that shape factors can depend on particle size. The dynamic and collision shape factors need not have the same value if the particles are entirely solid. Shape factors may vary over at least a range of 1 to 4 and may be as high as 12. There is, however, no mechanistic prediction of these shape factors, and their dependence on particle size is not incorporated into the available models of aerosol transport in the RCS. The issue of aerosol shape is of more concern in the RCS than in the reactor containment because there is no assurance that water condensing on the particles will draw agglomerates into spheres.[68]

The ongoing development of fractal geometry may provide a basis for prediction of aerosol shape factors. Currently, most models of aerosol behavior assume that the aerosol size increases with the one-third power of the number of coagulated primary particles. Numerical simulations of Brownian coagulation show, however, that the effective particle size as a function of coagulation is

$$\frac{r_p}{R_o} = \left(\frac{V}{V_o}\right)^{0.56} , \qquad (4.13)$$

*"Nuclear Aerosols in Reactor Safety," Supplementary Report, Organization of Economic Cooperation and Development, Paris, France (1985).

†A. M. Beard, D. R. Booker, and B. R. Bowsher, "The Role of Pressure on Nucleation of High Temperature Vapour," European Aerosol Society Meeting, Oxford, United Kingdom, September 6–11, 1992.

where

r_p = effective radius of agglomerate,

R_o = radius of primary particles,

V = volume of material making up the agglomerate,

$V_o = \frac{4}{3}\pi R_o^3$ (Ref. 55).

If it is assumed that the agglomerate is a convex body in outline, this result can be used to estimate size-dependent shape factors.

4.2.3 Aerosol Transport and Deposition

Interest in the behavior of aerosols in the RCS focuses on the deposition of these aerosols. Aerosol deposition processes are discussed subsequently. Deposition of aerosols may not permanently remove radioactive materials from source term considerations. Deposited aerosols may be resuspended by sudden increases in flow especially if surfaces supporting the aerosols are accelerated by shock waves or vibrations. Decay heating of deposits may raise temperatures to the point that volatile constituents, including volatile radionuclides, vaporize. Revaporization is of particular concern if the ambient chemistry of the RCS is suddenly changed, such as occurs when the RCS is depressurized or ruptured. Resuspension of aerosols and revaporization from aerosols are also discussed subsequently.

4.2.3.1 Aerosol Deposition

4.2.3.1.1 Basic Principles

Motions of aerosol particles are affected by a variety of phenomena and forces that can lead to deposition of the particles in the RCS. Aerosol particles are small enough that they are affected by Brownian motion, temperature gradients, concentration gradients, and electrostatic forces. On the other hand, aerosol particles are big enough that they can separate from flow streams by inertia or because of gravitational forces. Any of these forces or phenomena that bring aerosol particles to within about a particle diameter of surfaces in the RCS can lead to aerosol deposition. Aerosols are held to the surfaces by Van der Waals forces, electrostatic forces, or, when liquid is present, surface tension. Once on the surface, the particle can be further bound by chemical reaction with surface materials or by sintering with other deposited materials. Further discussion of some of the deposition mechanisms follows.

- Brownian motion

  Brownian motion of aerosol particles is produced by stochastic impulses imparted by collisions with gas molecules. Brownian motion induces a diffusive behavior to aerosol particles. The diffusion coefficients of aerosol particles vary with the reciprocal of the particle size:

$$D = \frac{CkT}{6\pi\mu_g r_p \chi}, \qquad (4.14)$$

  where

  C = Cunningham slip correction,

  μ_g = viscosity of the gas,

  k = Boltzmann's constant,

  r_p = particle radius,

  χ = dynamic shape factor.[55]

  Consequently, deposition of aerosol particles by diffusion is most important for very small particles (<0.1 μm). The diffusion coefficients are linearly dependent on temperature and independent of pressure at least to a first approximation.

- Thermophoresis

  Temperature gradients in the gas phase can impart a net velocity to aerosol particles in a direction opposite to the gradient. Thermophoretic velocity is proportional to the magnitude of the gradient with a proportionality constant that depends on the thermal conductivity of the particle. Metallic particles with high thermal conductivities are less affected by thermophoresis than oxide or hydroxide particles with low thermal conductivities. The dependence on the particle size is weak. Because there can often be large temperature differences between the gas phase and structures in the RCS, deposition of aerosol particles by thermophoresis is an important phenomenon to consider in reactor accident analyses. The model developed by Talbot et al.[69] is widely used today:

$$U_T = -\frac{2C_s\mu_g}{\rho_g} \frac{\left(\frac{k_g}{k_p} + \frac{C_t\lambda}{r_p}\right)\left(1 + \frac{\lambda}{r_p}\left(A + B\exp\left[-Cr_p/\lambda\right]\right)\right)\frac{\nabla T}{T_o}}{\left(1 + 3C_m\,\lambda/r_p\right)\left(1 + \frac{2k_g}{k_p} + 2C_t\,\lambda/r_p\right)}, \qquad (4.15)$$

where

U_T = thermophoretic velocity of the particle,
μ_g = viscosity of the gas,
ρ_g = density of the gas,
k_g = thermal conductivity of the gas,
k_p = thermal conductivity of the particle,
r_p = radius of the particle,
λ = mean free path in the gas,
∇T = temperature gradient,
T_o = mean temperature in gradient,
A = 1.20,
B = 0.41,
C = 0.88,
C_m = 1.14,
C_t = 2.18,
C_s = 1.17.

- Diffusiophoresis

  The fluxes of condensing or chemically reacting vapors toward surfaces in the RCS can sweep along aerosol particles. To a first approximation, this diffusiophoretic deposition is independent of particle size but linearly dependent on the vapor flux. Unless there is condensation of bulk gas such as steam, the effect of diffusiophoresis on aerosol concentrations in a volume is essentially linearly proportional to the fraction of the gas phase that condenses. Typically, this is not an important deposition mechanism in the RCS under severe accident conditions. Accident management activities, such as cooling the steam generator, could make diffusiophoresis a more important deposition mechanism.

- Electrostatic interactions

  As discussed previously, radioactive aerosols in the RCS can carry net electrostatic charges. Similarly, oxide layers on structural surfaces in the RCS can be charged electrostatically. Depending on the relative signs of the surface and aerosol charges, an attractive or a repulsive Coulombic force exists between the aerosol and the surface, which can either enhance or inhibit deposition.

- Gravitational deposition

  Aerosol particles can, because of gravity, fall across streamlines of flow through the RCS and settle on surfaces. Settling velocities vary with the square of the particle diameter. Consequently, gravitational settling is most important for large particles (>1 μm). Gravitational settling becomes an increasingly important deposition mechanism as flow velocities through the RCS decrease.

- Convective deposition mechanisms

  Perhaps the most important mechanism for aerosol deposition comes about because inertia of aerosol particles limits the ability of particles to follow rapidly varying flow streams. Thus, aerosol particles deposit on surfaces as flows pass through bends and when there are changes in flow direction, sudden contractions or expansion in the flow channel width, and when flows are turbulent. Because this deposition is an inertial effect, it increases in importance with aerosol particle size. The inertial deposition effect coupled with deposition by diffusion leads to particle capture efficiencies that pass through a minimum when plotted against particle size. Very small aerosol particles are efficiently removed from the flow stream by diffusion. Diffusion, however, becomes less effective as particle size increases. On the other hand, inertial deposition becomes more effective as particle size increases. Therefore there is a particle size where, typically, the sum of inertial and diffusive deposition is minimal. The particle size that is minimally affected by these processes varies with the geometry, flow condition, and particle properties. However, the minimally affected particle size typically has an aerodynamic diameter between 0.1 and 0.4 μm.

  Deposition in bends is especially important in the analysis of aerosol behavior in the RCS. Flow pathways from the reactor core through the RCS can be tortuous. Steam separators and steam dryers found in boiling-water reactors are obviously locations where aerosol deposition is likely.[70] Deposition of aerosol can be caused by any local turbulence induced by discontinuity in the flow. Deposition of particles at a discontinuity can enhance the local turbulence and induce more deposition. Because of this feedback effect, aerosols can plug even quite large flow passages.[71]

4.2.3.1.2 Status

Naturally, there is a vast literature base on the behavior of aerosol particles (see Ref. 55 for example). The literature encompasses both theoretical and experimental studies. Most of these studies, both theoretical and experimental, are for flow geometries that are quite simple relative to the flow geometries encountered in RCSs. Usually, laboratory studies of aerosol behavior have been designed to isolate a single deposition mechanism. Experimental results then are cast in terms of empirical correlations or are used to validate a theoretical model. These correlations and models for isolated deposition mechanisms in simple flow geometries have been adopted and adapted into models of aerosol behavior in the RCS.

Laboratory studies of most interest for the analysis of aerosol deposition in the RCS can be summarized as follows:

Thermophoretic Deposition—A substantial data base exists for thermophoretic deposition from laminar flows.[72] Thermophoretic deposition from turbulent flows, which would be of more interest for reactor accident analyses, has received little attention. What data are available suggest that thermophoretic forces are not greatly affected by turbulent flow conditions.

Gravitational Deposition—In general, there is confidence that gravitational deposition is well understood. Difficulties in accurate estimation of gravitational deposition arise primarily from properties of the particles and when gravitational deposition acts in concert with other deposition mechanisms.[55]

Deposition in Bends—A data base also exists for deposition in bends.[73] Typically, 90° bends in pipes much smaller than those of interest for reactor accident analyses have been studied. Theoretical models for deposition from laminar flows have been developed.[74,75] These models suggest that "secondary" flows in bends complicate the scaling of laboratory studies to sizes of interest in reactor accident analyses. Only an empirical correlation exists for deposition from turbulent flows in bends:

$$\eta = 1 - 10^{-0.963\,Stk} \quad , \qquad (4.16)$$

where

η = deposition fraction in turbulent flow through a bend,
Stk = stokes number = $C\rho_p D_p^2 U_o / 18 \mu R_t$,
C = Cunningham slip correction factor,
ρ_p = particle material density,
D_p = particle diameter,
U_o = mean axial fluid velocity,
μ_g = gas viscosity,
R_t = pipe radius.

Deposition at Expansions or Contractions in Flow Channels—Limited data on deposition at sudden contractions in flow are available.[76] These data have been obtained for very tiny flow channels. There are hydrodynamic analyses and aerosol deposition data for sudden expansions in the flow.[77] The data are for 5 and 10 μm particles, and it is difficult to know how these data may be applied to the smaller particles that typically are of interest in accident analyses.

Turbulent Inertial Deposition—An extensive data base exists on the deposition of particles in pipes from turbulent gas flows.[78]

Because flows encountered in reactor accidents are far more complex than those studied in the laboratory, and because there typically will be more than one deposition mechanism operative, there has been an interest in integral tests to validate models based on laboratory studies or theoretical models. One of the best of these integral tests was conducted by Gieseke and Jordan with full-scale steam separators and dryers from boiling-water reactors.[70] A notable finding made in this work was that electrostatic charging of aerosols drastically affected particle retention in the test apparatus. Gieseke and Jordan conducted their work with full-scale equipment but under laboratory conditions. Though they undertook elaborate efforts to scale their experimental conditions to reactor accident conditions, they concluded that models available to them may have been too simplistic to scale their tests properly.

Other integral tests of aerosol behavior such as the LACE[79] and Marviken-V[80] tests of aerosol behavior are discussed in Sect. 4.3. Though these tests have been large, they still suffer from the issues of scaling to reactor accident conditions. Ball et al.[81] recently announced the establishment of a facility to study aerosol behavior in piping systems. Other experiments are under way in France (see Sect. 4.3).

4.2.3.1.3 Remaining Uncertainties

In their review of turbulent deposition of aerosols, Agrawal and Lui[78] listed many factors that can affect aerosol deposition data:

- electrical charging of the aerosols,
- bounce of particles impacting surfaces,
- re-entrainment of deposited particles,
- local turbulence at discontinuities in the flow path,
- surface roughness, and
- nonspherical particles.

Presumably, these factors, which can affect experimental data, should also affect predictions of aerosol behavior in the RCS. Yet, there have been no systematic studies of these processes, and models addressing these factors are largely absent from computer codes. Certainly, issues of electrostatic charging of radioactive aerosols have been neglected in the models as discussed previously. The poor capacity to predict aerosol shape factors has also been mentioned.

Similarly, there have been no studies of the very important process of thermophoretic deposition from turbulent flows. It may be, however, that suitably accurate predictions can be made by application of laminar flow models to the boundary layers adjacent to surfaces.

Primary

Perhaps the biggest need for experimental data is to address the issue of complex flows with simultaneously operating deposition mechanisms. The work with steam separators and dryers by Gieseke and Jordan[70] is an example of the types of data needed. Systematic studies with real-scale systems provide the opportunity to test the ways in which correlations of experimental data and theoretical models are combined to predict deposition in reactor accident situations. Some hypothesized accident conditions are indeed complex. For instance, analyses of natural circulation during core degradation have predicted countercurrent flows in the reactor hot leg through the steam generator in a pressurized-water reactor.[32] The effects of such countercurrent flows on aerosol deposition have not been studied.

Because of phenomena like "secondary" flows, scaling of results to reactor accident scales may be more complicated than is typical for strictly hydrodynamic considerations. Applicability of test data taken even from large test fixtures (though small in comparison to the coolant systems of nuclear reactors) will depend on an accurate understanding of these scale issues.

4.2.3.2 Aerosol Resuspension

4.2.3.2.1 Basic Principles

Deposited aerosol particles can be resuspended if there is drastic change in flow conditions or acceleration of the surfaces loaded with deposited particles. Such changes in the flow conditions are expected to occur in the RCS. Collapse of molten core debris into water in the lower plenum of the reactor vessel, penetration of the reactor vessel by core debris, or even operation of safety relief valves could produce sufficient changes in the turbulent flows near the surface to lift particles off structural surfaces. Because shock waves will pass through the surfaces or the surfaces will vibrate during many of the changes in flow conditions, the conditions for resuspension clearly would be established.

There are resistances to resuspension of particles. Van der Waals or electrostatic forces that initially bound the particles to the surface may not be overcome by the turbulent lift forces. During the period the particles are at rest on the surface, there may be reaction with the surface or the deposited particles may be hot enough to sinter together into a compact mass that would be difficult to resuspend.

4.2.3.2.2 Status

A variety of laboratory studies of particle resuspension[82,83] and a few scoping studies at larger scales[84,85] have been made. These studies have examined the resuspension of particles not subject to all the factors that will affect particle resuspension in a reactor accident. Notably, the studies have not involved high temperatures that would allow particles to sinter and chemically react. In general, the studies have involved relatively constant, though elevated, flow velocities to produce resuspension. No effort has been made to simulate the violently turbulent, transient flows expected to produce resuspension in a reactor accident. Shocks and vibrations to the supporting structures, which should enhance resuspension, have not been simulated in the experimental studies. The studies have been confined to examination of resuspension from flat plates or pipes. Geometries expected to produce the most extensive aerosol deposition in the RCS, such as pipe bends, flow discontinuities, and sudden changes in flow channel width, have not been studied.

Experimental studies to date have established that resuspension does occur. The resuspension flux of particles decreases approximately exponentially with time. The initial resuspension flux varies approximately linearly with velocity once a threshold velocity is exceeded. Resuspension also increases with increasing depth of the deposit. Aging the deposited material seems to reduce rates of resuspension.

Studies have focused on the fractional amount of aerosol resuspended. Little attention has been given to the sizes of the resuspended materials. It is not known if resuspended particles will have the same size as deposited particles. Certainly, it is expected that larger particles will be more easily resuspended than small particles.[82] Surface agglomeration of particles may mean that resuspended particles are so large they readily redeposit elsewhere.

Various theoretical models of particle resuspension have been developed. Within the reactor safety community the Reeks-Hall model has become popular.[86,87] This model considers particles bound to the surface within an anharmonic potential well. Resuspension of particles occurs when the energy imparted by flow exceeds the potential energy barrier.

4.2.3.2.2 Remaining Uncertainties

Resuspension is *terra incognita* within the reactor safety community. Significant progress in this area requires:

- a more detailed characterization of the forces expected to arise in a reactor accident that will lead to resuspension and
- a better understanding of the nature of aerosol deposits within the RCS and the features of these deposits that will resist resuspension.

Progress in these areas will permit the design of resuspension experiments that will provide at least a prototypic, empirical data base on the phenomenon. A large-scale experimental program called the STORM project is being planned to study physical resuspension of deposited aerosols.[89]

4.2.3.3 Revaporization

4.2.3.3.1 Basic Principles

Early analyses[2] of radionuclide retention in the RCS assumed that chemical reactions of vapors with structural surfaces and aerosols were irreversible. Chemical reactions are always reversible in some sense. Reversal of reactions of vapors with structures and aerosols becomes of interest when radioactive vapors are regenerated. This regeneration of the vapors can reverse the source term mitigation that was achieved by deposition of the vapors and aerosols. Of particular interest is revaporization of deposited radionuclides late in a reactor accident when the integrity of the containment has been lost and radionuclides released from the RCS can easily escape the plant.

Chemical reactions and condensation in the RCS can reverse when the equilibrium vapor pressures over deposited material exceed the ambient partial pressures of these vapors [see Eq. (4.1)]. Common reasons for equilibrium vapor pressures to exceed ambient partial pressures include

- deposited materials being heated by decay of radionuclides and convective heating and
- changes occurring in the chemical environment within the RCS.

Decay heating of deposited materials is particularly important in regions where aerosols preferentially deposit. Areas of preferential deposition include bends, discontinuities in the flow paths, and regions that at least at one time involved sharp temperature gradients.

Continued convective heating of deposited materials is especially important in accidents in which the pressurization of the RCS has been maintained. Then, natural circulation is predicted to distribute substantial amounts of heat generated within the degrading core to structures in the balance of the RCS.[32] Temperatures of structures sufficient to cause rupture by creep (>1100 K) are predicted to develop. Such high temperatures could certainly cause revaporization of volatile materials such as species formed from cesium and iodine. They could also cause deposits to melt and flow into other regions of the RCS. Though this flow phenomena was observed in the Marviken-V experiments,[80] it is not modeled in accident analysis codes.

Rupture of the RCS can produce radical changes in the chemical environment of deposits. Air can be drawn into the system, and this air will dramatically raise the oxygen potential of the atmosphere. Oxidation of metal iodides could produce gaseous, elemental iodine, which could be readily swept from the RCS. Air could oxidize metal tellurides to produce volatile tellurium oxides. Deposited uranium dioxide could vaporize as $UO_3(g)$ in air. Ruthenium and molybdenum could be oxidized to the volatile species RuO_4, RuO_3, and MoO_3. On the other hand, high oxygen potentials could suppress the volatility of elements such as barium, strontium, and rare earths. Carbon dioxide in the air could react with deposited CsOH to form the less volatile species Cs_2CO_3.

The fate of revaporized materials depends on the same factors that affect vapors evolved directly from the core. The revaporized materials may redeposit in cooler regions of the RCS or they may be swept from the system.

Revaporization could be a very protracted process, occurring over many days after an accident starts. As interest develops in the long-term (>30 d) performance of reactor safety systems during severe accidents, there will have to be a better understanding of revaporization processes and the long term behavior of deposited radionuclides.

4.2.3.3.2 Status

Revaporization is now understood only through analysis.*,[89,90] Though there have been experiments that identified revaporization phenomena,[91] systematic experimental studies of revaporization from prototypic deposits have not been conducted. Analyses have indicated that the rates of revaporization are dependent on the chemical form and possibly on the physical form of the deposited materials.[92] Formation of very stable compounds or solid solutions on surfaces can greatly inhibit the rates of revaporization of even quite volatile radionuclides. Unfortunately, there is not now a good understanding of the chemical nature of deposits to be expected in the RCS.

4.2.3.3.3 Remaining Uncertainties

Like resuspension, the importance of revaporization in reactor accidents is very uncertain. To develop the understanding of the risk significance of revaporization, there will have to be better capabilities to predict

*P. Bieniarz and R. Deem, "Indian Point 3 Consequence Analysis for TMLB[1] Sequence," New York Power Authority, White Point, NY, 1984.

Primary

- heat generation and heat losses in deposits in the RCS,
- gas flows over deposits late in reactor accidents,
- chemical speciation and physical forms of deposits in the RCS, and
- long term diffusion of deposited radionuclides into the structures in the RCS.

That is, the prediction of revaporization is difficult because of uncertainty in the thermal hydraulics, chemical environment, and chemical form of deposits in the RCS. A more substantial body of experimental data and more complete models are needed to establish the effects that revaporization processes can have on severe reactor accident source terms. Certainly, it is anticipated that the ongoing Falcon program and the forthcoming Phebus-FP program described in Sect. 4.3 will provide substantive contributions to the needed data base.

4.2.4 References

1. M. Epstein and D. E. Rosner, *Int. J. Heat Mass Transfer*, 13, 1393 (1970).*
2. J. A. Gieseke et al., Battelle Columbus Laboratory, "Radionuclide Release Under Specific LWR Accident Conditions," BMI-2104, Vol. II–VII, 1984.†
3. I. Johnson et al., "Downstream Behavior of Volatile Iodine, Cesium and Tellurium Fission Products," EPRI-NP-6182, Argonne National Laboratory, January 1989.
4. A. M. Beard, C. G. Benson, and B. R. Bowsher, "The Interaction of Simulant Fission Product Vapours with Control Rod Aerosols in a Flowing System," Winfrith Technology Centre, AEEW-R2470, United Kingdom (December 1988).
5. I. R. Beattie, B. R. Bowsher, and P. J. Jones, "Vapour Transport of Indium in Steam," Atomic Energy authority, Winfrith, AEEW-R2391, United Kingdom (September 1988).
6. V. Brandani, G. Del Re, and G. D. Giacomo, *J. Solution Chem. 17*, 429, (1988).*
7. A. W. Cronenberg and D. J. Osetek, *Nucl. Technol.* 81, 347 (1988).*
8. D. J. Wren, "Kinetics of Iodine and Cesium Reactions in the Candu Reactor Primary-Heat Transport System under Accident Conditions," Atomic Energy of Canada, Limited, AECL-T181, Pinawa, Manitoba, Canada (1983).
9. W. B. White, W. M. Johnson, and G. B. Dantzig, *J. Chem. Phys.* 28, 751 (1958).*
10. S. R. Brinkley, *J. Chem. Phys.* 15, 107 (1947).*
11. T. J. Heames et al., Sandia National Laboratories, "VICTORIA: A Mechanistic Model of Radionuclide Behavior in the Reactor Coolant System Under Severe Accident Conditions," USNRC Report NUREG/CR-5545, 1990.†
12. D. R. Stull and H. Prophet, *JANAF Tables*, 2nd edition, NSRDS-NBS 37, National Bureau of Standards, June 1971.
13. C. A. Alexander and J. S. Ogden, "Real Time Mass Spectrometric Evaluation of Fission Product Transport at High Temperature and Pressure," Proceeding of the Symposium on Chemical Phenomena Associated with Radioactivity Releases During Severe Nuclear Plant Accidents, S. J. Niemczyk, Ed., USNRC Conference Proceedings NUREG/CP-0078, June 1987.†
14. S. Dickinson, "Matrix Isolation-Infrared and Mass Spectrometric Studies of High Temperature Molecules," Atomic Energy Authority, AEEW R-2227, Winfrith, United Kingdom (August 1987).
15. R. A. Sallach, Sandia National Laboratories, "Reactor Safety Research Semiannual Report January-June, 1987," USNRC Report NUREG/CR-5039 (10/2) [SAND87-2411 (10/2)], January 1988.†
16. R. J. M. Konings and E. H. P. Cordfunke, *J. Chem. Thermodynamics 20*, 103 (1988).*
17. See for example, E. H. P. Cordfunke, R. R. Van der Laan, E. F. Westram, Jr., "The Thermochemical and Thermophysical Properties of Cs_2RuO_4 and Cs_2MnO_4 from 5 to 1000 K," Netherlands Energy Research Foundation, ECN-RX-91-100, Petten, The Netherlands (October 1991).

18. E. H. P. Cordfunke et al., *Thermochemical Data for Reactor Materials and Fission Products* (North Holland, 1990).

19. R. G. J. Ball et al., "Thermochemical Data Acquisition," AEA Technology, AEA TRS 5068, Winfrith, United Kingdom (January 1990).

20. R. G. J. Ball et al., "ECN Petten Report," Netherlands Energy Research Foundation, ECN-C-92-033 Petten, The Netherlands (1992).

21. O. H. Kerkorian, *High-Temp High Pressures* 14, 387 (1982).*

22. I. Dzidic and P. Kebarle, *J. Phys. Chem.* 74, 1466 (1970).*

23. M. Ashadi, R. Yamdagmi, and P. Kebarle, *J. Phys. Chem. 74*, 1475 (1970).*

24. R. G. Keesee and A. W. Castleman, Jr., *J. Phys. Chem. Ref. Data 15*, 1011 (1986).*

25. C. F. Clement and R. G. Harrison, "Electric Charge Effects on Aerosol Behavior, Workshop on Aerosol Behavior and Thermal-Hydraulics in the Containment," Committee on the Safety of Nuclear Installations, CSNI Report No. 176, Paris, France (November 1990).

26. L. Brewer in *Chemical Processes and Products in Severe Nuclear Reactor Accidents: Report of a Workshop* (National Academy Press, Washington, D.C., 1989) Chap. 3, p. 15.

27. R. M. Elrick and R. A. Sallach, "Importance of Environment on High Temperature Reactor Accident Chemistry," pp. 3–19 in *Proceedings of the Symposium on Chemical Phenomena Associated with Radioactivity Releases During Severe Nuclear Plant Accidents*, S. J. Niemczyk, Ed., USNRC Conference Proceedings NUREG/CP-0078, June 1987.†

28. S. Kazikowski, L. G. Johansson, U. Malmestrom, and O. Lindquist, "Corrosion and Deposition Studies of Stainless Steel Exposed to Aerosols Containing Te, Cs, I, Sn, Mn, Ag, and B_2O_3 at 300-1000°C in a Reducing ($H_2/H_2O/N_2$) Environment," pp. 3–79 in *Proceedings of the Symposium on Chemical Phenomena Associated with Radioactivity Releases During Severe Nuclear Plant Accidents*, S. J. Niemczyk, Ed., USNRC Conference Proceedings NUREG/CP-0078, June 1987.†

29. A. B. Anderson, A. M. Beard, P. J. Bennett, and C. G. Benson, "Characterization of Boric Acid Aerosol Behavior and Interactions with Stainless Steel," AEA Technology, AEA TRS 5091, Winfrith Technology Centre, United Kingdom (March 1991).

30. M. W. Chase, Jr., J. L. Curnutt, R. A. McDonald and A. N. Syverud, *J. Phys. Chem. Ref. Data* 7, 793 (1978).*

31. R. B. Bird, W. E. Stewart, and E. N. Lightfoot, *Transport Phenomena* (John Wiley and Sons, Inc., New York, 1960), p. 646.

32. P. D. Bayless, Idaho National Engineering Laboratory, "Analyses of Natural Circulation During Surry Station Blackout Using SCDAP/RELAPS," USNRC Report NUREG/CR-5214, (EGG-2547), October 1988.†

33. J. O. Hirschfelder, C. F. Curtiss, and R. B. Bird, *Molecular Theory of Gases and Liquids* (John Wiley and Sons, Inc., New York, 1954).

34. R. M. Elrick, R. A. Sallach, A. L. Ouellette, and S. C. Douglas, Sandia National Laboratories, "Reactions Between Some Cesium-Iodine Compounds and the Reactor Materials 304 Stainless Steel, Inconel 600, and Silver: Volume I Cesium Hydroxide Reactions," USNRC Report NUREG/CR-3197/1 of 3 (SAND83-0395), June 1984.†

35. B. R. Bowsher, S. Dickinson, and A. L. Nichols, "High Temperature Studies of Simulant Fission Products, Part I, Vapor Deposition and Interaction of Caesium Iodide, Caesium Hydroxide and Tellurium with Stainless Steel," Atomic Energy Authority, AEEW-R1697, Winfrith, United Kingdom (July 1983).

36. V. F. Baston, K. J. Hofstetter, G. M. Bain, and R. M. Elrick, "A Comparison of TMI-2 and Laboratory Results for Cesium Activity on Reactor Material Surfaces," *American Nuclear Society* Winter Meeting San Francisco, CA, November 10–14, 1985, *Trans. Am. Nuc. Soc.*, 1985.

37. B. R. Bowsher, S. Dickinson, and A. L. Nichols, "High Temperature Studies of Simulant Fission Products: Part III Temperature Dependent Interaction of Caesium Hydroxide Vapour with 304 Stainless Steel," Atomic Energy Authority, AEEW R1863, Winfrith, United Kingdom (April 1990).

38. F. Sabathier, "Interaction of Caesium Hydroxide with 304 Stainless Steel and Inconel 600," Winfrith Technology Centre, AEA RS 5164, United Kingdom (August 1991).

39. R. M. Elrick and A. L. Ouellette, Sandia National Laboratories, "Interaction of Tin Telluride and Cesium Hydroxide with Reactor Materials in Steam," SAND89-2504, December 1991.†

40. R. M. Elrick, R. M. Merrill and A. L. Ouellette, Sandia National Laboratories, "The Thermal Instability of Cesium Iodide," USNRC Report NUREG/CR-5155 (SAND88-1187), August 1989.†

41. D. R. Wren, R. K. Rondeau and M. D. Pellow, "Studies on the Radiation Stability of Cesium Iodide," Atomic Energy of Canada Limited, EPRI-NP-6344, Panawa, Manitoba, Canada (April 1989).

42. B. R. Bowsher and S. Dickinson, "The Interaction of Caesium Hydroxide Vapour with Iron and Ferric Oxide (Fe_2O_3) Powders at 760°C," Atomic Energy Authority, AEEW-M2262, Winfrith, United Kingdom (July 1985).

43. R. M. Elrick, R. A. Sallach, A. L. Ouellette, and S. C. Douglas, "Boron Carbide-Steam Reactions with Cesium Hydroxide and with Cesium Iodide at 1270 K in an Inconel System," USNRC Conference Proceedings NUREG/CP-4963 (SAND86-1491), Sandia National Laboratories, September 1987.†

44. B. R. Bowsher and A. L. Nichols, "High Temperature Studies: Part IV, Interactions of Caesium Iodide with Boric Acid Over the Temperature Range 400 to 1000°C, Atomic Energy Authority, AEEW-R1973 Winfrith, United Kingdom (July 1985).

45. B. R. Bowsher and S. Dickinson, "The Interaction of Caesium Iodide with Boric Acid: Vapor Phase and Vapor-Condensed Phase Reactions," Atomic Energy Authority, AEEW-R2102 Winfrith, United Kingdom (May 1986).

46. I. R. Beattie, B. R. Bowsher, T. R. Gilson and P. J. Jones, "The Interaction of Caesium Iodide with Boric Acid," Atomic Energy Authority, AEEW-R1974, Winfrith, United Kingdom (June 1985).

47. G. C. Allen et al., "High Temperature Studies of Simulant Fission Products: Part VI, Surface Studies of the Interaction of Caesium Hydroxide Vapour with 304 Stainless Steel," Atomic Energy Authority, Winfrith, AEEW-R 1986, United Kingdom (July 1985).

48. R. A. Sallach, C. J. Greenholt, and A. R. Taig, "Chemical Interactions of Tellurium Vapors with Reactor Materials," NUREG/CR-1921 (SAND82-1145), Sandia National Laboratories, 1984.†

49. D. A. Powers and P. Bieniarz, "Influence of Chemical Form on Cesium Revaporization from the Reactor Coolant System, Chemical Phenomena Associated with Radioactivity Releases During Severe Nuclear Plant Accidents," S. J. Niemczyk, Ed., USNRC Conference Proceedings NUREG/CP-0078, p. 3–67, 1987.†

50. R. A. Sallach, R. M. Elrick, S. C. Douglas, and A. L. Ouellette, "Reactions Between Some Cesium-Iodine Compounds and the Reactor Materials 304 Stainless Steel, Inconel 600, and Silver. Volume II: Cesium Iodine Reactions," NUREG/CR-3197/2 of 3 (SAND83-0395), Sandia National Laboratories, August 1986.†

51. S. L. Nicolosi and P. Baybutt, "Vapor Velocity Measurements and Correlations for I_2 and CsI," USNRC Report NUREG/CR-2713, Battelle Columbus Laboratory, 1982.†

52. M. F. Osborne et al., "Iodine Sorption on Low Chromium Alloy Steel," ORNL/TM-7755, Oak Ridge National Laboratory, 1981.†

53. J. Kestin and W. A. Wakeham, *Transport Properties of Fluids: Thermal Conductivity, Viscosity, and Diffusion Coefficient* (Hemisphere Publishing Co., 1988).

54. P. Dumaz, "Analysis of the Falcon 3A Experiment Using VICTORIA," Winfrith Technology Centre, AEA RS 5257, United Kingdom (1992).

55. M. M. R. Williams and S. K. Loyalka, *Aerosol Science Theory and Practice with Special Applications to the Nuclear Industry* (Pergamon Press, 1991).

56. R. D. Spence and A. L. Wright, "The Importance of Fission Production/Aerosol Interactions in Reactor Accidents," *Nucl. Technol.*, 77, 150 (1987).*

57. J. Henshaw, M. S. Newland, and S. J. Wood, "Thermogravimetric Studies of Vapour-Aerosol Interactions," Atomic Energy Authority TRS 5074, AEA Technology, United Kingdom (January 1991).

58. E. Hontnon, "Theoretical and Experimental Research on Homogeneous Nucleation Phenomena," CTN-67/91, Catedra de Tecnologia Nuclear E.T.S. De Ingeniers Industriales, Madrid, Spain (1991).

59. J. Frenkel, *Kinetic Theory of Liquids* (Oxford University Press, London, 1946).

60. K. H. Im, R. K. Ahluwalia, and F. C. Chang, "RAFT: A Computer Model for the Formation and Transport of Fission Product Aerosols in LWR Primary Systems," *Aerosol Science and Technology* 4 125 (1985).*

61. J. M. Otter and E. U. Vaughan, "Evaluation of Empirical Aerosol Correlations," EPRI NP-4974, Rockwell International Corp., Canoga Park, CA, December 1986.

62. D. C. Williams and J. Tills, Sandia National Laboratories, "CONTAIN/MAEROS Sensitivity Studies," Appendix N, in R. J. Lipinski et al., *Uncertainty in Radionuclide Release Under Specific LWR Accident Conditions*, SAND84-0410, Vol. 2, February 1985.†

63. L. Baker, Jr., et al., "Source Term Experiments Project (STEP): A Summary," NP-5753M, Electric Power Research Institute, Palo Alto, CA, March 1988.

64. A. M. Beard, C. G. Benson, and B. R. Bowsher, "Fission Product Vapour–Aerosol Interactions in the Containment: Simulant Fuel Studies," Winfrith Technology Centre, AEEW-R2449, United Kingdom (December 1988).

65. F. Gelbard, L. A. Mondy, and S. E. Ohrt, *Statistical Physics* 62, 945 (1991).*

66. B. H. McDonald, "Comparison of the Physical Models and Numerical Methods Used for the GREST LWR Code Comparison Exercise," CSNI Report No. 116 Addendum, OECD Nuclear Energy Agency, Paris (1988).

67. J. E. Brockmann, Sandia National Laboratories, "Range of Possible Dynamic and Collision Shape Factors," Appendix F, R. J. Lipinski et al., *Uncertainty in Radionuclide Release Under Specific LWR Accident Conditions*, SAND84-0410, Vol. 2, February 1985.†

68. R. Adams, "Behavior of U_3O_8, Fe_2O_3, and Concrete Aerosols in a Condensing Steam Environment," p. 129 in *Proceedings Eleventh Water Reactor Safety Research Meeting*, Vol. 3, USNRC Report NUREG/CR-0048, January 1984.†

69. L. Talbot, R. K. Cheng, R. W. Schefer, and D. R. Willis, *J. Fluid Mechanics* 101, 737 (1980).*

70. J. A. Gieseke and H. Jordan, "Aerosol Deposition in BWR Steam Separators and Dryers," NP-5597, Electric Power Research Institute, January 1988.

71. V. J. Novick, *Aerosol Sampling and Transport Tube Plugging Criteria, American Association for Aerosol Research 1990 Abstract Book* (American Association for Aerosol Research, Philadelpha, PA), p. 46.

72. G. D. Fulford, M. Moo-Young, and M. Babu, *Canadian J. Chem. Eng.*, 49, 553 (1971).*

73. D. Y. H. Pui, F. Romay-Novas, and B. Y. H. Liu, *Aerosol Science and Technology* 7, 301 (1987).*

74. Y. S. Chen and C. S. Wang, *Atmos. Environ.* 15, 301 (1981).*

75. R. I. Crane and R. L. Evans, *J. Aerosol Sci.* 8 , 161 (1977).*

76. Y. Ye and D. Y. H. Pui, *J. Aerosol Sci.* 21, 1689 (1990).*

77. P. Kindler, M. A. Elliot, B. K. Stehenson, and M. J. Matteson, *J. Aerosol Science* 22, 259 (1991).*

78. B. Y. H. Liu and J. K. Agrawal, *J. Aerosol Science* 5, 145 (1974).*

79. F. J. Rahn, "The LWR Aerosol Containment Experiments (LACE) Program," LACE TR-012, (EPRI NP-6094-D), Electric Power Research Institute, November 1988.

80. "The Marviken - Fifth Series: Aerosol Transport Test 4 Results," MXE-204, Marviken, Studsvik (November 1985).

81. M. H. E. Ball, F. R. Brighton, and J. P. Mitchell, "Commissioning of the Winfrith Aerosol Deposition and Pipe Flow Facility (ADPFF)," AEA Technology, AEA TRS 5077 GNSR (DEn/TWP/P(91)44, Winfrith, United Kingdom (February 1991).

82. M. Corn, "Adhesion of Particles," *Aerosol Science*, C. N. Davies, Ed., (Academic Press, 1966), Chapter XI.

83. C. G. Benson and B. R. Bowsher, "Physical Resuspension and Revaporization Phenomena in Control Rod Aerosols," Winfrith Technology Centre, AEEW-R2427, United Kingdom (December 1988).

84. A. Fromentin, "Particle Resuspension from a Multi-Layer Deposit by Turbulent Flow," PSI-Bericht Nr. 38, Paul Scherrer Institut, Switzerland (September 1989).

85. A. L. Wright and W. L. Pattison, "Results from Simulated Upper Plenum Aerosol Transport and Aerosol Resuspension Experiments," *Proceeding CSNI Specialists' Meeting on Nuclear Aerosols in Reactor Safety Sept. 4–6, 1984 in Karlsruhe, FRG*, KfK-3800, CSNI-95, Kernforschungszentrum Karlsruhe, Germany (February 1985).

86. M. W. Reeks and D. J. Hall, *J. Fluids Eng.* 110, 165 (1988).*

87. A. Alonso, R. Bolado, and B. Hontanon, "Aerosol Resuspension in the Reactor Cooling System of LWRs Under Severe Accident Conditions," Commission of European Comunities Report EUR 13789 Italy (1991).

88. G. Agrati et al., "Simplified Tests on Resuspension Mechanisms - Preliminary Description of the Project," Ente Nazionale per l'Energia Elettrica, N6/91/01/MI, Milan, Italy (June 1991).

89. M. Donahue, M. Hazzan, J. Metcalf, and E. Warman, "An Analysis of Retention Revaporization in a Mark-II Power Plant," *Source Term Evaluation for Accident Conditions*, International Atomic Energy Agency, IAEA-SM-281/23, Vienna, Austria (1986).

90. IDCOR, "Peach Bottom Atomic Power Station Integrated Accident Analysis," Atomic Industrial Forum, Bethesda, Md., 1983.

91. C. G. Benson and B. R. Bowsher, "Physical Resuspension and Revaporization Phenomena in Control Rod Aerosols," Atomic Energy Authority, AEEW-R2427 Winfrith, United Kingdom (December 1988).

92. D. A. Powers and P. Bieniarz, "Influence of Chemical Form on Cesium Revaporization from the Reactor Coolant System," *Proceedings Symposium on Chemical Phenomena Associated with Radioactivity Releases During Severe Nuclear Plant Accidents*, S. J. Niemczyk, Ed., USNRC Conference Proceedings NUREG/CP-0078, June 1987.†

*Available in public technical libraries.
†Available for purchase from the National Technical Information Service, Springfield, VA 22161.

4.3 Description of Major Experimental Programs

A large number of experiments have been undertaken to provide data on fission product transport phenomena. These studies range from small-scale, separate-effects experiments designed to provide input data to the modeling codes to large-scale, integral experiments designed to test the coupling between individual models and allow the source term programs to be validated.

All the major programs are summarized in Table 4.1. This table groups the experiments in terms of the key phenomena. More details of these experiments can be found through the cited references and in Sects. 4.2 and 4.5.

Table 4.1 Summary of major fission product transport (primary circuit) experimental programs

Phenomena	Laboratory/Country	Manager	Description	Duration	Footnotes[a]
		Vapor-phase phenomena			
1. Thermodynamics and speciation	AEA (UK) ECN Petten (NL) Brussels University (Belgium) BCL (USA)	Bowsher Cordfunke Drowart Alexander	Provision of thermodynamic quantities for condensed and vapor-phase species using wide range of calorimetric, spectroscopic, and other techniques. Supporting capability in critical assessments of data.	1985– 1970– 1970–1990 1970	1,2 1,2 2 3
2. Vapor condensation	ORNL (USA)	Osborne/ Lorenz	HI and VI tests including analyses of condensation profiles along a thermal gradient by Norwood.	1975–1993	4
	AEA (UK)	Taylor/ Dickinson	Analyses of deposition profiles along thermal gradient tube of fission products released from simulant and irradiated fuel.	1965–1975/ 1985–1992	5,6
	Grenoble (France)	Leveque	VERCORS experiments involving heating irradiated and freshly re-irradiated pellets to 2800°C and thermal gradient.	1991–	7
	VTT (Finland)	Jokiniemi	Vapor condensation (fission product and bulk materials simulants) in a laminar flow reactor at controlled flow rates and temperature gradient.	1994–	8
3. Vapor interactions	SNL (USA)	Powers/Elrick	Data on CsI, CsOH and Te interactions with stainless steel and Inconel.	1982–1986	9
	BMT (USA)	Genco	Data on I_2 and HI interactions with stainless steel	1965–1970	10
	AEA (UK)	Bowsher/ Newland	Data on CsOH, Te, I_2 and HI interactions with stainless steel and aerosol substrates (Cd, MnO, CsI, Ag).	1984–	11
	ORNL (USA)	Spence/Beahm	Data on interaction of radiolabeled fission product compounds (CsI, CsOH and Te) with aerosol substrates (Ag, Mn_2O_3, Cr_2O_3, Fe, Fe_2O_3, SnO_2, and Ni). Some studies of interaction of I_2 and HI with aerosols for ACE program.	1983–1991	12,13

Table 4.1 (continued)

Phenomena	Laboratory/Country	Manager	Description	Duration	Footnotes[a]
3. Vapor interactions (cont.)	AECL (Canada) BCL (USA)	Wren Alexander	Analyses of CsI-H_2 equilibrium of relevance to interaction with stainless steel.	1985–1986	14
	Grenoble (France)	Leveque	DEVAP program to follow vapor deposition of CsI, CsOH, and Te on oxidized stainless steel and Inconel surfaces. AERODEVAP to study the influence of Sn- and Cd-bearing aerosols on the vapor interaction.	1990–	7
	Rossendorff (Germany)	Rettig	Program to follow absorption of radiolabeled fission product compounds on surfaces planned to begin in SPAREX facility in 1993.	1993–	15
	Siemens (Germany)	Hellman	Interaction of HI and I_2 with Inconel and stainless steel.	1990-	16
	VTT (Finland)	Jokiniemi	Gas-particle reaction rates (for fission product and inactive simulants) at high temperatures before condensation in a laminar flow reactor at controlled vapor and seed rates and temperature.	1994–	8
		Aerosol nucleation and transport			
4. Nucleation	AEA (U.K.)	Bowsher	Studies of nucleation as functions of temperature and pressure; work planned to follow control rod nucleation at 3.5 MPa.	1987–	17
	VTT (Finland)	Jokiniemi	Aerosol formation (fission product and inactive simulants) by homogeneous nucleation in a laminar flow reactor at controlled vapor feed rate and temperature gradient.	1994–	8
5. Aerosol growth and characterization	Grenoble (France)	Leveque	Characterization of fuel and control rod, aerosols in HEVA program involving irradiated and freshly re-irradiated pellets (program conducted from 1983 and extended through VERCORS—first phase from 1991 and second phase from 1994).	1983–	18

Table 4.1 (continued)

Phenomena	Laboratory/Country	Manager	Description	Duration	Footnotes[a]
	ORNL (USA)	Parker	Characterization of fuel, control rod and boric acid aerosols in an extensive series of induction furnace test.	1960–1988	19
	AEA (UK)	Bowsher	Characterization of control rod and boric acid aerosols.	1984–	20,21
6. Aerosol transport	ORNL (USA)	Wright	Aerosol transport and deposition studies (ATT program) to provide data for validation of TRAPMELT.	1983–1987	22
	Cadarche (France)	Albiol	Aerosol transport studies in TUBA to investigate thermophoretic removal processes.	1991–1993	23
	Cadarache (France)	Albiol/ Sabathier	TRANSAT program to study aerosol removal processes.	1992–	23
	AEA (UK)	Ball	Studies of aerosol transport and deposition in pipes of different cross section and diameter for comparison against ATLAS calculations.	1991–	24
	AEA (UK)	Benson	Falcon tests to follow transport of aerosols through primary circuit and containment. Two experiments form basis of CSNI International Standard Problem.	1985–	25
	BCL (USA)	Gieseke	Aerosol transport studies to provide data for testing TRAPMELT.	1980–1985	26
	Inhalation Toxicology Research Institute (USA)	Yeh	Small-scale studies on self-charging of ^{198}Au-labelled and $^{238}PuO_2$ aerosols.	1975–1977	27
7. Resuspension	AEA (UK)	Benson	Studies of control rod aerosol, with comparison against empirical model.	1987	28
	NE (UK)	Reeks	Sophisticated single-particle studies for comparison against mechanistic model.	1985–1990	29
	ORNL (USA)	Wright	Resuspension tests—mostly in dry atmospheres, but limited study conducted in condensing environment.	1984–1988	22
	PSI (Switzerland)	Fromentin	Limited experimental program for comparison with model.	1984–1988	30

Table 4.1 (continued)

Phenomena	Laboratory/Country	Manager	Description	Duration	Footnotes[a]
	Ispra (CEC/Italy)	De Santi	Planned STORM program to investigate aerosol transport and resuspension.	1994–	31
8. Revaporization	AEA (UK)	Newland	Separate effects tests using Knudsen cell mass spectrometry undertaken in support of integral Falcon experiments.	1990–	32
		Large-Scale Tests			
Marviken-V	Studsvik (Sweden)	Collen	Full-scale simulant studies to follow deposition behavior of fission products (CsI, CsOH, Te) and structrual material aerosols (Ag, Mn) in the primary circuit in order to validate modeling codes.	1983–1985	33
LOFT FP	Idaho INEL (USA)	Coryvell	Loss of fluid tests, two fission product transport tests to investigate fission product transport in just-beyond design basis and severe accident situations.	1984–1986	34
PBF-SFD	Idaho INEL (USA)	Hobbins	Severe fuel damage tests to investigate fission product release and timing of fuel degradation. Final test included effects of control rod alloy on fission product behavior.	1982-1986	35
STEP	EPRI (USA)	Vogel Hercey	Source Term Experimental Program: in-core studies in TREAT facility of aerosol release and fuel damage.	1984–1987	36
LACE	HEDL-EPRI (USA)	Rahn	LWR Aerosol Containment Experiments: aerosol containment studies with two containment-bypass experiments to assess attenuation in the primary circuit pipework and release to the auxiliary building.	1985–1988	22
ACE	HEDL-ORNL-AECL-EPRI (USA-Canada)	Merilo	Advanced Containment Experiments: analyses of vapor-aerosol interactions in CSTF supported by separate-effects studies.	1988–1992	37
ACRR-ST	Sandia (USA)	Reil	Source term experiments conducted in Annular Core Research Reactor (ACRR).	1985–1988	38

Table 4.1 (continued)

Phenomena	Laboratory/Country	Manager	Description	Duration	Footnotes[a]
Phebus-FP	CEA-CEC (France)	Tattegrain von der Hardt	Major fission product release and transport studies planned in the 1990s.	1993–	39

[a]Footnotes:

1. R. G. J. Ball et al., "Thermochemical Data Acquisition," AEA TRS 5068, CEC Report EUR 14004 EN (1991).
2. R. G. J. Ball et al., "Fission Product Thermodynamic Data," AEA RS 5254, CEC Report EUR 14844 EN (1992).
3. C. A. Alexander and J. S. Ogden, "Thermodynamic Activities in Zircaloy-4 Mass Spectrometry," *J. Nucl. Mater.*, 175, 1997 (1990).
4. K. S. Norwood, "Assessment of Thermal Gradient Tube Results from the HI Series of Fission Product Release Tests," USNRC Report NUREG/CR-4105, 1985.
5. D. A. Collins, A. E. McIntosh, R. Taylor, and W. D. Yuille, "Experiments Relating to the Control of Fission-Product Release from Advanced Gas-Cooled Reactors," *J. Nucl. Energy*, 20, 97 (1966).
6. B. R. Bowsher, S. Dickinson, and A. L. Nichols, "High Temperature Studies of Simulant Fission Products, Part I: Vapour Deposition and Interaction of Caesium Iodide, Caesium Hydroxide and Tellurium with Stainless Steel" AEEW-R 1697 (1983).
7. J.-P. Leveque, CEN Grenoble, France, private communication, 1993.
8. J. Jokiniemi, VTT, Technical Research Centre of Finland, private communication, 1993.
9. R. M. Elrick, R. A. Sallach, A. L. Ouellette and S. C. Douglas, "Reactions Between Some Caesium-Iodine Compounds and the Reactor Materials 304 Stainless Steel, Inconel 600 and Silver," USNRC Report NUREG/CR-3197, 1984.
10. J. M. Genco, W. E. Berry, H. S. Rosenberg, and D. L. Morrison, "Fission Product Deposition and its Enhancement Under Reactor Accident Conditions: Deposition on Primary-System Surfaces." BMI Report BMI-1863, 1969.
11. J. Henshaw, M. S. Newland and S. J. Wood, "Thermogravimetric Studies of Vapour-Aerosol Interactions," AEA TRS 5074 (1991).
12. R. D. Spence and A. L. Wright, "The Importance of Fission Product/Aerosol Interactions in Reactor Accident Calculations," *Nucl. Technol.*, 77, 150 (1987).
13. E. C. Beahm, M. L. Brown and W. E. Shockley, "Adsorption of Iodine on Aerosols," ACE Report ACE-TR-B5 (1990).
14. R. D. Wren, R. K. Rondeau, and M. D. Pellair, "Studies on the Radiation Stability of Cesium Iodide: Final Report," EPRI-NP-6344 (1989).
15. D. Rettig, Forschungszentrum Rossendorff, Germany, private communication, 1992.
16. F. Funke and S. Hellmann, "Reaction of Iodine with Stainless Steel," KWU Siemens, to be published as CEC Report, 1993.
17. E. R. Buckle and B. R. Bowsher, "Theoretical Calculations of Primary Particle Condensation for Cadmium and Caesium Iodide Vapours," AEEW-R 2414 (1988).
18. G. Le Marois and R. Warlop, "Source Term Experiments for Fission Product Transport Assessment: The HEVA Programme," International ANS/ENS Conference, Avignon, France, October 2-7, 1988.
19. G. W. Parker, "Chemistry of Nuclear Reactor Accidents: Problems and Progress," *Process of ACS Symposium on Chemical Phenomena Associated with Radioactivity Releases During Severe Nuclear Plant Accidents, September 9-12, 1986, Anaheim, USA, USNRC Conference Proceedings* NUREG/CP-0078, 2-1, 1987.
20. B. R. Bowsher et al., "Silver-Indium-Cadmium Control Rod Behaviour During a Severe Reactor Accident," AEEW-R 1991 (1986).
21. A. B. Anderson, A. N. Beard, P. J. Bennett, and C. G. Benson, "Characterization of Boric Acid Aerosol Behaviour and Interactions with Stainless Steel," AEA TRS 5091 (1991).
22. F. J. Rahn, J. Collen, and A. L. Wright, "Aerosol Behaviour Experiments on Light-Water Reactor Primary Systems," *Nucl. Technol.*, 81, 158 (1988).
23. T. Albiol, CEC Cadarache, France, private communication, 1992.
24. M. H. E. Ball, F. R. Brighton, and J. P. Mitchell, "Commissioning of the Winfrith Aerosol Deposition and Pipe Flow Facility (ADPFF)," AEA TRS 5077 (1991).
25. A. M. Beard, P. J. Bennett, B. R. Bowsher, and J. Brunning, "The Falcon Programme: Characterization of Multicomponent Aerosols in Severe Nuclear Reactor Accidents," *J. Aerosol Sci.*, 23, S831 (1992).
26. J. A. Gieseke et al., Battelle Columbus Laboratory, "Radionuclide Release Under Specific LWR Accident Conditions," BMI-2104, Vols. I-VII, 1984.
27. H. C. Yeh, G. J. Newton, O. G. Raabe and D. R. Boor, "Self-charging of ^{198}Au-labelled Monodisperse Gold Aerosols Studied with a Miniature Electrical Mobility Spectrometer," *J. Aerosol Sci.*, 7, 245 (1976).
28. B. R. Bowsher and C. G. Benson, "Physical Resuspension and Revaporization Phenomena in Control Rood Alloy Aerosols," AEEW-R 2427 (1990).
29. M. W. Reeks, J. Reed, and D. Hall, "On the Resuspension of Small Particles by a Turbulent Flow," *J. Phys. D: Appl. Phys.*, 21, 574 (1988).
30. A. Fromentin, "Dry Resuspension: State of the Art," PhD Thesis, Swiss Federal Institute for Reactor Research, Wurenlingen, 1987.
31. G. Agrati et al., "STORM: Simplifed Tests on Resuspension Mechanisms," CEC JRC Ispra, private communication, 1991.
32. S. Dickinson, "Resuspension of Caesium from Stainless Steel," AEEW-R 2473 (1989).
33. J. Collen, H. Unnebeg, and D. Mecham, "Overview of Marviken Experimental Procedures," *Proc. of ANS Meeting on Fission Product Behaviour and Source Term Research, July 15-19, 1984, Snowbird, USA*, NP-4133-SR, 20-1, 1985.
34. E. Coryell, Idaho National Engineering Laboratory, USA, private communication, 1990.
35. R. R. Hobbins, D. A. Petti, and D. L. Hagrman, "Fission Product Release from Fuel Under Severe Accident Conditions," *Nucl. Technol.*, to be published, 1993.
36. J. K. Fink et al., "Chemical Characteristics of Material Released During Source Term Experiments Project (STEP) In-Pile Tests," *Proc. of ACS Symposium on Chemical Phenomena Associated with Radioactivity Releases During Severe Nuclear Power Accidents, September 9-12, 1986, Anaheim, USA*, NUREG/CP-0078, 2-79, 1987.
37. R. L. Ritzman, "Overview of the ACE Iodine Project," *Proc. of Third CSNI Workshop on Iodine Chemistry, Tokai-Mura, Japan, September 11-13, 1991*, NEA/CSNI/R(91) 15, JAERI-M 92-012, 98, 1992.
38. K. O. Reil, Sandia National Laboratories, USA, private communication, 1988.
39. P. Van der Hardt and A. Tattegrain, "The Phebus Fission Product Project," *J. Nucl. Mater.*, 188, 115 (1992).

The remainder of this section provides more details of those experimental programs (typically involving integral tests) for which the data are available in the open literature and have been used for comparison with calculations made by primary circuit codes (as described in more detail in Sect. 4.5).

4.3.1 Marviken-V Aerosol Transport

The Marviken-V Aerosol Transport tests were conducted between 1983 and 1985 to study the transport and attenuation of aerosols and volatile fission products within typical light-water reactor (LWR) primary systems under conditions simulating severe accidents.[1] Nonradioactive materials were used to determine the transport properties of volatile fission products (fissium) and bulk materials' aerosols (corium) through a large-scale reactor system with a steam atmosphere. The fissium and corium mixtures simulated the materials volatilized during the early stages of a severe accident; thus, the fissium consisted of cesium iodide, cesium hydroxide, and tellurium, and the corium was a mixture of elemental silver and manganese oxide.

The test facility is shown in Fig. 4.2 (for the arrangement adopted for the final test) and consisted of an aerosol generation system, reactor vessel (160 m^3) with simulated LWR internals, pressurizer (50 m^3), relief tank (50 m^3), and filter. Five main tests of increasing complexity were conducted; the main features of these experiments are summarized in Table 4.2 (taken from Ref. 2). Although a number of problems were experienced with these tests (notably in meeting the aerosol input specifications and closing the mass balance), this program represents a valuable source of data on aerosol transport for code assessment (reflected in the number of analyses described in Sect. 4.5.3).

4.3.2 LWR Aerosol Containment Experiments

The LWR Aerosol Containment Experiment (LACE) program was established to study aerosol behavior in the containment and pipework of an LWR under severe accident conditions.[3] The experiments were conducted between 1985 and 1987. Although the main interest was in aerosol behavior within the containment, two tests (LA1 and LA3) focused on containment bypass sequences. These tests involved passing a simulant aerosol mixture (soluble cesium hydroxide and insoluble manganese oxide) along a complex test pipe 63 mm in diameter, 27 m long with five 90° bends, four horizontal sections, and two vertical test sections.

Test LA3 consisted of a series of three experiments in which the gas flow rate and aerosol composition were varied between tests (Fig. 4.3). In addition to the main LACE tests, the program included three containment bypass scoping tests (designated CB 1 to 3). A diagram of the aerosol generator, test assembly, and simulated auxiliary building used in these tests is shown in Fig. 4.4 (taken from Ref. 2). The conditions of the LACE and CB tests are summarized in Table 4.3 (taken from Ref. 2). Although the main emphasis of the LACE tests was on aerosol behavior in the containment, these experiments were well instrumented and provide an important data base on aerosol transport within primary circuit pipe work.

4.3.3 Oak Ridge Aerosol Transport and Resuspension Tests

A series of experiments was performed at Oak Ridge National Laboratory between 1985 and 1988 to provide data with which to validate aerosol models within the TRAPMELT code.[2] Two types of experiment were conducted:

- aerosol transport tests to investigate aerosol wall plateout in a vertical pipe geometry simulating conditions in the upper plenum of the reactor vessel and
- aerosol resuspension tests to provide a data base on resuspension from which analytical models can be developed.

The main components of the former tests are a plasmatorch aerosol generator system, a vertical test pipe, and associated temperature measurement and aerosol sampling equipment. The main features of the apparatus are illustrated in Fig. 4.5 (taken from Ref. 2); the experimental conditions for the four main tests (A105 to A108) are summarized in Table 4.4.

The aerosol resuspension tests (ART) are summarized in Table 4.5, and the apparatus used in these studies is illustrated in Fig. 4.6. Aerosols were initially collected on the interior of a series of 25-mm-diam, 76-mm-long stainless steel tubes [Fig.4.6(*a*)]; after weighing, these tubes were remounted into the second test section [Fig. 4.6(*b*)], and resuspension followed under dry atmospheres (nitrogen gas flow at a Reynolds number ranging from 6,000 to 90,000). These tests provided the first quantitative determination of the extent of resuspension and have been used to generate empirical relationships that have been incorporated into a number of codes.

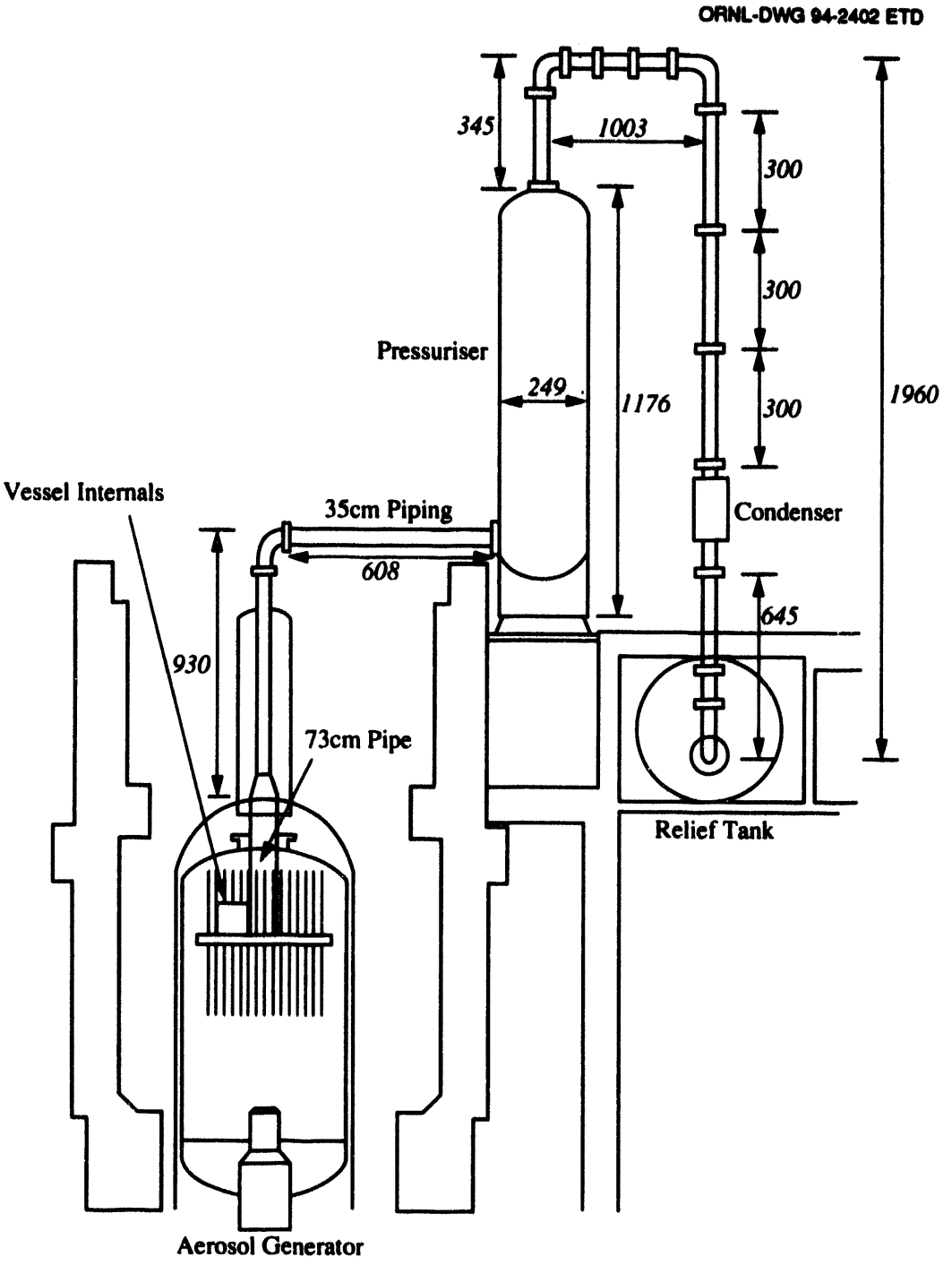

Figure 4.2 Marviken V Test Facility (Test 4)

Table 4.2 Summary of Marviken-V aerosol transport tests[a]

	Test 1 (11/10/83)	Test 2a (03/05/83)	Test 2b (01/17/84)	Test 4 (02/27/85)	Test 7 (07/11/84)
Test duration (min)	**138**	**115**	**118**	**79**	**69**
Aerosol generation					
Gross electrical power, kW	215	204	215	1650	2000
Cesium feed rate, g/s	6.1	8.8	9.6	15	15
Iodine feed rate, g/s	0.047	1.1	0.83	2[b]	1.9
Tellurium feed rate, g/s	1.6	~1.5	1.6	2.3	2.4
Argon feed rate, g/s	0	0	0	53	0
Manganese feed rate, g/s	0	0	0	3.8	0
Total feed, g/s	7.8	~11	12	73	19
Flow					
Total [m^3/h (101.3 kPa, 20°C)]	241	289[c]	235	506	481
Reactor vessel	Not used	Not used	Not used		
Wall temperature, °C				630 to 850	600 to 770
Gas temperature, °C				750 to >1200	~770
Retention, %[d]				30.3	10.9
Piping to pressurizer	Not used	Not used	Not used		
Wall temperature, °C				420 to 490	400 to 450
Gas temperature, °C				480 to 600	460 to 590
Retention, %[d]				7.6	2.5
Pressurizer					
Wall temperature, °C	360 to 430	270 to 350	275 to 385	280 to 350	250 to 300
Gas temperature, °C	365 to 550	300 to 400	285 to 420	290 to 350	300 to 490
Retention, %[d]	32	14	45	24.5	2.5
Piping to relief tank					
Wall temperature, °C	255 to 330	95 to 280	70 to 300	125 to 290	120 to 220
Gas temperature, °C	265 to 370	130 to 300	135 to 315	200 to 300	200 to 290
Retention, %[d]	4.1	0.8	4.6	10.9	19.9
Relief tank					
Water volume, m^3	0	20	19.6	20	20
Fluid temperature, °C	180 to 200	30 to 35	29 to 34	24 to 32	26 to 33
Wall temperature, °C	175 to 185	37 to 44	25 to 30	24 to 32	26 to 33
Retention, (%)[d]	20.1	85.3	49.0	26.1	59.2
Scrubber and condenser		Not used	Not used	Not used	Not used
Water volume, m^3	7				
Fluid temperature, °C	24 to 57				
Wall temperature, °C	20[e]				
Retention, (%)[d]	40				

Table 4.2 (continued)

	Test 1 (11/10/83)	Test 2a (03/05/83)	Test 2b (01/17/84)	Test 4 (02/27/85)	Test 7 (07/11/84)
Test duration (min)	**138**	**115**	**118**	**79**	**69**
Final filter					
Temperature, °C	20[e]	15[e]	20[e]	20[e]	15[e]
Retention, %[d]	0.3	0.1	0.04	0.1	0.2
Measured aerosol concentration (g/m^3)[f]	20 to 40	~80	40 to 50	30 to 120	28 to 60

[a] Intervals for temperatures and concentrations include both local variations and time variations.
[b] Fed for 5 min.
[c] Value uncertain because of steam leakage.
[d] Fraction of total amount recovered.
[e] Nominal value.
[f] At actual conditions. This concentration was measured in the pressurizer for tests 1, 2a, and 2b and in the reactor vessel for tests 4 and 7.

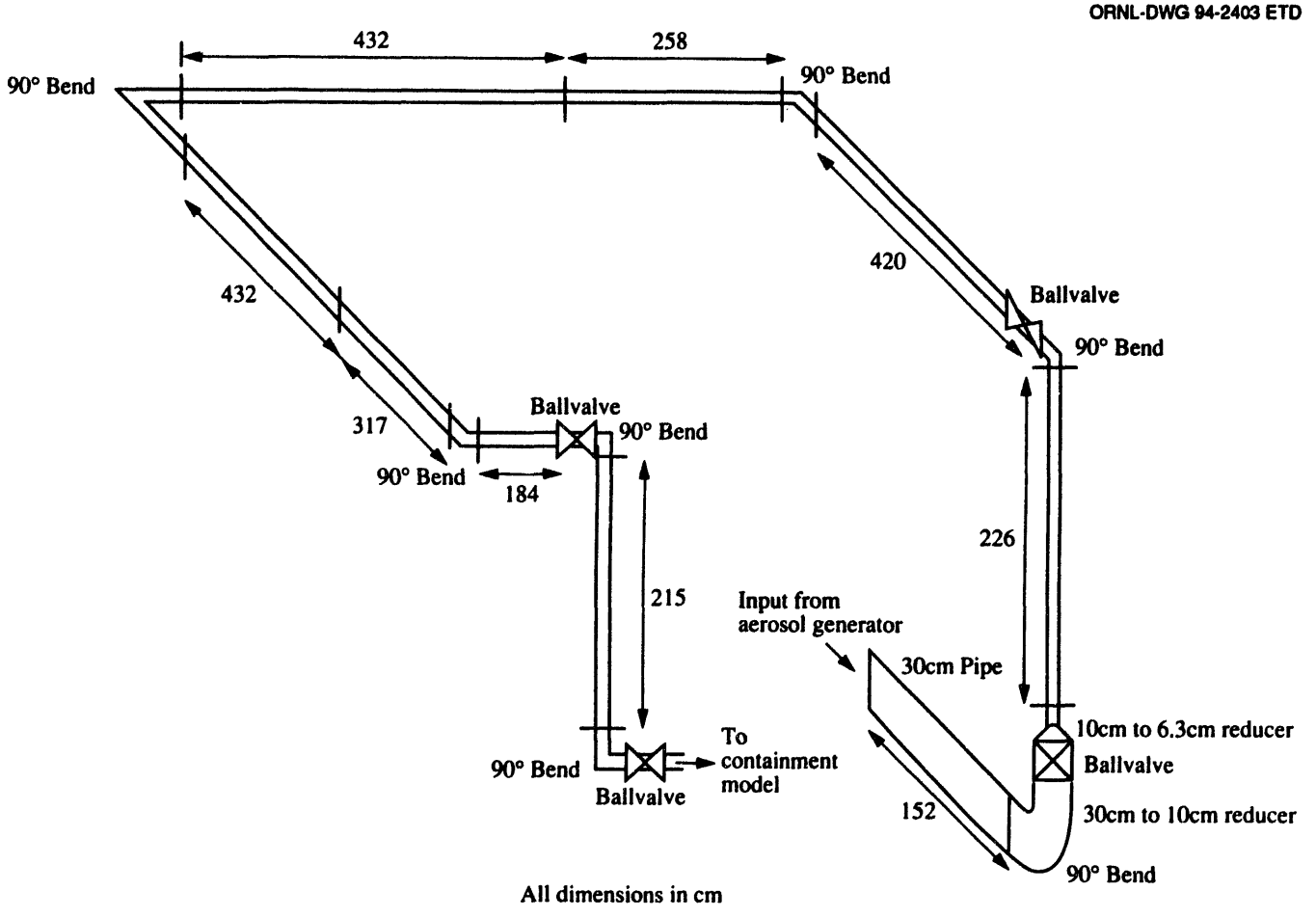

Figure 4.3 Diagram of piping system used in the LACE tests

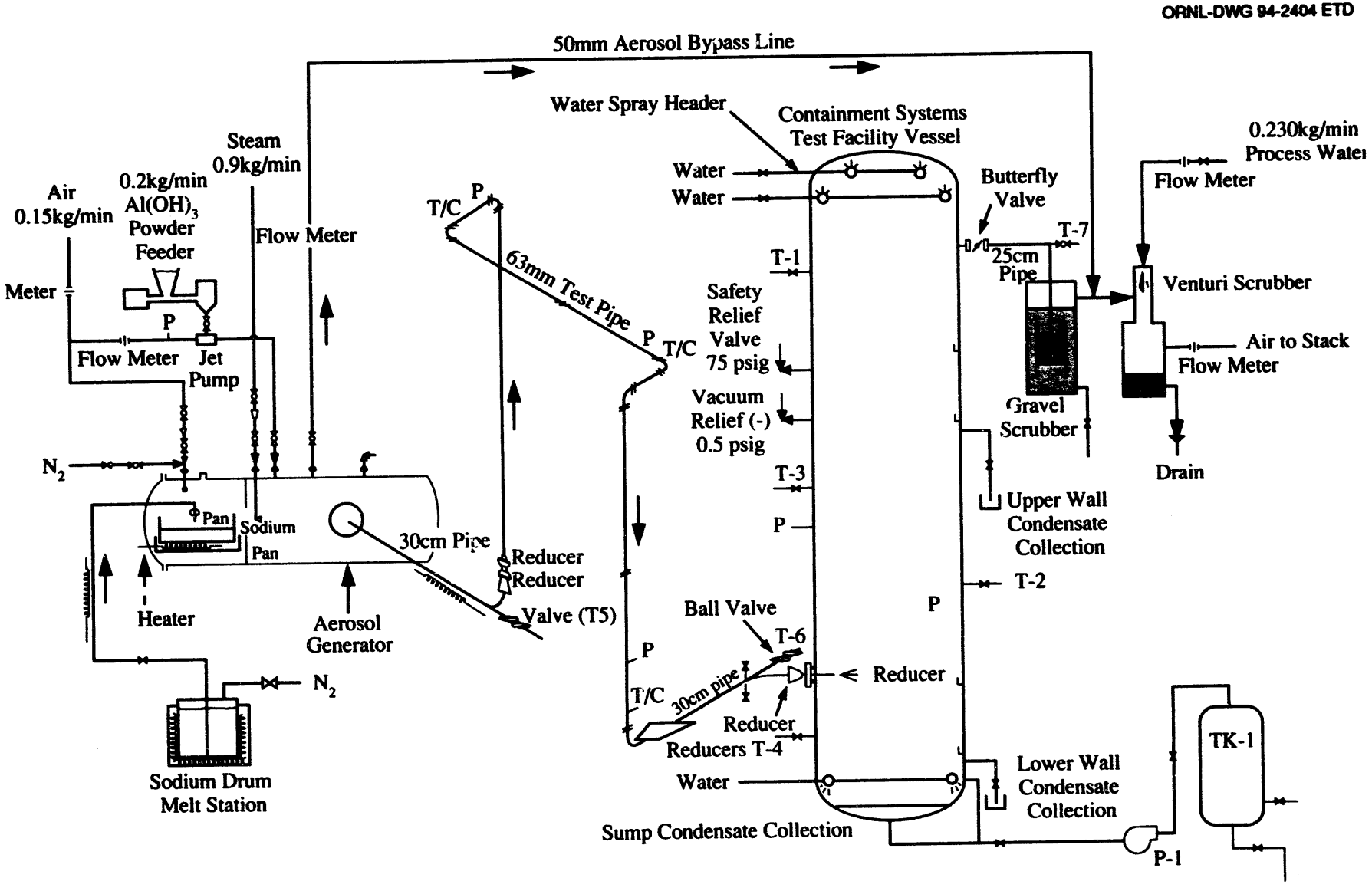

Figure 4.4 Diagram of the aerosol generator and test assembly for CB tests

Table 4.3 Summary of LACE primary circuit tests

Test	Aerosol	Soluble mass fraction	Carrier gas	Gas velocity (m/s)	Temperature (°C)	Degrees superheat (°C)	Auxiliary building conditions
CB1	Soluble NaOH	1.00	Air-steam	100	186	88	Saturated steam/air, 85°C
CB2	Soluble NaOH Insoluble $Al(OH)_3$	0.67	Air-steam	91	111	15	Saturated steam/air, 81°C
CB3	Insoluble $Al(OH)_3$	0	Air-steam	97	160	66	Saturated steam/air, 84°C
LA1	Soluble CsOH	0.18	N_2-steam	96	247	141	Superheated steam/air, 115°C
LA3A	Soluble CsOH Insoluble MnO	0.42	N_2-steam	75	298	208	No auxiliary building
LA3B	Soluble CsOH Insoluble MnO	0.12	N_2-steam	24	303	219	No auxiliary building
LA3C	Soluble CsOH Insoluble MnO	0.38	N_2-steam	23	300	215	No auxiliary building

4.3.4 Falcon

Falcon experiments have been conducted in the UK since 1986 to follow the transport and deposition of fission products released from small-scale representations of severe accidents in LWRs. Simulant and trace-irradiated fuel samples are heated up to 2300 K in the presence (and absence) of typical bulk materials found within the core, some of the primary circuit, and the containment (Fig. 4.7). Various analytical techniques are used to identify and characterize the resulting chemical species and their physical forms. Details of the facility may be found in Ref. 4.

Two main experimental programs were conducted as summarized in Tables 4.6 and 4.7. The initial series of experiments [designated either TG (thermal gradient configuration) or CT (containment configuration)] was designed to provide qualitative assessments of key phenomena. Detailed improvements were made to the thermal-hydraulic and measurement systems on the basis of code analyses of these experiments to enable more quantitative data to be generated for code analysis from the subsequent FAL series of experiments (Table 4.7). Two tests from Falcon are currently being used as the basis of a Committee on the Safety of Nuclear Installations (CSNI) international standard problem (ISP) exercise (ISP No. 34).

Few analyses have been made of fission product transport issues under the rigorous conditions required for an ISP, and considerable international interest has been shown in this work. The small scale of Falcon limits the applicability of some of the data (e.g., most experiments were conducted under laminar flow). However, this small scale also gives flexibility and means that a number of experiments can be conducted cost effectively to investigate specific phenomena. Although many of the early experiments generated only qualitative information, improvements in the facility offer the capability to address key chemistry issues that may arise from the integral Phebus-FP tests.

4.3.5 Power Burst Facility and Loss-of-Fluid Test Experiments

In-pile tests conducted at Idaho National Engineering Laboratory in the 1980s contributed to the understanding of fission product release and transport behavior. The main programs were the Severe Fuel Damage (SFD) experiments 1.1 to 1.4 conducted at the Power Burst Facility (PBF) and the two fission product experiments (LP-FP-1 and 2) conducted as part of the Organization for Economic Cooperation and Development (OECD) Loss-of-Fluid Tests (LOFT) program. Details of the facilities and test matrices are given in Chap. 3 as these programs primarily

1. Plasma Torch Assembly
2. Inlet Cone
3. Lower Sampling Station
4. Slide Valve
5. Lower Pipe Section
6. Centre Sampling Section
7. Centre Pipe Section
8. Upper Sampling Station
9. Upper Pipe Section
10. Transition Section
11. Pyrex Pipe
12. Aerosol Collection Bag

ORNL-DWG 94-2405 ETD

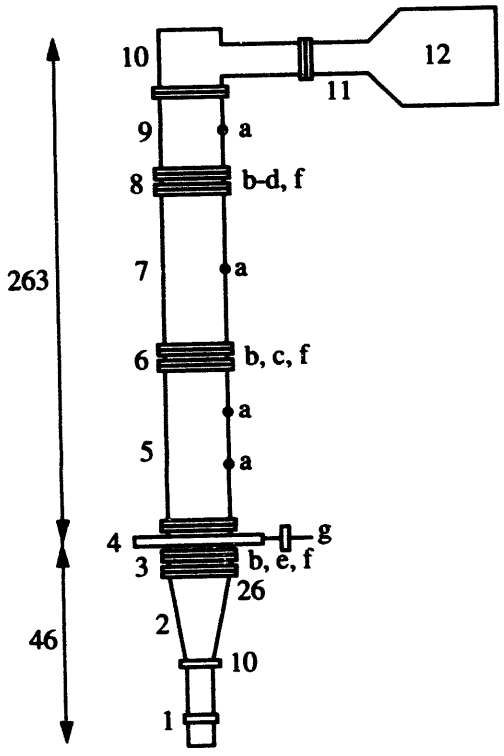

Measurements
a. Gas and Wall Temperatures
b. Aerosol Concentration
c. Agglomerate Size: Impactors
d. Primary Particle Size: Electrostatic Precipitators
e. Primary Particle Size: Settling Sampler
f. Metal-Foil Deposition Samples
g. Final Aerosol Concentration: Slide Valve

All Dimensions in cm

Figure 4.5 ORNL ATT apparatus

Table 4.4 Main parameters of ORNL aerosol transport tests

Test	Aerosol material	Mean flow residence time (s)	Mean test flow velocity (cm/s)	Mean temperature gradient range[a] (°C/cm)
A105	Iron oxide	56	4.7	14 to 56
A106	Iron oxide	26	10.3	20 to 73
A107	Zinc metal	54	4.9	17 to 77
A108	Zinc metal	24	11.2	31 to 88

[a]Values estimated from differences in temperatures measured at pipe wall and at 13 mm from wall.

Table 4.5 Test parameters for ORNL series-2 aerosol resuspension experiments

Test	Aerosol material	Sample mass loading (mg)[a]	Sample loading per unit area (mg/cm^2)[a]
ART-02	Manganese oxide	63	1.13
ART-03	Metallic zinc	72	1.29
ART-04	Iron oxide	82	1.47
ART-05	Tin oxide	332	5.94
ART-06	Metallic manganese	66	1.18
ART-07	Metallic zinc	114	2.04
ART-08	Tin oxide	34	0.61
ART-09	Iron oxide	11	0.20

[a]Average for all tests performed.

provided fission product release data rather than transport data.

4.3.6 Phebus-FP

Phebus-FP represents the major fission product release and transport program planned in the 1990s. The program is sponsored by the Commissariat a l'Energie Atomique (CEA), the Atomic Energy Commission, and the Commission of the European Communities (CEC), with additional support from the international community [notably the U.S. Nuclear Regulatory Commission (NRC), CANDU Owners' Group (COG), Nuclear Power Engineering Corporation (NUPEC), Japanese Atomic Energy Research Institute (JAERI), and Korean Atomic Energy Research Institute (KAERI)]. Most of the major source term phenomena are integrated into one program. Thus, it is planned to follow the release of fission products from a bundle of highly irradiated fuel (heated to induce at least partial melting) through a representative primary circuit and into a containment vessel. A scaling factor of 5000 has been adopted for Phebus-FP, based on the ratio of the fission product inventory in the Phebus bundle to that in a commercial reactor. All tests will be highly instrumented with extensive on-line and posttest analyses.

ORNL-DWG 94-2406 ETD

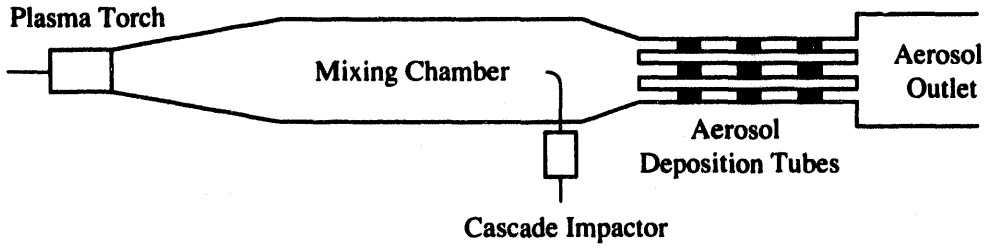

(a) Apparatus for collecting deposition samples (oriented verically)

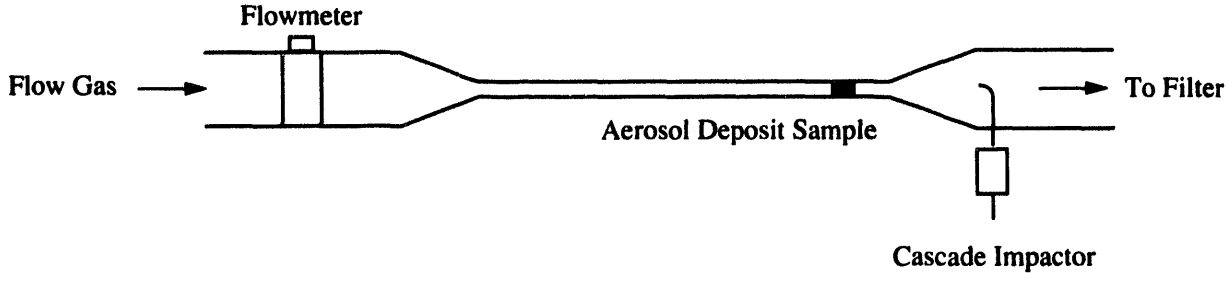

(b) Resuspension test apparatus

Figure 4.6 ORNL ART apparatus

Extensive code analysis studies have been conducted to aid in the test design and selection of parameters. The test matrix includes six tests to be conducted at a rate of one per year beginning in 1993. The first test will use trace-irradiated fuel, with the others using highly irradiated fuel in the range of megawatt day per kilogram uranium (MWd/kgu) burnup. The Phebus-FP experimental facility is shown in Fig. 4.8, and details of the test apparatus are presented in Fig. 4.9. The test matrix is summarized in Table 4.8; note, however, that details of some of the later tests are not yet finalized. In particular, proposals have been made to extend the scope of Phebus-FP to address late-phase issues such as debris bed behavior and air ingress phenomena. This program is also supported by a number of separate-effects tests (some of which are listed in Table 4.1) designed to resolve specific issues. Further details of the program may be found in Refs. 5 and 6.

4.3.7 STORM Project

The STORM project is planned by the Joint Research Centre (JRC) at Ispra for 1994 through 1998 and involves large-scale "single-effects" experiments to study the behavior of fission products and aerosols in reactor components. The experiments are focused on the investigation of the mechanical resuspension of aerosols under turbulent flow conditions involving multicomponent aerosols (soluble and insoluble simulants), multilayer deposits (mass loadings up to 200 mg/cm^2), and a variety of thermal-hydraulic conditions (gas and steam flows up to sonic values). Noninvasive measurement techniques will be used to characterize the gas-borne and deposited aerosols (particle size distributions, density, and shape) for the development and assessment of mechanistic or semi-empirical computer resuspension models. The STORM facility is shown in Fig. 4.10, and further details of the program be found in M. Eusebi et al.*

*M. Eusebi et al., "Preparatory Calculations for a New Experimental Program on Dry Aerosol Resuspension Mechanisms (STORM Project)," European Aerosol Conference, Oxford (UK), September 1992.

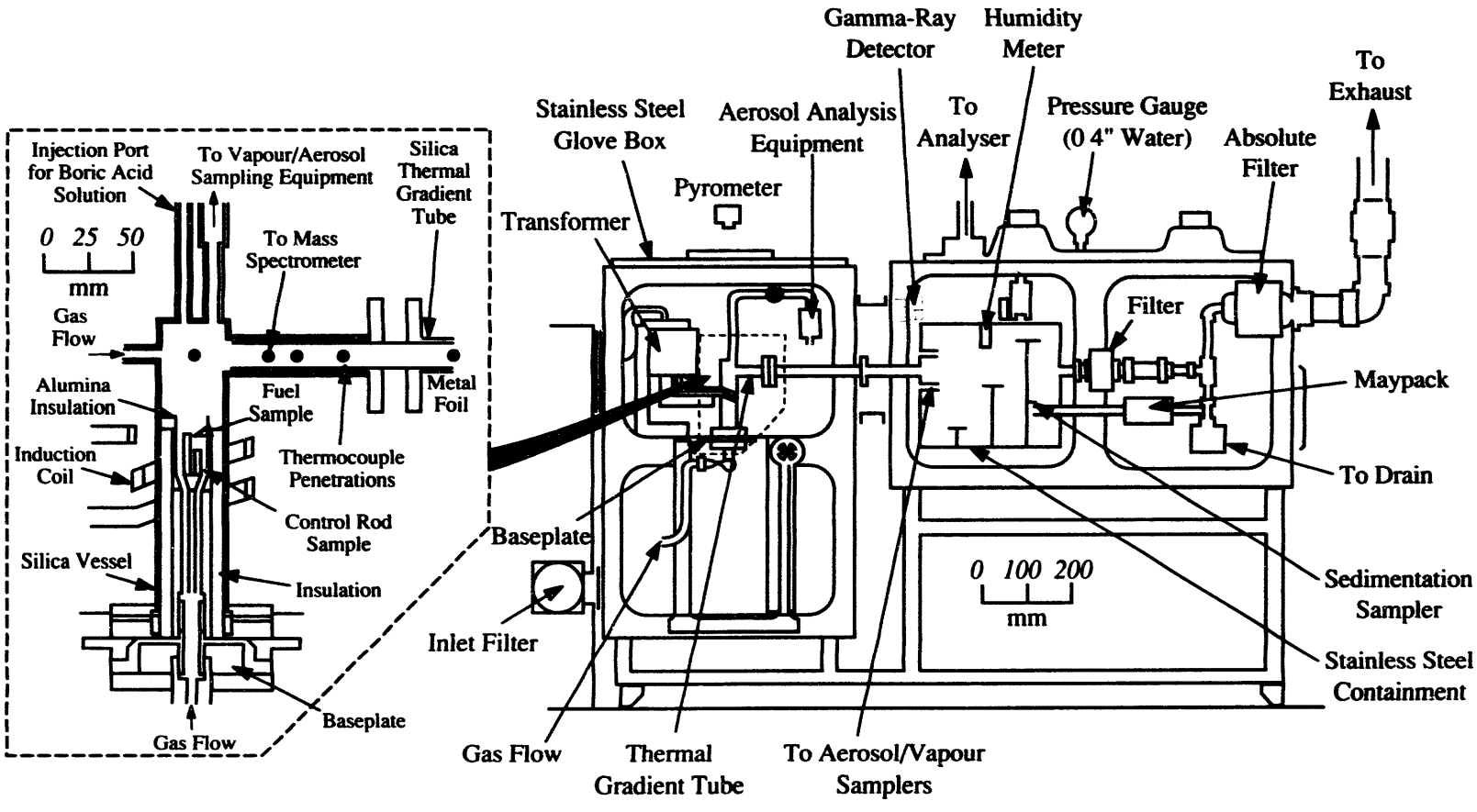

Figure 4.7 Falcon

Table 4.6 Falcon TG and CT series of experiments

Experiment No.	Fuel sample[a]	Control rod sample[b]	% Steam	Time (s)	Temperature (K)
TG-1	X	-	0	1070	~2000
TG-2	-	X	0	870	1670
TG-3	X	X	0	605	2400
TG-4	X_c	-	0	1830	2100
TG-5	X[d]	-	0	1830	1900
TG-6	X[e]	-	0	1860	2080
TG-7	X[e]	X	0	1020[f] 1040[g]	1400[f] 2200[g]
TG-8	-	X	3	1680	1530
TG-9	X	-	3	2200	1730
TG-10	X	X	3	1100[f] 2280[g]	1600[f] 1870[g]
CT-1	-	X	3	315	1700
CT-2	-	X	28	60	1700
CT-3	X	-	3	450	1700
CT-4	X	-	28	660	2200
CT-5	X	X	3	510	1650
CT-6	X	X	3	140	1650

[a]Fuel sample inventory—8.84 mg CsI, 56.94 mg CsOH, 10.64 mg Te, 21.66 mg SrO, 34.42 mg BaO, 55.80 mg Mo, 18.16 g UO_2.
[b]Control rod inventory—1.11 g Cd (5.06%), 17.56 g Ag (79.83%), 3.31 g In (15.07%).
[c]Unirradiated 3.1% enriched fuel sample.
[d]Irradiated at 1.2 kW for 47 min.
[e]Irradiated at 3.0 kW for 3 h.
[f]Estimated temperature at control rod failure.
[g]Estimated temperature at fuel rod failure.

Table 4.7 Falcon FAL-series test matrix

Expt	Configuration	Simulant fuel[a]	Irradiated fuel[b]	Control rod	Boric acid	Atmosphere	Containment humidity (%)	Paint	Sump (pH)	Date (dd.mm.yy)
FAL-1	CT	X	-	-	-	He-8% H_2O[c]	68	-	-	24.10.89
FAL-1A	CT	X	-	-	-	He-16% H_2O	73	-	-	23.04.90
FAL-2	CT	X	-	X	-	He-8% H_2O	52	-	-	02.11.89
FAL-3A[d]	CT	X	-	X	X	He-16% H_2O	95	-	-	28.02.90
FAL-3B[d]	CT	X	-	X	X	He-16% H_2O	88	-	-	14.03.90
FAL-4	CT	X	-	X	X	He-16% H_2O	61	-	-	08.03.90
FAL-5	CT	X	-	X	X	He-27% H_2O	92	-	-	22.03.90
FAL-6	CT	X	-	X	X	He-16% H_2O	88	X	-	08.08.90
FAL-7	CT	X[e]	-	X	X	He-16% H_2O	92	X	X (8)	19.12.90
FAL-8	CT	X	X	X	X	He-16% H_2O	95	X	-	19.09.90
FAL-9	CT	-	X	X	X	He-16% H_2O	85	X	X (5)	31.10.90
FAL-10	CT	-	X	X	X	He-27% H_2O	95	X	X (8)	09.10.90
FAL-11	TG	-	X	X	X	He	-	-	-	14.11.89
FAL-12	CT	-	-	X	-	He-16% H_2O	92	-	-	10.07.90
FAL-13	CT	X	-	X	X	He-16% H_2O	89	X	X (8)	20.08.91
FAL-14	TG	X	-	X	X	He-30% H_2O	-	-	-	27.09.91
FAL-15	CT	X	-	X	X	He-16% H_2O	92	X	X (8)	07.11.91
FAL-16	[f]	X	-	-	-	Vacuum	-	-	-	24.02.92
FAL-17	TG	X	-	X	X	He-3% H_2O	-	-	-	28.04.92
FAL-18	TG	X[e]	-	X	-	He-5 H_2-3% H_2O	-	-	-	18.11.92
FAL-19	CT	X	-	X	X	He-51% H_2O	100	X	X (8)	11.02.93
FAL-20	CT	X[e]	-	X	X	He-5% H_2 <5%H_2O	<80	X	X (8)	12.05.93

Table 4.7 (continued)

Expt	Configuration	Simulant fuel[a]	Irradiated Fuel[b]	Control rod	Boric acid	Atmosphere	Containment humidity (%)	Paint	Sump (pH)	Date (dd.mm.yy)
FAL-ISP-1	CT	X[e]	-	X[e]	X	He-5% H_2O	50	-	-	04.06.92
FAL-ISP-2	CT	X	-	X	X	He-51% H_2O	100	-	-	19.08.92

[a] 18.16 g of depleted UO_2 powder were mixed with 8.84 mg CsI, 56.94 mg CsOH, 10.64 mg Te, 21.66 mg SrO, and 55.80 mg Mo_2.
[b] 22 g of 3.09% enriched UO_2 were clad in Zircaloy-2, irradiated for 3 h at a neutron flux of 6.58×10^{10} neutron $cm^{-2}s^{-1}$ and cooled for 92 h to obtain ~MBq of mixed fission products.
[c] Inlet pipe was maintained at ~20°C, resulting in steam condensation prior to containment.
[d] FAL-3A and 3B were conducted under identical conditions to assess experimental reproducibility.
[e] Experiment with fuel bundle.
[f] Experiment FAL-16 designed to determine vapor phase species at high temperatures and involved matrix isolation-infrared spectroscopy and mass spectrometry.

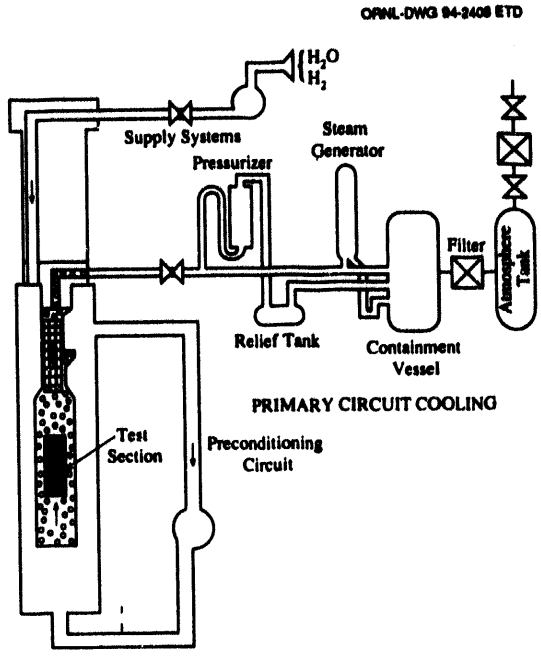

Figure 4.8 Phebus test facility

4.3.8 References

1. J. Collen, H. Unneberg, and D. Mecham, "Overview of Marviken Experimental Procedures," pp. 20–21 in *Proceedings of ANS Topical Meeting on Fission Product Behavior and Source Term Research, July 15–19, 1984, Snowbird, Utah*, NP-4113-SR, Electric Power Research Institute, 1985.

2. F. J. Rahn, J. Collen, and A. L. Wright, "Aerosol Behavior Experiments on Light Water Reactor Primary Systems," *Nucl. Technol.*, 81, 158 (1988).*

3. G. R. Bloom et al., "Status of the LWR Aerosol Containment Experiments (LACE) Program," *Proceedings of the International Symposium on Source Term Evaluation for Accident Conditions, Columbus, Ohio, October 28–November 1, 1985*, International Atomic Energy Agency, 1986.

4. A. M. Beard, P. J. Bennett, B. R. Bowsher, and J. Brunning, "The Falcon Program: Characterization of Multicomponent Aerosols in Severe Nuclear Reactor Accidents," *J. Aerosol Sci.*, 23, S831 (1992).*

5. P. Von der Hardt and A. Tattegrain, "The Phebus Fission Product Project," *J. Nucl. Mater.*, 188, 115 (1992).*

6. *The Phebus Fission Product Project*, Eds., W. Krischer and M. C. Rubinstein (Elsevier Applied Science, London, 1992).*

*Available in public technical libraries.

4.4 Review of Main Computer Codes

Fission product (FP) transport computer codes are designed to predict the behavior of FP vapors and aerosols inside the RCS and to estimate the importance of FP releases to the containment.

A number of computer codes have been developed that are able to model severe accident FP transport phenomena in the RCS. The TRAPMELT code, developed by Battelle Columbus Laboratories (BCL), U.S.A., with the support of the NRC, is considered to be a pioneer of this type; it was first released in 1979. This code represents further development of the TRAP-LOCA code, published by BCL in 1977, which was developed for application to loss-of-coolant accidents. Substantial improvements in FP transport modeling capability have occurred in recent years. A version of TRAPMELT has been developed by Ente Nazionale per l'Energia Elettrica (ENEL). The NRC-supported Cooperative Severe Accident Research Program (CSARP) is the source of the detailed FP release and transport code VICTORIA, first released in 1990. The CEC, through its Shared Cost Action Program, supports an ambitious research program on source term evaluation, which includes development and testing of the ESTER code. The Electric Power Research Institute (EPRI)

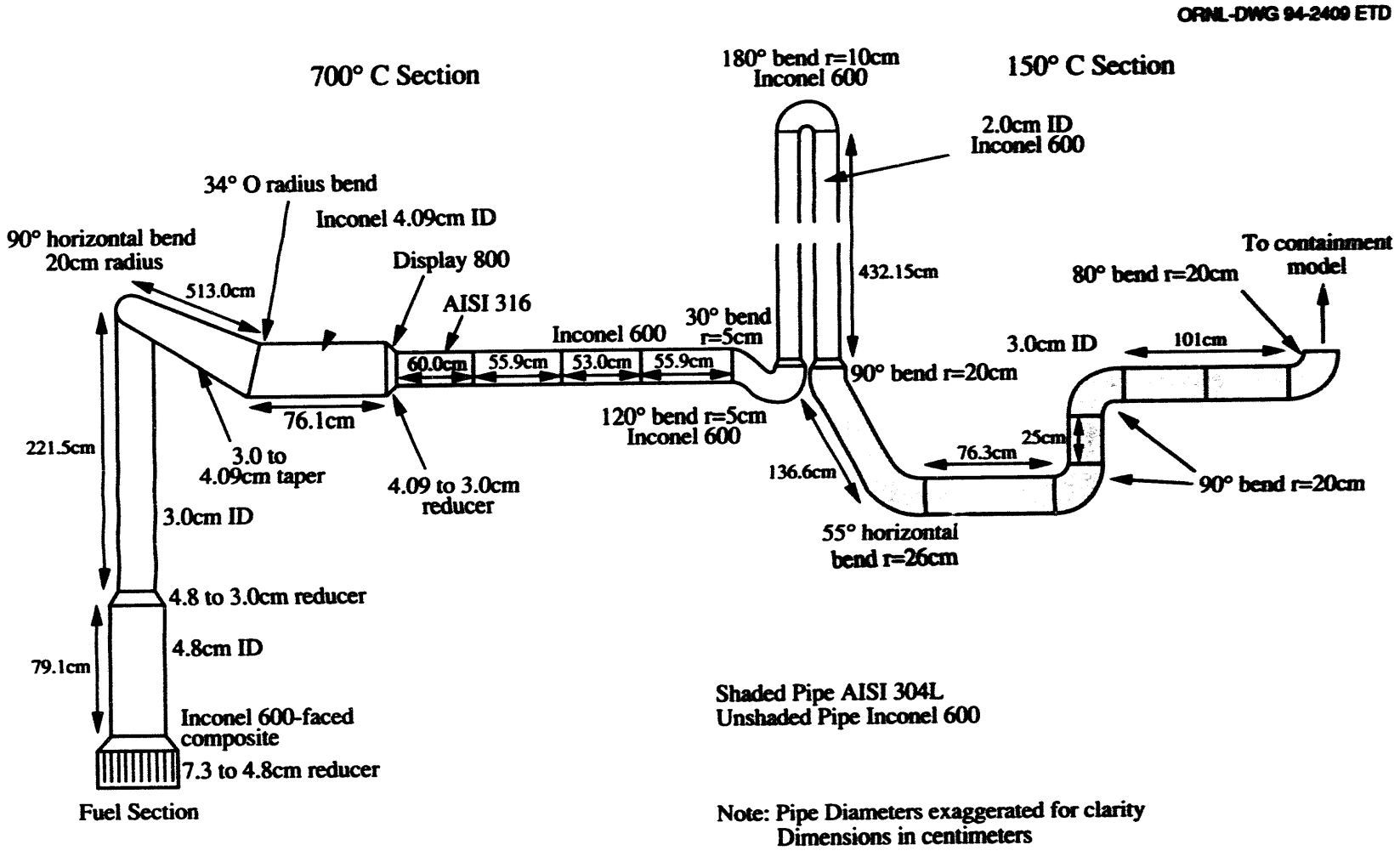

Figure 4.9 Diagram of the test apparatus to be used in the Phebus-FP project

Table 4.8 Phebus-FP test matrix

Test No.	System pressure	Fuel bundle: Burnup (MWd/kgU)	Fuel bundle: Sweep gas H_2/O_2 ratio	Primary circuit	Containment vessel
FPT-0	Low	Fresh, preconditioned	Low	Steam generator, noncondensing	Low humidity, sump water pH: acid
FPT-1	Low	~30, preconditioned	Low	as FPT-0	High humidity, initial pH: neutral
FPT-2	Low	~30, preconditioned	High	Steam generator or minimum line	Not yet defined
FPT-3[a]	Open test with three options: • Back-up test, • High-pressure test, or • BWR and/or advanced fuel test				
FPT-4[a]	Rubble bed test: Fuel degradation up to a molten pool, or FP release and behavior of low-volatile FPs.				
FPT-5[a]	Air ingression test.				

[a]Tests with high burnup fuel—test parameters not yet defined.

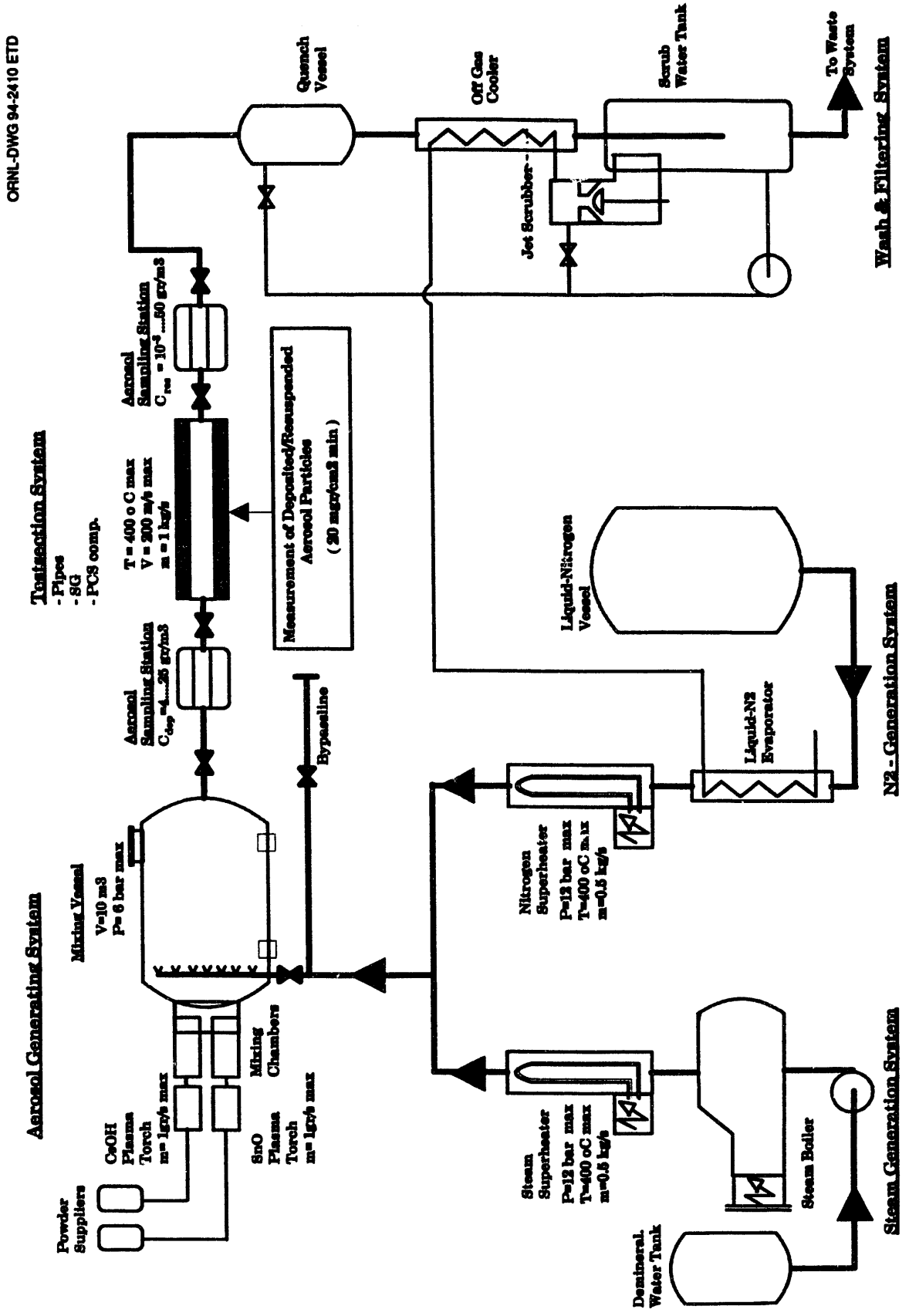

Figure 4.10 STORM facility

supports development of the RAFT code, first released in 1987. NUPEC and JAERI are the source of the MACRES and HORN codes. Developments concerning chemistry subroutines of the MAAP code have been made in the frame of the NORDIC Project.

System codes, which model severe accident phenomena inside the RCS in an integrated way, also incorporate FP transport subroutines and subcodes. Most system codes have developed their FP subroutines as versions of previously published FP transport codes. Some, as is the case of MAAP code, incorporate newly developed subroutines.

FP transport inside the RCS is the result of a number of phenomena that can be classified and linked as shown in Fig. 4.11, taken from Ref. 1. Generally, all FP transport codes calculate aerosol and vapor physical transport and behavior, all codes treat chemical reactions between gaseous phases and surfaces, and a few codes allow for calculation of chemical interactions in the gaseous phases. Thermal hydraulic boundary conditions are usually given as input, with only a few codes capable of being coupled to energy and mass balance codes.

Figure 4.12, taken from Ref. 1, depicts the "physical" phenomena relevant to FP aerosol and vapor transport inside the RCS. All codes model several aerosol agglomeration and deposition mechanisms. Only a limited number of codes can treat liquid phases and pool

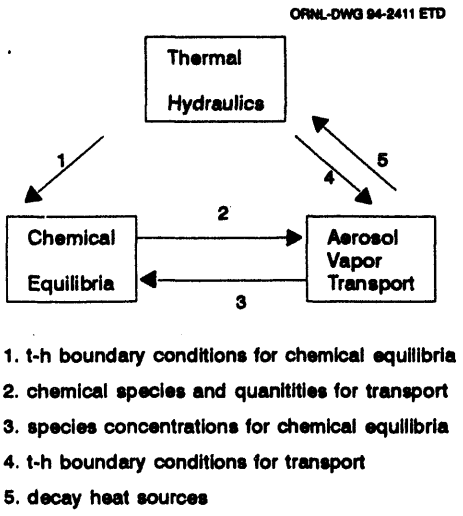

Figure 4.11 Structure of FP transport phenomena

scrubbing, as a steam-hydrogen atmosphere in the RCS is considered to be the most probable situation in an unrecovered accident.

FP-specific codes and the FP transport modules of system codes are described subsequently. The most important phenomena covered and the main features of the calculation methodology have been reviewed. This information has usually been derived from code manuals, which manifest large differences in the quality of the information provided. Tables 4.9 and 4.10 are a summary of the findings of this review.

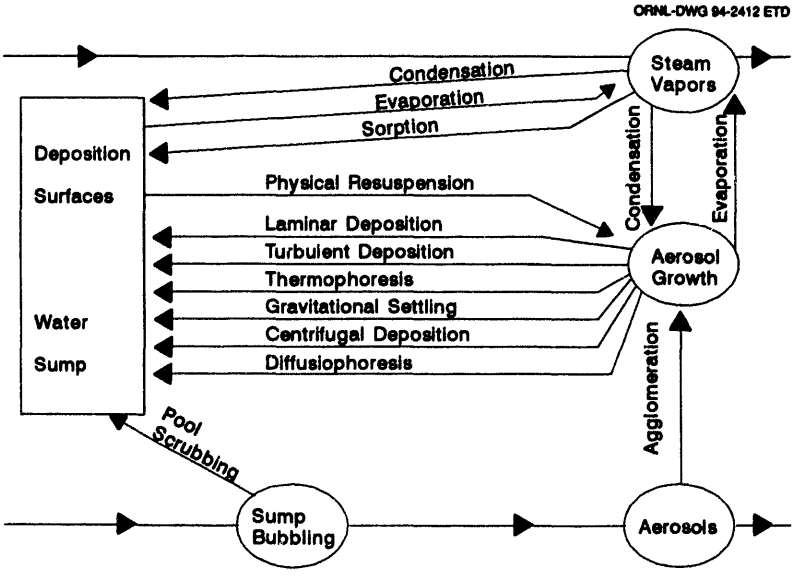

Figure 4.12 Schematic of the transport phenomena considered

Table 4.9 System codes summary

System code	SCDAP/RELAP5 Mod3	MELCOR Version 1.8.2	MAAP Version 3.0B	ESTER	ICARE Version 2.1	ESCADRE	ATHLET
General description	Aerosol and FP Behavior based on TRAPMELT 2.	Aerosol behavior based on MAEROS code. Operates on principle of material classes. Ongoing validation (MCAP program).	Parallel FP and TH treatment. Innovative, simplified aerosol transport model.	Portable software structure. Uses VICTORIA for FP transport calculations. Under development. There is a first running version.	FP transport modules under development, will be based on integration of SOPHIE, AEROSOLS, and TRAP-F. Implicit numerics.	Modular code system. Transport codes are AEROSOLS B2 and SOPHIE.	FP transport module based on TRAPMELT, under development.
Special capabilities	Minor changes from TRAPMELT 2 to treat aerosol behavior. Only I_2, CsI, CsOH, Te, Cd, Ag, and Sn are considered. Energy deposition model to treat FP decay heat.	Vapor condensation model follows TRAPMELT. Decay heat treatment. 15 material classes and limited chemical reactions.	No chemical reactions considered. A number of 12 species are calculated. Tracks energy associated with decay heat. Extensive validation matrix available. Wide use.				

Table 4.10 FP Transport dedicated codes

FP transport code	VICTORIA Version 1992	RAFT Version 1	TRAPMELT 2/3	SOPHIE	AEROSOLS B2	HORN	MACRES	ECART
General description	Internationally developed, mechanistic, very detailed code. Running time can be weeks.	EPRI vapor and aerosol transport code. Running time usually minutes.	Pioneer code. Coupling with MERGE in STCP structure. UK and Italian versions developed. Running time hours.	Vapor transport and deposition module of the French code ESCADRE.	Aerosol transport and deposition module of the French code ESCADRE, for circuits or contain-ments.	JAERI mechanistic code.	NUPEC aerosol and vapor transport code.	Under development, ENEL code based on coupled models.
Aerosol behavior	Aerosol treatment based on CHARM/MAEROS. Limited multicomponent aerosol model. Steam hydrogen mixture.	Detailed nucleation and growth model. Single component aerosol.	Based on QUICK. Single homogeneous aerosol in a steam-hydrogen carrier gas. No resuspension. No model for inertial impaction.		One or two aerosol populations. Dry or wet atmosphere.	Simplified heat and mass transfer models. Only dry conditions.	Limited treatment of homogeneous nucleation and standard aerosol removal mechanisms. Single component aerosol. Growth due to condensation.	TRAPMELT based. Integration with NAUA and SPARC. Water sumps and scrubbing of airborne particles considered.
Chemistry	State-of-the-art chemistry. 25 elements and 288 species chosen by Gibbs energy in all phases. Limited chemisorption and revaporization. Model for vapor condensation onto surfaces and particles.	Gibbs energy minimization procedure adopted for gas phase only. No revaporization. Model for vapor condensation onto surfaces and particles.	Stable chemical forms. Surface reactions for some species. 9 chemical species considered.	Allows condensation/ evaporation and ab-sorption onto walls. Steam-hydrogen mixture. 8 elements including hydrogen and water.	Allows vapor condensation onto particles and particle evaporation.	12 elements and 147 species. Limited to SOLGASMIX treatment.	Gibbs energy minimization procedure. Water existing conditions are treated.	Chemical equilibrium. Condensation/evaporation of chemical species, and reaction with surfaces follows TRAPMELT procedure. Particle growth due to vapor condensation.
Special features	New version includes resuspension of aerosols and chemisorption onto SS and Zircaloy surfaces. Under assessment.	Current version has Lagrangian numerics. Versions developed by users. Project to couple to ESTER.	Development has been stopped. Used in system codes. Extensive validation data available.	Validation ongoing, by DEVAP studies. Langmuir model for physical adsorption.	Validation program ongoing by TUBA and TRANSAT studies.	Limited validation against LOFT-FP-2.	Pool scrubbing included.	Can interface with a number of severe accident codes. Under development in RCA program.

Where available, information has also been included on future code developments and code use and validation.

4.4.1 Codes Dealing Specifically with Fission Product Transport

4.4.1.1 VICTORIA (Version 1992)

4.4.1.1.1 Code Scope

VICTORIA is a mechanistic code designed to model the release, transport, and deposition of fission products inside the RCS during a severe reactor accident.[2] VICTORIA development and validation is an international effort, involving three countries (U.S., U.K., and Canada) and five laboratories (Sandia, Argonne, Oak Ridge, Winfrith, and Chalk River). The overall effort is being coordinated by Sandia National Laboratory, under contract with the NRC.

A new version has recently been released. VICTORIA follows the evolution of 25 different elements and up to 288 species. It requires an initial element distribution and the variation of the pressures, temperatures, velocities, and geometry provided by a core degradation analysis code. The purpose of VICTORIA is to evaluate simplifying assumptions used in probabilistic risk assessment (PRA) analyses and provide guidance for future PRAs. This purpose is accomplished by simultaneously and mechanistically modeling chemical interactions and aerosol physics and transport.

4.4.1.1.2 Code Physical Models

General. The spatial domain of VICTORIA covers the interior parts of a reactor vessel (fuel rods, structural surfaces, and volume normally occupied by the reactor coolant). The spatial domain varies according to the accident progression. Debris beds and molten pools are not covered by the code.

The vessel is discretized into a two-dimensional cylindrical (r,z) Eulerian mesh. Boundary conditions must be prescribed at the outer surfaces of the mesh. The fuel rod can be further separated into several radial fuel zones, gap, and cladding. Within each transport cell are a maximum of five "chemistry regions": fuel grains, fuel open porosity, fuel/cladding gap, the bulk gas (which includes the aerosol particles), and the structure surfaces, where the species are allowed to experience chemical change. Structure surfaces are treated as either a vertical or a horizontal surface area.

VICTORIA discretizes the solution time domain into a series of equal time steps. During each of these steps, systems of equations are solved over the spatial meshes that describe the coupled phenomena. The calculation framework consists of five submodules, which are explicitly coupled:

- equilibrium chemistry calculations for all species, between vapor and aerosol in bulk, between surface and vapor, and deposit at surfaces;
- behavior and transport calculation of the species within the fuel rod geometry;
- transport calculation of the species in the bulk gas medium;
- species continuity calculation on all structure surfaces.
- aerosol formation, size evolution, and transport in the bulk gas and deposition onto structure surfaces; and
- decay heating.

Bulk Gas Species Transport. Transport is achieved by convection and/or diffusion between adjacent rings within an axial level and between adjacent axial levels within a radial ring. Transport of species in the cell is governed by the flux of species between the fuel film, the bulk gas, and the structure films. The annular volume of film surrounding the fuel rod has a constant thickness, and transport between the film and the flow channel is by diffusion. The structure surface film areas must be entered in the input. The transport equations model diffusive transport of gaseous species between the gas flow and the surface areas.

Equilibrium Chemistry. Chemistry calculations can dominate the computational cost of VICTORIA, so attention has to be paid to simplifying assumptions and calculational efficiency.

Liquid water is assumed not to be present in the vessel because VICTORIA is intended to model only unrecovered severe accidents. Plans are, however, to include liquid water in revised versions of the code. Steam may be present, and therefore chemical interactions involving steam are treated, including Zircaloy oxidation. The oxidation model is based on the work of Urbanic and Heidrick[3] and can interface with a severe accident code.

All interactions between chemistry regions are diffusion limited only to avoid computational costs associated with chemical rate limiting processes. Species diffusion is therefore treated as required, and chemical equilibrium pertains in all regions. Local equilibria are calculated by

minimization of free energies. At most, one condensed phase of each chemical species is allowed to exist.

All chemical phases are assumed to be ideal, the mass of any species within a cell being determined primarily from the availability of its constituent elements and by the mass fraction of the species. Transmutation and isotope effects are assumed to be unimportant.

Aerosol Behavior and Transport. The aerosol treatment in VICTORIA uses the CHARM[4] model. Aerosol behavior is modeled in a single computational cell. Time-varying external conditions are assumed to have been calculated in advance and are supplied as data to the model. The aerosol particles have a single, constant composition and can agglomerate, deposit on surfaces, or leak from the cell. A combination of the agglomeration and deposition models from MAEROS[5] and TRAPMELT[6] have been used in VICTORIA. In addition, models have been added to treat additional deposition by turbulence and to estimate boundary layer thicknesses and turbulence properties of the flow field.

The surfaces exposed to aerosols can be ceiling, floor, or wall type. Deposition mechanisms described by VICTORIA are

- gravitational settling,
- turbulence of submicron (Brownian) and supermicron particles,
- laminar diffusion,
- thermophoresis,
- diffusiophoresis, and
- pipe bends.

Three agglomeration processes are considered by VICTORIA: Brownian motion, differential gravitational settling, and turbulence.

The model assumes the aerosol to be well mixed throughout the cell, and the particles of a given mass to have the same size. In VICTORIA, a particle-particle efficiency, user supplied, is included in the equations to provide the coalescence probability.

The modeling of between cell aerosol transport is similar in approach to the modeling for bulk gas transport, but transport of aerosols to surfaces is calculated by the deposition models.

An aerosol multicomponent model is available, but it has not been extensively tested and is incompatible with the equilibrium chemistry calculation.

Decay Heat. Decay powers are calculated only for "VICTORIA species," the fuel, bulk gas flow and aerosol particles, and for the structures. VICTORIA calculates the new geometric distribution of decay heat caused by release of fission products from the fuel, but it does not solve the appropriate energy conservation equations. It would need a coupling to a reactor safety code to transfer this information every time step.

Decay chains are neglected in the VICTORIA scheme, isotopes are not lost from the number densities, and the creation of radioactive daughters upon decay of their parents is ignored. Also, there is no strict accounting of whether the decay emitted beta or gamma.

4.4.1.1.3 Developments

A new version of VICTORIA was released in 1992.* New FP transport models account for the following effects:

- structural heatup;
- aerosol resuspension;
- deposition of aerosols in sudden contractions, steam separators, and steam dryers;
- kinetically limited surface reactions; and
- more chemical species.

4.4.1.1.4 Code Use and Validation

The VICTORIA code was developed on a Cray-XMP at Sandia National Laboratories (SNL) and on a CRAY-2 and various SUN workstations at the Winfrith Technology Center. The code has been coupled to TRAC and MELPROG codes by the NRC, and it has also been coupled to ESTER. VICTORIA is a detailed code that usually requires several days of CPU time. Computer time is used largely to solve chemical equilibrium equations.

Code validation efforts already done include comparisons with Falcon, Marviken-V, ACRR-ST1, and ORNL HI-3 tests. Participation has also begun in the Falcon-ISP program and in the Phebus-FP series of tests.* Atomic

*N. E. Bixler et al. (SNL), and D. A. Williams (WTC), "Status of VICTORIA Development and Validation," presented at the CSARP Meeting, Washington, May 1992, U.S. Nuclear Regulatory Commission (1992).

Energy Authority Technology has reported an application for Sizewell NPP,[7] which includes a calculation of FP behavior in a TMLB sequence.

4.4.1.2 TRAPMELT 2.2 and TRAPMELT 3

4.4.1.2.1 Code Scope

TRAPMELT has been developed by BCL, under contract with the NRC, for analysis of FP transport and deposition in the RCS under fuel damaged conditions. Current versions are TRAPMELT 2.2 (Ref. 6,8) and TRAPMELT 3 (Ref. 9), which are modifications of the previously published TRAPMELT code.[10] Version 2.2 is an improved version[8] of the TRAPMELT 2 code, which includes new developments concerning fluid properties, vapor pressures, and diffusion coefficients and turbulent deposition of particles. Unless otherwise indicated, this description applies to both versions 2.2 and 3.

TRAPMELT calculates the transport and deposition of aerosol particles and a number of species that would be found in vapor state in portions of the RCS. TRAPMELT uses input information describing the system geometry, source rates of various vapors and particulate species, and thermal-hydraulic information.

Fluid transport data and surface temperatures are input into the TRAPMELT 2.2 code by time-dependent thermal-hydraulic data read into the code by the subroutine INPUT. The TRAPMELT 3 code is one of the elements of the STCP Mod1 code 10 (Ref. 9) and is a further development and coupling of the TRAPMELT and MERGE codes. MERGE was created to supply TRAPMELT with the necessary thermal-hydraulic history of the RCS. Important advantages of this coupling are that thermal-hydraulic information is updated with each MARCH code time step, and treatment of the decay heat contribution to the behavior of the RCS is possible.

Chemical species are fixed in the TRAPMELT code so that masses cannot move from one species to another. Chemistry is not treated explicitly in the code.

4.4.1.2.2 Code Models

General. TRAPMELT considers a system of up to 10 control volumes that can be connected by fluid flow in an arbitrary way. In each control volume, a species can reside in four states: suspended or deposited, in either in particle or vapor (molecular) form. A fifth state, surface reacted, is used to describe vapors that have reacted with RCS surfaces and are not subject to revaporization. Each volume is assumed to be well mixed. The suspended aerosol is treated in the code as consisting of particles residing in a set of up to 20 discrete size bins. TRAPMELT treats up to nine different chemical species.

Transport. The carrier is assumed to be a superheated steam-hydrogen mixture. Radionuclide transport can occur among the states of an individual control volume or between certain states of different control volumes, if these are connected by fluid flow. Transport between control volumes is assumed to occur in conjunction with carrier transport, which is imposed on the code. It is assumed that the transport rates of any species between states of a given control volume are the mass of the species in the state from which transport occurs, multiplied by the mass transfer coefficient or deposition velocity.

The code does not treat aerosol resuspension. Transport between control volumes is assumed to be a unidirectional, one-dimensional flow. TRAPMELT does not account for chemical reaction kinetics.

Intervolume Mass Transfer. Intervolume mass transfer is assumed to occur solely by convection and therefore occurs only for the suspended states. The transport rate of suspended species out of a volume is just the fractional rate of change of mass of the carrier gas.

Deposition. Deposition processes are calculated in the BETV and REMOVE subroutines. All processes are modeled as rate controlled by transport across a concentration boundary layer, whose thickness is very much less than the equivalent diameter of the RCS component considered. Such a situation exists for turbulent flow, and it is useful to employ a deposition velocity across the boundary layer. For laminar flow, transport through the fluid to the wall surfaces is continuous and the result of mass and temperature gradients. However, it is also possible to determine a fictitious deposition velocity for deposition from laminar flow.

Deposition mechanisms are assumed to be independent. The following processes are considered:

- vapor reaction with surfaces;
- submicron and supermicron particle deposition from turbulent flow, considering rough surface effects;
- deposition in bends;
- diffusion from laminar flow;
- thermophoretic deposition; and
- sedimentation.

Mass Transfer Involving Phase Changes. Because of condensation and evaporation, the ADHOC subroutine contains interphase mass transfer, which cannot readily be described by mass transfer coefficients. The mass of vapor condensed on walls, mass of vapor condensed on aerosol particles, and concentration of the vapor suspended are calculated by equations in the form of the general transport rate. They are treated separately from the transport equations because phase changes are much more rapid phenomena than either surface reactions or particle deposition.

Agglomeration. The code accounts for aerosol agglomeration caused by Brownian, gravitational, and turbulent mechanisms. The treatment of these processes is taken directly from the QUICK code.[11]

Decay Heat. TRAPMELT 3 assumes all gamma decay heat to be absorbed by control volume structures. The distribution of decay heat among structures is based on relatively simple sharing assumptions. Beta decay heat is treated similarly, except that allowance is taken for energy lost to the gas traversed by the beta rays.

4.4.1.2.3 Code Developments

No further developments of the stand-alone TRAPMELT code are foreseen. User-developed versions of TRAPMELT 2 have been reported by AEA[12] and ENEL.[13] Their unique features are described as follows.

TRAPMELT 2-UK is an enhanced version that results from the extensive assessment work on TRAPMELT 2 done in the UKAEA. The major differences are

- up to five structures modeled in each control volume. Evaporation, condensation, thermophoretic deposition, and gravitational sedimentation are calculated for each structure;
- improved calculation of the thickness of the thermal boundary layer between the bulk gas and the structure surfaces;
- updated thermophoretic accommodation coefficients; and
- adoption of the Pruppacher and Klett derivation of the collision efficiency pParameter.

ENEL has tested TRAMELT 2 against experimental data from Marviken and LACE and applied it to the Phebus-FP project. All this work led to TRAPMELT2/ENEL 88.1 code, which includes the following improvements:

- IBM Fortran 77 compatibility,
- time stepping control possibility,
- thermal-hydraulic data updated every time step,
- correction of errors in aerosol turbulent flow deposition and aerosol "puff" release to the containment,
- carrier gas modeled as a steam-nitrogen-argon-hydrogen mixture,
- thermophoretic boundary layer calculation revised,
- model of deposition in bend pipes, and
- model for gas recirculation because of natural convection in large components.

Two subcodes named TRAP-F[14] and TRAPG have been developed based on TRAPMELT and are being coupled respectively to the ICARE (CEA, France) and ATHLET-CD (GRS, Germany) system codes.

4.4.1.2.4 Code Use and Validation

TRAPMELT running time is proportional to the number of size bins, control volumes, and species treated. A typical 200-s run of nine species with seven volumes needs about 1000 s of computer time. The stand-alone TRAPMELT code has been used and tested against Marviken and LACE tests and in preparing the Phebus-FP tests. Coupling to a system analysis code, such as SCDAP/RELAP, seems to be the preferred way of using TRAPMELT presently. The VICTORIA and RAFT codes are generally the preferred codes for detailed FP transport calculations. The TRAPMELT code is the base of many developments of FP transport subroutines in codes such as MELCOR, ECART, and so forth.

4.4.1.3 RAFT Version 1.0

The RAFT code was initially developed by Argonne National Laboratory under funding by EPRI. Since then, it has been used by several European organizations who have independently proceeded with the development. In the meantime, EPRI decided to stop funding RAFT development and support.

4.4.1.3.1 Code Scope

The RAFT code[15] provides a one-dimensional mechanistic analysis of vapor or aerosol transport and deposition in the steam-hydrogen environment of LWR coolant systems. Users must supply data on thermal-hydraulic conditions, mass injection rates, and flow system. The code has been developed by Argonne National Laboratory (ANL), under contract with EPRI.

The code was originally written in PL1 language, and it has been translated to FORTRAN 77. The code is written in modular form, each subroutine being self-contained.

4.4.1.3.2 Code Models

General. A unique feature of the RAFT model is the inclusion of the homogeneous nucleation mechanism, which provides the capability to predict the particle size spectrum from the inception stage, without making any assumptions concerning initial size and number density. Besides the nucleation mechanism, other processes modeled in RAFT are heterogeneous nucleation, aerosol agglomeration and deposition, velocity difference between the particles and gas, gas-phase equilibrium chemistry, vapor condensation onto surfaces and particles, and chemisorption on structures.

An assumption used in RAFT is that the time constant of the gaseous reactions is sufficiently small (compared with that of vapor condensation) that the gas-phase species are essentially in local chemical equilibrium, but may be in nonequilibrium with respect to the condensed species.

RAFT is unique in that it uses a Lagrangian numeric methodology, in contrast to the Eulerian numerics of VICTORIA and most other codes.

The code constructs a direct solution of the aerosol population balance equation, which gives the size distribution and composition, containing terms for each of the processes just mentioned.

Homogeneous Nucleation. RAFT provides the user with the options to choose between the classical and nonclassical nucleation theories and to include the possibility of ion-nucleation. In classical nucleation theory, the rate expression is derived by considering a series of reactions that involve addition of a monomer to the cluster (condensation) or removal of a monomer from the cluster (evaporation). The nonclassical theory takes into account the change in surface tension of small particles as compared with the bulk liquid. Also, another nonclassical effect considered is the translational and rotational degrees of freedom possessed by the embryo-sized particles.

Heterogeneous Nucleation (Growth Rate). After the conventional simplified method of analysis of the Knudsen flow regime, the gas surrounding the particle is divided into two layers. RAFT uses a simplified approach, assuming that the gas outside the boundary between the two layers is in kinetic equilibrium.

Agglomeration. RAFT considers agglomeration caused by Brownian diffusion, turbulence, and gravitation.

Brownian coagulation is subject to two distinct limiting cases corresponding small and large Knudsen numbers.

The formulation of Saffman and Turner[16] is used to calculate the turbulent coagulation kernel. The formulation assumes that the particles are smaller than the microscale of turbulence (length scale characterizing the dissipation of turbulence energy). Interparticle collisions are governed by microscale turbulence assumed to be isotropic.

Particle and Vapor Deposition. Deposition models used in RAFT include diffusive phenomena (Brownian and thermophoresis), eddy turbulent impaction, inertial impingement across bends, sedimentation, centrifugal collection in a steam separator, and inertial collection in a steam dryer. Also, a model is included to treat vapor deposition on cool surfaces and reactive (chemisorption) vapor deposition. No revaporization model is included.

4.4.1.3.3 Code Development

A new version of RAFT (RAFT 1.1) has been developed and released under EPRI sponsorship, but no user's guide is available. Developments in version 1.1 include an enlarged species data base and improved physical properties. No major change in modeling has been reported. RAFT development is no longer funded by EPRI, and no new version is foreseen. However, a new version might be developed and released by ANL that would collect new independent developments by RAFT users. This version would adopt the classical Eulerian numerics. A project exists to couple the new RAFT code to ESTER as an alternative to VICTORIA aking into account that RAFT is a much faster code.

A number of user-developed improvements exist and have been used in calculation exercises:

- A UPM (Madrid, Spain) development concerning Te speciation and Te reactions with Ag aerosols and stainless steel structures has been tested against the Marviken-4 test.*
- A new PSAT subroutine, to calculate saturation pressures, has been implemented by JRC (Ispra, Italy) because the old one was not adequate when hydrogen is not injected at the circuit inlet.

*C. Gonzalez, "Improvements of Models to Treat Te in the RAFT Code," PhD Thesis, Polytechnical University of Madrid (EUR Report to appear in 1993).

- The Technical Research Centre of Finland (VTT) version considers boric acid, binary nucleation, stochastic cluster nucleation, chemisorption between vapors and aerosols and structural materials, and other improvements.

4.4.1.3.4 Code Use and Validation

EPRI has developed the SIAM code, which is a coupling of the RAFT, PSAAC, and CORMLT codes.

RAFT is being validated through analyses of the large-scale integrated Marviken experiments, the in-pile source term experiments (STEP) performed at ANL's TREAT reactor, and the bench-scale separate-effects experiments carried out at ANL's hot tube facility. The typical computer time for a RAFT run is in the order of several minutes. The code is widely used for calculations of the Phebus-FP tests.

4.4.1.4 SOPHIE Version 2.1

4.4.1.4.1 Code Scope

SOPHIE[17] is a module of the ESCADRE code system, which calculates vapor fission product transport and deposition of iodine, cesium, and tellurium (I_2, Cs, CsI, CsOH, Te) in parts of the RCS where the gas temperature exceeds the "transition" temperature between vapor and aerosol phases. The module was developed by a team from Institut de Protection et de Sureté Nucleaire (IPSN) (France). When integrated in the ESCADRE system, SOPHIE receives input from the primary circuit analysis module VULCAIN.

4.4.1.4.2 Code Physical Models

General. At each time step, the system of equations is solved by an implicit finite difference method. Automatic submeshing has been added to the code to enable the required calculation precision to be achieved.

Fission Product Vapor Transport. This calculation, in a fluid consisting of a steam-hydrogen mixture, is based on the mass transfer/heat transfer analogy and comprises determination of

- the fluid thermal-hydraulic properties and
- the vapor fission product mass transfer coefficient between fluid and wall for natural convection and forced convection.

Fission Product Adsorption on Walls. The Langmuir model is used. This theory assumes that the adsorbent surface comprises a predetermined, constant number of adsorption sites. A simplification is introduced to consider the surface as homogeneous.

The Langmuir model applies only to single-layer physical (reversible) adsorption. A second adsorption/desorption mechanism, which takes into account chemical adsorption or diffusion inside the metallic surfaces, in series with the first, is used in SOPHIE.

Condensation and Evaporation. The saturating vapor pressure vs temperature is calculated for each chemical element considered, using the thermodynamic data base. The condensation/evaporation current at the wall is calculated by a mass transfer coefficient in the control volume.

Vapor Transport and Deposition in Gaseous Fluid Flow. Mass transport through the carrier fluid is assumed to be the combined result of axial convection and radial diffusion, turbulent or otherwise. The calculation is performed in a control volume of predetermined geometrical characteristics, within which all parameters are constant. Adsorption/desorption and condensation are calculated separately. Each control volume can contain two surfaces at different temperatures.

4.4.1.4.3 Code Developments

An experimental program (DEVAP) is being implemented at the CEA to optimize data relating to adsorption isotherms that will then be integrated in the code.

An experimental program consisting of the HEVA-VERCORS-EMAIC tests has been set up to test FP and material release source characterization.[18] Measurements will include chemical species identification and fission product aerosol size distribution, and test results will be applied to SOPHIE validation.

4.4.1.5 AEROSOLS B2

4.4.2.5.1 Code Scope

AEROSOLS B2 (Ref. 19) has been developed by the French IPSN. The object of the code is to compute the behavior of an aerosol population injected inside a containment or into a circuit with known thermal-hydraulic conditions.

The code is a module of the ESCADRE code system and can receive input data from the SOPHIE code concerning vapor behavior in the RCS.

4.4.1.5.2 Code Physical Models

The aerosol size population is discretized in a maximum of 100 classes. The aerosol source is represented by one or two log-normal distributions: it is possible to follow two different aerosol populations. Thermal-hydraulic conditions and also the carrier gas composition are entered as data. The circuit or containment can be divided into a maximum of 20 compartments.

Aerosol Sedimentation. The removal rate is calculated by a modified Stokes law. Correction factors take into account gas velocity, large drops effect (higher Reynolds number), and drop shape.

Other Deposition Mechanisms. Thermophoresis, diffusiophoresis, Brownian diffusion, turbulent diffusion, turbulent impaction, and centrifugal impaction are calculated by the code.

Aerosol Agglomeration Mechanisms . The agglomeration kernel is the sum of three terms corresponding to Brownian motion, gravitational settling, and turbulence. A correction factor corresponding to the collision efficiency for larger particles has been introduced (Fuch's law or Prupacher-Klett law).

4.4.1.5.3 Code Use, Validation, and Developments

A separate-effects test program called TUBA-TRANSAT[18] has been set up to study FP aerosol behavior in pipes. Measurements will include deposition for aerosols. The program will include validation of the AEROSOLS B2 code against test results.

4.4.1.6 MACRES

4.4.1.6.1 Code Scope

MACRES* is a mechanistic computer code of aerosol and gaseous radioactive materials behavior in LWR cooling systems, for realistic estimation of the source term. The code has been developed by NUPEC for the Ministry of International Trade and Industry of Japan.

MACRES uses physical and chemical models based on up-to-date knowledge from source term research. MACRES can treat not only fully uncovered core conditions in the RCS but also water existing core conditions. Thermal-hydraulic conditions, plant data, and masses of released radioactive materials must be given as input data.

MACRES consists of 120 modules and has been written in FORTRAN 77. The code can be run by IBM-compatible machines or UNIX workstations.

4.4.1.6.2 Code Physical Models

General. MACRES divides the RCS into a number of component volumes such as core, piping, pressurizer, and steam generators. For each of the specified volumetric regions, the model considers liquid/gas phases and wall/floor geometries. The physical quantities to be treated in the basic equations are FP distributions in liquid and gas phases, in aerosol, and in wall deposition. A set of nonlinear differential equations gives the inventory of each chemical element in each phase and volume.

FP Chemical Form. After being released from the fuel, the FP's chemical form, which could exist in steam atmosphere, is determined by minimization of the Gibbs free energy.

Aerosol Nucleation. MACRES calculates the homogeneous phase aerosol nucleation velocity. Calculating the nucleation velocity for the system consisting of more than three components is difficult, and the surface tension for the mixture is unknown. MACRES assumes a constant number of atoms in one aerosol seed and calculates surface tension using saturation ratio as a parameter.

Aerosol Behavior. The MACRES model considers the following phenomena for the processes of aerosol particle growth:

- condensation of FP gas onto the aerosol particles,
- Brownian agglomeration,
- turbulent agglomeration, and
- gravitational agglomeration.

The following aerosol deposition phenomena are considered by the code:

- sedimentation,
- diffusion deposition,
- diffusiophoresis,

*J. Sugimoto, Japan Atomic Energy Research Institute, letter to J. A. Martinez, Spanish Nuclear Safety Council, June 1992.

- thermophoresis, and
- inertial collision.

Gaseous FP Behavior. The FPs existing in the gas phase can move into the liquid phase by dissolution, while those in the liquid phase can conversely move into the gas phase. Thus, the gas/liquid distribution of rare gases is determined by using Henry's constant based on experimental data, and the distribution of iodine is determined by using the equilibrium coefficient derived from experiments.

FP Removal by Pool Scrubbing. The MACRES code considers the following pool scrubbing phenomena:

- steam condensation,
- gravitational settling,
- diffusion deposition, and
- inertial collision.

Removal of gaseous FPs by scrubbing is evaluated by determining the amount of gaseous FPs absorbed or moving into the liquid phase during the bubble rising period. This evaluation is made by considering FP mass transfer from gas phase in the bubble to the liquid phase in water, in analogy to the heat transfer correlation functions.

4.4.1.7 HORN

4.4.1.7.1 Code Scope

The HORN[20] code has been developed by the Department of Fuel Safety Research of the JAERI to calculate the transport of volatile fission products in dry primary coolant systems under severe accident conditions.

HORN results are used to calculate the diffusional deposition rates of vapors and to estimate the nucleation rates of aerosols.

A total of 12 elements are considered by the code either as carrier gas or as elements for analysis in the present version. HORN determines the chemical forms of fission products both in the bulk gas and in the wall surface.

4.4.1.7.2 Code Physical Models

Elements for Analysis. HORN has selected a number of elements for analysis: H, O, Kr, Xe, Cs, I, Te, Sb, Ag, Cd, and Ba. The number of fission products for analysis has been minimized by using the periodicity of elements and by treating "less volatile" elements summed up as an imaginary element that always behaves as an aerosol. It is assumed also that volatile elements in the period around Xe: I, Cs, have similar behavior as those in the period around Kr: Br, Sr. Thus, only the first group is analyzed.

Chemical Form of Fission Products. To estimate the equilibrium concentrations of vapors in the bulk flow and at the wall surface, and to estimate the aerosol nucleation rate, HORN determines the chemical form of fission products and their concentration.

The code considers only gas-phase reactions. Surface reactions on the wall and radiation-induced reactions are neglected. The most important assumption is that the fission products instantaneously take their equilibrium chemical forms.

The equilibrium composition of vapors is calculated with the principle of minimum total free energy. The basic model is the same as that of the SOLGASMIX[21] code.

The assumption of instantaneous equilibrium means, in the case of phase change, that condensed-phase species instantaneously nucleate when the partial pressure of the gaseous species has exceeded the saturation pressure. However, the code needs a supersaturation factor as an input parameter that defines the supersaturation needed for gas molecules to condense by homogeneous nucleation.

Heat and Mass Transfer Models. Considering the enormous uncertainties involved, very simple models are used for both for heat and mass transfer. The HORN code assumes, for gas temperature and fission product removal calculations, that steady state is established within each time step. However, heatup of the tube wall is treated by a completely transient algorithm.

The flow path is divided into control volumes, characterized by three bulk temperatures. Wall temperatures are either given by input data or calculated from the heat balance at the end of each time step. In the latter case, calculation of the wall temperature is separated from that of the gas-wall heat transfer.

Volatile fission products are assumed not to affect the behavior of the bulk gas.

Convective heat transfer correlations are used to calculate the gas-to-wall heat transfer coefficient. The effective

emissivity between the gas and the wall is given by the formula for emissivity between two parallel planes. Material properties of the mixed gas are calculated from the properties of five monatomic component gases.

Only beta decay is considered when calculating decay heating of the control volume inner walls.

Condensation is the only deposition mechanism considered by HORN for fission products in gaseous form. The deposition rate is given by the molecular flux based on the concentration gradient.

Aerosol Growth Rate. HORN does not perform a complex calculation of particle size distribution as the residence time is assumed to be very small for sufficient growth to occur. In HORN, a log-normal size distribution is assumed for aerosols.

The rate constant for aerosol agglomeration is calculated assuming agglomeration caused only by Brownian motion. Other mechanisms are assumed to be unimportant because the code assumes that aerosols in the RCS remain submicron. Gas mean free path is calculated by the kinetic theory of gases. An initial particle size can be input either as a time-dependent value or a default value.

Aerosol Deposition. As the aerosol formed in the RCS is assumed to stay submicron, the removal processes caused by inertial motion in turbulent flow are assumed not to make a significant contribution to overall removal rate. In HORN, therefore, only diffusional deposition caused by Brownian motion, thermophoresis, and gravitational settling are considered as removal processes.

Removal rates are first expressed as group velocities toward the wall for each particle size class. Then they are averaged over the log-normal distribution weighted by mass.

4.4.1.7.3 Code Validation

According to Ref. 21, a preliminary code assessment has been done using the data from the FP LOFT experiments.

4.4.1.8 ECART

4.4.1.8.1 Code Scope

ECART[1] is a mechanistic and reasonably fast-running code used for the study of radionuclide transport throughout the nuclear island under severe accident conditions in all types of nuclear plants. ECART is aimed at unifying RCS and containment analysis and couples aerosol/vapor transport with thermal-hydraulic calculations.

The code has been set up by ENEL-CRTN of Milan, Italy. The code structure, developed by Synthesis-Milan, has been designed to make the code able to receive new models coming out from ENEL research activities performed within European Community cooperation projects.

ECART is based on three modules described subsequently; these modules can run separately.

4.4.1.8.2 Code Physical Models

General. ECART is designed to treat radionuclide transport in an arbitrary two-phase flow system divided into a number of control volumes.

Although ECART adopts the classic "well-mixed" hypothesis to describe the transport within each control volume, the deposition and resuspension phenomena are described by dividing each control volume into different subregions, where local thermal-hydraulic conditions are considered.

Thermal-Hydraulic Module. The carrier gas is considered as a multicomponent gas mixture with a catalog of ten gases available. Gas properties are calculated by the code.

The two-phase flow is expected to be in the stratified regime, with the phase distribution known a priori. ECART can consider water both in airborne form (condensation on aerosol particles) and as deposited liquid (collected in the control volume sump).

The thermal-hydraulic module provides for boundary conditions for the other two modules and has two activation levels:

- The module provides only for carrier and water physical properties and carrier/aerosol interaction parameters, if ECART is run with fixed thermal-hydraulic conditions.
- The module supplies complete thermal-hydraulic conditions taking into account both two-phase flows and thermal losses of the analyzed systems.

Aerosol and Vapor Transport Module. This module unifies TRAPMELT2, NAUA, and SPARC phenomenologies, with the addition of aerosol physical resuspension phenomena.

Condensation/evaporation of chemical species is calculated, as in TRAPMELT, using a diffusion model that does not require any feedback to thermal-hydraulic boundary conditions. Conversely, steam/water phase changes are based on mass transfer rates imposed to the aerosol module.

Irreversible reaction of vapors onto internal surfaces is modeled adopting the usual deposition velocity approach.

The ECART aerosol model is based on a discretized particle size distribution; the number of bins can be chosen by the user. The code adopts a simplified multicomponent description able to record the proportions of the different species in each size bin. This strategy prevents suspended species that have been released with different size distributions from being removed with the same depletion rate.

Agglomeration of suspended particles is based on the three mechanisms:

- Brownian, calculated with a Smoluchowski formulation;
- gravitational, as modeled in the QUICK code; and
- turbulent, shear, and inertial, calculated with the Saffman and Turner formulation.

Particle growth caused by bulk vapor/steam condensation is calculated taking into account the Kelvin effect. Particle deposition onto surfaces is calculated as the sum of several phenomena:

- inertial impaction from turbulent flow (Friedlander-Johnstone),
- diffusion from turbulent flow (Davies),
- diffusion from laminar flow (Gormley-Kennedy),
- thermophoresis (Brock),
- gravitational (Stokesian and non-Stokesian),
- inertial in bends, and
- diffusiophoresis (Schmitt-Waldmann).

Pool scrubbing of aerosols is modeled using the SPARC[9] code mechanistic method and aerosol depletion models.

For the calculation of resuspension of deposited aerosol particles, ECART incorporates an empirical model based on the aerosol resuspension tests performed at Oak Ridge National Laboratory (ORNL) and uses the force-balance criterion to calculate the resuspension rate for each particle size.

Chemical Equilibrium Module. Releases from the fuel, pressures, temperatures, and mass flow rates are calculated from separate subroutines and are given to the module. Calculation of chemical equilibrium is performed each time step for a "hard-wired" catalogue of species that can be considered representative for most of the accident sequences. Calculations are performed in a nonideal multiphase system to find the composition that contains minimum Gibbs free energy under the constraints of conservation of mass of each element and total pressure.

4.4.1.8.3 Code Use and Validation

The code is still under development at ENEL. The new aerosol transport models will be checked in the frame of the CEC Reinforced Concerted Action on Source Term. Validation programs, in cooperation with other research organizations, are planned for the near future. ECART is four to five times faster than TRAPMELT on similar severe accident problems. Additional speed and prevention of numerical instabilities is obtained by adopting implicit integration methods.

ECART can interface with the MARCH3 and VANESA codes of STCP, and with SCDAP/RELAP5, MAAP, and other severe accident codes.

4.4.2 System Codes

4.4.2.1 SCDAP/RELAP5 Mod3

4.4.2.1.1 General

Most aerosol and fission product behavior models in SCDAP/RELAP5 Mod 3 are based on the TRAPMELT 2 code,* but all of them have been recoded to make the formulation consistent with the SCDAP/RELAP5 scheme for dynamic dimensioning and to remove some of the limiting assumptions made in the development of TRAPMELT 2.

*C. M. Allison et al., "SCDAP/RELAP5/MOD3 Code Manual, Volume II," NUREG/CR-5273 Rev. 2, *(draft)*, September 1991.

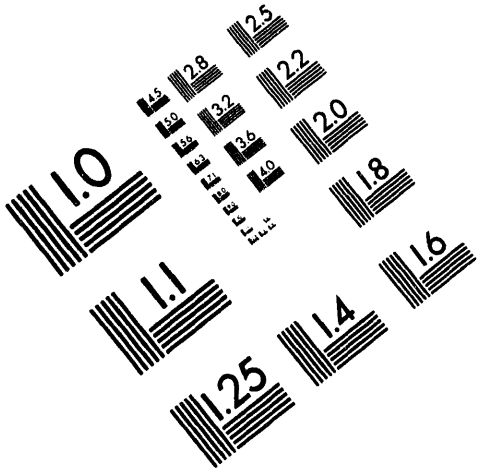
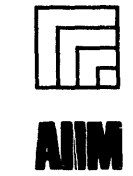
Association for Information and Image Management
1100 Wayne Avenue, Suite 1100
Silver Spring, Maryland 20910
301/587-8202
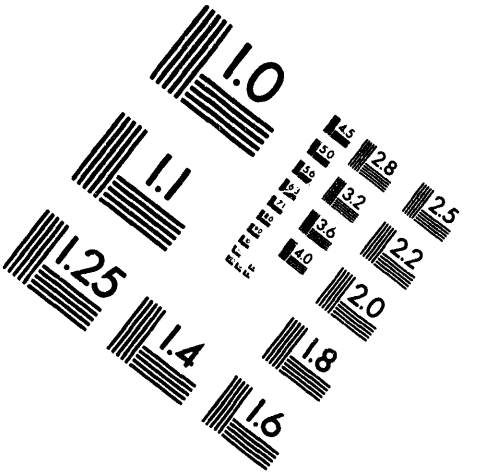
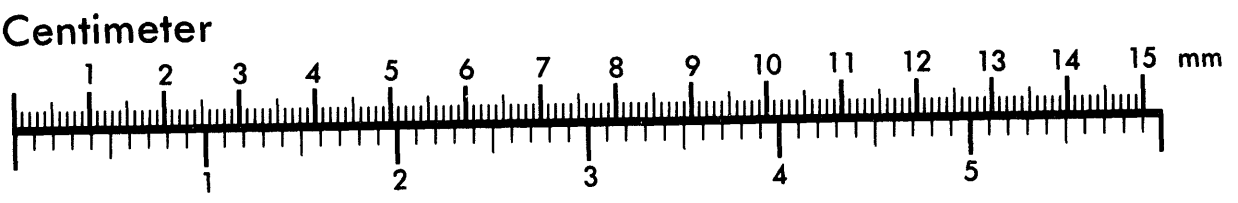

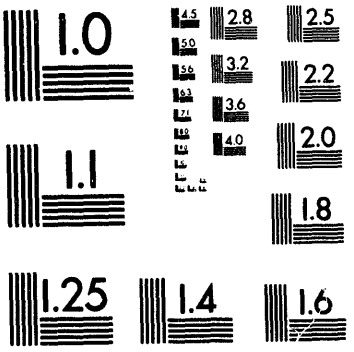
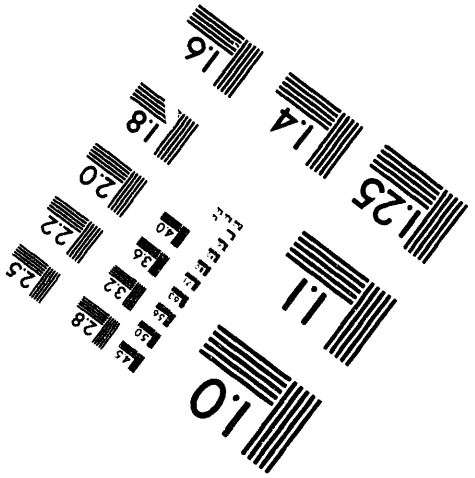
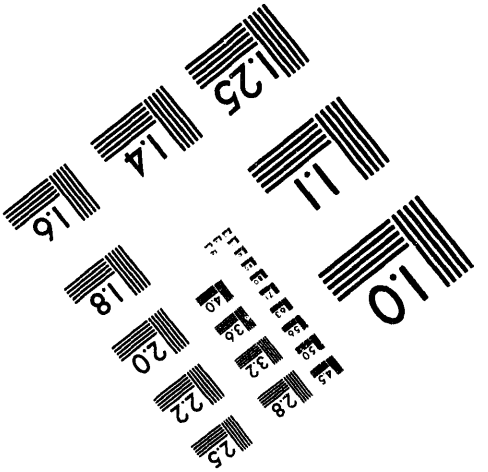

3 of 3

4.4.2.1.2 Code Physical Models

Formulation of the FP Transport Problem. The chemical species that can be considered by the FP transport models are iodine, cesium iodide, cesium hydroxide, tellurium, cadmium, silver, and tin. In contrast to TRAPMELT, all chemical species are allowed to evaporate or condense. The code does not consider silver in the FP transport equations.

The major states considered are aerosol, vapor, condensate, aerosol plateout, and absorbed states. Also, non-condensable gases and steam fields are modeled by the thermal-hydraulic behavior code.

Aerosol Agglomeration Models. Models are very similar to the QUICK code[11] agglomeration models used in TRAPMELT 2. The kernels for gravitational settling and turbulent fluid motion differ from those used in TRAPMELT 2 by a buoyancy factor. The net effect of the Brownian, gravitational, and turbulent kernels is assumed to be the sum of the three contributions.

Aerosol Deposition Models. Deposition velocity caused by gravitational settling differs from that used in TRAPMELT 2 by a buoyancy factor. Thermophoresis, diffusion, and inertial deposition from turbulent flow and diffusion from laminar flow calculation models are similar to the corresponding TRAPMELT 2 models. A new model for aerosol deposition caused by impaction at pipe bends has been developed.

Vapor Evaporation and Condensation. The rate equations have been taken from TRAPMELT 2 but differ by the use of separate equations for each particle bin size (TRAPMELT 2 uses a single representative particle radius).

Heterogeneous Chemical Reactions. Vapor deposition velocities on walls, from chemical reactions, have been changed slightly from those in the TRAPMELT 2 model.

Decay Heat Deposition Model. An energy deposition model has been connected to the fission product transport model. The model assigns decay energy either to the vapor space, the solid impacted by the particle, or the solid upon which the fission product is deposited. Gamma and beta are treated in a similar way, except that only beta energy is attenuated in the vapor space through which the particle must pass.

4.4.2.2 MELCOR Version 1.8.2

MELCOR is a full scope system analysis code, intended to be the main NRC tool for source term calculations in nuclear power plant severe accidents.

4.4.2.2.1 General

The Radionuclide Package of the MELCOR code[22] operates on the principle of material classes, which are groupings of elements. Typically, 15 classes are used by default in MELCOR, and a maximum of 20 classes are calculated. The default grouping is based on work by D. A. Powers of SNL. Just after release, combination of classes is permitted.

4.4.2.2.2 Code Physical Models

Aerosol Dynamics. The aerosol dynamics portion of the code is based on the MAEROS[5] program, without steam condensation. MAEROS is a multicomponent aerosol dynamics code that evaluates the dynamic size distribution of each component. The size distribution is described by the mass in each section, or size bin. A mapping between MELCOR material classes and components must be specified. Representation as a single component is the current default, since computation cost could otherwise be very high.

Steam condensation/evaporation is handled separately to reduce the stiffness of the differential equations. The amount of steam condensed or water evaporated is calculated by the thermal-hydraulics portion of the code.

The aerosol deposited on the various surfaces cannot now be resuspended. The aerosol resuspension process will be controlled by parameters that are accessed or modified by other packages. Currently no user input control is available to activate resuspension.

Condensation and Evaporation. The condensation and evaporation of FP vapors is calculated by the same equations as in the TRAPMELT 2 code.[6] The FP masses in the control volume atmosphere and on the aerosol surfaces, pool surfaces, and heat slab surfaces are described by rate equations based on the surface areas, mass transfer coefficients, present surface concentration, and the saturation surface concentration.

Deposition and Settling. Aerosols and FP vapors can be transported to and from heat slabs and water pools. The heat slab surface orientation is defined by default by the

heat slab geometry input and can be changed. In addition, aerosols can agglomerate and settle between or within control volumes through open flow paths. A pool scrubbing model, for the removal of aerosols only, includes condensation at the pool entrance, Brownian diffusion, gravitational settling, centrifugal impaction, and evaporative forces for the rising bubble.

Decay Heat. The decay heat from fission products suspended in the atmosphere can go to the gas phase in any volume or to any surface. The water pool is evaluated as a surface. The decay heat from FP deposited on any slabs can be directed to any heat slab or control volume gas phase. A correction is made for the reduced deposition of decay heat in small or low-density atmospheres.

Chemistry. Chemistry effects can be simulated in MELCOR through mass and energy transfer data given by the user for each stoichiometric reaction. Reversible and irreversible reactions can be used to model adsorption, chemisorption, and chemical reactions. Only FP vapors undergo chemical reactions.

4.4.2.2.3 Code Use, Validation, and Developments

An important effort is being made to set up an international validation program (MELCOR Cooperative Assessment Program, or MCAP). MCAP includes comparison exercises with LOFT, Phebus-FP, and Falcon tests. A new version, named MELCOR 1.8.2, was released in April 1993, but it did not include any substantial new development in terms of FP transport models.

MELCOR has been used in a large number of PRA analyses to provide source term radionuclide release, transport, deposition, and retention.

Validation has been made against ABCOVE, LACE, and Marviken test data and against LOFT FP-2.

4.4.2.3 MAAP Version 3.0B

MAAP is a system analysis code that has been developed by Fauske and Associates for EPRI. The code intends to simulate the full scope of a severe accident in any type of LWR and it is used mainly by utilities and their contractors.

4.4.2.3.1 General Structure of FP Subroutines

MAAP[23] is a modular code containing specific subroutines for pressurized-water reactor (PWR) or boiling-water reactor (BWR) calculations and a general subroutines package. FP treatment is done in a similar way both for PWR and BWR, and it is based on "Region FP Subroutines" for the primary system and for containment compartments proper to each type of plant.

There is a parallelism of the code architecture between thermal-hydraulic and FP calculations. The main program calls both the T/H integrator and FP integrator to update the T/H conditions and the FP masses throughout the RCS and containment. Each FP region subroutine calculates the convective transport and internal transitions between vapor, aerosols, and deposited masses for each of the 12 FP species.

FP species can exist in up to four states: vapor, aerosol, deposited, and contained in the core or corium. Where applicable, the FP subroutines also calculate the FP mass rates-of-change for FP contained in corium.

4.4.2.3.2 Mass Transport in the RCS

When subroutine PSFP is called, the rates of change of each FP chemical group are computed for each state in which the FP can reside: vapor, aerosol, or deposited. Each FP and structural material group is also tracked separately in the core or core debris. The masses in a node change because of flows between nodes, releases from the core and from transported corium, and internal transitions from one state to another.

The total rate of change of FP mass caused by convective flows can be determined explicitly by summing the mass rates for each FP group over the flow paths connected to the node. The explicit rates of change are converted into stable implicit rates of change to avoid the use of too-small time steps.

In the RCS, FP transport in liquid water is not considered as there are usually no water pools in the RCS associated with FP. Also, no convective transport by water of deposited FP is accounted for in the steam generators.

FP and structural materials that are not released from the core remain dissolved in the corium as it flows out of the original core boundaries. After vessel failure, these materials flow out of the lower plenum and into the reactor cavity.

4.4.2.3.3 Aerosol and Vapor Deposition Rates

Subroutine FPTRAN, common for PWRs and BWRs, calculates the aerosol and vapor removal rates from the gas

phases to surfaces, or the revaporization rates of deposited material under these conditions. The calculational procedure for aerosols, with particles growing by agglomeration, uses two correlations for the solutions of the Smoluchowski equation. This obviates the need to run a time-consuming computer subroutine. Correlations are used for "aging," sedimenting aerosol, and for "new" source reinforced aerosols. Removal rates are calculated for sedimentation, inertial impaction, steam-driven diffusiophoresis, and thermophoresis. Turbulent deposition has not been incorporated because FAI's analyses suggest that turbulent deposition is not nearly as important as other deposition processes.

The removal by vapor condensation on surfaces is dominated by steam condensation, and the removal rate is calculated accordingly. Water-soluble aerosols are assumed to grow to their equilibrium size before any removal process takes place.

4.4.2.3.4 Chemical States

Once FPs leave the core in-vessel, their chemical state is "frozen" and defined by the 12 FP species calculated by MAAP.

4.4.2.3.5 Decay Heat

The decay energy associated to the 12 FP species is summed and added to each core node. Deposited vapor and aerosol FP are assumed to fall into any existing water pools or to adhere to surrounding heat sinks if water is not present. The FP masses that are deposited on the face of each of the heat sinks is tracked separately, and the associated decay energy is assumed to go into that face. Decay energy associated with suspended FP is assumed to penetrate the gas and to heat a preselected heat sink face.

4.4.2.3.6 Code Use and Validation

There is an extensive MAAP validation matrix, described in Ref. 23, against aerosol transport and deposition experiments. Programmed experiments include ABCOVE, ORNL (NSPP), Marviken, CEA, and JAERI tests. The Swedish RAMA II Project Report[24] contains results of MAAP validation against Marviken and LACE experiments. The MAAP code is being widely used by utilities, vendors, and architects/engineers in evaluating the progression of accidents and in conducting IPEs.

4.4.2.3.7 Developments

A new version (4.0) of the MAAP code is being prepared by EPRI, but it does not seem to contain any major new development concerning FP transport. There is a development named CHMAAP 3b6,* which is basically a tool for sensitivity testing of MAAP with regard to the possible effects caused by chemical phenomena not modeled in the standard MAAP code. Some preliminary work is also under way on inclusion of radiation-enhanced chemical processes.

4.4.2.4 SOPHAEROS and TRAP-France

The SOPHAEROS† code is being developed by a team from IPSN. Code will model FP transport inside the RCS. Code manuals are not available yet, but its main features follow.

- Input data concerning fission product release will be taken from the ICARE2 code.
- State-of-the-art physical models from the SOPHIE, AEROSOLS B2, and TRAP-France (an IPSN numerically implicit version of TRAPMELT) will be collected and integrated into SOPHAEROS.
- RCS thermal-hydraulic data will be taken from the CATHARE code.
- A new totally implicit solution method, similar to that already developed in the TRAPF code, will be incorporated.

TRAP-France[14] is the result of modifications to the TRAPMELT 3 code, which involve:

- implicit numerical treatment;
- deposition by diffusiophoresis, and by inertial impaction in horizontal/vertical bends;
- new chemical species, such as cadmium vapor and tin telluride; and
- modification of the deposition formalism by thermophoresis: the particle thermal conductivity can be varied through the circuit.

4.4.2.5 ESCADRE

The ESCADRE system is a modular code structure, comprising separable codes, aimed at the analysis of PWR accident phenomenology. ESCADRE was developed by the French IPSN. The FP transport codes used in ESCADRE are SOPHIE (vapor transport) and

*J. O. Liljenzin et al., "Development, Implementation and Use of CHMAAP," NKS/SIK-2 Seminar in Halden, November 17-18, 1992.

†M. Cranga, IPSN/DRS/LEACS, France, letter to J. A. Martínez, Spanish Nuclear Safety Council, July 1992.

AEROSOLS B2 (aerosol transport). These codes were described previously.

4.4.2.6 ATHLET-CD

In ATHLET-CD, the module TRAPG* adapted from TRAPMELT 2 has been implemented to calculate FP transport. Besides the coding error corrections, the modeling of FP vapor sorption on walls and condensation/evaporation on walls and particles, as well as of aerosol agglomeration and deposition, remain basically unchanged.

TRAPG input and output are adapted to the ATHLET structure. Geometrical data, fluid conditions, and temperatures are taken from the ATHLET input data and transient solution of the thermal-hydraulics. The release rate data, calculated by the EFIPRE module, are regrouped and taken as source for the circuit calculation. There is no limitation in the number of fluid cells or structure surfaces.

The first code assessment calculations will be carried out as part of the ISP 34 Falcon exercise.

4.4.2.7 ESTER

ESTER (European Source Term and Research Code) is under development in the frame of the Shared Cost Actions supported by the CEC. ESTER is a portable software framework, able to accommodate with minimal changes existing or newly developed modules for the various components and phenomena involved in a severe accident. The VICTORIA code has been implemented as an ESTER module† to make available models for the transport, retention, and behavior of FP and other structural materials in the RCS. Moreover, VICTORIA will then be able to link with other severe accident analysis codes such as KESS and ICARE2.

VICTORIA/ESTER is a self-contained, stand-alone code that consists of a version of VICTORIA that uses ESTER for much of its data storage and a driver designed to run VICTORIA/ESTER as a stand-alone unit. If the code is linked to other ESTER-compatible code, such as ICARE2, the driver will be replaced by the compatible code. VICTORIA fuel release models will not be incorporated into the first working version.

A version of VICTORIA/ESTER is being run on a SUN computer at Ispra and a VAX computer at IKE. This version has been tested on Falcon and Phebus calculations.

A possible future development is the coupling between ESTER and a new version of the RAFT code. This work was expected to begin in 1993 as soon as a new version of RAFT, with Eulerian modeling, is released by ANL.

4.4.3 Conclusions on FP Transport Codes

An extensive review of FP transport calculation tools available today has been carried out in Sect. 4.4. This review gives the reader a broad idea of what has been done on FP transport code development and serves as the starting point for further reading. Some conclusions from this review are:

- The TRAPMELT code provides the foundation for many other more recent FP transport codes to build more refined or complete models, but its development has been discontinued in the U.S.A. The new generation RAFT and VICTORIA codes are more detailed, mechanistic FP transport codes and are widely used. An interesting feature of the RAFT code is that it requires little CPU time when compared with VICTORIA. FP transport codes have also been developed in France, Japan, and Italy; however, these codes seem to be less widely used. Important assessment is being done for these codes, particularly including Phebus-FP calculations.
- System codes couple thermal-hydraulic and material behavior subroutines to FP release and transport subcodes and are intended for calculation of severe accident sequences in nuclear power plants. TRAPMELT-derived subroutines are presently the preferred choice for system codes. The coupling of more detailed FP transport codes, such as RAFT and VICTORIA, to severe accident and system codes should be weighed carefully, taking into account the calculation costs involved.
- The potential user has a large number of different versions of FP transport codes available. A number of user-developed versions exist for TRAPMELT and RAFT. Choosing a code or version to treat a particular problem could be a difficult task. The diversity of available codes is an additional difficulty when the resources of the research community are to be allocated for code development and validation.
- Tables 4.9 and 4.10 give the reader a summary of FP transport code modeling. Conclusions from the code model review are:

*K. Trambauer, GRS Munich, letter to J. A. Martinez, Spanish Nuclear Safety Council, November 1992.

†N. Johns and D. Williams, "VICTORIA as an ESTER Module," AEA Reactor Services, Winfrith Center, presentation at the first ESTER seminar, Ispra, June 1992.

- There is a general consensus that sedimentation, thermophoresis, impaction, and turbulent diffusion are important deposition phenomena in the circuit. However, a good deal of variety in the treatment of deposition processes within each code has been observed. A benchmark study between the VICTORIA and RAFT codes has been published,[25] showing that a detailed examination is needed of the aerosol deposition models used in both codes to clarify differences and inconsistencies.
- Calculating chemical reactions accurately is generally a time-consuming task. Gas-phase chemistry is generally calculated by the minimum free-energy equilibrium model. Systems analysis codes tend to simplify chemistry.
- Treatment of aerosol resuspension and revaporization is planned in a number of codes. Current models existing in some of the codes are crude and poorly validated.
- Multicomponent aerosol models are standard in the containment but rare in RCS codes. Current models in the VICTORIA code have problems of consistency with the overall numerical scheme and of excessive CPU time.
- Revaporization models generally assume ideal behavior of the components of the deposited mixture. Extension to nonideal behavior requires significant addition to the existing data base.
- The codes generally assume a monophasic (steam-hydrogen mixture) gas carrier. Only a few codes consider the presence of liquid water. Two-phase chemistry will be an additional concern (e.g., in the VICTORIA code).

- The main international development program on FP transport codes is taking place in new versions of the VICTORIA code. Other developments are taking place in Europe concerning improvements to the RAFT code and in Italy with the ECART code. A new version of the RAFT code was expected to be released in 1993, containing user-developed improvements. The CEC, through the Ispra Research Establishment, has sponsored some of these developments.
- Researchers from several countries participate in the VICTORIA code development team. Peer review of this code has been scheduled; this may recommend new developments. The development work of VICTORIA is focused on validation against experimental data,[26] as soon as they are available, and the development of new models concerning revaporization, transport after vessel failure in air environment, and aerosol transport in the RCS. The Phebus-FP test program is expected to be an interesting source of data against which to test the code.

4.4.4 References

1. F. Parozzi, "Computer Models on Fission Product and Aerosol Behavior in the LWR Primary System, Part II," Commission of the European Communities EUR Report 14676 EN (November 1992).

2. T. J. Heames et al., Sandia National Laboratories, "VICTORIA: a Mechanistic Model of Radionuclide Behavior in the RCS Under Severe Accident Conditions," USNRC Report NUREG/CR-5545, Sandia National Laboratories, October 1990.*

3. V. F. Urbanic and T. R. Heidrick, "High Temperature Oxidation of Zircaloy-2 and Zircaloy-4 in Steam" *J. Nucl. Materials*, 75, 34-50 (1978).†

4. C. J. Wheatley, Sandia National Laboratories, "CHARM: a Model for Aerosol Behavior in Time-Varying Thermal-Hydraulic Conditions," USNRC Report NUREG/CR-5162 (SAND-0745), August 1988.*

5. F. Gelbard, Sandia National Laboratories, "MAEROS User Manual," USNRC Report NUREG/CR-1391, 1982.*

6. H. Jordan and M. R. Kuhlman, Battelle Columbus Laboratories, "TRAPMELT2 User's Manual," NUREG/CR-4205, May 1985.*

7. J. Lillington et al., "Sizewell B Plant Calculations: TMLB' Accident Scenario Results," AEA Reactor Services, Winfrith Technology Centre, AEA-RS-5110 United Kingdom (November 1991).

8. M. R. Kuhlman et al., Battelle Columbus Laboratories, "TRAPMELT2 Code: Development and Improvement of Transport Modeling," USNRC Report NUREG/CR-4677, July 1986.*

9. J. A. Gieseke et al., Battelle Columbus Laboratories, "STCP User's Guide," USNRC Report NUREG/CR-4587, April 1986.*

10. H. Jordan et al., Battelle Columbus Laboratories, "TRAPMELT User's Manual," USNRC Report NUREG/CR-0632, 1979.*

11. H. Jordan et al., Battelle Columbus Laboratories "QUICK User's Manual," USNRC Report NUREG/CR-2105, 1981.*

12. D. A. Williams, "Further Analyses of the Marviken Aerosol Transport Tests 1, 2a, and 2b using the TRAPMELT2-UK Computer Code," Atomic Energy Establishment Winfrith, AEEW-M 2298, United Kingdom (April 1986).

13. F. Parozzi, "User's Guide to ENEL-CRTN Version of TRAPMELT2 Code," Ente Nazionale per P'Energia Elettric, N6/88/02/MI (June 1988).

14. M. Cranga, "TRAPF Code Physics. Development and Validation Status. Correlations and Models," Institut de Protection et de Sureté Nucléaire, SEMAR/LEACS 91/72, France (December 1991).

15. K. H. Im et al., "The RAFT Computer Code for Calculating Aerosol Formation and Transport in Severe LWR Accidents," Electric Power Research Institute, NR-5287-CCM, July 1987.

16. P. G. Saffman and J. S. Turner, "On the Collision of Drops in Turbulent Fluids," *J Fluid Mech*, 1, 16-30 (1956).†

17. C. Leuthrot and G. Lhiaubet, "SOPHIE Reference Document," Commissariat à l'Energie Atomique, SEAC/91-06, Institut de Protection et de Sureté Nucléaire, France (1991).

18. C. Lecomte, "Recent Plans and Accomplishements of Severe Accident Research in France," Institut de Protection de Suretè Nuclèaire presentation at the CSARP meeting, Bethesda Maryland, May 1992, U. S. Nuclear Regulatory Commission (1992).

19. J. Gauvain and G. Lhiaubet, "AEROSOLS B2 Reference Document," Commissariat à l'Energie Atomique, SEAC/91-02, Institut de Protection et de Sureté Nucléaire DPEI, France (1991).

20. M. Uchida and H. Saito, "HORN: A Computer Code to Analyze the Gas-Phase Transport of Fission Products in RCS under Severe Accidents," Japan Atomic Energy Research Institute, JAERI report 86–158, Tokai, Japan (October 1986).

21. T. M. Bessmann, Union Carbide Corp. Nucl. Div., Oak Ridge National Laboratory, "SOLGASMIX, A Computer Program to Calculate Equilibrium Relationships in Complex Chemical Systems," ORNL/TM-5775, 1977.*

22. Sandia National Laboratories, Thermal Hydraulics Analysis Division, "MELCOR 1.8.1 Computer Code Manual," June 1991.*

23. R. E. Henry and M. G. Plys, "MAAP-3.0B Computer Code Manual," Electric Power Research Institute NP-7071-CCML, November 1990.

24. A. Hedgran et al., "RAMA II Final Report," Reactor Accident Mitigation Analysis, RAMA II 87/01, Sweden (September 1987).

25. J. A. Capitao et al., "A Comparison of the RAFT and VICTORIA Computer Codes for Simple Geometries in Chemically Reactive Systems," *J. Aerosol Science*, 22, 45-49 (1991).†

26. U.S. Nuclear Regulatory Commission, "Severe Accident Research Plant Update," NUREG-1365, December 1992.*

*Available for purchase from the National Technical Information Service, Springfield, Virginia 22161.
†Available in public technical libraries.

4.5 Comparison of Codes with Experiments

4.5.1 Introduction

Even if a code has an impeccably sound modeling strategy, and even if its programming has undergone the most rigorous quality assurance procedures, the results of reactor calculations performed using this code will be believed only if they have successfully predicted the results of a number of experiments where similar phenomena are encountered. The calculation of these experiments does not have a long history. A report in 1985 by Kress[1] surveying the state of validation of severe accident codes contains no code-experiment comparisons in the fission product transport field. In fact, there were few codes to validate and few experiments to check against them. TRAPMELT was the only code

mentioned, and at this stage it was still under development and unvalidated.

The situation has now improved. As we have seen, there are now a large number of computer codes that are capable, in theory, of modeling the phenomena that govern the transport of fission products as well as a reasonable number of experiments to check them against. Assessment statements have been made for TRAPMELT-2, by Kuhlman et al.,[2] TRAPMELT-ENEL, by Parozzi,* VICTORIA, by Williams et al.,[3] and for MELCOR, by Kmetyk.[6] In this chapter we aim to build on this work and assess the predictive power of fission product transport codes. Some effort has been made to be thorough. We have tried to summarize all calculations that can be compared to experiments and where the results of both code and experiment are freely available. Experiments where the measurement results are thought to be scarce are included because useful information can always be obtained from their analysis.

*F. Parozzi, "Relevance of Marviken and LACE Project Results in Validating TRAP-MELT/ENEL Code," Marviken-V/DEMONA/LACE Workshop, Montreux, Switzerland, June 28-July 1, 1988, ENEL report N6/88/04/MI.

4.5.2 Overview of Experiments Studied

Table 4.11 is an attempt to classify the subset of fission product transport experiments that have been analyzed by codes according to the main deposition mechanisms. In-pile and out-of-pile experiments are listed separately because the advantages of the in-pile experiments' use of a more representative source have to be balanced by the very poor data that is available from those carried out so far.

Normally the temperature is a guide as to whether the transport is by vapor and aerosol or by aerosols only. For

Table 4.11 Overview of phenomena

Experiment	Vapor phase	Gravitational setting	Turbulent deposition	Thermophoresis	Resuspension
		Out-of-pile experiments			
Marviken 4,7 (pressure vessel)	Yes	More in test 7	Probably	No	No
Marviken 4,7 (hot pipe)	Possibly	Big particles	Yes	Small particles	No
Marviken 1,2a,2b,4,7 (pressuriser)	No	Dominant	Possibly	Some	No
Marviken 1,2a,2b,4,7 (cold pipe)	No	Yes	Some	Little	No
LACE LA1	No	Little	Dominant	Little	No
LACE LA3a,3b,3c	No	Little	Mostly bends	Little	Maybe
Falcon, Fal	Dominant	Little	No	Yes	No
ORNL ATT A105,106	No	No	No	Yes	No
ORNL ART-04	No	No	Yes	No	Mechanical
TUBA, TRANSAT	No	No	No	Yes	No
DEVAP	Yes	No	No	No	No
		In-pile experiments			
PBF 1.4	Yes	Yes	Yes	Probably	No
PBF 1.3	Yes	Yes	Yes	Probably	No
LOFT LP-FP-1	Yes	Yes	Yes	Probably	No
LOFT LP-FP-2	Yes	Yes	Yes	Probably	No

those tests that are hot enough to allow the presence of vapors, at least for those included here, it is very difficult experimentally to know whether the vapors condensed onto walls or onto aerosols or reacted chemically with them. Therefore, no attempt has been made in this table to subdivide vapor phenomena. Of the aerosol depletion mechanisms, gravitational settling in a component is normally straightforward to detect because there is more deposition at the bottom than the top. It is harder to distinguish between thermophoresis and turbulent deposition. High Reynolds numbers or deposition at flow restrictions and bends indicate a turbulent mechanism, but turbulent deposition has also been postulated for tests with neither of these attributes. Some entries to the table are marked "possible" or "probable" so this table should be taken as a guide only. More details are to be found later in the chapter where each experiment is discussed individually.

4.5.3 Marviken Experiments

The Marviken tests are a valuable source of data for code assessment, and the large number of analyses carried out reflects this. Their value lies in the scaling, which is almost full size. Analysis of tests 1, 2a, and 2b was carried out by Williams and Butland in 1984,[5] again by Williams in 1986,[6] by Kuhlman et al.[2] and by Parozzi et al.[†] [**] Tests 4 and 7 included a reactor pressure vessel, and these tests were analyzed by Williams in 1986,[7] Gonzalez and Alonso in 1991,[8,9] Bond and Johns in 1991,[10] and Parozzi[††] in 1986. Tests 2b and 4 were analyzed by Kmetyk in 1993.[11] The results of all these calculations are summarized as follows.

[†]F. Parozzi, G. Sandrelli, and M. Valisi, "Analysis of Marviken Test 1 and Test 7 Using TRAPMELT Code," Presentation at Marviken V Analysis Meeting, June 26–28, 1986.

[**]F. Parozzi, G. Sandrelli and M. Valisi, "Analysis of Marviken Test 2b Using TRAP-MELT2/ENEL Code. Preliminary Calculations," Presentation at Marviken V Analysis Meeting, Argonne National Laboratory, July 15-17, 1986.

[††]F. Parozzi, "Analysis of Marviken Test 4 Using TRAP-MELT2/ENEL Code, Benchmark Calculation Calculations," Presentation at Marviken V Analysis Meeting, Argonne National Laboratory, July 15-17, 1986.

Boundary Conditions. The most important boundary conditions are presented in Sect. 4.3.1 of this report. Other important data for assessing the representativeness of the tests are given in Table 4.12. Only tests 4 and 7 used the complete Marviken facility. Only test 4 used a corium simulant.

Results of the Calculations. Tables 4.13 to 4.17 summarize the experimental and calculation results. The percentages given are percentages of the injected mass. Not all of the material mass injected in the experiments was collected. The missing mass is noted separately in the following discussion. Many analysts made several calculations. The most popular parameter to change for these sensitivity calculations was the aerosol size at the inlet of the experiment, so a separate column is allocated to this.

Clearly, it can be misleading to present only the global retention for each component. For instance, Kuhlman et al.[2] noticed that although they managed to predict quite well the overall retention in the pressurizer during test 1, they predicted too much deposition on the floors and not enough on the walls. Thus the overestimation of settling compensated for other errors. Nevertheless a comparison of global results does illustrate rather well the sensitivity of the results to the code, the user, and the assumptions.

Test 1. In this experiment, 12% of the cesium was lost, 57% of the iodine, and 10% of the tellurium. The main results are given in Table 4.13.

Test 2a. In this experiment, 21% of the cesium was lost, 17% of the iodine, and 39% of the tellurium. This test was performed at a lower temperature than test 1. Many features of the test, including a 25% uncertainty in the flow rate, make it difficult to analyze. Few calculations have been performed, and these are presented in Table 4.14.

Table 4.12 Conditions for Marviken tests

	Vessel	Pipe	Pressurizer	Pipe
Diameter, m	5	0.35	2.5	0.3
Flow length, m	7	16	3.32	10
Velocity (test 4), m/s	0.03	4.5	0.05	3.5
Reynolds Number (test 4)	200-300	15300	8100	22120

Table 4.13 Marviken test 1

Date	Code	Organization	Inlet AMMD[a]	Pressurizer Cs	Pressurizer I	Pressurizer Te	Pipe Cs	Pipe I	Pipe Te	Relief tank Cs	Relief tank I	Relief tank Te
1983	Experiment		?	27	11	27	4	3	4	20	10	14
1984	TRAPMELT-2	UK	0.8	5	5	11	8	9	8	22	22	21
1986	TRAPMELT-2UK	UK	1	5			5			27		
1986	TRAPMELT-2UK	UK	10	15			9			30		
1986	TRAPMELT-2UK	UK	30	60			10			18		
1985	TRAPMELT-2.2	ENEL	2.6	41	41	47	7	7	6	24	24	22
1986	TRAPMELT2	BCL	3.6	11			2			17		

[a]Aerodynamic mass median diameter (μm).

Table 4.14 Marviken test 2a

Date	Code	Organization	Inlet AMMD	Pressurizer Cs	Pressurizer I	Pressurizer Te	Pipe Cs	Pipe I	Pipe Te
1983	Experiment		?	5	5	2	1	1	0
1984	TRAPMELT-2	UK	0.8	9	9	11	12	11	12
1986	TRAPMELT-2UK	UK	1	7			7		
1986	TRAPMELT-2UK	UK	10	20			12		
1986	TRAPMELT-2UK	UK	30	65			12		

Test 2b. This test was a repeat of test 2a and was much more successful. In the experiment, 8% of the cesium was lost, 13% of the iodine, and 6% of the tellurium. The results are summarized in Table 4.15.

Test 7. This was the first test to include the reactor pressure vessel. The temperature in this component was between 1000 and 1350 K, high enough for vapor phenomena to occur. In the experiment, 16% of the cesium was lost, 5% of the iodine, and 15% of the tellurium. The deposition is summarized in Table 4.16.

Test 4. As in test 7, this test included a hot pressure vessel. This was the only test in which nonvolatile "corium" was injected. In the experiment, 8% of the corium was lost, 18% of the cesium, 66% of the iodine, and 19% of the tellurium. The results are summarized in Table 4.17.

Behavior in the Reactor Vessel. This component, included in tests 4 and 7, was the only one where temperatures were high enough for the fission products to exist as vapor as well as aerosols.

In test 7, there was little deposition here (<10%) and no indication that the speciation affected the results. Cesium, iodine, and tellurium were deposited in roughly the same proportions. The U.K. TRAPMELT calculations significantly overpredicted vapor condensation onto walls in this test and found that they could obtain any aerosol deposition they desired simply by changing the aerosol size. RAFT[12] predicted that most of the tellurium retention was by condensation and chemisorption on walls, although the non-negligible deposits found on the floor would indicate that aerosol settling was also an important mechanism. Table 4.18 shows the experimental distribution of deposition for the two tests as a percentage of the injected mass.

Table 4.15 Marviken test 2b

Date	Code	Organization	Inlet AMMD	Pressurizer			Pipe		
				Cs	I	Te	Cs	I	Te
1983	Experiment		?	41	39	41	4	4	3
1984	TRAPMELT-2	UK	0.8	20	20	21	14	14	14
1986	TRAPMELT-2UK	UK	2	10			10		
1986	TRAPMELT-2UK	UK	10	25			15		
1986	TRAPMELT-2UK	UK	30	65			12		
1986	TRAPMELT-2ENEL	ENEL	2.5	31	31	31	11	11	11
1987	TRAPMELT-2ENEL	ENEL	13.2	46	46	46	14	14	14
1991	VICTORIA	UK	2	23	23	23	11	11	11
1992	MELCOR 1.8.1	SNL	5	41	41	41	22	22	22
1992	MELCOR 1.8.1	SNL	10	63			10		
1992	MELCOR 1.8.1	SNL	1	12			15		
1986	TRAPMELT2	BCL	0.2	20			10		
1986	TRAPMELT2	BCL	3.4	68			18		
1986	TRAPMELT2	BCL	2	51			17		

Test 4 was more interesting still. This was the only Marviken test where simulated core materials (silver and manganese), as well as the fission product simulants, were injected. Speciation may have played a role in this test; whereas the cesium deposited in more or less the same location as the corium material (mostly on the upper wall), the tellurium deposition was less and the iodine deposition much less.

Gonzales' work[8,9] showed that the addition of new tellurium species does not influence the results as much as the introduction of a model for the interaction of tellurium vapor with silver aerosol particles. The standard RAFT model allows condensation of vapors onto aerosol but not the reaction of vapor species with particles of another species.

TRAPMELT-UK predicted that 12% of the injected cesium condensed onto walls and none condensed onto aerosols. This is incorrect if the almost identical deposition of cesium, silver, and manganese means that the cesium was deposited as aerosols. Williams[7] thought this was a coincidence, the low measured cesium deposition being caused by TRAPMELT's neglect of chemical reactions between vapors and aerosols and between vapors and surfaces. Indeed, Gonzalez showed that vapor-aerosol reactions, previously neglected in RAFT, could lead to the formation and retention of silver telluride. The TRAPMELT results from ENEL show similar errors to the U.K. results.

The MELCOR base calculation predicted some features of the experiment quite well, in particular the very low deposition of iodine compared to cesium. The only species containing these elements were cesium iodide and cesium hydroxide, and because cesium iodide has a lower vapor pressure and hence lower volatility, the difference in the calculated deposition must be because of a higher deposition rate of vapor than of aerosols in the vessel. Because there is no chemisorption model in MELCOR, the mechanism would be vapor condensation. In fact, MELCOR predicts vapor condensation on the cylinder wall in the upper vessel to be the predominant deposition phenomena for cesium hydroxide, and presumably cesium iodide was already an aerosol here. The difference in experimental depositions between cesium and iodine could be explained by the MELCOR calculation, but

Table 4.16 Marviken test 7

Date	Code	Organization	Inlet AMMD	Vessel			Pipe			Pressurizer			Pipe		
				Cs	I	Te	Cs	I	Te	Cs	I	Te	Cs	I	Te
1983	Experiment		?	9	8	8	1	1	1	5	5	5	17	19	14
1986	TRAPMELT-2UK	UK	5	22			2			9			7		
1986	TRAPMELT-2UK	UK	10	30			10			21			11		
1986	TRAPMELT-2UK	UK	18	37			20			30			11		
1985	TRAPMELT-2ENEL	ENEL	1.7	16	13					11	11				
1991	RAFT	USA				0			11			2			10
1991	RAFT-1.0	UPM				8			9			5			20
1991	RAFT-1.0[a]	UPM				8			9			5			19
1991	RAFT-1.1	UPM				19			12			0			3
1991	RAFT-1.1[a]	UPM				19			12			0			1
1991	VICTORIA	UK	2				2	1	2	5	5	5	10	10	10
1986	TRAPMELT2	BCL	3.8	58						8					
1986	TRAPMELT2	BCL	0.1	15						10					

[a]The RAFT version was modified by adding new tellurium species.

Table 4.17 Marviken test 4

Date	Code	Organization	Inlet AMMD	Vessel				Pipe				Pressurizer				Pipe			
				Corium	Cs	I	Te	Corium	Cs	I	Te	Corium	Cs	I	Te	Corium	Cs	I	Te
1983	Experiment		?	27	27	3	15	3	2	2	2	24	15	10	20	10	7	15	9
1986	TRAPMELT-2UK	UK	5	14	12			1	4			5	5			4	6		
1986	TRAPMELT-2UK	UK	10	25				3	8			8	9			10	10		
1986	TRAPMELT-2UK	UK	20					4	15			24	16			10	10		
1986	TRAPMELT-2ENEL	ENEL	5	14	1	2	0	4	6	4	36	22	25	26	16	10	12	12	8
1991	RAFT	USA					0				16				2				-
1991	RAFT-1.0	UPM					6				11				17				18
1991	RAFT-1.0[a]	UPM					5				10				25				25
1991	RAFT 1.1	UPM					7				17				18				12
1991	RAFT 1.1[a]	UPM					6				14				27				12
1991	RAFT 1.1[b]	UPM					29				4				27				12
1992	VICTORIA	UK	2						3	3	3		8	10	9		12	17	14
1993	MELCOR 1.8.1	SNL	5	36	14	1	19	4	5	6	5	14	19	26	17	9	11	14	11
1993	MELCOR 1.8.1	SNL	1	15			9	2			2	15			15	12			12
1993	MELCOR 1.8.1	SNL	25	81			57	1			4	2			6	1			5
1986	TRAPMELT2	BCL	0.1	25								26							

[a]The version of RAFT had been modified by the inclusion of new tellurium species.
[b]The version included a model for the interaction of tellurium with silver aerosol particles. This only allowed vapor-aerosol interactions in the standard RAFT model are condensation and evaporation.

Table 4.18 Experimental distribution of deposits in Marviken reactor vessel

	Test 4				Test 7		
Location	Corium	Cs	I	Te	Cs	I	Te
Floor	8.6	7.6	0.6	5.7	2.8	3.0	2.8
Lower wall	3.9	1.9	0	1.9	1.4	1.2	0.8
Upper wall and internals	10.8	16.5	0.5	5.7	5.0	4.2	3.9
Center plate	1.9	0.8	0	1.2	0.1	0	0.1
Total	27.5	26.9	3.4	15.4	9.4	8.3	7.7

experimental error cannot be excluded because 66% of the injected iodine was lost, a much higher percentage than for any other element. Furthermore, a low deposition of iodine in the pressure vessel would likely lead to iodine-rich aerosols downstream, and this was not observed. MELCOR calculated the cesium deposition to be about half that of manganese and silver, unlike in the experiment where they were, as we have said, more or less the same.

No calculations of this component have been made with VICTORIA.

Behavior in Hot Pipe Work. This is the pipe between the core and the pressurizer. In experiment 4, a higher proportion of the corium was deposited than of the volatile products. All calculations (TRAPMELT-UK, TRAPMELT-ENEL, and MELCOR) predicted the reverse.

Behavior in the Pressurizer. The codes managed to reproduce the experimental finding that most of the deposition was on the floor. Williams calculated (using TRAPMELT2) that this should be the case for particles with an aerodynamic mass-median diameter (AMMD) greater than 0.5 μm in tests 2b and 7, and although the particle size was not measured, nobody expected it to be smaller than this. Table 4.19 gives the percentage of the total deposition for each element that deposited on the floor.

All the codes assume that the flow is well mixed and unidirectional. Indications are that this is not a good approximation in this case. Parozzi[13] reproduces three-dimensional fluid dynamics calculations using the FLUID-3-D code that indicates fast recirculation inside the pressurizer. Williams' VICTORIA validation statement indicates that he also suspects that some recirculation took

Table 4.19 Percentage of pressurizer deposition on floor

Test	Corium	Cs	I	Te
1		80	55	63
2a		67	60	82
2b		85	85	84
4	85	84	83	85
7		62	64	73

place. Turbulent impaction, caused by these flow patterns and exacerbated by the horizontal injection position, was probably responsible for the greater proportion of the aerosols that were deposited towards the bottom of the vessel, near the injection point. Masnaghetti[14] made a detailed study of this component and attempted to estimate the deposition using calculated recirculation velocities but could not reproduce the experimental deposition pattern.

None of the experiments had significant differences between the behavior of the different elements. The code calculations agreed with this.

The percentage deposition in test 2b was 50% more than in the similar test 1, presumably because of the higher aerosol density. Most of the U.K. calculations, whether with TRAPMELT-2 or TRAPMELT2-UK, predicted this. Parozzi, using TRAPMELT-2 ENEL, found the reverse: the calculated retention in test 1 was higher than in test 2b. The final verdict on the pressurizer is then:

1. The codes are capable of calculating that the dominant mechanism is gravitational settling.
2. The code predictions of the quantity deposited cannot be evaluated because the aerosol size was not measured and this has a strong influence on gravitational settling.
3. Deposition onto the walls was generally underpredicted by the codes. Wall deposition may have been caused by thermophoresis (which is modeled by the codes) but could also have been caused by turbulent impaction caused by recirculation (which is not modeled by the codes).
4. There were no obvious speciation effects. All the elements deposited in the same proportion. Assuming that the source was a single-component aerosol seemed to be a good approximation.

Behavior in Cold Pipe Work. The pipe work leading from the pressurizer is relatively cold, and transport is mostly in the form of aerosol. Corium, cesium, iodine, and tellurium all deposited in more or less the same proportions. Bond and Johns[10] predicted that the aerosols in this pipe would deposit by thermophoresis, settling, and bend impaction. They performed many different calculations with VICTORIA, varying the initial aerosol size and shape, but no combination of parameters led to a calculation that correctly partitioned the deposition between horizontal and vertical sections and bends. Other researchers came to similar conclusions.

Behavior in the Relief Tank. This report is concerned only with the transport of fission products up to the pressure boundary condition, so phenomena in the relief tank are relevant only for test 1—the only test where the tank did not contain subcooled water. Even for this test, analysts devoted little attention to the relief tank; this is partly because it is intrinsically difficult to analyze but also because it is the last component in the chain. The aerosol source to this component depended on the deposition in all upstream components. Because the codes had mostly not managed to predict the upstream deposition well, the characteristics of the aerosol particles arriving into the relief tank were not well estimated either.

4.5.4 LACE Experiments

Full information about code-experiment comparisons for test LA1 can be found in Wright et al.'s comparison report.[15] Corresponding information for test LA3 can be found in Wright and Arwood's report on pretest calculations[16] and their report on blind posttest analyses.[17] The results reported are of particular value because the calculations reported are "blind"— the participants to these exercises did not know the experimental results.

Subsequently, Bond, Johns, and Williams performed other calculations using VICTORIA.[18]

Understanding the Tables. For test LA1, the circuit is divided into six sections, and the deposition in each is given. In the LA3 tests, the overall deposition only is given. The code users assumed that all the recovered mass was injected. In fact some of the injected mass in the experiment was not recovered, and this gives an uncertainty to the experimental measurements. Percentages are given as a percentage of the recovered mass.

The source aerosol was a mixture of manganese oxide and cesium hydroxide. The percentage of cesium hydroxide in the deposited mixture is given as a percentage of the total mass deposited at that point.

Test LA1. The test pipe was 0.063 meters in diameter, 30 meters long, and contained six bends. The test velocity was 100 meters per second at inlet and 200 meters per second at outlet. The results are summarized in Table 4.20. Although for the most part the codes correctly calculated the very low overall transmission factor of around 3%, they did not calculate where the deposition occurred. In fact, Table 4.20 shows that the codes overpredicted deposition in the first sections and underpredicted it in later sections. The difference between the ENEL and U.K. results was because of input errors. Later U.K. results were similar to those of ENEL.

The measured inlet AMMD was 1.64 μm. The codes correctly predicted that the larger particles would preferentially deposit and hence that the outlet diameter would be smaller than that at the inlet. Calculations such as those performed by BCL using TRAPMELT2 that overpredicted the overall deposition also tended to overpredict the size reduction and therefore underestimate the size of the particles at the outlet of the pipe.

Test LA3. Three tests in this series have been analyzed. The geometry is the same as for LA1.

In LA3A the pipe diameter was 6.3 cm, the steam flow 62 g/s, the nitrogen flow 92 g/s, the average source rate 0.59 g/s, the pressure atmospheric, and the velocity about 77 m/s. The results are summarized in Table 4.21.

Table 4.20 Deposition in test LACE LA1

Date	Code	Organization	Deposition (%)[a]					Transmission (%)[a]	Outlet AMMD (μm)
			4-5	6v-6	7-11v	12-15	16-19		
1987	Experiment		7	19	47	25	2	2	0.9
1987	AEROSIM-M	UK	28	25	18	6	1	37	1
1987	AUX2.9	Sweden	4	4	8	4	5	76	
1987	RETAIN-2C	Finland	7	40	44	7	2	3	
1987	TRAPMELT2	BCL	43	31	24	4	1	1	0.4
1987	TRAPMELT2	ENEL	23	15	32	15	4	4	0.85
1987	TRAPMELT2	UK	14	19	27	16	4	23	1

[a]Percent of mass injected in the test.

Table 4.21 LACE test LA3A

Date	Code	Organization	Deposition			Outlet AMMD (μm)
			%	Mechanism[a]	%CsOH	
1987	Experiment		77 +/- 2	40% bend 49% straight	19	1.05
1987	AEROSIM-M	UK	49	T (100%)	23	1.3
1987	HAA4	Rockwell	44		16	0.8
1987	RAFT	VTT-Finland	20		17	0.8
1987	MCT-2	NYPA	38	T (>99%)	17	1.1
1987	TRAPMELT2	ENEL	51	T (99%)	17	0.65
1987	TRAPMELT2	JAERI	48	T (99%)	17	0.85
1987	TRAPMELT2[b]	UK	49	T (99%)	2	0.85
1987	TRAPMELT2[c]	UK	49	T (99%)	17	0.85
1987	TRAPMELT 2.2	BCL	61		17	0.85
1991	VICTORIA (vs90mod1)	UK	59		17	1.65

[a]Information about mechanisms comes from pretest calculations.
[b]Time-averaged source size.
[c]Time-dependent source size.

Note: T = Turbulent impaction

In LA3B the pipe diameter was 6.3 cm, the steam flow 12 g/s, the nitrogen flow 18 g/s, the average source rate 0.85 g/s, and the pressure atmospheric and the velocity about 25 m/s. The results are summarized in Table 4.22.

In LA3C the pipe diameter was 6.3 cm, the steam flow 12 g/s, the nitrogen flow 18 g/s, the average source rate 0.66 g/s, the pressure atmospheric, and the velocity about 24 m/s. The results are summarized in Table 4.23.

Lesson from LACE Experiments. The LACE experiments are a rich source of experimental data, and the tables summarizing the deposition do not do full justice to them. The most important lessons learned from these tests were:

1. Figure 4.13 shows the experimental deposition in LA3B in each pipe section expressed as a percentage of the total mass recovered. The sections marked with a "b" are bends. Most codes overpredicted deposition in the straight sections and underpredicted it on the bends. In LA3B, bend deposition in the test was about a factor of three greater than that predicted by the codes. The BCL TRAPMELT2.2 calculation showed the same trends as the other codes, but the margin of error was less.
2. Many experiments have conclusively demonstrated that the rate of turbulent impaction depends on the aerosol size, and in fact the available correlations take this into account. If different species are associated with different size distributions (multicomponent aerosols), it would seem logical that each species

Table 4.22 LACE test LA3B

			Deposition			
Date	Code	Organization	%	Mechanism[a]	%CsOH	Outlet AMMD (μm)
1987	Experiment		44 +/- 10	89% bend 9% straight	12	1.77
1987	AEROSIM-M	UK	20	T (100%)	12	1.7
1987	HAA4	Rockwell	28		11	1.42
1987	RAFT	VTT-Finland	11		11	1.62
1987	MCT-2	NYPA	14	T (>95%)	11	1.45
1987	TRAPMELT2	ENEL	27	T (72%) Th (32%)	11	1.52
1987	TRAPMELT2	JAERI	15	T (63%) S (36%)	11	1.52
1987	TRAPMELT2[b]	UK	11	T (78%) Th (14%)	2	1.40
1987	TRAPMELT2[c]	UK	22		11	1.40
1987	TRAPMELT 2.2	BCL	46		11	1.35
1991	VICTORIA (vs90mod1)	UK	27		11	1.13

[a]Information about mechanisms comes from pretest calculations.
[b]Time-averaged source size.
[c]Time-dependent source size.

Note: T = Turbulent impaction.
Th = Thermophoresis.
S = Gravitational setting.

Table 4.23 LACE test LA3C

Date	Code	Organization	Deposition %	Deposition Mechanism[a]	Deposition %CsOH	Outlet AMMD (μm)
1987	Experiment		78 +/- 14	36% bend 53% straight	43	0.64
1987	AEROSIM-M	UK	13	T (100%)	46	1.67
1987	HAA4	Rockwell	19		41	1.42
1987	RAFT	VTT-Finland	13		41	1.62
1987	MCT-2	NYPA	19	T (>94%)	41	1.44
1987	TRAPMELT2	ENEL	21	T (73%) Th (25%)	41	1.52
1987	TRAPMELT2	JAERI	9	T (62%) S (37%)	41	1.47
1987	TRAPMELT2[b]	UK	16	T (79%) Th (14%)	41	1.4
1987	TRAPMELT2[c]	UK	16		41	1.4
1987	TRAPMELT 2.2	BCL	42		41	1.35
1991	VICTORIA (vs90mod1)	UK	34		41	0.9

[a]Information about mechanisms comes from pretest calculations.
[b]Time-averaged source size.
[c]Time-dependent source size.

Note: T = Turbulent impaction.
Th = Thermophoresis.
S = Gravitational setting.

would deposit at a different rate. In LACE, the evidence is not conclusive. Figures 4.13 and 4.14 show the experimental deposition of each species as a percentage of the total recovered mass of that species. The cesium hydroxide deposits are significantly greater than those of manganese oxide in the straight sections but not in the bends. Unfortunately it is not clear whether this is because of a difference in deposition velocities or because the cesium hydroxide (being liquid) was harder to resuspend than the manganese oxide. Overall the difference in deposition between the species was less than the difference between calculation and experiment.

3. A more striking feature was the difference between tests LA3B and LA3C. The boundary conditions are

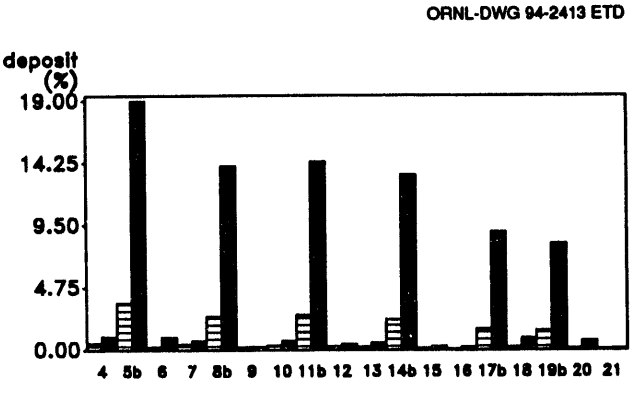

Figure 4.13 Measured deposition in test LA3B as function of position along pipe (CsOH-light, MnO-dark)

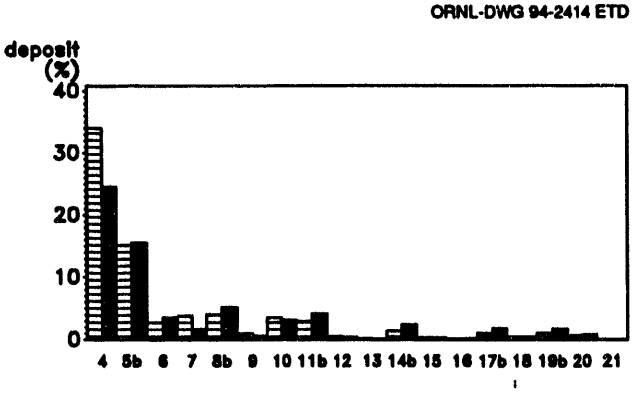

Figure 4.14 Measured deposition in test LA3C as function of position along pipe (CsOH-light, MnO-dark)

very similar except that in LA3C there was a higher proportion of CsOH in the aerosol. This strong dependence of the deposition on the composition of the aerosol particles is not predicted by any code.

4. In general, the codes are correct in predicting that it is the large particles that deposit; hence the aerosol particles are smaller at the outlet than at the inlet of the pipe.

4.5.5 Aerosol Transport Experiments at ORNL

A series of aerosol transport tests (ATTs) have been performed at ORNL to study the deposition of aerosols in a vertical tube. The tube has as inner diameter of 0.26 m and is 2.63 m long; the carrier gas and aerosol particles enter from the bottom. The results of two of these tests, A105 and A106, have been compared to TRAPMELT-2 by Rahn, Collen, and Wright.[19] Both experiments used an iron-oxide aerosol, and the flow boundary conditions are shown in Table 4.24.

Calculations were compared to experimental results for the top, middle, and bottom portions of the test pipe. The pipe was hotter at the bottom than the top; the temperatures are shown in Table 4.25.

The resulting plateout was calculated first using a standard TRAPMELT-2 (case 1) and then one modified as follows:

Case 2: Aerosol collision shape factor of 10.

Case 3:

- Improved correlation to calculate wall temperature gradient.
- Slip coefficients in Brock thermophoresis model changed.

Case 4:

- Measured temperature differences included as code input.
- Slip coefficients in the Brock thermophoresis model changed.

The total experimental plateout in test A105 was about 54% of the injected mass and about 43% in A106. The calculations predicted less. The values in Table 4.26 give plateout at each location for each calculation expressed as a percentage of the recovered mass.

Rahn, Collen, and Wright[19] concluded that no reasonable change in the thermophoresis model would increase the predicted deposition to the level of that measured so thermophoresis was not the dominant mechanism for retention. Despite the low Reynolds numbers (<1000), they thought that turbulent convection was responsible for the deposition, the turbulence being caused by natural convection. This was suggested by the high calculated Grashof numbers (>10^7) that could induce net downward flow near the pipe walls and enhanced upwards flow near the axis. Because the flow patterns were not measured, this remains a hypothesis.

4.5.6 Aerosol Resuspension Experiments at ORNL

The aerosol resuspension tests (ARTs) were carried out in two stages. Aerosols generated by a plasma torch were deposited inside tubes with a diameter of 2.5 cm and a length of 7.6 cm. The rate of aerosol removal was measured for

Table 4.24 Boundary conditions for ATTs

Experiment	Mean velocity (cm/s)	Residence time (s)	Mean Reynolds Number	Mean Grashof Number
A105	4.7	56	480	4-6 × 10^7
A106	10.3	26	850	3-6 × 10^7

different flow velocities of nitrogen and different sample exposure times. Resuspension is not modeled by most codes, and the only known posttest calculation of these tests was by Parozzi,* who calculated the ART-04 resuspension experiment using the ECART code. In this experiment, an iron-oxide aerosol was used. Parozzi managed to predict quite well the resuspended amount using a method based on a force balance for the suspended particles.

4.5.7 Falcon Experiments

Despite the large amount of data that has being generated by the Falcon experiments, only a limited number of attempts have been made to analyze them with codes. Experiments TG-1, TG-2, TG-3, TG-6, and TG-7 have been calculated by Chown and Williams[20] using VICTORIA, and Dumaz[21] has analyzed FAL-1a, FAL-12, and FAL-3a, again using VICTORIA. Pretest calculations for Falcon 17 (Ref. 22) and 18 were made by Mason and Williams,[23] who also made posttest calculations,[24] as did Shepherd et al.,[25] with the ESTER version of VICTORIA. The TG series of tests were of a qualitative nature and not suitable for detailed quantitative analysis.

Falcon consists of an induction furnace, used to heat up fuel and control rod samples, and some downstream pipe work. Most of the Falcon analysis of relevance to this report has concentrated on part of this pipe work—a 48-cm-long, 2.5-cm-diam horizontal silica thermal gradient tube that is at the heart of the experiment. The material released into this tube and the temperatures at its inlet and outlet were as shown in Table 4.27 for tests FAL-1a, FAL-12, FAL-3a, FAL-17, and FAL-18. The release was not measured on-line but was deduced after the test by collecting and weighing all the deposited and collected material. Inevitably some errors were associated with this method, especially for elements such as iodine that are present only in small quantities.

The release rate during an experiment was not constant. The analysts performing calculations used known events such as control rod burst times to decide how to partition the release of material during the experiment, and their choices affected the results. For instance, the speciation and hence deposition of fission products will depend on whether they were released simultaneously with or subsequent to the release of control rod material. Most calculations assumed a steady state.

*F. Parozzi, "Final Report on Contract ENEL/CEC," Contract Number 3558-88-12 EL ISP I, July 1991, to appear as EUR report.

Table 4.25 Temperatures in ATTs

	Gas temperature (°C)			Wall temperature (°C)			Wall temperature gradient (°C/cm)		
Experiment	Bottom	Middle	Top	Bottom	Middle	Top	Bottom	Middle	Top
A105	237	127	77	61	39	30	56	25	14
A106	309	173	103	73	31	36	73	48	20

Table 4.26 Results of ATTs[a]

	Test A105			Test A106		
Calculation	Bottom	Middle	Top	Bottom	Middle	Top
Experiment	34	13	5	26	10	7
Case 1	2	1	0.2	1	1	0.5
Case 2	1	0.5	0.3	1	1	0.2
Case 3	4	2	1	3	1.5	0.5
Case 4	4	2	1	3	1.5	1

[a]Results are percent of recovered mass.

Table 4.27 Boundary conditions in Falcon experiments

Experiment	Fuel	Control rod	Boric acid	Inlet temperature, °C: Gas, 3 cm from pipe entrance	Inlet temperature, °C: surface	Outlet temperature, °C: Gas, 39 cm from pipe entrance	Outlet temperature, °C: Surface
FAL-1a	Simulant	No	No	735	420[a]	206	163[c]
FAL-12	Simulant	Yes	No		785[a]	457	302[c]
FAL-3a	Simulant	Yes	Yes	206	262[a]	371	286[c]
FAL-17	Simulant	Yes	Yes	800	705[b]		222[d]
FAL-18	Simulant	Yes	No	1104	800[b]		235[d]

[a] 9 cm from pipe entrance plus 100°C.
[b] 4 cm from pipe entrance.
[c] 45 cm from pipe entrance.
[d] 46 cm from pipe entrance.

The overall retention in the silica pipe as a percentage of the total mass recovered is shown in Table 4.28. No error margins are stated for these calculations, although presumably they are quite wide. In FAL-1a, no control rod material was injected, but some was recovered after the experiment. Similarly, low concentrations of boron were found in FAL-18, and the iodine collected after the experiment was 30% more than the assumed inventory of the fuel sample. Dumaz[21] supposed that it resulted from contamination during previous experiments. In these experiments it is more useful to examine where the deposition took place rather than the overall transmission factors. This is summarized in Figs. 4.15 to 4.26, which show the deposition in kilograms in sections of the 48-cm-long thermal gradient tube as a function of position for FAL-1a, FAL-3a, and FAL-12. The dark bars are the experimental results. The lighter bars are VICTORIA results. Figures 4.27 to 4.30 show cesium and iodine deposition in FAL-17 and FAL-18. The thicker lines show experimental results (kg/m^2) measured at the top ("UP") and bottom ("DOWN") of the tube. Generally, deposition at the bottom of the tube was less than that at the top, although the difference is not great. This is consistent with VICTORIA's prediction that aerosol particles settle under gravity but that this is not the dominant mechanism. The main difference between the various calculations for these two tests is that Shepherd et al.'s ESTER calculation[25] assumed that some release from the fuel continued after the control rod release had finished, whereas the others assumed that the releases were contemporary and performed a steady-state analysis.

Table 4.28 Overall retention[a]

	Cs	I	Te	U	Cd	In	Ag	B
Experiment FAL-12	48	61	57	100	53	42	86	
FAL-12 VICTORIA	31	32	28	16	42	27	47	
FAL-12 VICTORIA (no control rod material)	34	31	25	17				
Experiment FAL-3a	48	13	79	86	48	57	99	18
Experiment FAL-17	42	20	100		57	68	49	22
Experiment FAL-18	51	75	16		31	49	33	

[a] Retention values are percent of recovered mass.

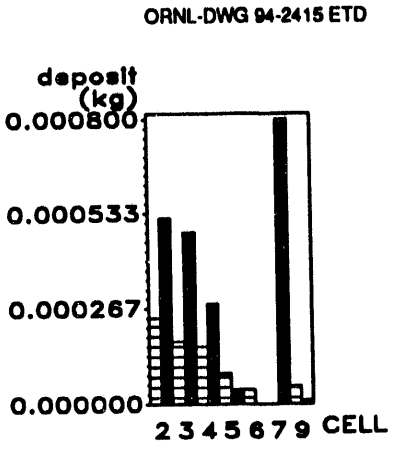

Figure 4.15 FAL-1a cesium deposition

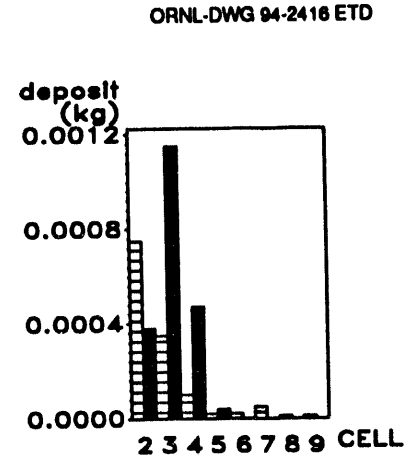

Figure 4.16 FAL-3a cesium deposition

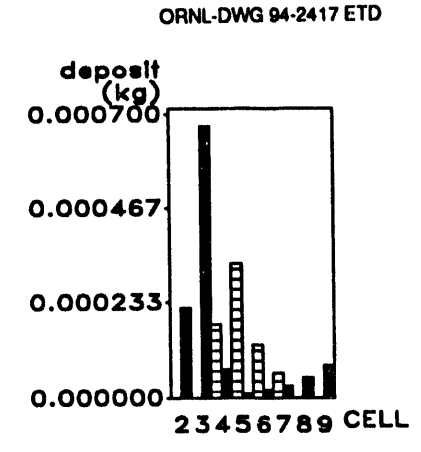

Figure 4.17 FAL-12 cesium deposition

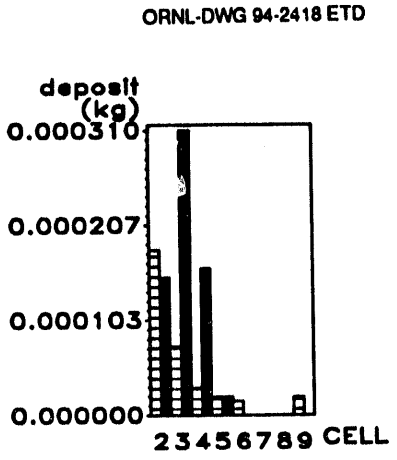

Figure 4.18 FAL-1a iodine deposition

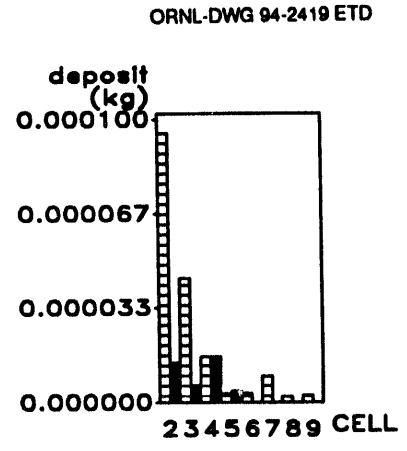

Figure 4.19 FAL-3a iodine deposition

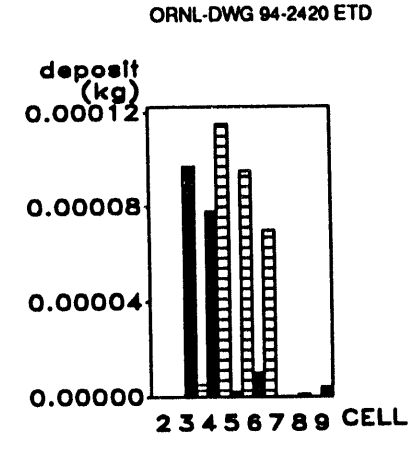

Figure 4.20 FAL-12 iodine deposition

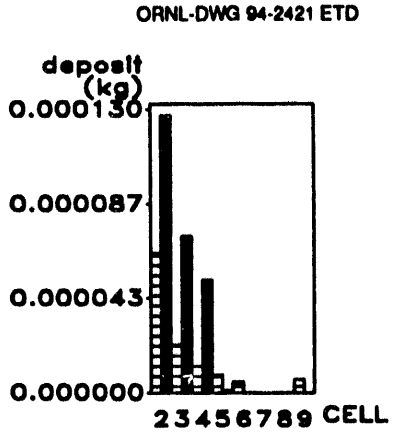

Figure 4.21 FAL-1a tellurium deposition

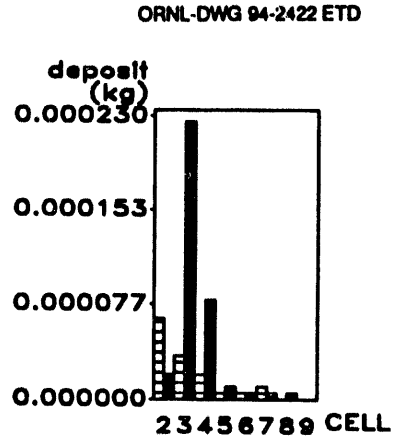

Figure 4.22 FAL-3a tellurium deposition

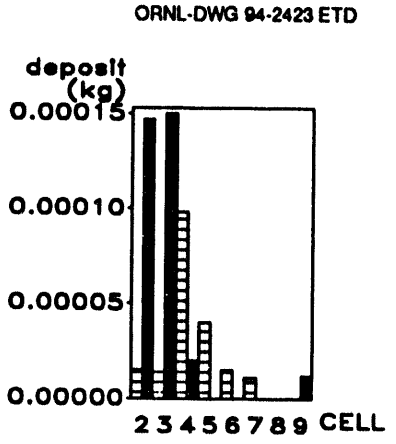

Figure 4.23 FAL-12 tellurium deposition

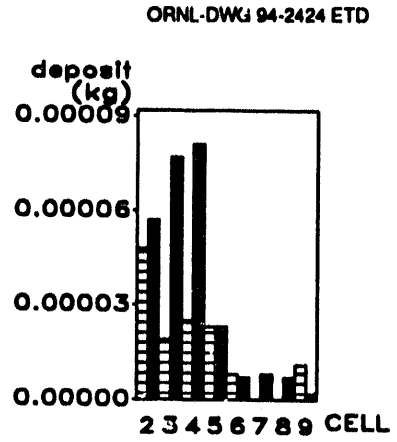

Figure 4.24 FAL-1a cadmium deposition

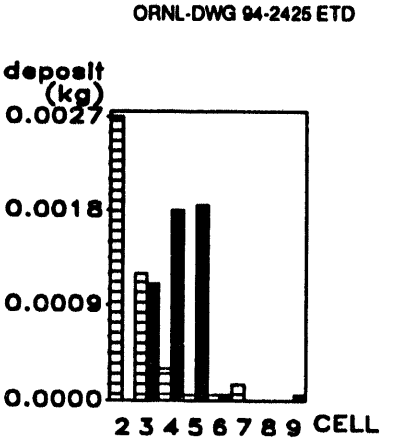

Figure 4.25 FAL-3a cadmium deposition

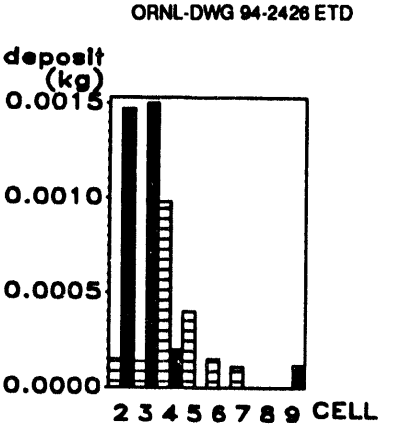

Figure 4.26 FAL-12 cadmium deposition

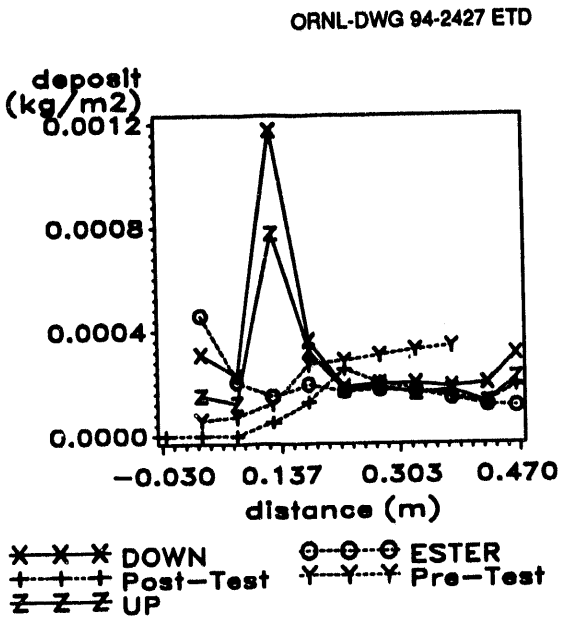

Figure 4.27 FAL-17 cesium deposition

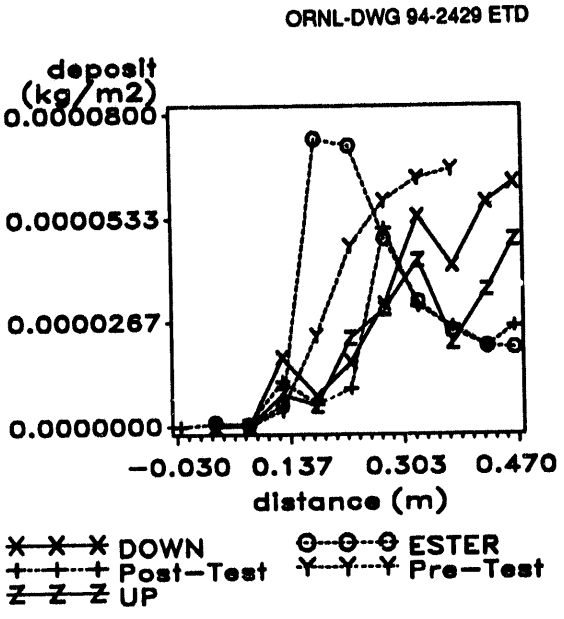

Figure 4.29 FAL-17 iodine deposition

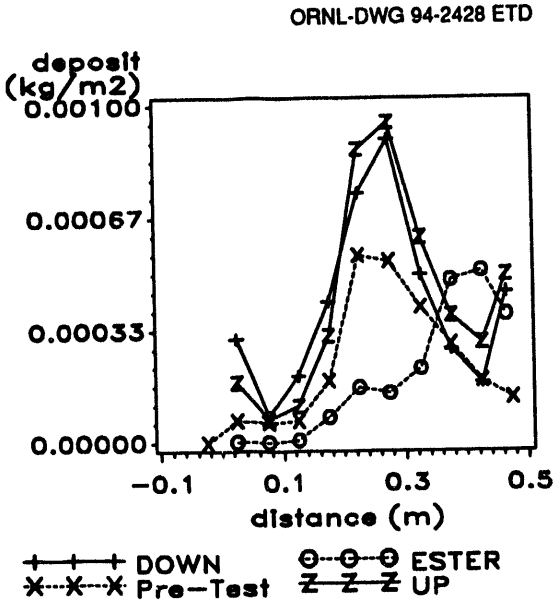

Figure 4.28 FAL-18 cesium deposition

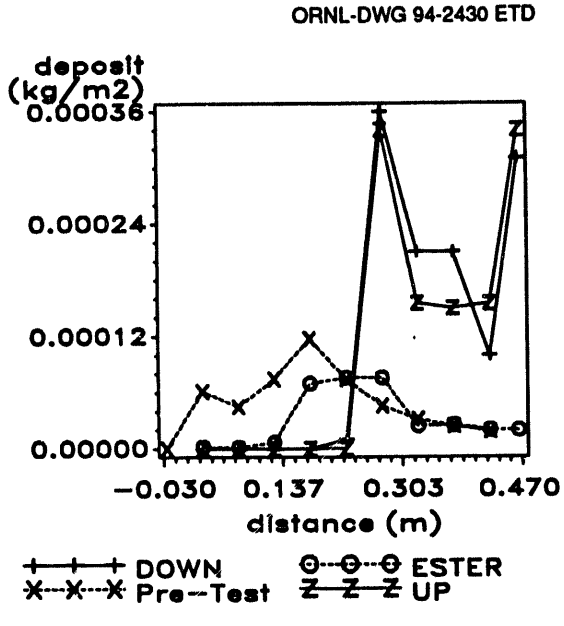

Figure 4.30 FAL-18 iodine deposition

VICTORIA modeling suggests that deposition is by vapor condensation on the pipe walls and vapor condensation onto aerosol particles followed by thermophoresis, but the code is unable to predict the deposition in the pipe. In the first set of calculations (TG series), Chown and Williams[20] noted that some features of the experiments make analysis difficult. For instance, the temperature was not measured in the upper plenum, before the entrance of the thermal gradient tube, whereas VICTORIA predicts a sensitivity to it (in TG-2). Another unknown was the timing of the control rod release. Apart from the quantitative discrepancies shown in the figures just mentioned, the results are qualitatively wrong. In TG-1 and TG-6, VICTORIA predicted aerosol deposition, whereas the experiments indicated vapor deposition.

Dumaz[21] made the same point, in the later FAL series tests, about the necessity to have more precise thermal boundary conditions. His attempts to match the deposition profiles by varying the temperatures were not very successful, so all of the blame cannot be attributed to this.

FAL-17, described by Beard et al.,[22] and FAL-18 were nearly identical except that FAL-17 had boric acid and FAL-18 did not. The experimenters claim that the boric acid made a significant difference to the experimental results and believed that the high iodine transmission factor in the test with boric acid, FAL-17, was because of the formation of hydrogen iodide by the reaction:

$$CsI + H_3BO_3 \rightarrow CsBO_2 + HI + H_2O \ .$$

They suggested that the hydrogen iodide then reacted preferentially with smaller aerosol particles and that this enhanced transmission. There was no experimental evidence for this other than the transmission factor itself. The difference between the cesium deposition between the two experiments was slight, although in the test with boric acid it did deposit at a higher temperature. VICTORIA calculations suggested that the transmission of cesium as cesium borate instead of cesium hydroxide should have influenced the deposition by more than was in fact observed.

Williams did not include any Falcon results in his VICTORIA validation statement;[3] probably the main benefit to VICTORIA in these tests has been in the extensive testing of the code with different chemical combinations, the elimination of some errors, and an improvement in the code's robustness. Falcon also benefited from the pinpointing of areas where more careful measurements were required. The later experiments are significantly more useful for code validation than the early ones.

The first ever CSNI ISP to be based on a fission product transport experiment is being organized around the Falcon facility, and an exceptionally large number of organizations and codes will be participating. Usually these ISPs result in a rigorous scrutiny of measurement and codes, and it is hoped that the Falcon exercise will be no exception.

4.5.8 French Analytical Experiments

Some of these French experiments, summarized by Lecomte and Lhiaubet,[26] are currently under way, so only a limited number of code comparisons have been carried out. The TUBA and TRANSAT experiments study thermophoresis in pipes of 20 and 400 mm diameter.

Calculations have been made first by Albiol and Dumaz,* using AEROSOLS-B2 and comparing the Brock model to the Derjaguin model, and second by Dumaz et al.,[27] who compared TRAPF, VICTORIA, and RAFT. Agreement in both cases was rather good.

Dumaz et al.[27] also studied vapor condensation in the DEVAP experiment and found more variation in the code results. VICTORIA predicted considerably less deposition than the other codes; these measurements are shown in Fig. 4.31.

4.5.9 PBF Experiments

Test 1-4. The transport and deposition of fission products and aerosol through the upper plenum in the PBF tests have been calculated by PULSE—a version of TRAPMELT—and VICTORIA. The PULSE calculation is described by Petti et al.[28] and the VICTORIA calculation by Dumaz.† Figures 4.32 and 4.33 show the deposition of cesium and cadmium in the upper plenum plotted against distance from the bottom of the core. The upper plenum

*P. Dumaz, "Interpretation with AEROSOL-B2 Code," American Association for Aerosol Research Annual Meeting, Philadelphia, June 18-22, 1990.

†P. Dumaz, "Analysis of Fission Product Transport in PBF-SFD 1-4 Experiment Using VICTORIA," CEA Note Technique SEMAR 92/07, January 17, 1992.

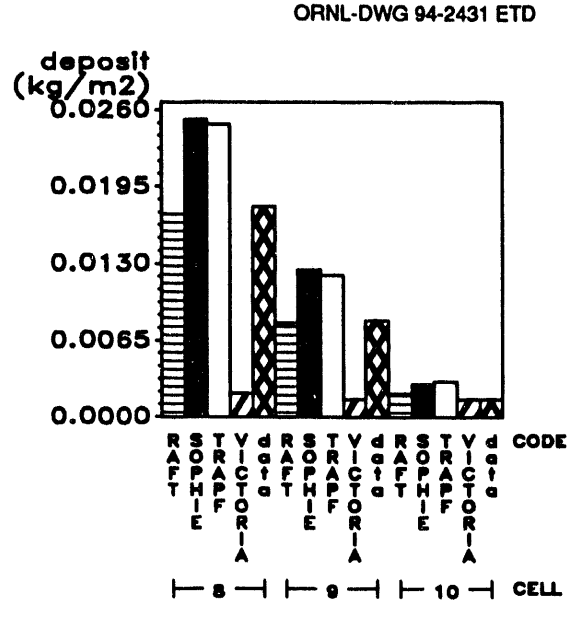

Figure 4.31 Test DEVAP08 cesium iodide deposition

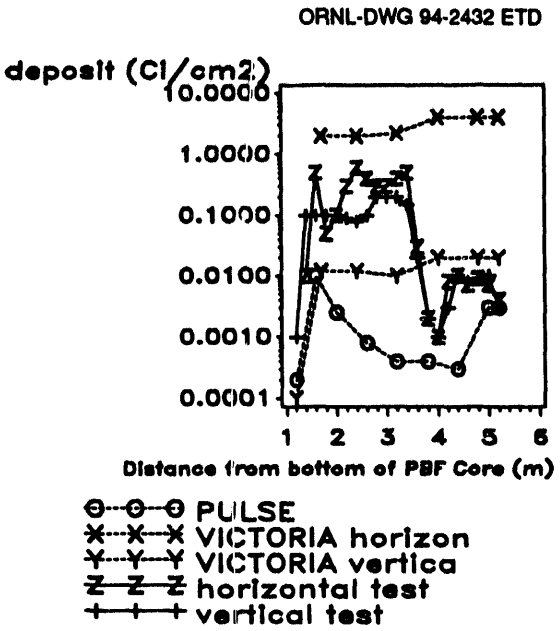

Figure 4.32 Deposition of cesium in upper plenum of test PBF 1.4

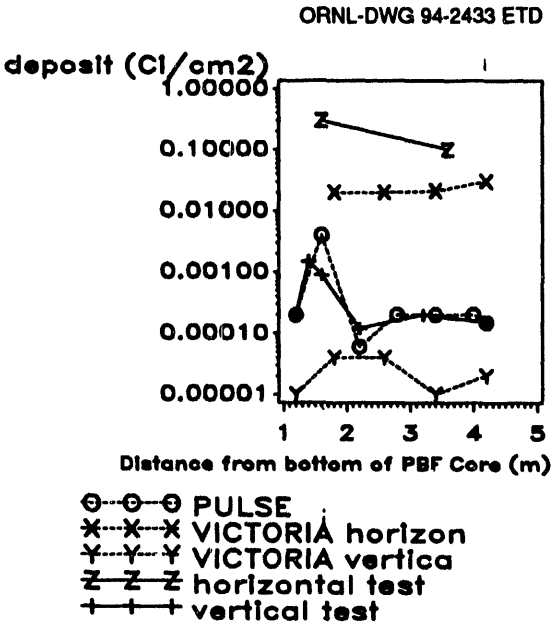

Figure 4.33 Deposition of cadmium in upper plenum of test PBF 1.4

starts at a position of 1.6 m. The experiment and the VICTORIA calculation are divided into deposition onto horizontal surfaces and onto vertical surfaces. An average value, as calculated by PULSE, is dominated by vertical deposition because the area is much greater.

The code predictions are flattered by the logarithmic scale. For the volatile fission product cesium, both VICTORIA and PULSE hugely underpredict the vertical deposition. VICTORIA predicts too much horizontal deposition for cesium (by settling) but underpredicts the settling for cadmium. VICTORIA predicts that the main mechanism for deposition was wall condensation for the vapor species (CsI, CsOH, SnTe, etc.) and thermophoresis for the low volatile species ($BaZrO_3$, $SrZrO_3$, etc.). Petti et al.,[28] however, suggest that most deposited material was trapped aerosol particles, and the relatively large deposition on horizontal surfaces would tend to confirm this. According to their analysis, the vertical deposition was mostly caused by turbulent impaction in recirculating eddies behind the deposition rods.

Both sets of researchers would have liked more precise boundary conditions and tried sensitivity calculations with plausible variations in them. Even so they could not reproduce the experimental results.

Test 1-3. The only calculation of transport in test 1-3 has been made by Martinson et al. using PULSE.[29] Figure 4.34 shows the iodine deposition in the upper plenum. The experimental results are divided into horizontal and vertical deposition. PULSE predicted that these should be the same, so only one curve has been drawn for the calculational results. PULSE greatly overpredicts the experimental results. The results for cesium, not shown here, were better, but not by much.

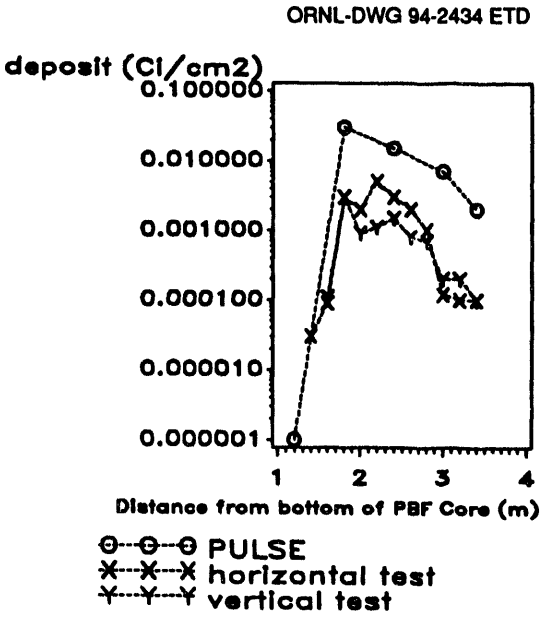

Figure 4.34 Deposition of iodine in upper plenum of test PBF 1.3

4.5.10 LOFT Experiments

Test LP-FP-1. The objective of this test was to study the release rather than the transport of fission products. In fact the part of the Experimental Analysis Summary Report devoted to fission product behavior[30] does not mention transport at all. The only known calculation for this test has been performed by Garcia Cuesta et al.[31] using TRAPMELT. They predicted the deposition up to the blowdown suppression tank, as shown in Table 4.29.

TRAPMELT predicted that the deposition in the upper plenum was by thermophoresis, but the authors warn against drawing too many conclusions from this analysis because the experimental data are unreliable.

Test LP-FP-2. At an open forum summarizing the LOFT achievements, Merilo and Mecham[32] presented results of a code comparison exercise for this test. Subsequently, Kmetyk[33] performed a calculation as part of the MELCOR assessment program. The data presented in Table 4.30 show the results of calculations for the fission product transport part of the test. All of these calculations used measured data as boundary conditions and calculated data when this was not possible.

The codes agreed that most of the deposition in the upper plenum was by vapor condensation except for tellurium, which the Spanish predicted to be deposited primarily by chemical absorption. JAERI and INEL assumed that the iodine was transported as silver iodide, whereas Spain and EPRI assumed that it was cesium iodide. The basis for the choice of silver iodide were the deposition-coupon measurements in the upper plenum. Carboneau[34] noticed that the ratio Cs/I was 0.074 in this case. Clearly, there are equally strong grounds for suggesting other iodine species.

Table 4.29 LOFT test LP-FP-1

Code	Date	Iodine transmission (%)	Cesium transmission (%)
Experiment		61	13
TRAPMELT2.2	1989	97	83

Table 4.30 LOFT test LP-FP-2

			Upper plenum deposition (% of release)			LPIS deposition (% of LPIS source)			Transport out of system (% of release)		
Date	Code	Organization	Cs	I	Te	Cs	I	Te	Cs	I	Te
1985	Experiment		17	39	9	87	74	97	11	16	2
1990	TRAPMELT	INEL	8	29		91	61		8	28	
1990	TRAPMELT2	Spain	35	13	2	99	89	100	1	9	0
1990	MAAP	EPRI	25	25					77	77	
1990	TRAPMELT (using Liu-Agarwal model)	JAERI				16	28				
1990	TRAPMELT (using Friedlander Johnstone model)	JAERI				62	58				
1992	MELCOR	SNL	38	31	42	Not modeled separately			40	52	33

4.5.11 Phebus-FP

The authors of this report hesitated before including Phebus-FP calculations in this chapter because the experiments have not yet been performed, so no comparison of results is possible. Nevertheless it was felt worthwhile to include them for two reasons:

1. The forthcoming Phebus-FP experiments are of such importance for the study of fission product transport that they deserve at least a mention.
2. Comparison of code calculations for deposition in pipe work has played an important role during all phases of the project. The most up-to-date versions of the most important codes have been used in these comparisons.

The results of the first comparison study are reported by Shepherd and Markovina,[35] who summarized calculations made by various organizations for different postulated geometries. The results from these studies were useful in designing an experimental circuit capable of reproducing phenomena that resembled as much as possible those taking place in a full-scale reactor circuit under accident conditions. Another benchmark exercise, reported by Fermandjian et al.,[36] compares deposition using boundary conditions rather close to those likely to be used in the test. Table 4.31 compares the overall deposition in the circuit divided between that deposited as an aerosol and that deposited as a vapor.

All codes predict that most deposition of cesium (mainly cesium hydroxide according to the codes) and iodine (mainly cesium iodide again according to the codes) will be in the simulated steam generator where the surface temperature is 150°C and the gas temperature drops from about 700°C at the inlet to 150°C some distance later. The mechanisms were predicted to be vapor condensation and thermophoresis, although the proportion predicted by each code varies considerably. RAFT predicts mostly vapor condensation (about 80% depending on the version), TRAP-FRANCE predicts about half and half, and VICTORIA predicts nearly all thermophoresis. Whether the experimental measurements will distinguish between the two processes is not yet clear.

The tellurium predictions also vary enormously. All RAFT versions predicted that the tellurium was deposited fairly evenly over the circuit by chemisorption. The other codes predicted tellurium deposition by condensation either on particles or surfaces from the steam generator onwards.

4.5.12 Conclusions

In general, the codes are useful for interpreting experimental measurements, but they should be used with caution as tools for predicting reactor transients. We have some understanding of aerosol physics phenomena, but the transport and retention of fission products at higher temperatures cannot be predicted with confidence. The reasons for this assessment are outlined as follows.

Fission Product Vapors. Experiments to validate the vapor phase behavior of fission products are few because they are difficult. The temperature has to be higher and more carefully measured than for the purely aerosol experiments.

Analysis of these few experiments is also hard. There is no measurement in any of the experiments analyzed in this chapter that gives the speciation of the fission products either in the bulk gas or at the moment they are deposited, or

Table 4.31 Predictions for Phebus test FPT-0

		Total deposition in circuit (percentage of release to circuit)					
		Cesium		Iodine		Tellurium	
Code	Organization	Particles	Vapor	Particles	Vapor	Particles	Vapor
TRAP-FRANCE	CEA, Cadarache	13	24	17	13	10	9
VICTORIA	JRC, Ispra	33		36		45	
MACRES	NUPEC, Japan	24	11	24	3	21	0.1
RAFT	CEA, Cadarache	6	78	6	80	0	100
RAFT	JRC, Ispra	13	70	20	56	0	100
RAFT	UPM, Madrid	11	66	22	55	12	84

even whether they were deposited as an aerosol or a vapor. Normally, the only information available to analysts in experiments like Falcon is the mass of each element deposited at a certain position. Thus when the codes are quantitatively wrong in the prediction of the deposition rate, it is difficult to know whether or not they are qualitatively wrong as well. Only if the quantitative predictions are good can we say that the code is validated. At present they are not.

The in-pile tests, LOFT-FP2 and PBF 1-3 and 1-4, are useful because of their representative fission product sources. Although measurements are meager and boundary conditions uncertain, their results indicate that the codes cannot reproduce the experimental results. LOFT-FP2 measurements indicated that iodine was not transported as cesium iodide in the upper plenum. Some experiments that were considered primarily as release experiments such as the STEP tests or ACRR-ST could also be analyzed using transport codes, but no such analyses have been reported in open literature.

Aerosol Physics. Historically, aerosol physics was studied in the containment before being applied to the RCS, so phenomena that are also present in the containment are generally the best understood. Thus the codes identified correctly that gravitational settling was a significant phenomenon in the Marviken pressurizer. This is not to say that the settling models in the codes are validated, because they are not. The actual magnitude of deposition caused by gravitational settling depends mostly on the particle size. If this was not measured accurately, as was the case in Marviken, then the accuracy of the deposition rate as calculated by the codes cannot be adequately assessed.

Attempts to study thermophoresis have often foundered because in experiments designed to validate the models' thermophoresis seems to be dominated by other deposition mechanisms. In LACE LA3 and the ORNL ATT experiments, some, but not all, codes predicted that thermophoretic deposition might be a significant phenomenon, but it is now thought that most of the deposition was by turbulent impaction and that thermophoresis will probably only dominate in laminar flow. In Falcon thermal gradient tubes, on the other hand, the Reynolds number was around 20, the flow laminar, and the dominant aerosol deposition mechanism, according to VICTORIA, was thermophoresis. Analysis of the results is complicated because the aerosol size and thermal-hydraulic conditions were not known precisely, and in some cases it was not known whether elements were deposited as vapors or aerosols. Nevertheless, analysis of some of the later Falcon tests and of the TUBA tests suggests that the codes' thermophoresis models are capable of predicting these experimental results. On the other hand, the codes were not unanimous in their predictions for thermophoresis in the Phebus-FP steam generator, reflecting a genuine uncertainty in modeling thermophoresis when the temperature difference between the pipe wall and the carrier gas is high. This temperature difference is expected to be around 500 K in Phebus-FP; in Falcon and TUBA it was around 30 K.

For settling and thermophoresis it is possible that a careful examination of experimental measurements may in the end reveal that the present models are adequate: this is not the case for turbulent impaction. Where the flow is turbulent, some aerosol particles will deposit, but it is difficult to predict how many. Careful analysis of calculations for experiments such as LACE has shown that the present models for turbulent impaction cannot predict the deposition rate and have particular difficulty with predicting the deposition caused by bends and flow obstructions. It is unfortunate that the experiments show that this is where most of the deposition will occur.

The composition of the aerosols had an unexpected, at least as far as the codes were concerned, influence on the retention. In LACE, aerosol particles rich in cesium hydroxide deposited more than those with lower CsOH mass fractions.

Some codes can predict the mechanical resuspension in the ORNL-ART resuspension tests, but the range of conditions is not large enough to say that the models are validated. No experiments model the revaporization of deposits following a temperature rise caused by, for instance, decay heat or a change in carrier gas composition. There are few experimental data with which to check code predictions.

None of the experiments studied in this chapter clearly indicated a need to move to multicomponent aerosol modeling. It had been suggested that aerosol particles of a particular species could be of a significantly different size to those of another and so be deposited or transmitted differently, but this has not been observed. In LACE LA3B and LA3C, some differences in deposition between CsOH and MnO were observed, but this may have been caused by resuspension, and the effect was, in any case, small. Otherwise there was no experiment where one element behaved significantly differently from the others. The coagglomeration approximation seems to be justified for all of the experiments considered in this section. It remains to be seen whether this is true only for the rather limited number of species used in these experiments or under more representative conditions as well.

The Codes. Some codes, notably TRAPMELT, consider a limited number of species—normally cesium iodide, cesium hydroxide, and tellurium—to be stable from their release in the core to their entry into the containment. Others, such as RAFT and VICTORIA, calculate the changing speciation as the fission products are transported through the system. Although it is clear that the TRAPMELT approximation is wrong, it is not felt that this approximation made a significant difference to the analyses reported in this chapter. There are several reasons for this:

1. Most of the experiments considered were at low temperatures. Once an element is in aerosol form, its behavior is, according to all codes, independent of the chemical form of the aerosol.

2. Codes such as VICTORIA and RAFT that predict speciation indicated that cesium iodide was the predominant form of iodine, even in cases, such as Falcon Test Fal-17, where the experimental measurements indicate that it was not.

We expect that as the codes are further developed and the results of more high-temperature experiments such as Phebus-FP become available, we will be able to understand better whether or not a frozen chemistry model is acceptable.

Although one or two codes have a theoretical capability of calculating multicomponent aerosol behavior, this option has not been used to calculate the behavior of aerosols in experiments. The experimental results examined here do not indicate that different chemical species deposited differently because they were associated with different size aerosol particles.

Some of the calculations described in this report were nodalized rather coarsely, sometimes with temperature gradients of more than 50°C between meshes. This is no doubt a consequence of the long running times of some the codes. An increase in speed could allow finer nodalization and better modeling of condensation phenomena.

Nearly all the calculations reported in this chapter are integral experiments that model many coupled phenomena. The codes have not been thoroughly checked against separate-effects tests where one phenomenon is investigated over a range of conditions.

The plethora of versions of codes, particularly TRAPMELT and RAFT, is confusing. ENEL's version of TRAPMELT predicts more deposition in LACE LA3B than LA3C. The UK TRAPMELT calculations predict the reverse. There is no documented evidence that some versions being used for reactor cases and Phebus-FP pretest calculations have ever been checked against experiments at all. The developers of other codes such as VICTORIA and MELCOR have, on the other hand, issued validation statements, and this is a step forward.

4.5.13 References

1. T. S. Kress, Martin Marietta Energy Systems, Inc., Oak Ridge National Laboratory "Review of the Status of Validation of the Computer Codes Used in the Severe Accident Source Term Reassessment Study" ORNL/TM-8842 (BMI-2104), April 1985.*

2. M. R. Kuhlman, V. Kogan, and P. M. Schumacher, Battelle Columbus Laboratories, "TRAP-MELT2 Code: Development and Improvement of Transport Modeling," USNRC Report NUREG/CR-4677, 1986.*

3. D. A. Williams, H. S. Bond, and N. A. Johns, "VICTORIA Validation Statement", Atomic Energy Establishment Winfrith Report R-5131, United Kingdom (October 1991).

4. L. N. Kmetyk, Sandia National Laboratory, "Survey of MELCOR Assessment," SAND92-1273, 1992.*

5. D. A. Williams and A. T. D. Butland, "Preliminary Analysis of the Marviken Aerosol Transport Tests 1, 2a and 2b using the TRAPMELT-2 Computer Code," Atomic Energy Establishment Winfrith Report AEEW-M 2147, United Kingdom (October 1984).

6. D. A. Williams, "Further Analyses of the Marviken Aerosol Transport Tests 1, 2a and 2b using the TRAPMELT2-UK Computer Code," Atomic Energy Establishment Winfrith Report AEEW-M 2298, United Kingdom (April 1986).

7. D. A. Williams, "Analyses of the Marviken Aerosol Transport Tests 4 and 7," Atomic Energy Establishment Winfrith Report AEEW-M 2371, United Kingdom (December 1986).

8. C. Gonzalez and A. Alonso, "Improvement and Validation of Tellurium Transport Models in the RAFT Code," *Third CSNI Workshop on Iodine Chemistry in Reactor Safety at Tokai-mura, Japan, September 11-13, 1991*, Committee on the Safety of Nuclear Installations, NEA/CSNI/R(91)15, France (March 1992).

9. A. Alonso and C. Gonzalez, "Modeling the Chemical Behavior of Tellurium Species in the Reactor Pressure Vessel and the Reactor Cooling System under Severe Accident Conditions," Commission of the European Communities Report EUR13787EN (July 1991).

10. H. S. Bond and N. A. Johns, "Analysis of Marviken ATT Experiments Using VICTORIA," Atomic Energy Establishment Winfrith Report AEA R-520, United Kingdom (June 1991).

11. L. N. Kmetyk, Sandia National Laboratory, "MELCOR 1.8.1 Assessment. Marviken-V Aerosol Transport Tests ATT-2b/ATT-4," SAND92-2443, 1993.*

12. A. L. Nichols and D. A. Williams, "Report on the Second Marviken-V Analysis Meeting: 15-17 July 1986 at the Argonne National Laboratory," Atomic Energy Establishment Winfrith Report AEEW-M 2486, United Kingdom (August 1986).

13. F. Parozzi, "Relevance of Marviken and LACE Project Results in Validating TRAP-MELT/ENEL Code," Marviken-V/DEMONA/LACE Workshop, Montreux, Switzerland, June 28-July 1, 1992, ENEL Report N6/88/04/M.

14. A. Masnaghetti, "Influence of Recirculation on Aerosol Deposition in a Pressurized PWR During an Accident with Core Melting," Tesi di Laurea in Ingegneria Nucleare Politecnico di Milano - Facolta di Ingegneria Nucleare, ENEL report N6/88/05/MI (September 1988).

15. A. L. Wright, P. C. Arwood, and J. H. Wilson, Martin Marietta Energy Systems, Inc., Oak Ridge National Laboratory, "Summary of Posttest Aerosol Comparisons for LWR Aerosol Containment Experiment (LACE) LA1," ORNL/M-365 (LACE TR-022), October 1987.*

16. A. L. Wright and P. C. Arwood, Martin Marietta Energy Systems, Inc., Oak Ridge National Laboratory, "Summary of Pretest Aerosol Code Results for LWR Aerosol Containment Experiment (LACE) LA3," ORNL/M-352 (LACE TR-023), November 1987.*

17. A. L. Wright and P. C. Arwood, Martin Marietta Energy Systems, Inc., Oak Ridge National Laboratory, "Summary of Posttest Aerosol Code-Comparison Results for LWR Aerosol Containment Experiment (LACE) LA3," ORNL/M-492 (LACE TR-024), June 1988.*

18. H. S. Bond, N. A. Johns, and D. A. Williams, "Analysis of the LACE Experiments Using VICTORIA," Atomic Energy Establishment Winfrith Report R 5143, United Kingdom (June 1991).

19. F. R. Rahn, J. Collen, and A. L. Wright, "Aerosol Behavior Experiments on Light Water Reactor Primary Systems," *Nucl. Technol.*, 81, 158-182 (May 1988).†

20. N. M. Chown and D. A. Williams, "Analysis of the Falcon Thermal-Gradient Tube Experiments," Atomic Energy Establishment Winfrith Report AEE R 5063, United Kingdom (December 1990).

21. P. Dumaz, "Interim Report On: Analyses of the Falcon Experiments Using VICTORIA," Atomic Energy Establishment Winfrith Report AEE R-5267, RSSD Note 186, United Kingdom (February 1992).

22. A. M. Beard, P. J. Bennet, and J. Brunning, "Falcon Experiments: A Comparison of Falcon Tests Fal-17 and Fal-18," Atomic Energy Authority R-2380 (March 1993).

23. A. Mason and D. A. Williams, "Pre-Test Calculations for FAL-17 and FAL-18 Using the VICTORIA Code," Atomic Energy Authority Winfrith Report AEA R-2321 (August 1992).

24. A. Mason, "Post-Test Calculations for FAL-17 and FAL-18 Using the VICTORIA Code," Atomic Energy Establishment Winfrith Report AEA R-5409 (November 1992).

25. I. Shepherd, J. Areia Capitão, and Y. Drossinos, "Post-test Calculations of Falcon-17 and Falcon-18 Using RAFT and the ESTER Version of VICTORIA," in J. Areia Capitão et al., *Fission Product Chemistry in Support of the Phebus-FP Programme, Volume 2: Code Analyses*, Commission of the European Communities (1994).

26. C. Lecomte and G. Lhiaubet, "CEA Analytical Activities: HEVA, PITEAS, Mini-Containments," *The*

Phebus Fission Product Project: Presentation of the Experimental Program and Test Facility, ISBN 1 85166 765 2 (Elsevier Applied Sciences, 1992).

27. P. Dumaz, Y. Drossinos, J. A. Capitao, and I. Drosik, "Fission Product Deposition and Revaporization Phenomena in Scenarios with Large Temperature Differences," 1993 National Heat Transfer Conference, Atlanta, Georgia, August 8-11, 1993.

28. D. A. Petti et al., "Power Burst Facility (PBF) Severe Fuel Damage Test 1-4 Test Results Report," USNRC Report NUREG/CR-5354 (EGG-2565), September 1989.*

29. Z. R. Martinson et al., "PBF Severe Fuel Damage Test 1-3. Test Results Report," USNRC Report NUREG/CR-5354 (EGG-2565), September 1989.*

30. E. Schuster and W. Morrell, "Experimental Analysis Summary Report (EASR) of OECD LOFT LP-FP-1 Volume 4 Fission Product Behavior," Centro de Investigaciones Energéticas, Medioambientales y Tecnologicas Report TN/TS-16/R-8, Madrid, Spain (March 1989).

31. J. C. Garcia Cuesta, E. R. Mayguez, and A. I Lontanaros, "Analysis of Fission Product Behavior During the SECA Phase of Experiment LOFT-LP-FP-1," Centro de Investigaciones Energéticas, Medioambientales y Tecnologicas Report TN/TS-16/R-8, Madrid, Spain (February 1981).

32. M. Merilo and D. C. Mecham, "Code Comparison Results for the LOFT-FP-2 Experiment," *Proceedings from an Open Forum: The OECD/LOFT Project: Achievements and Significant Results: 9-11 May 1990, Madrid, Spain*, Organization for Economic Cooperation and Development, ISBN 92-64-03339-4, Paris, France (1991).

33. L. N. Kmetyk, Sandia National Laboratory "MELCOR 1.8.1 Assessment: LOFT Integral Experiment LP-FP-2," SAND92-1373, December 1992.*

34. M. L. Carboneau, "Highlights of the OECD LOFT LP-FP-2 Experiment Including Hydrogen Generation, Fission Product Chemistry, and Transient Fission Product Release Fractions," *Proceedings from an Open Forum: The OECD/LOFT Project: Achievements and Significant Results: 9-11 May 1990, Madrid, Spain*, Organization for Economic Cooperation and Development, ISBN 92-64-03339-4, Paris, France (1991).

35. I. Shepherd and A. Markovina, "Summary of the Dimensioning Verification Studies of the Phebus-FP Studies," Commission of the European Communities Report EUR 13906EN, Luxembourg (1992).

36. J. Fermandjian et al., "Presentation of the Results of Exploratory Circuit Calculations for Phebus FPT-0 (Reference Scenario)," Phebus-FP Report SAWG 92-035/2, Ispra, Italy (June 1992).

*Available for purchase from National Technical Information Service, Springfield, Virginia 22161.
†Available in public technical libraries.

4.6 Conclusions

4.6.1 Thermodynamics and Speciation

The chemical form of the fission products will influence their transport within the RCS both as vapors and aerosols. Thermodynamic data are required to predict the main species stabilized and their likely properties. Good progress has been made in recent years in understanding the vapor and condensed phase chemistry that can occur within the reactor coolant circuit during a severe accident. A substantial data base of thermodynamic properties has been assembled of species likely to be present in the RCS. Efforts are under way to ensure that the data base is self-consistent and broadly accepted.

However, there are fewer data on species such as hydroxides and hydrides that may become more important at high pressures of steam and hydrogen. Furthermore, the effects of intense radiation fields on chemistry in the reactor coolant circuit have received little attention. The major uncertainty for code validation purposes is believed to be the lack of data on the chemical forms of the fission products stabilized within the RCS. The Phebus-FP program is expected to provide an indication on the fission product speciation from experiments using a realistic source.

4.6.2 Vapor Interactions with Surfaces and Aerosols

Interactions of fission product vapors with primary circuit surfaces and aerosols can substantially modify the magnitude and nature of the source term to the containment. However, the relative importance of the

processes is uncertain: while the extensive surface area of the aerosol surfaces indicates that vapor-aerosol interactions should predominate, heat and mass transfer limitations can considerably affect the balance.

A number of deposition kinetics studies have been conducted using the following vapor species: CsOH, I_2, HI, Te, SnTe, and CsI. Other vapors could well play important roles, and the data base needs to be extended to include them. Note that, in reality, surfaces could be oxidized and coated with aerosols, and work is required on such representative surfaces. The effect of carrier gas oxidation potential is also an important consideration.

Some data are available on vapor interactions with deposited aerosols, but few studies have addressed vapor interactions with suspended aerosols. Consideration of time scales indicates that the latter process will be governed by diffusion limitations rather than chemical kinetics. Lack of data on the diffusion of fission product vapors through reactor gases prevents accurate prediction of condensation phenomena.

Representative data are required (e.g., from Phebus-FP) to indicate the nature of the surface deposits and the competition between vapor-surface and vapor-aerosol reactions. Such data should guide the requirement for separate-effects studies and the development of more sophisticated models to treat these processes.

4.6.3 Aerosol Nucleation and Growth

The behavior of fission product aerosols within the RCS will be determined predominately by the size and, to a lesser extent, the shape of the aerosol. The chemical form of the fission product vapors will determine the point at which condensation will occur to form aerosols, their size distribution, and morphology. Uncertainties in defining the chemical speciation of the fission product vapors represent an important uncertainty in determining the subsequent aerosol transport.

Experimental studies have shown that chemically distinct aerosols can be produced with different transport properties, although their significance with respect to transport in the RCS remains to be assessed. The role of pressure on aerosol nucleation is uncertain; however, scoping tests have indicated that the primary size of aerosol particles decreases with increasing system pressure.

The general requirement for a detailed treatment of aerosol nucleation has not been demonstrated (for example, while a sophisticated model is used in RAFT, only a limited approach is adopted within VICTORIA). The need for a detailed understanding of these phenomena should be assessed through sensitivity studies and additional scoping experiments, if appropriate.

4.6.4 Aerosol Transport and Deposition

The basic processes governing aerosol transport are generally well understood, although the neglect of electrostatic forces within the codes remains a concern. Areas of weakness include:

- deposition in bends,
- application of the fundamental aerosol physics models to treatment of complex structures at a large scale (such as steam separators or steam dryers),
- aerosol deposition arising from abrupt changes in the flow channel width, and
- thermophoretic deposition from turbulent flows.

4.6.5 Resuspension and Revaporization

Two processes may lead to a significant release of radioactivity at late stages of the accident:

- physical resuspension (or re-entrainment) of aerosols (increased flow and shock and vibration in the substrate) and
- revaporization of deposits (increased temperature or variation in gas composition).

Resuspension of aerosols has been demonstrated in a number of experiments; however, the importance of this phenomenon in determining the consequences of severe accidents is uncertain. All experimental studies conducted to date have relied on the use of simple aerosol stimulants, and more realistic experiments such as Phebus-FP are required to define the nature of the initial deposit more clearly. Uncertainties persist as to the size distribution of the resuspended material and the synergisms between the effects of gas flow and structural vibration on resuspension. However, the complexity of physical resuspension for realistic systems (involving multicomponent, multilayered deposits in a variety of thermal-hydraulic conditions) makes it unlikely that a fully mechanistic analysis will be possible.

Primary

Plant calculations and code analyses indicate the potential importance of revaporization to the consequences of severe reactor accidents. In the absence of interactions with surfaces and other materials, revaporization can be modeled simply on the basis of the temperature and partial vapor pressures of the system. However, reactions could modify any release significantly. The study of a number of key systems is recommended to acquire the relevant activity coefficients. More detailed modeling of the interactions of deposits with surfaces is also needed to interpret and apply these data.

4.6.6 Codes and Benchmarks

A large number of alternative codes and different versions of transport codes are available. In many cases there is no documented evidence that some of the current versions of codes have ever been checked against experiments. The production of validation statements (as for VICTORIA and MAAP for example) is recommended.

Although assumptions and approximations are made, no code appears to be significantly better than the others in predicting deposition. In general, code comparison exercises show that the codes are capable of predicting which aerosol deposition mechanism will dominate, but they are less successful in determining the extent of deposition. Few integral experiments have been conducted to allow the vapor models to be tested.

There is a general consensus that sedimentation, thermophoresis, turbulent diffusion, and impaction are important aerosol phenomena in the RCS. However, significant variety in the treatment of the deposition processes within each code has been observed. Comparison of the models within the codes would clarify differences and inconsistencies. Such an exercise would assist in identifying the best models that warrant continued use and development.

Detailed code comparison exercises are needed both to validate individual models (separate-effects studies) and to assess the coupling between models and the applicability of the source term programs (integral tests). Data from the Falcon ISP and Phebus-FP program should address some of these concerns.

Parametric assessments/sensitivity studies (e.g., variation of aerosol size, concentration, composition) are urgently needed to link the primary circuit calculations to eventual accident-specific source terms to the containment and environment. Such analyses should assist in defining the requirements for a detailed understanding of speciation calculations, the treatment of aerosol nucleation and resuspension, and the assessment of multicomponent aerosol behavior. The risk-dominant phenomena can be highlighted, allowing future work to concentrate on those phenomena contributing most to uncertainties in the consequences of the accident. Such calculations are planned as part of the CEC Reinforced Concerted Action on Source Term.

4.6.7 Thermal Hydraulics

There has been a significant change over the last ten years in the understanding of flows in the RCS during core degradation, particularly for the accidents in which the circuit remains pressurized during core degradation. Complex natural circulation loops are predicted to develop that could markedly influence aerosol and vapor behavior. The uncertainties in the results of source term calculations stem as much from uncertainties in the thermal hydraulic boundary conditions as from limitations in source term modeling. Examples of thermal-hydraulic uncertainties include the treatment of late-phase core behavior, the effect of the carrier gas on fission product speciation and transport, the 1-D or 2-D approach adopted within the majority of severe accident thermal-hydraulic codes, decay heat effects, and the coupling of source term with thermal-hydraulic modeling. Decay heat is important in determining local surface temperatures and hence phenomena such as revaporization. The relocation of liquid and slurry deposits under hydrodynamic and gravity forces therefore merits attention.

5 Main Conclusions and Recommendations

This chapter summarizes the main conclusions and recommendations from this report. Note that specific conclusions from the state-of-the-art assessment are presented at the end of Chaps. 3 and 4. These conclusions and other information presented in Chaps. 2, 3, and 4 are integrated and summarized from the standpoint of source term analyses for severe accident conditions. Recommendations to the Committee on the Safety of Nuclear Installations (CSNI) are also presented in this chapter.

Significant improvement has been made in understanding fission product release and transport in the reactor coolant system (RCS) since the accident at Three-Mile Island. The ability to predict behavior of radionuclides in the RCS under severe accident conditions has advanced greatly. These capabilities have demonstrated that radionuclide retention in the RCS can significantly attenuate and transform the potential release of radioactivity from a nuclear power plant during an accident. Careful modeling of these release and transport phenomena is an essential element of reactor accident analyses. For example, in accident scenarios involving containment bypass through lines connected to the RCS (V sequence) or late containment failure and revaporization and revaporization of radionuclides, the in-vessel behavior of radionuclides would have a direct bearing on the consequences of the accident.

However, the phenomena associated with RCS release and transport are complex, and not all of the relevant source term issues have been resolved. The conclusions and recommendations presented in this chapter concern the phenomena and issues that the writing group considered to have the greatest need for further understanding and potential impact on our ability to perform realistic source term analyses for severe accidents.

5.1 Assessment of Overall Importance and Knowledge of RCS Release and Transport Phenomena

Both Chaps. 3 and 4 included discussions of the major phenomena that must be modeled to assess RCS fission product release and transport. The writing group qualitatively assessed the importance of each of these phenomena to the prediction of RCS release and transport, and the needs for additional experimental data to resolve uncertainties in the phenomena.

Tables 5.1 and 5.2 summarize the rankings that members of the writing group gave to each of the phenomena in terms of importance and the data needs. These rankings ["high, medium, and low" (HML)] represent our best effort to prioritize the needs for further release and transport phenomena assessments in terms of importance to source term issues for severe accident analyses. A high ranking for a release phenomenon means that the writing group thinks it has a strong influence on release from the core. A high ranking for a transport phenomenon means that the writing group thinks it has a strong influence on the source to the containment or, in the case of bypass sequences, to the auxiliary building. Note that for phenomena where there was not a consensus on the HML rankings, a range (such as L-M) was agreed to. The experimental needs identified when assigning knowledge rankings are in addition to and not alternative to existing programs such as Phebus-FP and Falcon and potential future programs such as STORM.

5.2 Major Needs for Further Understanding of RCS Release and Transport Phenomena

Tables 5.1 and 5.2 illustrate the writing group view that there are many release and transport phenomena where an adequate data base exists for understanding and model development. A limited number of phenomena were ranked high in importance and were viewed by the writing group as needing additional experiments to permit the phenomena to be understood and included in RCS release and transport codes. The writing group recommends additional experiments (with supporting analysis and model development) concerning the following release and transport phenomena:

1. For fission product release, new experiments, or extension of planned experiments, are needed to characterize the fission product release from fuel under air or highly oxidizing conditions and low-volatile fission product release from molten pools in the reactor vessel. In our view, these release phenomena have the potential (depending on the plant design characteristics) for high impact on accident source term analyses, and adequate information is not available to model them in the release codes.

2. For fission product transport, additional experiments are needed to address vapor interactions with aerosols and surfaces and material revaporization phenomena. We assess these to be of high importance to RCS transport and source term analysis and think that an adequate experimental data base is not available to permit appropriate code models to be developed.

Table 5.1 Phenomena summary table for RCS fission product release

Phenomena affecting FP release	Importance (High-Med-Low)[a]	Knowledge ranking (1-4)[b]	Comments
Chemistry of FPs in fuel	M-H	2	Thermodynamic data are mostly adequate for current needs, and modeling tools exist for equilibrium calculations.
FP mobility in fuel	H	2	Extensive data exist, but they need to be consolidated and reviewed. More data may be required on the effect of oxygen potential and burnup on diffusion rates.
Evolution of fuel microstructure	M	3	Important for early phase of release (e.g., venting of grain boundaries). Need data to support model calculations at different grain sizes, burnups, and power histories.
UO_2 liquefaction	M	3	Need separate-effects test data to support models.
UO_2 oxidation	H	3	Important for post-vessel failure releases with air oxidation of exposed fuel. Data are required at high temperatures.
Quenching/reflood	M	3	Requires tests with high burnup fuel.
Debris bed formation/heatup	L-M	3	Requires integral test data. Need knowledge of local temperatures, fuel morphology, and carrier gas conditions.
Molten pool formation	H	3	Data required for low-volatile FPs after extended melt duration.
Molten fuel-coolant interaction	L	4	Not expected to contribute significantly to source term.
Non-FP material releases	H-L	2	Ag-In-Cd, boric acid, and Sn-Zr releases rated M/H, others as M/L. Data need to be reviewed/consolidated. Some integral test data, particularly at high pressures, may be required.

[a]IMPORTANCE RANKING: (level of importance with respect to impact on FP source term from the core).
[b]KNOWLEDGE RANKING: (level of understanding for each phenomena):

1: Current understanding (data and modeling) is adequate.
2. Further modeling or review/consolidation of data is required. Existing data appear to be adequate.
3. Understanding is incomplete. New experimental data would provide adequate information to develop the necessary understanding, and this could be achieved in the near future.
4: Understanding is incomplete. New experimental data would be required to provide adequate information to develop the necessary understanding, but the data are not likely to be available in the near future.

Table 5.2 Phenomena summary table for RCS fission product transport

FP transport phenomena	Importance (High, Med., Low)[a]	Knowledge ranking (1-4)[b]	Comments
Thermodynamic data	H	1[c]	Generally well understood, but there is a need for high-pressure data and data for more complex compounds.
Vapor interactions with surfaces and aerosols	H	3	There is a clear need for vapor-aerosol interaction data. Vapor-surface interaction tests may need to be done with more complex FP species. Data on appropriate species will hopefully come from Phebus-FP tests.
Aerosol nucleation and growth	M	2	The need for detailed nucleation/growth modeling in the codes has not been clearly established.
Aerosol deposition and transport	H-M	1[c]	Generally well understood in terms of basic physics, though there is a need for improved understanding of deposition in bends and in complex geometries.
Aerosol resuspension	L-M	3	The need for detailed resuspension models in the codes has not been clearly established. Phebus-FP can help to define the aerosol species to be used in any tests.
Revaporization	H	3	There is a need for revaporization tests performed with appropriate FP chemical species. Again, Phebus-FP can help.

[a]IMPORTANCE RANKING: (level of importance with respect to FP source term from the RCS).
[b]KNOWLEDGE RANKING: (level of understanding for each phenomena):

1: Current understanding (data and modeling) is adequate.
2: Further modeling or review/consolidation of data is required. Existing data appear to be adequate.
3: Understanding is incomplete. New experimental data would provide adequate information to develop the necessary understanding, and this could be achieved in the near future.
4: Understanding is incomplete. New experimental data would be required to provide adequate information to develop the necessary understanding, but the data are not likely to be available in the near future.

[c]As noted in the comments, the knowledge base for these phenomena is generally well understood. Although there were outstanding data needs, the writing group did not believe that these needs warranted giving these phenomena a "2" or "3" knowledge ranking.

5.3 Other Principal Conclusions and Recommendations to the CSNI

In this section we present additional conclusions and recommendations from this state-of-the-art assessment; these were developed from the specific conclusions presented at the ends of Chaps. 3 and 4.

1. Two types of fission product (FP) release codes are in use—empirical and mechanistic. The empirical codes are based on correlations between experimental conditions and release rates and are widely used because of their simplicity. However, they are often used under conditions differing from those on which they are based.

   We recommend that the CSNI encourage efforts to extend the usefulness of the empirical codes by including recent experimental data on the effects of burnup, fuel oxidation, and perhaps other phenomena such as liquefaction, quenching, and so forth. This will make the empirical codes applicable to a wider range of accident conditions.

2. The release code-to-data comparisons presented in Chap. 3 illustrate that (a) empirical release codes tend to overpredict volatile FP release data and (b) mechanistic release codes are capable of producing better agreement with experiment, but these codes appear to require very careful application (detailed fuel conditions) to obtain good results. However, detailed assessments of FP release code-experiment comparisons have never been performed (and none of the comparisons have been blind), so it is difficult to assess the validity and robustness of the models.

   We recommend that coordinated efforts be made to assess the validity of the FP release models and codes (current and future versions) using both benchmarks and International Standard Problems (ISPs). Comparisons with both simplified and well-controlled separate-effects tests, as well as with more global tests--especially with Phebus-FP data—should guide the need for further model improvements and developments. The additional experiments recommended in Sect. 5.2, point 1 (FP release from fuel under air-oxidizing conditions and low-volatile FP release from molten pools in the reactor vessel) will also be necessary as a data base for future code development.

3. The FP transport code-comparison results presented in Chap. 4 indicate that the codes have not been sufficiently validated for reliable use in reactor source-term analyses. From the standpoint of aerosol transport, the codes can correctly predict which deposition phenomena are most important in an experiment but are not capable of predicting the magnitude and distribution of the deposition when compared with experimental data. Few of the benchmark experiments discussed in Chap. 4 permit definitive validation of the vapor interaction models presently in the codes.

   We recommend the continued development and assessment of the FP transport codes. This should, at a minimum, include (a) improved transport code models based on the experimental needs highlighted in Sect. 5.2, (b) well-coordinated comparisons of code predictions to results from Falcon and Phebus-FP experiments (ISPs) and assessment of the FP transport codes based on these comparisons, and (c) additional code-comparison exercises to identify differences in code models used to analyze the same phenomena (e.g., bend deposition).

4. The importance of mechanistically modeling aerosol nucleation has not been assessed. At issue is whether ad hoc treatments of nucleation phenomena are adequate for the purposes of reactor safety analyses. In addition, the importance of mechanical resuspension of aerosols (and mechanistic modeling of this process) has not been clearly established. Consequently, while additional experiments would be useful to permit appropriate models for these phenomena to be developed, it is not possible to make a clear case for doing so.

   We recommend that coordinated efforts be initiated to determine the importance of aerosol nucleation and aerosol resuspension phenomena to RCS fission product transport analyses. These assessments would provide the basis for determining if experiments are needed in addition to those already performed or planned.

5.4 Other Writing Group Comments

1. With regard to any future integral FP release and transport experiments and particularly the Phebus-FP tests, the writing group recommends that attention be given to using the test data to guide future separate-effects tests. For example, appropriate analyses of deposition samples may indicate the fission product chemical species that should be included in future small-scale revaporization tests.

2. Although the writing group did not perform any detailed assessments of the impact of thermal-hydraulic and core-degradation uncertainties on FP release and transport and the importance of scaling of experiments, we view these issues as sufficiently important to be considered regarding release and transport analyses and experimental design. We think for example, that the core degradation codes should provide sufficiently accurate information on fuel conditions to the mechanistic FP release codes for release

calculations. The writing group encourages efforts to link existing mechanistic release models with existing mechanistic core degradation models.

Appendix
Description of OECD, NEA, and CSNI

Organization for Economic Cooperation and Development

Pursuant to Article 1 of the Convention signed in Paris on 14th December 1960, and which came into force on 30th September 1961, the Organization for Economic Cooperation and Development (OECD) shall promote policies designed:

- to achieve the highest sustainable economic growth and employment and a rising standard of living in Member countries, while maintaining financial stability, and thus to contribute to the development of the world economy;
- to contribute to sound economic expansion in Member as well as non-member countries in the process of economic development; and
- to contribute to the expansion of world trade on a multilateral, non-discriminatory basis in accordance with international obligations.

The original Member countries of the OECD are Austria, Belgium, Canada, Denmark, France, Germany, Greece, Iceland, Ireland, Italy, Luxembourg, the Netherlands, Norway, Portugal, Spain, Sweden, Switzerland, Turkey, the United Kingdom and the United States. The following countries become Members subsequently through accession at the dates indicated hereafter: Japan (28th April 1964), Finland (28th January 1969), Australia (7th June 1971) and New Zealand (29th May 1973). The Commission of the European Communities takes part in the work of the OECD (Article 13 of the OECD Convention).

Nuclear Energy Agency

The OECD Nuclear Energy Agency (NEA) was established on 1st February 1958 under the name of the OEEC European Nuclear Energy Agency. It received its present designation on 20th April 1972, when Japan became its first non-European full Member. NEA membership today consists of all European Member countries of OECD as well as Australia, Canada, Japan, The Republic of Korea, and the United States. The Commission of the European Communities takes part in the work of the Agency.

The primary objective of NEA is to promote cooperation among the governments of its participating countries in furthering the development of nuclear power as a safe, environmentally acceptable and economic energy source.

This is achieved by:

- encouraging harmonization of national regulatory policies and practices, with particular reference to the safety of nuclear installations, protection of man against ionizing radiation and preservation of the environment, radioactive waste management, and nuclear third party liability and insurance;
- assessing the contribution of nuclear power to the overall energy supply by keeping under review the technical and economic aspects of nuclear power growth and forecasting demand and supply for the different phases of the nuclear fuel cycle;
- developing exchanges of scientific and technical information particularly through participation in common services;
- setting up international research and development programs and joint undertakings.

In these and related tasks, NEA works in close collaboration with the International Atomic Energy Agency in Vienna, with which it has concluded a Cooperation Agreement, as well as with other international organizations in the nuclear field.

Appendix

CSNI

The NEA Committee on the Safety of Nuclear Installations (CSNI) is an international committee made up of scientists and engineers. It was set up in 1973 to develop and coordinate the activities of the Nuclear Energy Agency concerning the technical aspects of the design, construction and operation of nuclear installations insofar as they affect the safety of such installations. The Committee's purpose is to foster international cooperation in nuclear safety amongst the OECD Member countries.

CSNI constitutes a forum for the exchange of technical information and for collaboration between organizations which can contribute, from their respective backgrounds in research, development, engineering or regulation, to these activities and to the definition of its program of work. It also reviews the state of knowledge on selected topics of nuclear safety technology and safety assessment, including operating experience. It initiates and conducts programs identified by these reviews and assessments in order to overcome discrepancies, develop improvements and reach international consensus on technical issues of common interest. It promotes the coordination of work in different Member countries including the establishment of cooperative research projects and international standard problems, and assists in the feedback of the results to participating organizations. Full use is also made of traditional methods of cooperation, such as informaion exchanges, establishment of working groups, and organization of conferences and specialist meetings.

The greater part of CSNI's current program of work is concerned with safety technology of water reactors. The principal areas covered are operating experience and the human factor, reactor coolant system behaviors, various aspects of reactor component integrity, the phenomenology of performance, risk assessment, and severe accidents. The Committee also studies the safety of the fuel cycle, conducts periodic surveys of reactor safety research programs and operates an international mechanism for exchanging reports on nuclear power plant incidents.

In implementing its program CSNI establishes cooperative mechanisms with NEA's Committee on Nuclear Regulatory Acitivities (CNRA), responsible for the activities of the agency concerning the regulation, licensing and inspection of nuclear installations with regard to safety. It also cooperates with NEA's Committee on Radiation Protection and Public Health and NEA's Radioactive Waste Management Committee on matters of common interest.

Internal Distribution

1. E. C. Beahm
2. M. H. Fontana
3. E. C. Fox
4. W. Fulkerson
5. S. R. Greene
6. S. A. Hodge
7. J. E. Jones Jr.
8. T. S. Kress
9. K. Lenox
10. R. A. Lorenz
11. M. F. Osborne
12. L. J. Ott
13. C. E. Pugh
14. C. C. Southmayd
15. J. O. Stiegler
16. R. P. Taleyarkhan
17. R. P. Wichner
18–22. A. L. Wright
23. ORNL Patent Section
24. Central Research Library
25. Document Reference Section
26–27. Laboratory Records Department
28. Laboratory Records (RC)

External Distribution

29. R. Barrett, OWFN, U. S. Nuclear Regulatory Commission, Office of Nuclear Reactor Regulation, Washington, D.C. 20555
30. J. H. Flack, NLS324, U. S. Nuclear Regulatory Commission, Office of Nuclear Reactor Regulation, Washington, D.C. 20555
31. L. Soffer, NLN324, U. S. Nuclear Regulatory Commission, Office of Nuclear Reactor Regulation, Washington, D.C. 20555
32. A. C. Thadani, OWFN 8E2, U. S. Nuclear Regulatory Commission, Office of Nuclear Reactor Regulation, Washington, D.C. 20555
33. E . S . Beckjord, NLS007, U. S. Nuclear Regulatory Commission, Office of Nuclear Regulatory Research, Washington, D.C. 20555
34. F. Eltawila, NLN344, U. S. Nuclear Regulatory Commission, Office of Nuclear Regulatory Research, Washington, D.C. 20555
35. N . Grossman, NLN344, U. S. Nuclear Regulatory Commission, Office of Nuclear Regulatory Research, Washington, D.C. 20555
36. T. L. King, NLN370, U. S. Nuclear Regulatory Commission, Office of Nuclear Regulatory Research, Washington, D.C. 20555
37. R. V. Lee, NLN344, U. S. Nuclear Regulatory Commission, Office of Nuclear Regulatory Research, Washington, D.C. 20555
38. A. Behbahani, NLN344, U. S. Nuclear Regulatory Commission, Office of Nuclear Regulatory Research, Washington, D.C. 20555
39. R. L. Palla, Jr., OWFN 10 E 4, U. S. Nuclear Regulatory Commission, Office of Nuclear Regulatory Research, Washington, D.C. 20555
40. A. M. Rubin, NLN344, U. S. Nuclear Regulatory Commission, Office of Nuclear Regulatory Research, Washington, D.C. 20555
41. B. W. Sheron, NLN369, U. S. Nuclear Regulatory Commission, Office of Nuclear Regulatory Research, Washington, D.C. 20555
42. T. P. Speis, NLS007, U. S. Nuclear Regulatory Commission, Office of Nuclear Regulatory Research, Washington, D.C. 20555
43. C. G. Tinkler, NLN344, U. S. Nuclear Regulatory Commission, Office of Nuclear Regulatory Research, Washington, D.C. 20555
44. M. D. Houston, PHIL P-315, U. S. Nuclear Regulatory Commission, Office of ACRS, Washington, D.C. 20555
45. U. S. Nuclear Regulatory Commission Division of Technical Information and Document Control, 7920 Norfolk Avenue, Bethesda, MD 20014
46. B. Spencer, Argonne National Laboratory, 9700 South Cass Avenue, Argonne, IL 60439
47. W. H. Rettig, U.S. Department of Energy, Idaho Operations Office, 785 DOE Place, Idaho Falls, ID 83401-1134
48. C. Alexander, Battelle Columbus Laboratory, 505 King Avenue, Columbus, OH 43201

49. T. Pratt, Brookhaven National Laboratory, 130 BNL, Upton, NY 11973
50. M. Merilo, Electric Power Research Institute, P.O. Box 10412, 3412 Hillview Avenue, Palo Alto, CA 94303
51. R. J. Hammersley, Fauske and Associates, Inc., 16W070 West 83rd Street, Burr Ridge, IL 60521
52. F. E. Panisko, Reactor Systems, Fuels & Matls. P8-35, Pacific Northwest Laboratory, P.O. Box 999, Richland, WA 99352
53. N. Bixler, Sandia National Laboratory, P.O. Box 5800, Albuquerque, NM 87185
54. D. Powers, Sandia National Laboratories, Dept. 6404, MS-0744, 1515 Eubank SE, Albuquerque, NM 87123
55. S. Thompson, Sandia National Laboratory, P.O. Box 5800, Albuquerque, NM 87185
56. K. Washington, Sandia National Laboratory, P.O. Box 5800, Albuquerque, NM 87185
57. K. O. Reil, Sandia National Laboratory, P.O. Box 5800, Albuquerque, NM 87185
58. I. Catton, University of California Los Angeles, Nuclear Energy Laboratory, 405 Hilgaard Avenue, Los Angeles, CA 90024
59. C. M. Allison, MS 3840, Idaho National Engineering Laboratory, EG&G Idaho, Inc., P.O. Box 1625, Idaho Falls, ID 83415
60. R. Schneider, ABB/CE, 1000 Prospect Mill Road, Winsor, CT 06095
61. D. Buttermer, PLG Inc., 191 Calle Magdalena, Suite 240, Encunitas, CA 92024
62. James Metcalf, MS 245-2, Stone and Webster, 245 Summer Street, Boston, MA 02107
63. John Conine, D2-221, G. E. Knolls Atomic Power Lab., Box 1072, Schenectady, NY 12501
64. J. Sugimoto, Japan Atomic Energy Research Institute, Tokai-mura, Naka-gun, Ibaraki-ken, 319-11, Japan
65. Hee-Dong Kim, Korea Advanced Energy Research Institute, P.O. Box 7, Daeduk-Danji Taejeon 305-353, Korea
66. Kenji Takumi, Nuclear Power Engineering Center, Fujitakanko Building, 17-1, 3-Chrome, Toranomon, Minato-Ku, Japan, Tokyo 105
67. J. W. Wolfe, ZAP 34N, Westinghouse Bettis Atomic Laboratory, P.O. Box 79, West Mifflin, PA 15122
68. S. Inamati, General Atomics, P.O. Box 85608, San Diego, CA 92138-5608
69. M. Kazimi, Massachusetts Institute of Technology, Nuclear Engineering Department, 77 Massachusetts Avenue, Cambridge, MA 02139
70. N. Todreas, Massachusetts Institute of Technology, Nuclear Engineering Department, 77 Massachusetts Avenue, Cambridge, MA 02139
71. E. Stubbe, Belgonucleaire, Department of LWR Fuel, Rue de Champde Mars. 25, B-1050 Brussels, Belgium
72. L. A. Simpson, Whiteshell Laboratories, AECL Research, Reactor Safety Research Division, Pinawa, Manitoba Canada ROE lLO
73. B. Kuczera, Kernforschungszentrum Karlsruhe, Postfach 364O, 75 Karlsruhe, Germany
74. P. Hofmann, Kernforschungszentrum Karlsruhe, Postfach 364O, 75 Karlsruhe, Germany
75. G. Petrangeli, Nucleare e della Protezione Sanitaria (DISP), Ente Nazionnle Energie Alternative (ENEA), Viale Regina Margherita, 125, Casella Postale M. 2358, I-00100 Roma A. D., Italy
76. S. I. Chang, Institute of Nuclear Energy Research, P.O. Box 3, Lungtan, Taiwan 325, Republic of China
77. J . Bagues, Consejo de Seguridad Nuckan, SOR Angela de la Cruz No 3, Madrid 28056, Spain
78. A. Alonso, E. T. S. Ingenieros Industriales, Jost Gutierrez Abascal, 28006 Madrid, Spain
79. W. Frid, Statens Karnkraftinspektion, P.O. Box 27106, S-10252 Stockholm, Sweden
80. K. J. Brinkman, Reactor Centrum Nederland, 1755 ZG Petten, The Netherlands
81. Paola Fasoli-Stella, Thermodynamics and Radiation Physics, CEC Joint Research Center, Ispra I-201020 Ispra (Varese), Italy
82. P. Vaisnys, VATESI, Gediminis Prospect 36, Vilnius, Lithuania
83. S. Elo, Hungarian Atomic Energy Commission, H-1374 Budapest, P.O. Box 565, Budapest, Hungary
84. J. Stuller, State Office for Nuclear Safety, Slezska 9, 120 00 Prague 2, Czech Republic
85. S. Kinnersly, 203/A32, UKAEA, Winfrith, Dorchester DT2-8DH, Dorset, England, United Kingdom
86. D. Williams, UKAEA, Winfrith, Dorchester DT2-8DH, Dorset, England, United Kingdom
87. J. A. Martinez, Consijo De Seguridad Nuclear, Justo Dorado 11, 28040 Madrid, Spain
88. V. Asmolov, I. V. Kurchatov Institute of Atomic Energy, Nuclear Safety Department, Moscow, 123182, Russia
89. M. LiVolant, Institut de Protection et de Surete Nucleaire, CEN/FAR–B. P. No. 6, F-92265, Fontenay-aux-Roses, Cedex, France
90. P. Hosemann, Paul Scherrer Institut, Programm LWR-Sicherheit, CH-5232 Villigen, PSI, Switzerland
91. Y . Yanev, Committee on the Use of Atomic Energy for Peaceful Purposes, 69 Shipchenski, prokhod Blvd., 1574, Sofia, Bulgaria
92. J. Misak, Nuclear Regulatory Authority, Slovak Republic, Bajkalska 27, 827 21 Bratislave, Slovak Republic
93. A. Meyer-Heine, Cadarache Center for Nuclear Studies, F-13108 Saint Paul-Lez-Durance, Cedex, France
94. J. Leveque, Cadarache Center for Nuclear Studies, F-13108 Saint Paul-Lez-Durance, Cedex, France
95. B. Andre, Cadarache Center for Nuclear Studies, F-13108 Saint Paul-Lez-Durance, Cedex, France

96. S. Chakraborty, Swiss Federal Nuclear Safety, Inspectorate, CH-5232 Villigen - HSK, Switzerland
97. P. Kloeg, N. V. Kema. P.O. Box 9035, 6800 ET ARNHEM, The Netherlands
98. L. Bolshov, Russian Academy of Sciences, Nuclear Safety Institute, 52, B. Tulskaya, Moscow, 113191, Russia
99. E. Cordfunke, Netherlands Energy Research Foundation, P.O. Box 1 1755 ZG Petten, The Netherlands
100. B. Mavko, Jozef Stefan Institute, Jamova 39 61111 Ljubljana, Slovenia
101. P. Stoop, Netherlands Energy Research Foundation, P.O. Box 1, 1755 ZG Petten, The Netherlands
102. B. Adroguer, CEA/IPSN, Bat 702, CEN Cadarache, 13108 Saint Paul lez Durance, Cedex, France
103. B. R. Bowsher, AEA Technology, Winfrith Technology Centre, Dorchester, Dorset DT2 8DH, United Kingdom
104. U. Brockmeier, University of Bochum, IB4-128, 44780 Bochum, Germany
105. D. S. Cox, AECL Research, Chalk River Nuclear Laboratory, Chalk River, Ontario, Canada, K0J 1J0
106. R. R. Hobbins, RRH Consulting, P.O. Box 971, Wilson, Wyoming 83014
107. K.-D. Hocke, IKE, Universitat Stuttgart, P. O. Box 80 11 40, D-70550 Stuttgart, Germany
108. F. Iglesias, Ontario Hydro, H11E14, 700 University Avenue, Toronto, Ontario, Canada M5G 1X6
109. A. V. Jones, Commission of the European Communities, Joint Research Centre, Ispra, 21020 Ispra (Va) Italy
110. D. E. Leaver, Polestar Applied Technology, Inc., Four Main Street, Los Altos, CA, USA, 94022
111. I. Shepherd, Commission of the European Communities, Joint Research Centre, Ispra, 21020 Ispra (Va) Italy
112. H. Holmstrom, OECD/NEA, 38 Boulevard Suchet, F-75016 Paris, France
113. K. Trambauer, Gesellschaft fur Anlagen-und Reaktor-sicherheit (GRS)-mblt Forschungsgelande, D-8046 Garching Allemagne, Germany
114. Office of Assistant Manager for Energy Research and Development, DOE-ORO, Oak Ridge, TN 37831
115–116. Office of Scientific and Technical Information, P. O. Box 62, Oak Ridge, TN 37831

NRC FORM 336 (2-89) NRCM 1102, 3201, 3202

U.S. NUCLEAR REGULATORY COMMISSION

BIBLIOGRAPHIC DATA SHEET

(See instructions on the reverse)

1. REPORT NUMBER (Assigned by NRC, Add Vol., Supp., Rev., and Addendum Numbers, if any.)

NUREG/CR-6193
NEA/CSNI/R(94)2
ORNL/TM-12681

2. TITLE AND SUBTITLE

Primary System Fission Product Release and Transport

A State-of-the-Art Report to the Committee on the Safety of Nuclear Installations

3. DATE REPORT PUBLISHED

MONTH	YEAR
June	1994

4. FIN OR GRANT NUMBER

L2250

5. AUTHOR(S)

A. L. Wright

6. TYPE OF REPORT

Technical

7. PERIOD COVERED *(Inclusive Dates)*

8. PERFORMING ORGANIZATION – NAME AND ADDRESS *(If NRC, provide Division, Office or Region, U.S. Nuclear Regulatory Commission, and mailing address; if contractor, provide name and mailing address.)*

Oak Ridge National Laboratory
Oak Ridge, TN 37831-6050

9. SPONSORING ORGANIZATION – NAME AND ADDRESS *(If NRC, type "Same as above"; if contractor, provide NRC Division, Office or Region, U.S. Nuclear Regulatory Commission, and mailing address.)*

Division of Systems Research
Office of Nuclear Regulatory Research
U.S. Nuclear Regulatory Commission
Washington, DC 20555-0001

10. SUPPLEMENTARY NOTES

11. ABSTRACT *(200 words or less)*

This report presents a summary of the status of research activities associated with fission product behavior (release and transport) under severe accident conditions within the primary systems of water-moderated and water-cooled nuclear reactors. For each of the areas of fission product release and fission product transport, the report summarizes relevant information on important phenomena, major experiments performed, relevant computer models and codes, comparisons of computer code calculations with experimental results, and general conclusions on the overall state of the art. Finally, the report provides an assessment of the overall importance and knowledge of primary system release and transport phenomena and presents major conclusions on the state of the art.

12. KEY WORDS/DESCRIPTORS *(List words or phrases that will assist researchers in locating the report.)*

Fission Product Release
Fission Product Transport
Reactor Coolant System
Source Terms
Severe Accidents

13. AVAILABILITY STATEMENT

Unlimited

14. SECURITY CLASSIFICATION

(This Page) Unclassified

(This Report) Unclassified

15. NUMBER OF PAGES

16. PRICE

DATE
FILMED
8/15/94
END